TL
569
.R0334
PR
c.1

System

North Atlantic Complex

FLN

DPL

CONTRA

PROJ

SERVICE

SYSTEMS ANALYSIS OF THE NORTH ATLANTIC AIR TRAFFIC COMPLEX

FINAL REPORT

DECEMBER 1962

RESEARCH DIVISION PROJECT NO 116-9R

This report has been prepared by the ARCON CORPORATION for the Systems Research and Development Service, Federal Aviation Agency, under Contract No FAA/BRD-334 The contents of this report reflect the views of the contractor, who is responsible for the facts and accuracy of the data presented herein, and do not necessarily reflect the official views or policy of the FAA

Arcon Corporation
Lexington, Massachusetts
R62-3

ARGON CORPORATION, Lexington, Massachusetts
SYSTEM ANALYSIS OF THE NORTH ATLANTIC AIR TRAFFIC COMPLEX
December, 1962, 283 pp , including 62 illus , 7 tables, Ref R62-3,
Final Report
(Contract No FAA/BRD-334)

ABSTRACT

This report contains a detailed analysis of the North Atlantic Air Traffic Control System Emphasis is placed upon the effects on system performance of potential modifications in navigation, communications, weather forecasting, aircraft characteristics, control procedures and separation standards Mathematical models are developed and applied to operational data The models provide realistic representations of the significant functional characteristics of the basic system areas The report includes a description of the present system (Section III) The relationships between separation standards and other system areas are developed with emphasis on comparative evaluations of alternate system configurations (Section V) System performance is measured in terms of traffic capacity and economic penalties imposed by air traffic control restrictions (Sections VI, VII) The effects of various system modifications are then determined (Section VIII) Although emphasis is placed on subsonic jet aircraft operations over the North Atlantic, a brief discussion of other environments is also given (Section IX)

The body of the report (Sections I - IX) stresses the application and interpretation of the models Detailed mathematical developments are given in several Appendices These are A Statistical Model of Wind Behavior, B The Effect of Winds on Longitudinal Separation, C Monte Carlo Evaluation of Longitudinal Separation, D Analysis of Fix Errors, E Lateral Track-Keeping Errors, F System Capacity, G Analysis of the Minimal Time Path

PREFACE

This is the final report of the study performed by ARCON CORPORATION for the Federal Aviation Agency under Contract FAA/BRD-334, System Analysis of the North Atlantic Air Traffic Complex The study is part of the LODISNAV program of the Federal Aviation Agency Its purpose is to supply a comprehensive analysis of the North Atlantic Air Traffic Complex as it exists today, and the quantitative objective criteria for the evaluation of various proposed modifications of the present system

In the course of our work, we have profited greatly from the help, advice and encouragement freely tendered by many people and organizations We are particularly grateful to Mr Chester E Dunmire, of the Federal Aviation Agency, for his invaluable assistance and continuous support which were indispensable to the successful completion of this work We also wish to thank Mr Nathaniel Braverman for useful advice For assistance in the difficult task of data reduction, we are indebted to Mr James Grambart and Lt Cmdr H A LaQue

We also wish to express our gratitude to the International Air Transport Association, in particular to Messrs S Krzyczkowski, P Kearvell, and S Krejcik, and to all air carriers, especially the Trans-World Air Lines and the Pan American Air Lines, for providing important information on flight planning and navigational procedures

We are greatly indebted to members of the Ministry of Aviation and the Royal Aircraft Establishment of the United Kingdom, especially to Messrs. N R Norfolk, I M Lucas, K H Treweek, P G Reich, F L Sawyer, and D E Lloyd for thoughtful cooperation and several stimulating discussions It is a pleasure to acknowledge especially useful and pertinent information provided by Mr C S Durst, also of the United Kingdom.

TABLE OF CONTENTS

		Page
I	INTRODUCTION	1
II	SUMMARY	5
III	DESCRIPTION OF THE PRESENT SYSTEM	12
IV.	ORGANIZATION OF THE ANALYSIS	29
V	SEPARATION STANDARDS	35
VI	CAPACITY OF AIR TRAFFIC SYSTEMS	67
VII	ECONOMIC FACTORS	79
VIII	POTENTIAL SYSTEM IMPROVEMENTS	89
IX	APPLICATIONS TO OTHER ENVIRONMENTS	103
APPENDIX A	STATISTICAL MODEL OF WIND BEHAVIOR	107
APPENDIX B	THE EFFECT OF WINDS ON LONGITUDINAL SEPARATION	132
APPENDIX C	MONTE CARLO EVALUATION OF LONGITUDINAL SEPARATIONS	162
APPENDIX D	ANALYSIS OF FIX ERRORS	184
APPENDIX E	LATERAL TRACK-KEEPING ERRORS	212
APPENDIX F	SYSTEM CAPACITY	233
APPENDIX G	ANALYSIS OF THE MINIMAL TIME PATH	257
BIBLIOGRAPHY		278

I. INTRODUCTION

This study may be described briefly as an analysis of the air traffic control system in the North Atlantic environment, with special emphasis on the role of navigational devices and procedures. It is demanded by an urgent need for an increase in traffic handling capacity of the system without sacrifice in safety of operation.

The basic objective of this study is to investigate and evaluate various methods through which the capacity of the system can be increased All proposed system modifications are studied and compared with this objective in mind. Particular emphasis is placed on those system aspects which are more likely to affect the capacity in a significant way.

Thus, this study is more concerned with an interpretation of the available data rather than with a presentation of such data for its own sake. In other words, this document is not a compilation or statistical reduction of experimentally collected data, although the availability of such data is vital to the success of this work. Therefore, the reader will find here only a few tabulations and graphical representations of experimentally obtained numerical information attempting to describe the statistical aspects of the operation of the present North Atlantic Air Traffic Control System. For a more complete presentation of such data, the reader is referred to an excellent work by C. E. Dunmire[10] and other sources [15, 17]

In order to determine what improvements are needed (or, indeed, if they are needed at all) in any single area such as navigation, it is first necessary to develop a clear understanding of the interrelation hips among different areas of the system. It then becomes possible to determine how changes in one area affect the system, and whether such changes must be accompanied by additional modifications in other system areas.

Rather than to proceed with an assumption that improvements in navi-

gation (or any other specified area) are needed, a systematic approach requires that we first ask what determines the traffic capacity of the North Atlantic system and how this capacity relates to navigation techniques, communications coverage, separation standards, and air traffic control procedures. We organize the course of our analysis to correspond with the natural sequence in which the individual broad system areas depend on each other. Thus, we begin with the description of the system environment, including aircraft operational characteristics, traffic distribution, communications coverage, navigational techniques, weather forecast limitations, and so forth. Next, we consider operational procedures. Together, these two areas constitute the basic points of departure in the analysis. We find that they completely determine the choice of separation standards when safety considerations are taken into account. The study of separation standards then naturally leads to an evaluation of capacity and economic penalties associated with various system modifications.

To facilitate the use of this report, the detailed description of each individual study phase, including a complete mathematical analysis, has been placed in a separate Appendix. Thus, each of the seven Appendices can be regarded as a self-contained paper dealing with the appropriate part of the analysis. However, the Appendices do not consider the effects of interaction among various system areas. These problems, as well as a complete discussion and interpretation of the consequences of the analysis, are treated in the main part of the report. Here, the entire system analysis and its results are discussed in the same natural order described above.

Section II is a brief summary of the most important results and conclusions of this study with recommendations for further work.

Section III contains a description of the present North Atlantic Air Traffic Control System, emphasizing those system aspects which are most important to the analysis. The description includes both the equipment environment and the operational procedures.

Section IV discusses the fundamental organization of the analysis of the system. It describes an outline of the course of the study and stresses the interdependence of the various system areas.

Section V treats the problem of separation standards, and discusses their dependence on the significant features of system environment and control procedures. Emphasis is placed on the correct interpretation and operational use of separation standards. The longitudinal, lateral and vertical separation standards have different characteristics and are treated separately. Also included is a discussion of the relationships between separation standards and collision probabilities. This Section draws heavily on the results of Appendices B, C, D, and E.

Section VI describes the results of the analysis of system capacity. It formulates a realistic definition of capacity and, using the results of Appendix F, obtains useful relationships between capacity and the basic variables describing the environment and control procedures.

Section VII is concerned with the economic penalties associated with diversions of aircraft from preferred routes and altitudes. The penalties are expressed in terms of increased flight time and fuel consumption. This Section discusses the significance of the minimum time path and, using the results of Appendix G, evaluates the economic penalties associated with departures from it.

Section VIII discusses potential improvements in the system. In particular, it compares several proposed system modifications in terms of the associated economic penalties and effects on capacity.

Section IX is concerned with applications of the results of this study to other environments. Included here are considerations of propeller aircraft, supersonic aircraft, and operations in geographical regions other than the North Atlantic.

The following is a brief outline of the contents of the Appendices:

Appendix A is a self-consistent derivation of a mathematical model of the statistical wind behavior.

Appendix B uses the results of Appendix A to evaluate analytically the effects of winds on longitudinal separations.

Appendix C describes a Monte Carlo evaluation of longitudinal separations used to validate the conclusions of Appendix B and to obtain further insight into the relationships between longitudinal separations and other system variables.

Appendix D contains a detailed study of fix errors for various navigational techniques.

Appendix E performs an analysis of lateral track-keeping errors.

Appendix F evaluates the system capacity using realistic models of traffic distribution.

Appendix G is an approximate analysis of economic penalties associated with lateral departures from the minimum time path.

It should be noted here that the present urgent need to increase the traffic capacity of the system refers mainly to subsonic jet flight levels. Moreover, it is known that no other aircraft, propeller or supersonic, is likely ever to use these altitudes. For these reasons, this report is basically concerned with the operation of subsonic jet aircraft. However, frequent comments referring to propeller and supersonic aircraft are made throughout the report, wherever appropriate. In addition, a summary of such comments and partial results is presented in Section IX.

Emphasis is placed in this report on east-west traffic in the Gander and Shannon-Prestwick oceanic regions, where problems of traffic congestion are most acute. The application of analytic techniques to other regions is also indicated in Section IX.

II. SUMMARY

The purpose of this summary is to present in a brief and condensed form the significant results and main conclusions of the study. For a detailed discussion and interpretation of the analysis, the reader is referred to other parts of this report.

1. Objectives of the Study

The basic objective of this study is to investigate and evaluate various methods by which the capacity of the present North Atlantic Air Traffic System can be increased. All system modifications are considered with this objective in mind. Special emphasis is placed on those system aspects which are more likely to influence the capacity in a significant way. In the comparison of various modifications, due consideration is given to realistic constraints such as safety and economic factors.

2. Methods to Increase System Capacity

There are two fundamental methods to increase the capacity of the North Atlantic Air Traffic System:

a. Modifications of the environment.

b. Modifications of procedures.

Because of economic constraints, it is often easier to modify procedures than to change environment. Changes in environment are usually very costly and time consuming. Since the present subsonic jet traffic load is pressing the North Atlantic system nearly to its saturation point, immediate measures must be taken to increase capacity. Also, since the present procedures do not make optimum use of the North Atlantic environment, we first ask what can be achieved through changes of procedures alone.

3. Modifications in Procedures

An air traffic control system can be classified according to its basic control doctrine. Thus, a system which controls traffic by making short term predictions into the future can be described as TACTICAL. On the other hand, a STRATEGIC system predicts the future course of each flight all the way to its destination. Similarly, a system classification can be made on the basis of the degree of control exercised over the route pattern, with extremes described as FREE and ORGANIZED. Detailed discussion of such classification is included in Section III.

The present North Atlantic Air Traffic System lies between these extremes but can be described as tending toward STRATEGIC-FREE. This combination of procedures does not make optimum use of the existing environment. Therefore, a judicious change of procedures can increase the capacity of the system. In fact, the capacity of the present system can be more than doubled through modifications of operational procedures alone. No significant economic penalty is associated with these modifications.

A shift from FREE toward ORGANIZED systems would be quite compatible with present traffic characteristics. It should be understood that an ORGANIZED system does not necessarily imply a fixed route structure. A system in which the routes are determined by a common wind forecast each day offers most of the advantages of fixed routes. Unlike a fixed route structure, however, such a system does not impose significant economic penalties.

An example of an ORGANIZED system is the jet reference scheme described in Section VIII. If adopted, this system would allow a universal application of the 20 minute longitudinal standard and a capacity increase for subsonic jet traffic exceeding 100 percent. An even greater reduction in the longitudinal separation standard and a greater increase in the capacity of this system might be realized if unified weather forecasting were adopted. For comparison, the infrequent use of the conditional 20 minute longitudinal

separation standard permitted in the present system will yield less than a 3 percent capacity increase.

As mentioned above, an organized route structure will not impose a noticeable economic penalty. The reason for this is twofold. First, the economic penalty for the lateral deviations of the order of one degree latitude from an actual minimum time path is negligible. Second, the low accuracy of wind forecasts, as evidenced by the large spread of preferred routes requested by various carriers for the same day, renders the average penalty associated with a deviation from a preferred route even less significant. Naturally, the air routes in an ORGANIZED system (except fixed-route systems) would be clustered around the actual minimum time path computed for the day. The lateral spread of one-way routes in a system such as the jet reference scheme would be of the order of four degrees latitude.

While studying various system modifications, one may consider a transition toward a TACTICAL control doctrine. This transition requires rapid and highly reliable air-to-ground and ground-to-air communications. Since communications in the North Atlantic are not likely to satisfy these requirements in the near future, a change to a TACTICAL system cannot be recommended. It may also be noted that a TACTICAL approach is not compatible with the prevailing traffic patterns. Moreover, such an approach would not be suitable for the control of supersonic aircraft in the future.

4. Modifications in Environment

Introduction of improved navigation equipment would be motivated by the desire to reduce the lateral separation rule. There are two approaches toward improvements which will permit such a reduction. The first approach is to introduce new equipment or to extend the coverage and accuracy of in-service equipment so that accurate position fixes can be made throughout the oceanic region. The second approach is to improve the accuracy of dead

reckoning to a point where each aircraft can follow closely its assigned route through regions where accurate fix coverage is not provided.

If a system providing complete oceanic coverage of position measurement with errors in the range 2-3 n. mi. were made available, either present dead reckoning techniques would have to be improved, or position determinations would have to be made at frequent intervals (every 100 miles or so) in order to take advantage of the improved fix. The use of Doppler-DR computer would relax the requirement for frequent fix determination somewhat, but the dead reckoning errors associated with Doppler-DR equipment presently in service dominate the assumed 2-3 mi. fix error if the interval between resets is, say, 600 mi.

Alternatively, if improved Doppler-DR or some other accurate dead reckoning system were introduced, it might be possible to refine air-borne equipment and procedures sufficiently to take advantage of the inherent capability offered by Loran A in regions covered by ground wave.

A reduced lateral separation rule does not, however, guarantee a substantial increase in traffic handling capacity. Halving the lateral separation rule, for example, only provides a capacity increase of about 40% (for subsonic jet aircraft) under existing control procedures. The advantage of a reduced lateral separation rule can only be fully realized if an organized route structure is adopted.

Neither improvements in fix accuracy nor improvements in dead reckoning justify any reduction in the vertical separation rule. Significant gains could be achieved through the introduction of equipment which would permit an increase in the number of available flight levels, since the result is a greater than proportional increase in capacity. To take advantage of this increase, however, the controller must have freedom to reassign flight levels during peak periods, and he must have adequate coordination with adjacent domestic control centers to permit vertical rearrangement of the traffic prior to its entry into the oceanic region.

Longitudinal separation errors depend on air speed errors and on wind effects. Because of the relationship between errors in ETA differences and lateral wind gradient, the longitudinal separation rule for aircraft following the same flight path depends partly on the magnitude of lateral deviations from flight plan. Thus, in an organized system, accurate navigation may permit reduction of the longitudinal separation rule. A free system, however, requires an improved wind forecast. For either type of system, more accurate air speed indication will allow a small reduction of the longitudinal rule. In an organized system, adoption of a unified forecast should permit a reduction of the longitudinal rule. Halving the longitudinal rule nearly doubles capacity when the range of air speed is small (as is the case for subsonic jets).

Improvements in communications will not increase system capacity unless procedures are also modified. The required modifications would be directed toward a more tactical doctrine of control. As already stated, major improvements in communications are necessary. Even then, the gain in capacity would be marginal.

5. Recommendations for Further Study

In the course of this study, the need for further analytical and experimental investigation in various system areas has become apparent. This Section should not be interpreted as a list of recommendations for further work by ARCON. Indeed, some of the investigations in the following list have already been initiated or planned by other organizations. The intent of this Section is to point out those areas of investigation in which further progress should contribute to the solution of problems which at this time are not completely resolved.

a. Altitude errors

A comprehensive evaluation of vertical track-keeping errors is

needed, including a study of altimeter errors and the dynamic characteristics of the vertical autopilot control loop.

b. Air speed errors

A study of air speed errors should be made, including an evaluation of air speed measuring instruments and the effects of temperature forecast errors.

c. ETA errors

Data on ETA errors is required to determine correlations of errors for leading and following aircraft. Distinctions should be made according to whether aircraft follow identical or converging flight plan tracks and according to whether ETA's are based on the same or different weather forecasts.

d. Blunders*

A better understanding of the statistics of blunders is needed in order to obtain realistic estimates of collision probabilities. An experimental program, supported by a statistical analysis is recommended for this purpose. Particularly important is the evaluation of blunders associated with the use of new navaids such as Doppler. Data on actual operational performance is required rather than the results of controlled experiments.

e. Departures from minimum time path

An initial analysis of the economic penalties associated with lateral departures from the minimum time path has been performed. [cf. Appendix G]. A realistic validation of its results should be undertaken. Of particular importance here are the effects of wind forecast errors.

f. Inter-system coordination

Important improvements in system capacity can be realized by advance preparations for traffic entering the oceanic area from domestic regions. Coordination of oceanic and domestic control is essential for this purpose, and a study of the requirements for such coordination is recommended.

---

*Some authors have used the term "blunder" to designate human errors only. In this report, the term represents all large errors, regardless of cause.

g. Weather forecasting

The feasibility of employing a unified weather forecasting service for North Atlantic operations should be investigated. The possibility of using pilot reports on found winds, derived from Doppler measurements, to improve wind forecasts also merits consideration.

h. Organized route structures

The feasibility of adopting organized procedures (jet reference schemes) should be investigated.

III. DESCRIPTION OF THE PRESENT SYSTEM

We shall discuss briefly some of the more salient features of the present North Atlantic Air Traffic System. The system description is not complete and is intended only to provide background information essential to an understanding of this report. The interested reader will find a more detailed discussion in Reference 10.

1. Environment

The most critical ATC problems in the present system are related to the control of subsonic jet aircraft, which are expected to dominate North Atlantic operations for several years. Consequently, this discussion will emphasize the traffic problems associated with such aircraft and their relevant operational characteristics. A similar emphasis will be found in the remainder of this report, although applications involving other types of aircraft are considered in Section IV. Separate analyses of the problems associated with different classes of traffic are feasible because of a natural vertical separation of the different types of aircraft operating over the North Atlantic. Thus, subsonic jet operations are limited to altitudes between 28,000 ft. and 41,000 ft., while propeller aircraft are confined to much lower altitudes. Future supersonic jets will fly well above the flight levels of subsonic aircraft.

The total flight time for a transatlantic, subsonic jet flight is ordinarily about 6–9 hours. Approximately 3 hours are spent crossing the oceanic region between 10° W and 50° W, and the remaining time is spent over domestic regions or in oceanic areas near the coast lines. The oceanic portion of transatlantic flights will be emphasized in this report. Domestic regions will be considered primarily with respect to transitional problems associated with traffic entering or departing from the oceanic region.

The majority of civil flights cross the North Atlantic in an east-westerly direction through a region bounded by the 45°N and 60°N lines of latitude. This region, which is illustrated in Figure III-1, is encompassed almost entirely by two oceanic control areas (OCA's) having a common boundary at 30° W. The control of the western OCA is centered at Gander, Newfoundland, and control of the eastern OCA is shared by centers at Prestwick, Scotland, and Shannon, Ireland. Occasionally, the mid-Atlantic portions of civil flights pass through other OCA's or flight information regions (FIR's), but most of the traffic is contained within the Gander-Shanwick complex.*

The vast air space available over the region shown in Figure III-1 suggests that a virtually unlimited number of aircraft should be able to cross the North Atlantic in a 24 hour day. The actual number of aircraft which can be accommodated under the present system is limited, however, not only by the large separations required between aircraft, as described in the next Section, but also by the effects of scheduling, aircraft performance characteristics, and weather.

Because of time-zone differences, passenger preferences, and noise control measures in terminal areas, most eastbound jet flights depart from North American terminals in the early evening and arrive in Europe in the early morning (local times). Most westbound jet flights depart from European terminals in the afternoon with arrivals in North America scheduled for the late afternoon or early evening (local times). Because of these scheduling practices, most jet traffic passes through the oceanic region during certain peak periods, as illustrated in Figures III-2 and III-3.** These

---

*ICAO has recently decided to modify the boundaries shown in Figure III-1. An even greater majority of traffic will pass through the Gander and Shannon-Prestwick OCA's.

**Cf. Reference 10, pp. 30-31.

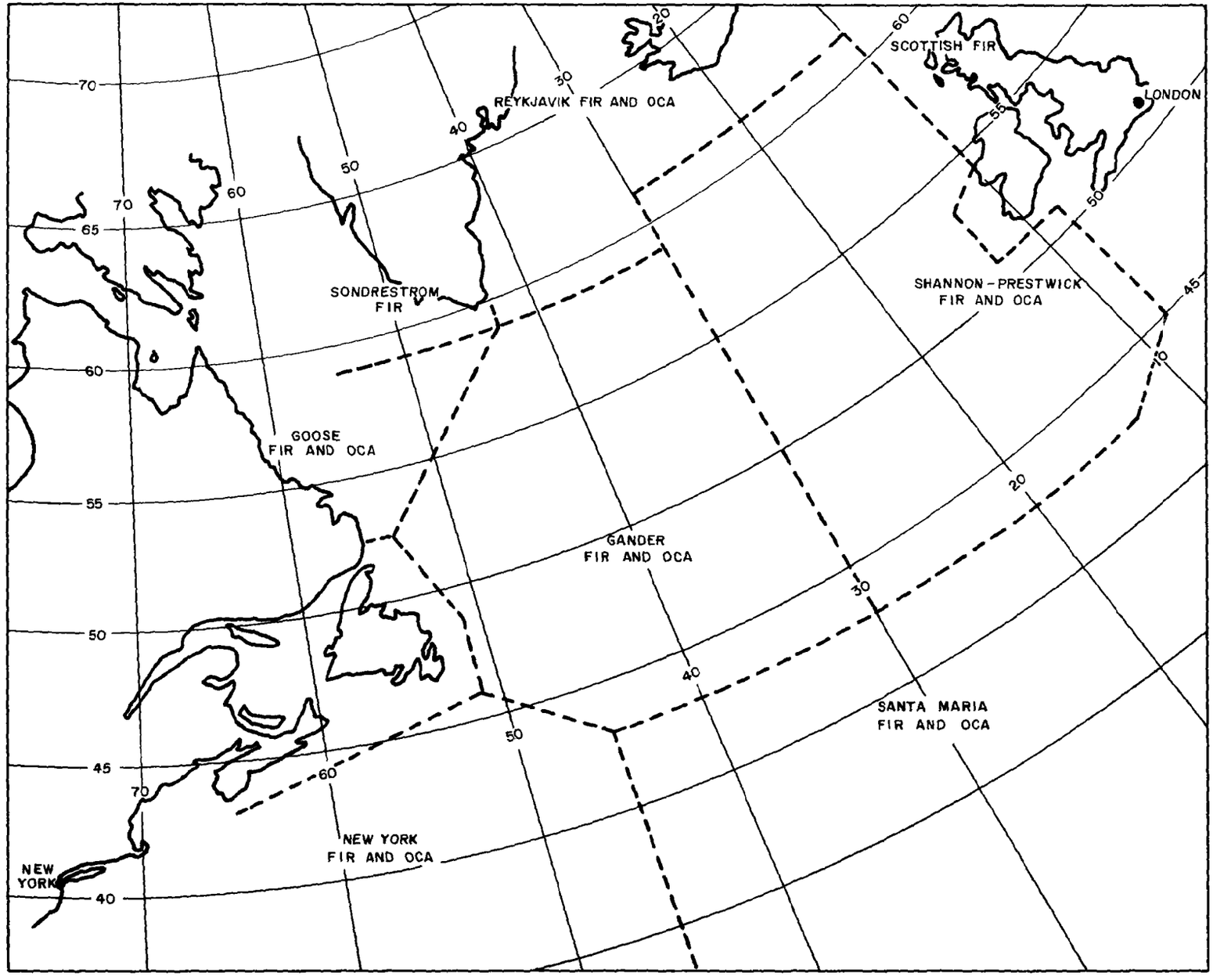

FIG. III-1 NORTH ATLANTIC FIR AND OCA BOUNDARIES

Figures have been prepared from data provided by Prestwick Control Center on the times at which aircraft cross the 30° W meridian. Although the data was recorded during the summer months of 1961 and is not necessarily characteristic of other seasons, Figures III-2 and III-3 do illustrate a non-uniform hourly distribution of traffic which is prevalent throughout the year.

Fortunately, traffic congestion is relieved by a separation of eastbound and westbound traffic peaks, although interference does occur in the Shannon-Prestwick OCA between the tail of the eastbound peak and the leading part of the westbound peak. The analogous problem in the Gander OCA is less serious because of the longer gap following the westbound peak.

Traffic over the North Atlantic is not only compressed in time but also in altitude. Only a narrow band between 28,000 ft. and 41,000 ft. is available to subsonic jet aircraft. Most airlines consider the use of the lower levels within this band as uneconomical. The upper levels are not attainable by jets during the early part of a flight. Because of ATC procedures described in Section 3, most jets cross the North Atlantic at a constant altitude. The result is that the highest attainable altitudes are used only by those aircraft which are air-borne for a relatively long period before entering the oceanic region. Thus, most aircraft compete for the mid-levels within the available altitude band.

Traffic is also compressed in the lateral dimension. Most air lines prefer flight plans based on minimal time paths (MTP's), which are determined each day from the weather forecast. Since each air line has its own facility for computing MTP's, there is some lateral scattering of the flight plans. Other factors contributing to this scatter are the difference between wind forecasts available at the various terminals and the geographic spread of points of origin and destination. In general, the latter factor broadens the pattern of flight paths to a greater extent on the eastern half of the North Atlantic than on the western half. Although the flight plan paths preferred

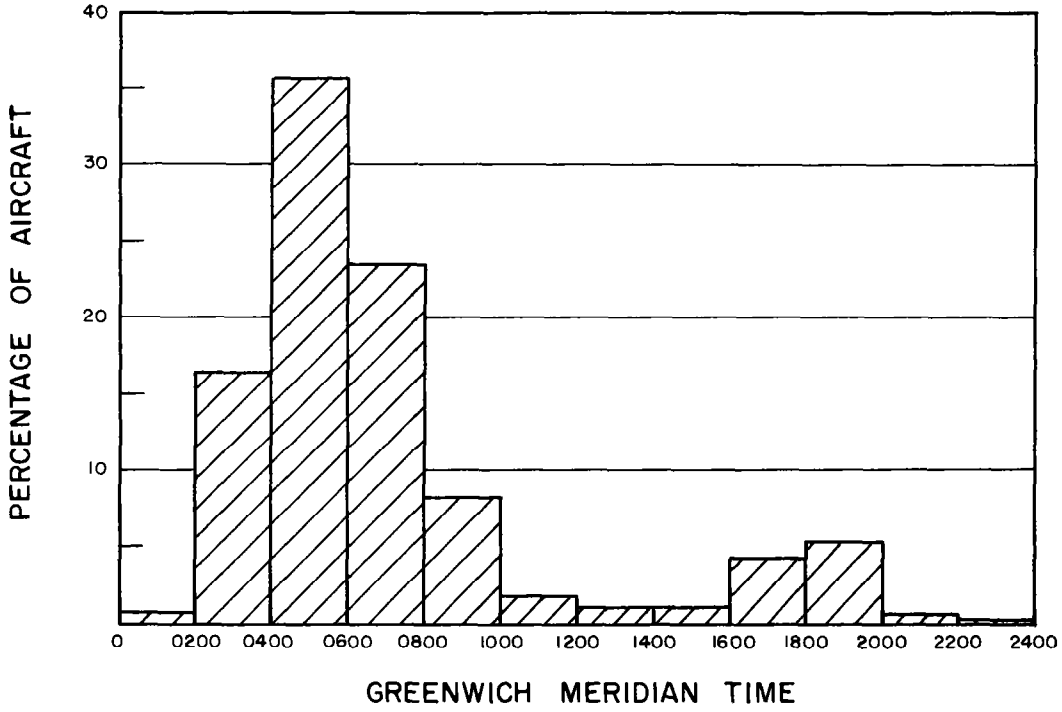

FIG. III-2 TIME DISTRIBUTION OF EASTBOUND CIVIL JETS CROSSING THE 30° MERIDIAN

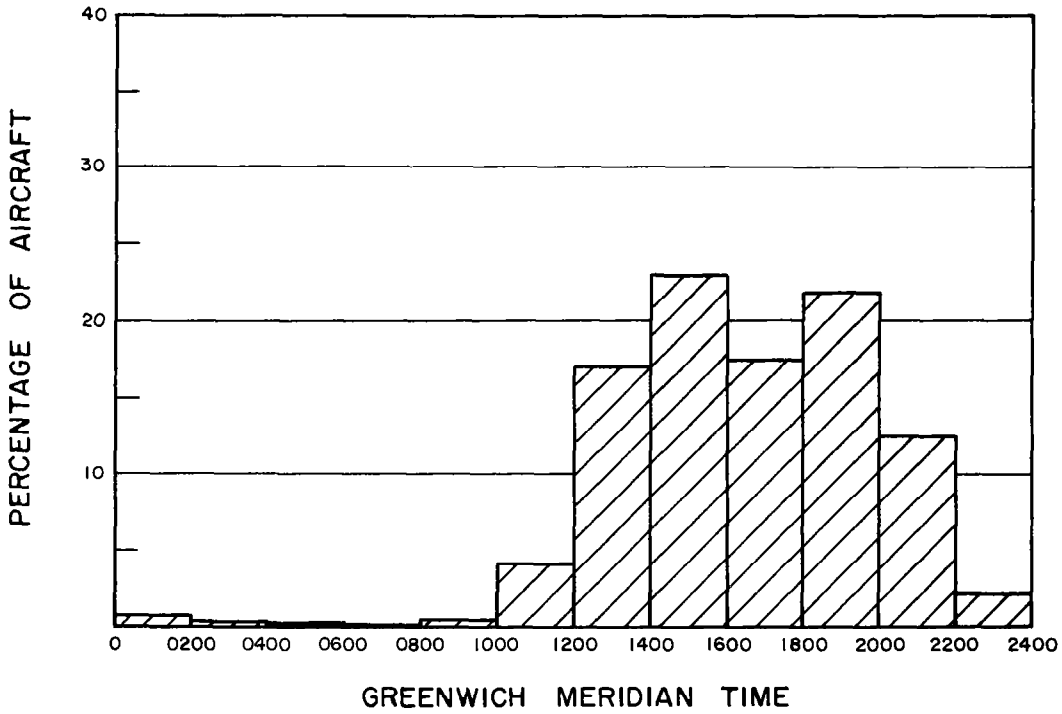

FIG. III-3 TIME DISTRIBUTION OF WESTBOUND CIVIL JETS CROSSING THE 30° MERIDIAN

by two carriers are frequently different, they are seldom so diverse as to provide lateral separation adequate to satisfy separation standards across the entire oceanic region. Thus the flight plans preferred by the air lines on any given day form a rather irregular pattern concentrated within a narrow lateral band. The location of this band varies from day to day with the weather.

Although traffic is constricted in three dimensions, as just described, there would be no serious problems in accommodating existing traffic loads if large separations were not required between aircraft over the North Atlantic. The separation standards described in the next Section are conservative because of difficulties in predicting and monitoring the progress of aircraft across the oceanic region. It is, therefore, important to consider those features of the North Atlantic environment which contribute to these difficulties.

Two important features of the environment are wind and temperature variability. The effects of wind variability are especially significant and are analyzed in great detail in this report. The variation of wind with time introduces errors in the predicted progress of aircraft across the North Atlantic, but the variation of wind with distance causes more significant errors in the relative positions of aircraft flying on different tracks. Temperature variability has a similar, though less critical, effect. Since most subsonic jet aircraft fly at a constant Mach number, air speed is a function of temperature. Thus, temperature variations introduce uncertainties in relative air speeds.

Certain features of both air-borne and ground-based support equipment are also critical. This equipment may be classified under the broad categories of communications and navigation.

A general view of the communications picture in the North Atlantic is that ground-to-ground (G-G) communications are good but that air-to-ground

(A-G) and ground-to-air (G-A) communications have serious failings. A new cable link provides direct voice communications between all oceanic control centers contiguous to the Gander and Shannon-Prestwick areas, except Santa Maria. When direct voice communications are not available between oceanic centers or between oceanic and domestic centers, radio teletype is used. The delays inherent in this form of communication do not impose serious limitations, so long as adequate data handling procedures are used.

Aircraft operating near the domestic boundaries of the North Atlantic can be contacted on VHF radio which is rapid and reliable. Beyond the line of sight VHF limits, HF radio telephony is the only direct link between ground and air. The ground HF stations are connected to the control center by teletype. As a result, some delays are encountered. Occasionally, HF propagation disturbances make it difficult or impossible to contact aircraft in the region. Total blackouts occur rarely, perhaps a few times each year. When they do occur, they persist for periods comparable to or longer than the time required for jet transit of the North Atlantic. Under these circumstances, some contact is maintained via VHF relay from one aircraft to the next. A report from an aircraft then frequently fails to reach the controller or arrives long overdue. HF communication cover is usually good over large portions of the North Atlantic, and usually the HF channels are not congested. Even when conditions are favorable, however, a few aircraft cannot be contacted and some reports are seriously delayed. The origin of these delays and missed reports during normal propagation is difficult to determine.

Even if communications were perfect, the controller would have imperfect information on the positions of aircraft in the region for which he is responsible. Indeed, each flight crew has only a limited knowledge of the progress of its own aircraft along the flight plan. This limitation arises primarily because of imperfections in navigation. When crossing the North Atlantic, the navigator never knows precisely where he is. When a position

fix is completed, he is able to determine only his approximate position at a time in the recent past. His present and future positions are estimated by means of dead reckoning procedures.

Most fixes in the North Atlantic are currently determined with the aid of Loran equipment, sextant observations of celestial bodies, Consol or Consolan, or advisory service from ocean station vessels.* Other means such as Vortac, Decca, and radio direction finding are restricted to coastal regions. An analysis of fix accuracy is given in Appendix D. The standard deviation of the vector error in fixes taken over the mid-Atlantic is estimated to lie in the range of 5–15 nautical miles. This estimate may not be appropriate for certain types of fix taken in regions nearer the coast lines; for example, 2-line Loran fixes, for which the methods of analysis in Appendix D are inapplicable. Not all air lines carry the same equipment and the accuracy and availability of a specific type of fix varies for each aircraft with location and time.

The principal devices presently used in navigation for purposes other than position-fix determinations are the Machmeter or air speed indicator, compass, pressure altimeter, radar altimeter, and, in some instances, Doppler radar. Errors in the measured air speed are not known precisely but are estimated by the air lines to be of the order of 2 or 3 knots and are probably less significant than fluctuations in air speed caused by temperature variations. Precise data is not available at present on compass instrument errors or on uncertainty in magnetic variation, although studies are currently in progress to determine their effects on heading accuracy. Present indications are that heading errors may vary from about 0.5° to 4°,

*For the purposes of this study, a fix is defined as a position determination which is independent of the navigator's previous estimates of position. Accordingly, pressure altimetry, which provides a line of position drawn from the last fix, is considered as a dead reckoning technique rather than as a method of fix determination.

but that most errors lie in the range of 1–2 degrees. Special efforts by some carriers to minimize the sources of error may result in average heading errors below this range.

The pressure altimeter and Doppler radar are useful in dead reckoning between fixes and provide a means for determining the drift angle of the aircraft with respect to the flight path. Dead reckoning procedures are discussed in Section 3. Errors in dead reckoning are difficult to assess and are treated in Appendix E.

2. Separation Standards

The key to the ATC procedures discussed in the next Section is the requirement that each aircraft follow a flight plan separated from all other flight plans according to at least one of three separation standards:

Vertical – 1000 ft. below flight level 290
2000 ft. above flight level 290

Lateral – 120 nautical miles (in practice, 2 degrees of latitude for flights which are approximately parallel to latitude circles).

Longitudinal – 30 minutes for leading and following aircraft. (ICAO has recently approved a 20-minute separation for aircraft with identical or diverging flight plan tracks. The 30-minute rule applies otherwise.)

The longitudinal separation requirement is augmented by the controller if the indicated air speed of a following aircraft exceeds that of a leading aircraft. At Shannon-Prestwick, a 60 n. m. lateral separation at the entry points into the OCA is accepted for westbound aircraft, providing they are on diverging tracks. There is no occasion to make the corresponding exception at Gander, since all entry points are separated by at least 120 n. mi.

3. Procedures

The following description is based, in part, upon information received at the Prestwick Control Center. It may be assumed, however, that the same procedures are used at Gander, with certain exceptions which will be specified.

All aircraft operating in oceanic areas are required to file a flight plan prior to departure. Flight plans are forwarded by the carriers to an International Flight Service Station and relayed to the OCA's and FIR's through which the flights will pass. Each flight plan for a jet aircraft must specify the latitude, expressed as an integral number of degrees, at which each of the 10° meridian lines (10° W, 20° W, etc.) will be crossed. The same information is required in the flight plans for propeller aircraft at each of the 5° meridian lines (10° W, 15° W, etc.). Because pilots are required to report certain information when they arrive at these meridian lines during flight, the points of crossing are called "reporting points". The estimated time elapsed and the predicted air speed between each pair of reporting points are also specified in the flight plan. For jet flights along an essentially north-south direction, reporting points are chosen at parallels of latitude spaced at 5° intervals.

The flight level must also be stated in the filed flight plan. Levels 290, 330, 370, and 410 are reserved for eastbound jet flights and 280, 310, 350, and 390 for westbound jet flights. Fortunately, the controllers are usually able to increase the number of flight levels available to traffic in each direction because of a natural separation between eastbound and westbound flights. This separation permits a "datum line" to be established each day by agreement between Shannon-Prestwick and Gander. The datum line is specified by the latitude at which it intersects 40W, 30W and 20W, and is determined from weather forecasts so that it lies south of most westbound MTP's and north of most eastbound MTP's. During the peak westbound period, some

of the eastbound flight levels can be assigned to westbound aircraft provided they remain at least one degree north of the datum line. Gander, during this period, will assign these same levels to eastbound aircraft only if they remain at least one degree south of the datum line. Similar arrangements permit greater flexibility in flight level assignments for eastbound traffic during the eastbound peak. The datum line technique relies upon two features of the traffic pattern, the time separation between eastbound and westbound peaks, and the tendency for westbound MTP's to lie north of eastbound MTP's. Occasionally, weather conditions are such that the second condition is not met and, on these days, no datum line is established. Since westbound jet aircraft can rarely reach level 390 upon entry and since level 280 is generally considered undesirable, the opportunity to use levels 330 and 370 nearly doubles the number of preferred flight levels available to westbound traffic. A similar comment may be made for eastbound flights, although a somewhat greater number of requests may be made for level 290 by eastbound flights than for level 280 by westbound flights.

The controller will clear a flight plan only at a fixed flight level, although the pilot may later request a change in altitude when he is enroute over the oceanic region. Because of the infrequency with which such requests are granted, most carriers plan fixed-altitude rather than step-climb flights. An exception is made for SAC which is permitted to file step-climb flight plans for flights between Canada and England provided that they are restricted to one of two fixed routes separated laterally from one another by two degrees throughout the Gander and Shannon-Prestwick OCA's. The exception is also made on a third SAC fixed route from New York to Lisbon, which passes through the southern part of the Shannon-Prestwick OCA at a considerable distance from the main east-west traffic stream.

When an aircraft departs from a terminal area, a message specifying the actual time of departure is forwarded to each of the flight plan

addressees. The controller is then able to determine an estimated time of arrival (ETA) at each of the reporting points specified in the flight plan. When an aircraft approaches the boundary of an OCA, the pilot transmits a request for clearance. Because of delays in G-G communications, this request will occasionally arrive ahead of the flight plan message. Such incidents have a disturbing effect on traffic planning.

The "clearance controller" honors the request for clearance, provided that the filed flight plan does not conflict with other flight plans already cleared. Otherwise, the controller must determine flight plan revisions adequate to resolve all potential conflicts. The pilot is then informed of the alternate flight plan(s) available to him. When there is a choice, the final cleared flight plan is determined by pilot preference. Pilots tend to prefer changes in altitude to lateral revisions of the filed flight plan, up to a point.

The clearance controllers at Shannon-Prestwick carry out their check for conflicts in westbound flight plans beyond the 30° W boundary of their OCA. A clearance to enter the Shannon-Prestwick OCA is given only when the flight plan is free of conflicts up to and including the 40° W reporting line. During periods of poor HF propagation, clearance is issued only if westbound flight paths are free of conflicts through 50° W. The same modification applies when HF propagation forecasts indicate a deterioration in communications within the next few hours. Similarly, the Gander controller separates eastbound aircraft through to 20° W. The need for separation of eastbound flights through to 10° W by Gander rarely arises, because of the diversity in HF ground stations serving Shannon-Prestwick and because of the greater proximity of 20° W to Shannon VHF limits than of 40° W to the Gander VHF zone of coverage.

After an aircraft has entered an OCA, it is the task of the "enroute controller" to maintain the required minimal separation provided by the initial clearance. Reroutings are sometimes required to resolve conflicts

which may develop when one or more aircraft fail to conform to their cleared flight plans. Conflicts usually occur because of a deterioration in longitudinal separation and may be resolved by one of three methods. The method most commonly used in the past is a change in flight level for one of the conflicting aircraft. Under a recent ICAO ruling, a transition under visual flight rules (VFR) from one flight level to another through an intermediate occupied flight level will not be permitted. If changes in flight level are unacceptable, the controller may alter the routes of one or both aircraft, thus providing lateral separation. The third method for resolving a conflict is to hold the following aircraft in order to provide longitudinal separation. Application of the holding procedure occurs very rarely.

The enroute controller must depend upon pilot position reports in order to check for the development of conflicts. For east-west flights, the pilot is required to report when each 10° meridian line is crossed. The report must specify the aircraft position and actual time of arrival (ATA), as well as the ETA at the next reporting point. This information is based upon the navigator's most recent fix. The ETA is usually computed by adding the flight plan interval for the next leg to the time of the position report. The flight plan intervals are computed prior to take-off on the basis of forecast winds and temperatures (for converting Mach number to air speed). Differences in weather forecasts provided at various airports often lead to inconsistent ETA's for aircraft following the same path and present the controller with fictitious conflicts or conceal actual ones.

The position report also includes the flight level or altitude, information on weather (especially found winds and temperature), flight conditions, and remaining fuel. By a recent ICAO ruling, a change in the flight plan air speed of more than 10 knots must be reported. Formerly, reports were required only on changes exceeding 20 knots. Because of communications difficulties, the controller occasionally fails to receive a report from a

particular aircraft. In such cases, he must assume that the aircraft adheres to the flight plan (updated by the most recent position report available).

The majority of A-G messages are routine position reports. Other pilot-initiated messages, such as requests for revised clearances, are less common. Controller-initiated messages include requests for supplementary position information or instructions required for conflict resolution and are relatively infrequent.

It is the task of the controller to check against conflicts which arise because of deteriorations in longitudinal separation. The pilot does not attempt to correct longitudinal deviations from his flight plan. On the other hand, it is the responsibility of the pilot and navigator to maintain the flight plan track laterally and vertically. The controller does not act on reported small lateral deviations from flight plans, although he issues warnings to the appropriate aircraft if a situation is potentially dangerous.

By an ICAO ruling, if a navigator finds that he is off the flight plan track by any distance, the aircraft heading must be altered so that the desired track will be regained at a point not more than 200 nautical miles ahead. Although this procedure helps to prevent large lateral deviations from the flight plan, an aircraft is seldom actually on track. Errors in the navigator's fix and in the dead reckoning procedure between fixes are responsible.

The accuracy of dead reckoning is limited by the compass error, uncertainty in magnetic variation, and the error in the drift angle. The correct heading depends both upon the current aircraft position and the cross-track component of the wind ahead. The wind ahead may be estimated from the forecast or from the winds encountered previously during the flight. The drift angle is sometimes estimated between fixes by means of pressure altimetry, which can also be used to determine a line of position (L.O.P.) drawn from the last fix.

Doppler navigation may also be used to determine the drift angle. In this connection, it should be noted that Doppler radar does not provide position fixes since it measures ground velocity* only and is essentially a dead reckoning device. A computer can be employed together with a Doppler radar to calculate the distance and direction of the aircraft from an initial position and thereby provide an estimate of current position. This procedure differs from other dead reckoning techniques only in that the computer integrates the instantaneous velocity measured continuously by the Doppler radar, whereas in the case of other techniques an estimated average velocity is multiplied by the time elapsed. In the former case, the error in the estimate of current position is the integrated error** in the instantaneous velocity measurements; in the latter case, the error** is the product of the time elapsed and the error in the estimated average velocity.

In either case, the cumulative dead reckoning error can be determined and corrected only if a fix is taken. The accuracy with which the cumulative error is corrected depends upon the navigational aids and the procedures used. After a fix has been taken, a new heading is required to correct any lateral deviation from the flight plan and, if Doppler equipment is used, the computer must be reset to correct the cumulative error in estimated current position.

4. Classification of Procedures

In classifying air traffic control systems, it is useful to consider two extremes in the possible types of control doctrine, which may be termed "strategic" and "tactical".*** In a region where a purely "strategic" doctrine is employed, each aircraft is assigned a flight plan for which separation from

---

*Velocity is, of course, a vector quantity with components both along and across the flight path.

**Similarly, this error is a vector quantity.

***This terminology has previously been proposed by P. G. Reich.[12]

all other aircraft during the entire flight through the region is provided by pre-entry planning. After entry of the aircraft into the strategic region, modifications of the flight plan are not required and communications are unnecessary for traffic control purposes.

In a region where a purely "tactical" doctrine is employed, no long-range pre-entry planning is required. Instead, the traffic situation is continually scrutinized throughout the entire tactical region for potential conflicts that may occur in the relatively near future. Such conflicts are dealt with as they appear. Communications are clearly an essential element of a tactical control system.

In practice, of course, all control doctrines lie somewhere between the two extremes. However, the control doctrine applied at present in the North Atlantic lies much closer to the strategic than the tactical extreme. In the present system, the controllers endeavor to avoid conflicts by advance checking of flight plans over an extensive oceanic region. Because of errors in navigation, tactical procedures are occasionally employed to resolve conflicts which arise between enroute aircraft; however, only limited reliance is placed on such procedures because of the unreliability of A-G communications.

It will also be useful to consider two extremes in the possible types of route structures, which will be called "free" and "organized." In a "free" system, an operator may request any flight plan track it pleases, and the controller must honor the request unless it is found to conflict with flight plans already cleared. In an "organized" system, each aircraft is limited in choice of flight plan track to a relatively small number of pre-determined routes. The routes may be rigidly fixed or may vary from day to day according to weather, traffic characteristics, or other criteria.

The system of routes employed at present is basically "free", since the requested flight plan tracks are limited only by the requirement that the

10° meridian lines be crossed at integral degrees of latitude. Thus, in the present North Atlantic system, a primarily strategic control doctrine is imposed upon an essentially free route structure. The superposition of these two basic philosophies, underlying the procedures in the present system, has not been entirely successful. Indeed, the requirement for advance, long-range conflict checking results in frequent rejections of requested flight plans, and the rather arbitrary patterns formed by the resulting flight plan tracks impose difficulties upon the controller attempting to fit arriving aircraft into the system.

IV. ORGANIZATION OF THE ANALYSIS

Before proceeding with the detailed analysis of the air traffic system, it is first necessary to establish a sound approach and to formulate a plan of attack. The system under consideration is so large and complex, and the objectives of the analysis so involved, that a direct attempt to obtain useful solutions, without a firm reference for the adopted point of view and without due regard for the subtle relationships among various system elements, is just not possible. To be sure, such a detailed philosophy cannot always be completely established before a substantial part of the analysis has been performed. Frequently, as in our case, only the main outline of the basic approach is initially understood, while the details are added in the course of the study. The framework of the analysis unfolds itself gradually, focusing attention on the important aspects of the system, isolating key variables, and indicating significant relationships among them.

An obvious way to simplify the analysis is to try to subdivide the main problem into its component parts. Thus the North Atlantic Air Traffic System can be regarded as a complex aggregate of several component subsystems. One can list three basic subsystems:

1. Navigational techniques.
2. Communications.
3. Control procedures.

At first glance, it might appear that this simple classification would yield the most direct and fruitful approach to the analysis of the entire system. One is tempted to study the individual subsystems independently and to confuse the sum of their analyses with the analysis of the overall system. However, interrelationships among the individual subsystems play a very important role and it is not possible to ignore them in the analysis. A more fruitful approach toward an understanding of the North Atlantic Air Traffic System consists of

a simultaneous analysis of several broad system areas and their interrelationships. Such principal areas of investigation are:

a). environment

b). operational procedures

c). separation standards

d). system capacity

e). economic considerations.

The environment of the North Atlantic System is determined by aircraft operational characteristics, the distribution of traffic in time and space, the weather, weather forecast limitations, communications coverage and reliability, and navigational equipment characteristics.

Operational procedures include the conventions governing route and altitude selection, the methods used by controllers to establish and maintain separations between aircraft, communications procedures, and the manner in which navigational equipment is used.

Separation standards play a central role in the determination of system performance. Not only do they depend upon the environment and procedures, but the latter are, in turn, influenced and modified by the separation standards actually practiced.

The traffic handling capacity and economic characteristics of the North Atlantic System are functions of the environment, procedures, and separation standards. In turn, user requirements introduce a feedback process by which the latter system areas are influenced by considerations of capacity and economics.

The interrelationships existing between different system areas, and within a single area, are complex and diffuse. For example, it can be shown that certain improvements in communications coverage afford little or no advantage unless accompanied by appropriate modifications in navigation and in ATC procedures. It is usually not possible to determine the effect on

system performance of a change in one area without considering how other areas are affected and whether additional changes are required.

Because of the multiplicity of feedback relationships among the various system areas, it is difficult to choose a point of departure from which to discuss the system. Nevertheless, it is necessary to consider the different areas in a sequential order. This implies postulating a sequence in which the various system areas influence each other. In other words, we require a guide to our analysis in the form of a general block diagram indicating the main trends of influence among the system areas. To be useful, such a diagram must have well defined inputs and outputs, without any feedback paths joining them. Unless this is done, it is not possible to conduct a simple analysis of the overall system that would permit us to assign arbitrary input conditions. The essential feedback paths must be provided later. The actual form of the block diagram is not unique. ARCON has chosen a particular form here which, ARCON thinks, corresponds most closely with the natural system structure, and which is most useful in our analysis. The organization of the discussion in the next Sections, as well as the manner in which the analytic tools presented should be used, can be explained with the aid of this block diagram, which is shown in Figure IV-1.

It may be noted that a number of feedback paths between certain system areas in the diagram have been severed, for reasons already given. These paths must be introduced later when the analytical techniques developed in the next Sections are applied to specific systems. To a considerable extent, it is necessarily the responsibility of the users of this report to determine the appropriate feedback relations. This statement will be clarified in the following discussion.

The block diagram of Figure IV-1 indicates the general structure of the process by which the tools provided in this report may be used to analyze air traffic systems. Two variable inputs to the process are indicated in the

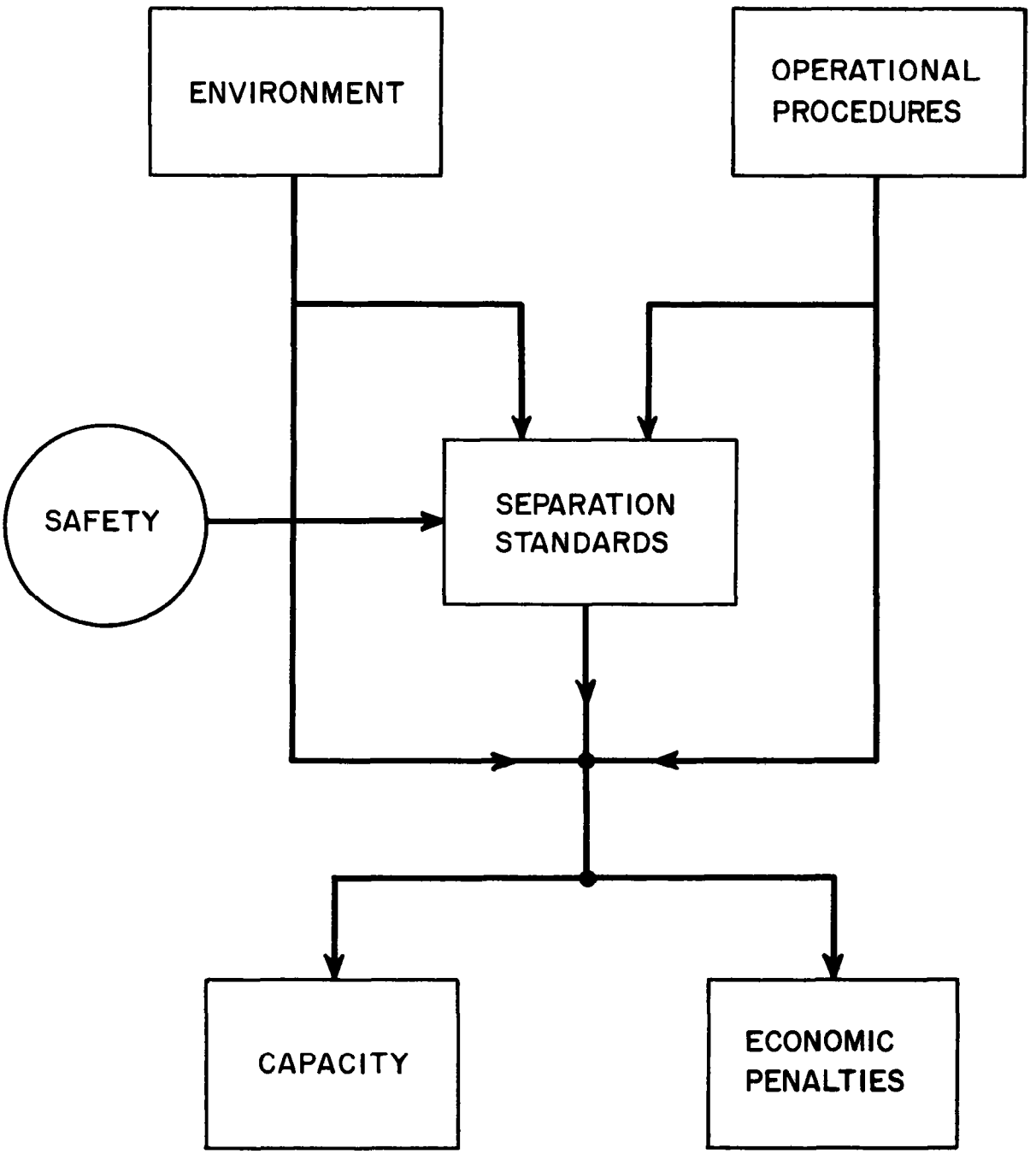

FIG. IV-1 BLOCK DIAGRAM OF NORTH ATLANTIC SYSTEM AREAS

diagram, the system environment and the operational procedures. A third input, safety, is also indicated. In this report, it is assumed that safety requirements are not to be compromised and, therefore, should be considered as a fixed input.

The separation standards for an air traffic system are determined from the three inputs according to criteria discussed in Section V. The two variable inputs may reflect any of a variety of proposed modifications in the environment and procedures.

The analytic process then leads from the given environment and set of procedures, together with the resulting separation standards, to evaluations of system capacity and certain "economic penalties." These evaluations are the outputs of the process.

A technical definition of system capacity and techniques for its evaluation are presented in Section VI. Loosely speaking, capacity is the ability of a system to accommodate traffic without imposing excessive penalties (ATC diversions). It is important to understand that capacity is independent of the traffic density that a system may be required to accommodate. When density exceeds capacity, the system is overloaded and excessive penalties are incurred. When density falls below capacity, the system is simply not fully used.

The economic penalties considered in this report are those associated with ATC imposed diversions of aircraft from preferred altitudes and from preferred routes. Criteria for assessing these penalties are discussed in Section VII. Other economic considerations, such as the costs of possible improvements in communications or navigation, are not analyzed. The costs of such system modifications must be determined by the responsible agencies and are, of course, a dominating element in the choice of a solution to North Atlantic air traffic problems.

When the evaluations of the capacity and economic penalties associated

with a given system configuration are complete, it is then necessary to determine whether system requirements are met. This question must be answered in terms of anticipated traffic loads. The acceptability of the costs of the proposed system modifications, as well as the economic penalties of the type treated in this report, must also be considered. If system requirements are not satisfied, it is then necessary to vary the inputs (environment and procedures) and repeat the analytic process until acceptable outputs are found. It is in this manner that the feedback loop must be closed.

V. SEPARATION STANDARDS

1. Introduction

Separation rules have been adopted in order to facilitate safe passage of aircraft from point of origin to destination. Their specific purpose is to prevent mid-air collisions between aircraft. The nature of the errors inherent in the determination of aircraft position makes it impossible, from a practical standpoint, to set separation minima which guarantee absolute safety for all aircraft. It is possible only in principle to make such a guarantee. For example, if only one aircraft were allowed off the ground at any time, there would obviously be no mid-air collisions. Economic reasons, however, make it impractical to go to such an extreme. Separation rules then represent a compromise between safety and the expedition of the flow of air traffic. This compromise must be treated with caution, however. An increase in traffic density creates a demand for increased traffic handling capacity. This demand cannot be met simply by reducing separation minima. On the contrary, if all other factors are held constant, an increase in traffic density requires an increase in the separation rules in order to maintain the same level of safety. The reason for this is that higher traffic density leads to an increase in the number of occasions on which a given aircraft comes into proximity with other aircraft. In order to maintain the necessary level of safety for the entire flight, the probability of collision at each single occasion of proximity must be reduced.

For reasons discussed in the next Section, a realistic evaluation of collision problems is not feasible, although notable attempts have been made in this direction.[13] It is possible, however, to establish criteria for comparing the relative levels of safety provided under different conditions. One may then ask whether proposed system modifications will improve, maintain, or degrade the existing level of safety. A choice among different possible

modifications may also be determined on a meaningful comparative basis. In this report, the evaluation of system changes is based on the premise that safety is not to be compromised; i.e., changes are justified only if established safety levels are maintained.

It is obvious then that, for a given environment and set of procedures, separation standards must be chosen to meet a specified level of safety. The separations required are related in a general way to accuracy of aircraft position measurement. Specifically, the basis for the determination of separation standards is the error in the estimated future position of the aircraft as known to the controller. The accuracy of aircraft position as known by the pilot or navigator is not the proper criterion, since it is the controller who provides separation between pairs of aircraft. Accuracy of present aircraft position as known to the controller is also an unsatisfactory criterion because the controller must have available a safe interval of time within which to resolve conflicts that arise. Let us first consider errors in the controller's knowledge of the present position of an aircraft and then investigate how these errors increase as the controller extrapolates the aircraft's position into the future.

In domestic air traffic control systems, two methods are utilized by controllers to obtain information on current aircraft positions. Where radar coverage is available, the controller himself can determine these positions. He uses his communications system only to identify aircraft on his display. In the absence of radar cover, the controller relies upon the pilot or navigator's measurement of position as transmitted to the controller. In the North Atlantic there is only limited radar coverage, and the controller usually must rely upon the pilot's position report. During the occasional periods of communications blackout, the controller's only source of position information is the cleared flight plan of the aircraft.

Thus, communications reliability and navigational accuracy both limit

the controller's knowledge of current aircraft positions. However, they affect his ability to predict the three components of future positions, lateral, vertical and longitudinal, in fundamentally different ways. In almost all present day air traffic control systems, the controller assumes that the aircraft's future movement will coincide with its cleared flight plan in the lateral and vertical dimensions. Errors in his prediction of the lateral and vertical components of the future position are simply the track-keeping errors in the navigation of the aircraft. In this report, track-keeping error refers to the difference between the actual position of the aircraft and its flight plan position. The basis for the controller's method of predicting future aircraft positions in the lateral and vertical dimensions is the requirement that the pilot maintain the flight plan in these dimensions and correct track-keeping errors whenever they are discovered.

A similar requirement does not apply to the longitudinal dimension, however, and the controller does not necessarily assume that the future position will coincide with the flight plan in this dimension. Instead, he must extrapolate the longitudinal position of an aircraft from the last reported position, that is, compute its ETA, on the basis of the reported air speed and his knowledge of the winds to be encountered along the flight plan path. Alternatively, he may accept the pilot's ETA. In the domestic system, where the controller need extrapolate only a short time ahead and where he has fairly accurate estimates of wind velocities, errors of extrapolation are small. In the North Atlantic, the controller must extrapolate over long time intervals on the basis of inaccurate wind forecasts and air speeds which are based on inaccurate forecast temperatures. In actual practice, the oceanic controller usually relies on navigator ETA's. These ETA's are based on a variety of different wind and temperature forecasts, which are not only inaccurate but often inconsistent.

It is apparent then that different control philosophies underlie the

methods by which separations in the three dimensions are maintained. Vertical and lateral separation standards are based on a strategic approach. The separation provided in either of these two dimensions by the cleared flight plans of two aircraft may deteriorate because of track-keeping errors. When this happens, the controller does not attempt to resolve minor deviations. Instead, it is the responsibility of the pilots to correct such deviations. On the other hand, it is not the responsibility of the pilots to resolve a conflict which arises because of deterioration of the longitudinal separation provided by the cleared flight plans. The controller endeavors to detect such conflicts on the basis of ETA computations and issues instructions for flight plan revisions when the need appears. Thus, tactical control procedures are employed in the maintenance of longitudinal separations. However, only limited reliance is placed on such procedures because of navigational and communications limitations.

It would appear then that the separation standards which should be set in the lateral and vertical dimensions depend primarily upon navigational devices and procedures, while the longitudinal standard depends upon both navigation and communications. We shall find, however, that other system characteristics, both environmental and procedural, also influence the separation standards and that the effects of improvements in communications and navigation cannot be evaluated independently of these characteristics.

2. Collision Probabilities

The probability of collision between two aircraft may be represented as the probability that the aircraft separations in all three dimensions, longitudinal, lateral, and vertical, will simultaneously diminish to values smaller than tolerances determined by the physical sizes and shapes of the aircraft. The separation in each dimension may be expressed as the sum of two components, the flight plan separation and a random variable. The random component

in each dimension is the difference in the track-keeping errors of the two aircraft in that dimension. Conventional attempts to evaluate collision probabilities are based on the following assumptions:

(1). The separations in the three dimensions are statistically independent.

(2). The track-keeping errors of two aircraft in the same dimension are independent, zero-mean random variables drawn from the same population.

(3). In each dimension, the distribution of track-keeping errors is Gaussian.

Under these assumptions, the aircraft separations in the three dimensions may be represented as independent, Gaussian variables. The mean value of each of these variables is the flight plan separation, while the standard deviation is related linearly to the standard deviation of the track-keeping errors in the corresponding dimension. The probability of collision is then determined by conventional mathematical techniques. Certain additional assumptions may be made in the form of approximations which simplify the mathematics and, in themselves, are not objectionable. However, assumptions (1) - (3) ignore important features of the North Atlantic environment and lead to a mathematical model which simply does not yield realistic results.

Assumption (1) fails to take account of certain features of the physical environment. It is reasonable to suppose that the lateral and vertical separations are independent. However, the longitudinal separation of two aircraft does depend upon their lateral separation, because the relative velocity of two aircraft is subject to the effect of horizontal wind gradient. This effect is analyzed in Appendices B and C and discussed in Section 3 of this Section. Temperature gradient also influences longitudinal separation, although less critically than the wind gradient. Similarly, longitudinal separation may be correlated with vertical separation because of the vertical gradients of wind

and temperature. However, the correlation of longitudinal and lateral separations is more significant because of the small vertical separations involved.

The assumption of independence in (2) is also suspect, although in some cases the track-keeping errors of two aircraft in a particular dimension may be independent. Independence of the track-keeping errors in the vertical dimension appears to be a reasonable assumption, since there is little reason to suppose that altimeter errors for two aircraft are correlated. It is also reasonable to suppose that most of the sources of error in lateral track-keeping are independent; but if two navigators use the same erroneous wind forecast to determine the drift angle required to maintain their respective aircraft on course, then the corresponding components of the track-keeping errors are clearly dependent. The longitudinal errors of aircraft following the same flight plan track are obviously not independent, since the winds encountered are correlated.

Assumption (3) leads to especially serious errors in calculated collision probabilities. When the cleared flight plans of two aircraft provide separation in just one dimension, then the probability that this planned separation will diminish to zero or near-zero values, because of large track-keeping errors by one or both aircraft, is of critical importance. The results of the assumption that the distribution of track-keeping errors is Gaussian are seriously misleading. This assumption is based on the central limit theorem, which asserts that, under quite general conditions, the distribution of a sum of a large number of random variables is approximately Gaussian. Since a number of different sources do contribute to track-keeping errors, the central limit theorem is pertinent. However, the error in the Gaussian approximation is small only near the mean of the distribution and becomes large for regions of the distribution farther removed from the mean. In other words, the central limit theorem cannot be used to obtain an accurate estimate of the probability of a rare event. But it is just the probability of rare events; i.e.,

large track-keeping errors, or blunders, for which an accurate estimate is required. Studies of data on both lateral and longitudinal track-keeping errors demonstrate that large errors, within certain ranges, are considerably more probable than those that can be associated with a Gaussian distribution.[7, 14, 15]

The actual distributions of track-keeping errors in each of the three dimensions are not known. Empirical data have been collected on large lateral and longitudinal errors occurring near the coast lines.[10, 15] Little information is available, however, on lateral errors occurring in the mid-Atlantic, a region which is critical because of the poor coverage by ground-based navigational aids. Since longitudinal errors, or ETA errors, of leading and following aircraft are correlated, statistics on the differences in ETA errors are required. These differences are the errors in predicted longitudinal separation. Information on vertical track-keeping errors is especially limited.

The Gaussian characterization of track-keeping errors is useful, if it is desired to determine the probability of coincidence of aircraft positions in a dimension for which the flight plan separation is nominally zero. For example, suppose that the longitudinal separation of two aircraft following the same route at the same flight level does diminish to a zero or near-zero value. The conditional probability of collision, given that this event has occurred, is determined by the probabilities that the aircraft positions also coincide (within appropriate tolerances) in the lateral and vertical dimensions. The Gaussian assumption may be employed to determine these probabilities, since it is the small track-keeping errors that are important in this case. A similar statement may be made concerning the conditional probabilities associated with the collapse of a separation provided by the cleared flight paths in either the lateral or vertical dimensions. Such conditional probabilities might be used to establish certain comparative relationships; however, it

should be noted that they are related only to the "instantaneous probability" of collision, that is, the probability of collision at any given moment when the cleared flight plan separation in one dimension has collapsed. Not only is the probability of the latter event unknown, but it is also difficult to determine the persistence in time of such a dangerous occurrence, once it has arisen. The collapse of the flight-planned longitudinal separation of two aircraft is likely to continue for a relatively long time, since pilots do not endeavor to correct ETA errors. Collapse of a flight-planned lateral or vertical separation is less likely to persist unless, perhaps, it is caused by an abnormally large bias error in the navigation of an aircraft.

It is apparent that the calculation of realistic collision probabilities is not feasible without much more extensive information than is presently available on track-keeping errors, particularly blunder probabilities, and on statistical dependencies of errors.

It is, however, often an easier problem to determine how collision probabilities may change with varying system characteristics. Thus, one may ask whether a particular system modification will permit a reduced separation standard without degrading existing safety levels. Such comparative relationships must be developed with caution. For example, if it can be shown that a new navigational device will cut the standard deviation of lateral track-keeping errors to half its present value, it does not necessarily follow that the lateral separation standard can be cut in half. Indeed, it is conceivable that the blunder rate, or probability of large errors, is greater even though the standard deviation is smaller.

A smaller separation standard may reasonably be associated with a smaller standard deviation of error, if the error distributions under comparison are of the same basic form (e.g., both Gaussian, rectangular, etc.). Specifically, it is not so important whether the standard deviation of lateral track-keeping errors is cut in half by a new navigational device as whether

the probability of errors exceeding, say, 30 n. mi. will be no larger than the present probability of errors exceeding 60 n. mi. In fact, a reduction of the standard deviation without a reduction of the blunder rate may in some cases even increase the probability of collision, although separation standards remain fixed. This possibility may occur because of certain secondary effects. For example, consider two aircraft following the same flight plan track at adjacent flight levels. If the vertical separation of the aircraft should deteriorate, then a smaller standard deviation of lateral track-keeping errors implies a greater probability that the aircraft positions will simultaneously coincide in both the vertical and lateral dimensions.

In subsequent Sections, certain quantitative relationships will be described which are useful in comparing the separation standards required under varying conditions.

3. Longitudinal Separation

The longitudinal separation standard is not determined on the basis of track-keeping errors. Although the navigator attempts to correct lateral and vertical deviations from the flight plan, no attempt is made to control speed in order to reduce deviations in the longitudinal dimension. Longitudinal separation depends upon the accuracy of the predicted time separation of aircraft, or differences in ETA's. There are three sources of error in the computation of ETA's. The first is the error in the position of the aircraft at the initial time from which future ETA's are extrapolated, or predicted. The second is the error in the forecast of winds to be encountered. The third is the uncertainty in the future air speed of the aircraft.

The contribution of the error in the initial fix to ETA errors is of little consequence if the fix is obtained with a reliable aid (available in most domestic regions). On the other hand, fix errors corresponding to a time error in the range of 2 to 3 minutes are not at all unusual in the mid-Atlantic.

In view of the slow rate of growth of extrapolation errors with distance, recomputed ETA's based on oceanic position fixes are of questionable value. This suggestion is confirmed by the results of studies conducted recently at the Prestwick Control Center.

A principal source of error in ETA's is the wind uncertainty. Considering only wind forecast errors, the standard deviation of the error in ETA's computed for Gander from Shannon is 11 minutes for jet aircraft. But it is the error in the ETA difference for two aircraft which determines longitudinal standards. Since aircraft on similar paths encounter similar winds, the error in the difference between computed flight times for two aircraft is considerably less than the error in the ETA's themselves.

Errors in air speed arise for two distinct reasons. The first is simply the error in the measurement of aircraft velocity. No statistical data are available on the magnitude of this error. However, jet operational economy is highly sensitive to Mach number, and the fact that an operational distinction is made between Mach .82 (normal cruise) and Mach .84 (high speed cruise) suggests that errors in the desired Mach number are not likely to introduce errors in air speed exceeding 5 knots. Since large deviations in Mach number would be reflected by the fuel flow rate, a check is provided against this source of error. The second factor is based upon the fact that aircraft fly at constant Mach number and that the relationship between Mach number and air speed depends upon temperature. Examination of data on the horizontal temperature gradient and temperature forecast errors indicates that the magnitude of these effects is less than 20% of the effect due to wind gradient and wind forecast errors.

We shall now describe the results of the analysis of wind effects presented in Appendices A, B and C. A mathematical model of the winds, developed in Appendix A, makes it possible to express the correlations of wind components in various directions and at different geographical points in

terms of existing statistical data.* This model is then used in Appendix B to evaluate the effect of winds on the longitudinal separation of aircraft. Two cases are considered, one in which both aircraft have filed the same flight plan path and follow actual paths close to one another, and a second case in which the two aircraft have filed flight plans which cross or converge at some point. The results of Appendix B are corroborated by a Monte Carlo evaluation, described in Appendix C, which also demonstrates in greater detail how wind effects vary with range, or flight path length, and with air speed.

In the following discussion, the effect of wind variation on longitudinal separation will be evaluated for aircraft with ETA's predicted on the basis of the same weather forecast. Thus, only the effect of the horizontal gradient of winds is considered. Adequate information is not available on the correlations of errors in the different weather forecasts currently used by aircraft operating over the North Atlantic. Consequently, the additional errors in predicted longitudinal separation contributed by inconsistencies in different forecasts are not evaluated. The cause of these errors is artificial and should be eliminated by a change in procedures [cf. V.6 and VIII.4].

It may be argued that the time separation between two aircraft following the same flight plan track at the same air speed must remain very nearly constant. Although this statement is correct, no two aircraft ever do actually fly the same path. The actual paths for two aircraft with identical cleared flight plan tracks will differ because of lateral track-keeping errors. The relationship between lateral track-keeping errors and ETA difference errors has been treated in Appendices B and C, and the standard deviation, $\sigma_{\Delta T}$, of the error in predicted longitudinal separation has been computed. The parameter $\sigma_{\Delta T}$ represents the standard deviation of the error component caused by wind effects only, that is, by differences in the tail winds encountered by the

*This data is available in a paper by C. S. Durst.[3]

aircraft. In both Appendices B and C, the actual flight paths of two aircraft, following the same nominal flight plan track, are represented as parallel paths separated by a distance, d, related to the lateral track-keeping errors. The actual flight paths are, of course, not parallel and may even cross on occasion; however, it can be shown that the effect of wind differences on longitudinal separation is equivalent to the effect on two aircraft flying along parallel paths separated by a suitably defined equivalent distance d.

With the aid of the mathematical model of wind correlations in Appendix A, it is shown in Appendix B that the standard deviation $\sigma_{\Delta T}$ of the longitudinal separation of two aircraft flying at the same flight level and at the same air speed, A, along such parallel paths is represented by an equation of the form

$$\sigma_{\Delta T} = \frac{\sigma_w}{A^2} I(d, L) \quad . \qquad (V.1)$$

The parameter σ_w is the standard deviation of the wind component in the direction of the parallel paths. I(d, L) is a function of the path separation d and the path length L and is determined by integrating the effect of the wind correlations over the flight paths. Numerical values of $\sigma_{\Delta T}$ are plotted in Figure B-11 for various values of d and L. The results are based on wind statistics at the 300 mb. level and an air speed of 480 knots. The mean error $\mu_{\Delta T}$ is also determined and is found to be negligible [cf. Figure B-10].

In the second case considered in Appendix B, two aircraft follow flight plan tracks which cross or converge. The tracks considered are straight line segments meeting at an angle 2θ. No allowance is made for track-keeping errors, since it may be assumed that these errors do not significantly affect the average lateral separation of the aircraft. The standard deviation $\sigma_{\Delta T}$ of the longitudinal separation of two aircraft flying at the same air speed,

A, along such paths is shown in Appendix B to satisfy an equation of the form

$$\sigma_{\Delta T} = \frac{\sigma_w}{A^2} J(\theta, L) \quad . \tag{V.2}$$

The parameter σ_w is the standard deviation of the wind component in the direction of either flight path. $J(\theta, L)$ is a function of the semi-angle θ of intersection and the length L of the two paths and is determined by integrating the effects of wind correlations over the flight paths. Numerical values of $\sigma_{\Delta T}$ are plotted in Figure B-12 for various values of θ and L. These results are also based on wind statistics at the 300 mb. level and an air speed of 480 knots. It is reasoned in Appendix B that the mean difference $\mu_{\Delta T}$ in the flight times along two converging or crossing tracks is accounted for by the time difference predicted on the basis of wind forecasts. Consequently, only the standard deviation $\sigma_{\Delta T}$ is relevant to an evaluation of errors in the predicted longitudinal separation of aircraft flying on such paths.

The results of Appendix B show that the standard deviation $\sigma_{\Delta T}$ is smaller for parallel tracks than for converging tracks, even when the average lateral separations are comparable, because parallel tail wind components are more highly correlated than nonparallel ones. This effect is illustrated in Figure B-13.

The average lateral separation of two aircraft following the same flight plan track is, of course, much smaller than that of two aircraft flying on converging tracks. A much larger standard deviation $\sigma_{\Delta T}$ is naturally anticipated for the latter case. The results of Appendix B verify this expectation, as illustrated by the following comparison of two specific cases.

In the first case, we shall consider two aircraft which follow the same flight plan track but, because of track-keeping errors, actually fly on approximately parallel tracks separated by an average distance d = 20 n. mi. This

value of the track separation d corresponds to a standard deviation in lateral track-keeping errors of 14 n. mi., assuming that the errors of the two aircraft are independent. A positive correlation in track-keeping errors would imply a somewhat smaller separation. For the assumed separation d = 20 n. mi. and a path length L = 720 n. mi., it can be seen from the curve labeled d = 20 n. mi. in Figure B-11 that the standard deviation $\sigma_{\Delta T}$ is 0.47 minutes. This value represents the standard deviation of the difference in the ETA's of the two aircraft, or the error in the predicted longitudinal separation, that is contributed by the cumulative effect of differences in winds encountered over a range of 720 n. mi. This range is approximately twice the distance between consecutive reporting points for jet aircraft.

We shall now consider two aircraft following flight plan tracks which initially have a lateral separation of 2° and converge after a distance of about 720 n. mi. For example, one aircraft might proceed eastbound from 40° W, 57° N to 20° W, 57° N and the other from 40° W, 55° N to 20° W, 57° N. For simplicity, we may take both flight path lengths to be about 720 n. mi. The angle of intersection at the point of convergence is approximately $2\theta = 10°$. It is seen from the curve labeled $\theta \approx 5°$ in Figure B-12, that the standard deviation $\sigma_{\Delta T}$ for a path length L = 720 n. mi. is 1.98 minutes. This value represents the standard deviation of the ETA difference, or error in the predicted longitudinal separation, at the point of convergence.

The ratio of values of the standard deviation $\sigma_{\Delta T}$ for the converging and parallel track cases is more than 4 : 1. It must be recalled, however that $\sigma_{\Delta T}$ represents only the standard deviation of the component of the error in predicted longitudinal separation caused by wind effects. The other principle component is caused by air speed errors. Since a predicted difference in air speed between the leading and following aircraft is compensated by an adjustment in the initial longitudinal separation, we shall suppose that the aircraft are assumed by the controller to fly at the same air speed A (480 knots in these

examples). An unpredicted difference ΔA, or error, in the average air speeds of the aircraft will cause an error in the predicted longitudinal separation. It can be shown that the standard deviation, $\sigma_{\Delta T'}$, of the component of the longitudinal separation error contributed by this effect over a path length L is approximately

$$\sigma_{\Delta T'} \approx \frac{L\Delta A}{A^2} \quad . \tag{V.3}$$

Assuming that the initial longitudinal separation of two aircraft is established on the basis of accurate fixes taken over domestic regions, then the principal components of the error, e, in predicted longitudinal separation are those contributed by wind effects and air speed errors. It is reasonable to assume that these two error components are independent. Hence, the standard deviation σ_e of the error in longitudinal separation is given by

$$\sigma_e^2 = \sigma_{\Delta T}^2 + \sigma_{\Delta T'}^2 \quad . \tag{V.4}$$

Adequate statistical information on air speed errors is not presently available. As indicated previously, the effects of inaccuracies in Machmeter reading should be small, and temperature effects are known to be less significant than wind effects. We shall assume an air speed difference ΔA of 10 knots for two aircraft with identical filed air speeds of 480 knots. Then from eq. (V.3), the error component $\sigma_{\Delta T'}$ for a path length L = 720 n. mi., is 1.86 minutes. If we assume the same air speed difference ΔA = 10 knots for both the converging and parallel tracks considered in our examples, then the values of the standard deviation, σ_e, as defined by eq. (V.4), for these two cases are 2.73 and 1.93 minutes, respectively. The ratio of these values is about 1.4 : 1.

The assumption of an identical air speed difference, ΔA, for both the parallel and converging track cases should be modified slightly, because the effect of temperature gradient is somewhat greater for the converging track case. Moreover, very large errors in longitudinal separation, caused by the abnormal wind gradients associated with jet streams, are more probable for the converging track case. Thus, the ratio 1.4 : 1 represents a low estimate of the ratio of separation standards required, respectively, for aircraft which follow the same flight plan track, with a small average separation, and aircraft which follow converging flight plan tracks. It is interesting to note that, under a recently approved modification of the longitudinal separation standard, the ratio of the standards required by ICAO for these two cases is 1.5 : 1.

Additional comparisons may, of course, be derived by the same methods for other examples with different path lengths and different angles of intersection for converging paths. It has been amply demonstrated, however, that a larger separation standard is required when aircraft fly on converging paths than when they follow the same flight plan track. In considering collision probabilities associated with converging paths, it should be noted that a distinction is required according to whether the aircraft follow identical or diverging paths beyond the point of convergence. The period of time over which a dangerous situation may exist is clearly greater in the former case.

Eqs. (V.1) - (V.4) may be used to obtain an interesting relation between the standard deviations of the longitudinal separation error for jet and propeller aircraft. For this purpose, it is necessary to know how errors in air speeds compare for the two types of aircraft. Adequate statistical information is not available; however, in order to illustrate how comparative relationships may be derived, we shall suppose that the error ΔA in the predicted difference of the air speeds of leading and following aircraft, expressed as a percentage of the true air speed A, is the same for both jet and propeller aircraft. That is, we assume that the ratio $\Delta A/A$ is a constant. Eq. (V.3)

shows that, under this assumption, the ratio of the standard deviations of the error in predicted longitudinal separation, caused by air speed errors for propeller and jet aircraft, is given by

$$\frac{\sigma_{\Delta T'(prop)}}{\sigma_{\Delta T'(jet)}} = \frac{A_{(jet)}}{A_{(prop)}} \quad . \tag{V.5}$$

In order to compare the effects of winds on the longitudinal separation of the two aircraft types, it is necessary to obtain data on wind correlations at the altitudes conventionally flown by propeller aircraft, say at 500 mb. Although such data has been provided at the 300 mb. level,[3] it does not appear to be available at 500 mb. The additional data could be readily derived by meteorologists. It seems likely that the wind correlation functions at the 300 mb. and 500 mb. levels are similar. If we assume that the functions I(d, L) and J(θ, L) appearing in eqs. (V.1) and (V.2) do not change with flight level, it follows from these equations that the ratio of the standard deviations of the longitudinal separation error components, caused by wind effects on propeller and jet aircraft, is

$$\frac{\sigma_{\Delta T(prop)}}{\sigma_{\Delta T(jet)}} = \frac{\sigma_{w(500\ mb.)}}{\sigma_{w(300\ mb.)}} \left(\frac{A_{(jet)}}{A_{(prop)}} \right)^2 \quad . \tag{V.6}$$

It appears from charts in reference 2 that the standard deviation of the wind at the 500 mb. level is about 75% of that at the 300 mb. level. If we assume that the air speed of propeller aircraft is half that of jets, we may then determine a comparison of the standard deviation σ_e, defined by eq. (V.4), for the two aircraft types. Consider the example given previously, in which jet aircraft follow the same flight plan track for a distance of 720 n.

mi. We have already determined the values $\sigma_{\Delta T'} = 1.86$ min. and $\sigma_{\Delta T} = 0.47$ min. for this example. It then follows from eqs. (V.5) and (V.6) that the corresponding values for propeller aircraft are $\sigma_{\Delta T'} = 3.72$ min. and $\sigma_{\Delta T} = 1.41$ min., respectively. Then, according to eq. (V.4), the standard deviation σ_e of the error in predicted longitudinal separation for propeller aircraft is 3.98 min. The corresponding value $\sigma_e = 1.93$ min. has already been determined for jet aircraft. Thus, in this example, the ratio of the standard deviations of the error in predicted longitudinal separations for propeller and jet aircraft is 2.1:1. Similarly, it can be shown that in the converging track example previously considered for jet aircraft, the ratio of standard deviations for propeller and jet aircraft is 2.6:1.

These comparative relationships for propeller and jet aircraft based on eqs. (V.5) and (V.6) should be regarded as conjectural until more adequate data becomes available on wind correlations at the altitudes flown by propeller aircraft and, especially, on the air speed errors of both aircraft types. It should also be noted that the analysis has been completed only for aircraft flying at fixed altitudes and that the effect of climb or descent on ETA errors has not been included. In addition, it is important to consider that the effects of large wind gradients associated with jet streams may be more significant at the flight levels flown by jet aircraft. It is, nevertheless, apparent that a larger longitudinal separation standard is indicated for propeller aircraft than for jets.

As a final comment, we may note from eqs. (V.1) and (V.2) that wind effects on longitudinal separation decline rapidly with increasing air speed and that they should be much smaller for supersonic jets than for aircraft currently in operation over the North Atlantic. This fact is amply demonstrated in Appendix C [cf. Figures C-8 and C-9], where a wide range of aircraft speeds is considered and it is shown that the effect of winds on the separation of supersonic aircraft is negligible.

4. Lateral Separation

The accuracy of the flight-planned separation of aircraft in the lateral dimension is limited by the track-keeping errors in that dimension. In the present system, the navigator endeavors to minimize these errors by determining intermittent position-fixes, with the aid of one or more navigational devices, and by dead reckoning between fixes. Dead reckoning requires estimates of both the aircraft position and the ground velocity. The former is known most accurately when fixes are taken. Ground velocity is derived from the compass heading, air speed measurement, and an estimate of the drift angle. The drift angle may be calculated from the wind forecast or by extrapolation from measurements of the cross-track component of the wind already encountered.

At present, fixes are usually taken at least twice an hour, or typically about once every 200 n. mi. The analysis in Appendix D indicates that the standard deviation of the vector error in 3-line fixes lies in the range of 5—15 n. mi.,* depending upon the type of equipment used, the geographical area and other factors. It has already been emphasized, however, that a knowledge of the standard error is not adequate to determine the level of safety that can be attributed to any given separation standard. The answer to this question requires a knowledge of the probability of large errors.

It should be further emphasized that it is track-keeping accuracy rather than fix accuracy that is critical. Even if the navigator were able to take a perfect fix, his knowledge that the aircraft has not conformed to the flight plan would not alter the fact that deviations have occurred. He can only endeavor to return the aircraft to its course by use of a dead reckoning technique; i.e., by requesting the pilot to make a heading change calculated to return the aircraft to the flight plan path at some point ahead. The efficacy

*The analytical techniques of Appendix D apply only to 3-line fixes. Consequently, estimates of the accuracy of other types of fix, including the 2-line Loran fixes frequently used in coastal regions, have not been derived.

of the dead reckoning procedure depends upon the accuracies of the compass heading, the air speed indication, and the estimate of future winds to be encountered, or mainly the heading reference in the case of Doppler-DR computer navigation. Thus, extremely accurate but infrequent fixes may allow large track-keeping errors to accumulate, unless highly accurate dead reckoning processes are used. Clearly, a trading relation exists between fix accuracy and fix frequency. Two approaches may be taken toward the problem of minimizing lateral track-keeping errors. One approach is to establish reliable navigational aids which provide wide coverage and make accurate and frequent, or even continuous, fixes available. The alternative approach is to employ accurate and reliable dead reckoning processes together with accurate, but infrequent fixes. The second approach relaxes the coverage requirements for accurate fix availability.

An analysis of track-keeping errors is developed in Appendix E for several different methods of dead reckoning. A simple model is first constructed which discloses certain illuminating relationships. This model is based on the assumption that the position of an aircraft is determined by intermittent fixes and that the flight path of the aircraft consists of a series of straight line segments, each corresponding to a particular choice of compass heading. Since the model is concerned with lateral track-keeping errors, only that component of the fix error perpendicular to the track need be specified. In order to compute track-keeping errors, the operational procedure or technique by which the navigator maintains track must also be described. It is assumed in this model that, if the fix indicates that the aircraft is off course, the navigator chooses a heading calculated to return the aircraft to its flight plan track at the time when the next fix is to be made. The error in the heading may be expressed as an angle measured in radians. If this angle is small, then the corresponding component of the track-keeping error can be represented approximately as the product of the angle and the distance between

fixes. This approximation is reasonable when applied to jet aircraft, for which air speeds are considerably in excess of typical wind velocities. The standard deviation of this component of the track-keeping error, therefore, is directly proportional to the distance between fixes. This last statement, must be qualified, however, since the heading error itself is, under certain circumstances, dependent upon the distance between fixes. This effect is included in the more detailed models developed later.

Under the assumptions described, the track-keeping error is equal to the sum of the previous fix error and the product of the heading error and distance between fixes. If we also assume that fix errors are independent of heading errors, then the standard deviation of the track-keeping error will be the RMS sum (square root of sum of squares) of the two components. A significant feature of this result is that track-keeping errors can never be less than fix errors.* Consequently, no matter how many improvements are made in heading references or in methods of estimating the drift correction angle, or how frequently the fixes are taken, the fix error is the absolute lower bound on the track-keeping error. This fundamental principle is also supported by the more complete results in Appendix E.

The models developed in Appendix E are essentially synthetic and lead to estimates of the standard deviation of lateral track-keeping errors for various navigational techniques. The results are based on the assumption that the navigator employs his available dead reckoning aids to optimal advantage. In order to evaluate dead reckoning procedures, the following sources

*An exception might occur in cases, not considered in the model, where the dead-reckoned position and the fix-position are "weighted," a procedure which is feasible when a reliable dead reckoning process is used to navigate from an accurate initial fix into a region where fixes are less accurate. In this region, it may happen that a weighted combination of the dead-reckoned position and the fix-position is superior to the fix-position alone. Such weighting procedures are not used in present practice, however.

of heading error must be considered.

1. Error in the estimated drift angle.
2. Error in magnetic variation.
3. Error in compass deviation (calibration error).
4. Error in the maintenance of the desired heading by pilot or autopilot.

Adequate statistical data on the last three sources of error is not readily available. It has therefore been necessary to use information obtained by interviewing pilots and by studying navigator's logs in order to estimate the magnitude of these errors.

The first source of error in the preceding list is frequently the most serious, unless a Doppler-computer or inertial system is used, and is evaluated in Appendix E by mathematical modeling techniques. These techniques establish statistical relationships between the error in the measured drift angle and the variation of winds. The drift angle depends upon the cross-track component of the wind to be encountered by the aircraft. Thus, in order to choose a heading which will bring the aircraft back to its flight plan, the navigator must somehow estimate the winds ahead (unless a Doppler-computer or inertial system is used). Several techniques currently used for this purpose are analyzed in Appendix E.

It is assumed in the computation of numerical values that fixes are taken every 200 n. mi., and that the standard deviation of the lateral fix error is 7 n. mi. (except for the model of Doppler-computer navigation). The 7 n. mi. value is based on a standard vector error of 10 n. mi. and the reasonable assumption that fix errors are approximately radially symmetric. The results of Appendix D indicate that a vector fix error of 10 n. mi. is appropriate for navigational devices and procedures currently employed in the

North Atlantic.* The calculations in Appendix E also assume a standard deviation of .025 radians, or about 1.4 degrees, for the component of the heading error caused by the cumulative effect of errors in magnetic variation, compass calibration, and compass following by the pilot or autopilot. Although this value is reasonable, it is not based on a statistical study. The results of Appendix E do not depend critically on the actual value, however, as long as it is limited to about 2°. It may be that some carriers can achieve smaller heading errors than the estimated 1.4°. Given a different estimate of heading error, the corresponding value of lateral track-keeping error can be obtained simply by substituting the new estimate in the model given in Appendix E.

The simplest technique that the navigator may use to estimate the wind ahead is to read it from a meteorological forecast. The error in the drift angle implied by this estimate may be derived from data on the spatial correlation of actual and forecast winds. The standard deviation of the lateral track-keeping error associated with this dead reckoning technique is approximately 15 n. mi.

In the remaining techniques to be described, the navigator measures the wind already encountered and identifies the wind ahead with this measured wind. The error in the drift angle implied by such techniques may be expressed in terms of the measurement errors and the spatial correlation of actual winds.

The least accurately measured winds that the navigator may use are called "fix-derived." The measurement is based on the assumption that the flight path segment indicated between the last two position fixes is identical to the path segment that was actually flown. The wind encountered over this

---

*The data on which the results of Appendix D are based emphasize the mid-Atlantic region. The fix errors in coastal regions may have a significantly lower standard deviation than 10 n. mi.

segment is then calculated from the indicated air speed and the compass heading that had been chosen for the segment. The contribution of fix errors to the error in the measured wind is especially significant, and the standard deviation of lateral track-keeping errors is estimated to be 21 n. mi. for this procedure.

In some cases, a navigator will combine both the forecast and fix-derived winds to determine a compromise between the headings which would be chosen when either of these wind estimates is used separately. It is shown in Appendix E that, if the navigator uses an optimal weighted average of the two estimates, the standard deviation of the track-keeping error is reduced to 14 n. mi. How closely the navigator approaches this optimum depends, of course, upon his skill.

Pressure altimetry provides a more effective method of measuring cross-track winds. This method is based on the geostrophic assumption which relates winds to differences in the altitudes measured by pressure and radar altimeters. If this technique is used to determine the drift angle at the time each fix is taken, the standard deviation of the lateral track-keeping error is found to be about 15 n. mi. If, in addition, it is used halfway between fixes and the aircraft heading is adjusted at that time, the standard deviation drops to 10 n. mi. This last procedure is similar to that used by many of the commercial carriers in oceanic regions, and it should be noted that the value of the standard track-keeping error is close to the assumed fix error of 7 nautical miles.

Two different dead reckoning techniques which employ Doppler radar are considered in Appendix E. The first method is similar in principle to the pressure altimetry technique just described. Since Doppler provides direct measurements of the components of ground velocity both along and across the direction in which the aircraft is headed, the navigator is able to estimate the drift angle at any time. Limited information is presently avail-

able on Doppler sensing errors; however, it is likely that they are small compared to compass deviation and other sources of heading error. If it is assumed that Doppler measurements are perfect and that they are used to determine the drift angle and to correct the heading once at each fix and again halfway between fixes, the standard deviation of the lateral track-keeping error is about 9 n. mi. This result implies that little improvement can be achieved by more frequent measurements of the drift angle, since the value 9 n. mi. already approaches the 7 n. mi. fix error assumed in the model. The lower limit dictated by the fix error can be realized only if all sources of heading error are eliminated. It should be recalled, however, that the value assumed in the model for the standard deviation of the fix error has been shown in Appendix D to be appropriate for the mid-Atlantic only and that different fix accuracies may be characteristic of other regions.

The second method of navigation using Doppler employs a computer which integrates the measured ground velocity and provides a continuous indication of aircraft position. The computer output may be read by the pilot, or it may be coupled directly to the autopilot. The growth of error in the integrated aircraft position depends upon the errors in Doppler measurement, compass calibration, etc. The accumulated error can be corrected only if the computer is reset to a fix-determined position. Thus track-keeping accuracy is again limited by fix errors.

One method of using Doppler-computer equipment in the North Atlantic is to reset the computer only when fixes can be taken in regions covered by Loran A ground wave and to dead reckon elsewhere; i.e., across the mid-Atlantic region lying roughly between 20° W and 40° W. The breadth of this region is about 600 n. mi., and since the dead reckoning error grows as a function of distance, the lateral track-keeping error occurring at the time a fix is taken just after the mid-Atlantic region has been crossed is of special interest. It can be shown that the standard deviation of this error is 9.2 n.

mi., assuming that the lateral component of the Loran A ground wave fix error is 2 n. mi. and that the lateral component of the dead reckoning error is 1.5% of the total distance flown since the last fix.

This error might be reduced in two possible ways. One way is to decrease the rate of growth of the dead reckoning error. It appears that the Doppler sensing errors are small and that the greatest potential for improvement in Doppler-computer dead reckoning is in the heading reference. An alternative way to reduce lateral track-keeping errors is to increase the accuracy of fixes in the mid-Atlantic region so that more frequent resettings of the computer become feasible.

The preceding estimates of errors in lateral track-keeping were all based on the assumption that a maximum effort is maintained by the navigator and pilot to hold the aircraft on course and that heading changes, no matter how small, are always made whenever the need is indicated. This assumption is, of course, optimistic, and does not allow for more casual navigational procedures. Indeed, a comparison made in Appendix E between empirical data and the model results indicates that the estimates of the standard track-keeping errors that have been given for various navigational techniques are lower than those achieved in practice by about 5 n. mi. The model results, therefore, represent lower bounds on lateral track-keeping errors which may be approached more closely by disciplinary measures. The absolute lower bound is the fix error. How closely it may be approached depends both upon the dead reckoning technique used and operational discipline.

Finally, it must be emphasized that the standard deviation of track-keeping error for a particular navigational technique does not reflect the blunder rate, or probability of large errors, for that technique. There is a need for data on the probability of large errors, since their effect cannot otherwise be evaluated realistically.

5. Vertical Separation

Track-keeping in the vertical dimension differs considerably from the lateral case. Where it takes a considerable time to deviate 60 miles from the flight plan, a change in altitude of 1000 feet can occur in seconds. In the North Atlantic, vertical track-keeping is usually done automatically by means of the altitude holding feature of the autopilot. The characteristics of the autopilot control loop are such that it is possible to deviate considerably from the measured pressure altitude in conditions of moderate atmospheric turbulence. The accuracy of the pressure altimeter itself is difficult to evaluate. Although it is known that changes in pressure altitude of 10 to 20 feet can be measured, far greater errors may be encountered in the calibration of the instrument.

An evaluation of the adequacy of existing or proposed vertical separation standards requires measurement data on vertical track-keeping accuracy under realistic operational conditions. Such data is not available at present.

6. Conclusions

We are now prepared to discuss improvements in the present North Atlantic System which might justify reductions in current separation standards. Potential improvements in communications, navigation, weather forecasting, and ATC procedures will be considered.

At present, the North Atlantic controller cannot depend upon air-to-ground and ground-to-air communications and should not depend upon them until a level of reliability is achieved comparable to that of the present domestic system. What would be the advantages of such an improvement? Obviously, a reduction of vertical or lateral separation standards would not be justified. It might be argued that a reduced longitudinal rule would be warranted, since separations could then be predicted ahead on the basis of the most recent pilot reports. However, the large error in position fixes

taken over the mid-Atlantic, as compared to those taken prior to entry into the oceanic region, eliminates much of the advantage of the shorter prediction interval. Thus, combined improvements in both communications reliability and navigational fix accuracy are required to achieve even a moderate reduction of the longitudinal separation rule. Moreover, it should be emphasized that only a major increase in communications reliability will be adequate for this purpose and that it must be accompanied by a shift in control philosophy toward a more tactical approach.

A different area in which improvement might lead to a reduction of the longitudinal standard is weather forecasting. More accurate forecasts would, of course, be helpful, however, it is possible to achieve an immediate improvement simply by requiring that ETA computations be based on a unified forecast. This possibility is also discussed in Section VIII-4. Without adequate information on the correlations of different weather forecasts presently used, it is difficult to determine a quantitative estimate of the error in predicted longitudinal separation that is contributed by inconsistencies in these forecasts. It is clear, however, that there is a real possibility to achieve an important system improvement by a relatively simple change in procedures.

Another procedural change which might allow some reduction of the longitudinal separation rule is the introduction of speed control. The adoption of Doppler-computer equipment would make this possibility feasible, since this equipment does provide a fairly accurate indication of the progress of an aircraft in the longitudinal dimension (for which compass errors are not significant). The economic penalties associated with this type of control have not been assessed but are certainly not inconsequential. Moreover, if the recommendation that ETA computations be based on unified weather forecasts were adopted, then the highly correlated ETA errors for aircraft following the same flight plan track would make speed control of doubtful value.

It was shown in Section 3 that a smaller longitudinal separation standard

is warranted for aircraft following the same flight plan track than for aircraft flying on paths which converge or approach one another at some point. A system of routes organized to take advantage of this fact is well worth consideration. A detailed discussion of the potential benefits of such a system is given in Section VIII-3.

The results discussed in Section 4 demonstrate that the lateral separation standard depends critically upon the accuracy of position fixes. Altimetry and Doppler are of comparable effectiveness when used for drift angle measurement. If used for this purpose to their full potential, both make it possible to achieve track-keeping errors close to the limit prescribed by the fix errors assumed in the model. Thus, more accurate fixes over the entire oceanic region together with an effective use of altimetry or Doppler may justify a reduction of the lateral standard. It should be understood explicitly, however, that this statement is based on the proviso that the improved fixes are taken at least as often as at present. If Doppler-computer dead reckoning is used, then two possibilities for reducing the lateral separation standard might be considered. One approach is to reduce fix errors over the entire oceanic region so that frequent, accurate resettings of the computer are possible. The alternative approach is to reduce heading errors so that accurate fixes are required in regions relatively near the coastlines but not necessarily in the mid-Atlantic. In this connection, it should be noted that a statistical evaluation of fix accuracy in coastal regions has not been completed during this study.

Any attempt to justify a reduction of the lateral separation standard should be based on a consideration of the blunder rate as well as the standard deviation of lateral track-keeping errors. Accordingly, it is important to note that dead reckoning navigation as currently practiced in the North Atlantic involves considerable redundancy of computation and measurement. This redundancy aids the navigator in detecting and eliminating errors.

Although carriers using Doppler-computer navigation may employ duplicate devices to guard against equipment malfunctions, there may still be inadequate checking against other sources of error; for example, in the resetting of the computer by a crew member. Even if the standard deviation of track-keeping errors is lower for Doppler navigation than for conventional dead reckoning techniques, it does not necessarily follow that large errors are less probable for Doppler navigation. It is not clear whether automation of the dead reckoning computation will reduce or increase the probability of large errors, and extensive experience with Doppler navigation is needed before a complete evaluation of its performance is possible.

An evaluation of large errors is also critically important for other proposed navigational aids. Thus, in evaluating Loran C, the possible confusion of sky wave and ground wave reception must be considered. Similarly, Dectra carries the possibility of a displacement of aircraft position to a lane parallel to the intended one.

The geographical coverage afforded by navigational aids also requires consideration because of the broad extent of the envelope of MTP's currently flown by jets during the course of the year. This problem is especially relevant to a consideration of the possible use of ocean based navigational aids. This possibility would clearly be more feasible for a fixed route system than the present system. Fixed routes, however, carry more significant economic penalties for the air lines than other organized route structures which can be adapted to the weather. One example is the "jet reference scheme" described in Section VIII-3, where it is shown that organized routes provide benefits apart from any possible reduction of separation standards.

It is not possible at present to speculate upon the possibility of a reduced vertical separation rule. It can only be recommended that a study of altimeter errors, particularly large calibration errors, and of the characteristics of altitude holding be conducted.

In order to evaluate the adequacy of existing or proposed separation standards in any of the three dimensions, it is necessary to learn more about the distribution of errors for that dimension. It is possible to gain some insight concerning an error distribution by analyzing the effects of various sources of error. If adequate statistical information on these sources is available, the error distribution may then be synthesized by appropriately combining their effects. An evaluation of this kind should be validated, however, by comparing it against a sufficiently large sample of measured errors chosen from the actual distribution in question; i.e., the errors that really occur in practice. Validation is required because the synthetically derived error distribution may fail to represent the actual error distribution realistically if the analysis has not been sufficiently comprehensive to include all significant error sources or if the data on these sources have been obtained under laboratory conditions.

An example of the need for validation is afforded by considering the following approach which might be employed to analyze Loran fix errors. Given experimental data on the timing errors in the readings taken from Loran receivers, it is possible to translate this data into information on the distance errors in the lines of position corresponding to the Loran readings. A statistical evaluation of the fix errors caused by timing errors can then be obtained by suitable methods. In addition, an experimental program might be undertaken to obtain data on the performance of human operators in drawing on navigational charts the lines of position that correspond to Loran readings. The study could be designed so that the data would reflect the effects of human inaccuracy in drawing the lines, the map scale, the thickness of the lead in the pencil used, etc. It would then be possible to determine a distribution for fix errors from the data on errors from various sources, including both those associated with the Loran equipment and those arising in the plotting of fixes. However, the results may fail to reflect important sources of error. For

example, since the lines printed on navigational charts for various Loran stations appear in different colors (purple, red, etc.), they are printed separately from the green colored lines of latitude and longitude and, therefore, are subject to alignment errors. Examination of charts actually used by navigators reveals that this source of error can, in some cases, be as significant as the Loran timing errors, yet it is one that can easily be overlooked. How can one be certain that he has not overlooked other significant error sources, particularly the causes of rare, but critical blunders? Clearly, a satisfactory check on an error analysis requires a large sample of independent measurements of errors from the actual distribution.

VI. CAPACITY OF AIR TRAFFIC SYSTEMS

1. Definition of Capacity

In discussing the relationship between separation standards and traffic capacity, some authors have compared the volume occupied by a single aircraft, given by the product of the lateral, longitudinal and vertical separation minima, with the total volume of air space presently utilized by aircraft. This type of comparison fails to bring out several important features of the air traffic control process. It is not possible to fill the available air space completely because of the random pattern presented to the controller by the aircraft entering the region. This simple volume comparison greatly overestimates the actual capacity of the system, and the extent to which capacity is overestimated varies from one set of traffic control procedures to another. A second difficulty arises when one attempts to compute the total volume of air space available. If the lateral dimension of available air space is taken as the envelope of all flight paths traversing the North Atlantic in a given year, the fact that there tends to be a concentration of flight plans around the so-called minimal time route on any given day is obscured. But it is precisely this lateral concentration of filed flight plans which has contributed to the present state of congestion in the North Atlantic. An additional contribution is made by the randomness in the arrival times of entering aircraft.

These features of the North Atlantic environment limit the number of aircraft that can be accommodated in a given period of time, without lateral revisions of requested flight plans or undesirable altitude changes. The number of aircraft which can be so accommodated corresponds to our intuitive notion of the traffic handling capacity of a system. In the subsequent discussion, we shall introduce a formal definition of capacity, applicable to a variety of systems including the present one. For heuristic purposes, we shall first estimate the maximum number of aircraft that might be accommo-

dated per hour by the present system, when only the lateral concentration of flight plans is considered and the ideal condition is assumed that aircraft arrive at equally spaced time intervals. We shall then indicate the effect on capacity of random aircraft arrivals. The following remarks are made with specific reference to westbound jet traffic, although similar statements also apply to eastbound traffic.

An estimate of the maximum number of requested flight plans that can be cleared per hour, by the Shannon-Prestwick OCA, without lateral revisions or undesirable altitude changes, may be determined as follows: when the datum line technique is used, the flight levels 280, 310, 330, 350, 370, and 390 are available to westbound flights. Level 390 is unusable for almost all flights, and not many carriers regard level 280 as desirable. Level 370 is attainable by only a minority of flights. In order to simplify the present discussion, we shall assume that the other three levels are all equally acceptable to the carriers. If all filed flight plans conflicted laterally, then each of these three levels could be interpreted as a channel into which at most one aircraft can be fed at any given time without lateral revision of the requested flight plan. With a longitudinal separation of 30 minutes, the three flight levels could then accommodate a maximum of six aircraft per hour. It should be allowed, however, that occasionally two filed flight plans with less than 30 minutes separation may be free of lateral conflicts across the entire oceanic region and, in addition, that some carriers are able and willing to accept levels 280 or 370. On rare occasions, level 390 can also be used. At times, therefore, there are more than three useful channels in the system; and each channel is sometimes able to accommodate more than one aircraft within a time interval of thirty minutes An ARCON study of data furnished by the Prestwick Control Center on filed flight plans reveals that a maximum average of about ten aircraft per hour could be accommodated by the system, without imposing undesirable flight plan revisions, if aircraft arrived at the OCA

boundary at equally spaced time intervals. This estimate may be optimistic, since it is based on the assumption that the controller can freely interchange assignments at the flight levels 310, 330, and 350 without significantly penalizing the carriers.

Moreover, the preceding estimate must be reduced drastically, because the assumption that aircraft arrivals are evenly spaced in time is not realistic. An ARCON study of data furnished by Prestwick reveals that aircraft arrivals at the eastern boundary of the Shannon-Prestwick OCA are randomly distributed in time and may be realistically represented by a Poisson distribution. The effect of the random character of aircraft arrivals is demonstrated by a comparison of filed flight plans with those that are actually cleared in the present system. The comparison shows that, when aircraft arrive at an average rate of 5 aircraft per hour, more than 10% of the arrivals are diverted laterally. These figures contrast sharply with the previously determined estimate of the ability of the system to accommodate traffic that is uniformly distributed in time.

If a random distribution of aircraft arrivals is assumed, then some revisions of requested flight plans must be countenanced for any traffic system, no matter how low the arrival rate. This is apparent, because the probability is non-zero that arriving aircraft will occasionally accumulate in sufficient numbers to overload any system capable of handling only a finite number of aircraft at any given time. On the other hand, unlimited diversions of aircraft from requested flight plans are not acceptable. Otherwise, the present system would be more than adequate to meet current, as well as all reasonable future, demands. Indeed, if the controller were free to impose unlimited lateral diversions from requested flight plans, then more than 64 aircraft per hour (both eastbound and westbound) could be fed into the Prestwick OCA at the flight levels 310, 330, 350, 370 alone (assuming 30 minute longitudinal and 2° lateral separation rules). If aircraft departures

could also be rescheduled with complete freedom, then more than 1000 aircraft per day (in both directions) could be accommodated by the present system.

The economic penalties associated with such flight plan revisions cannot be ignored, however, and an appropriate definition of system capacity must take them into account. The capacity of a traffic system should therefore be defined in terms of the maximum acceptable level of ATC imposed economic penalties. It is not the function of this study to determine this maximum level; however, it has already been demonstrated that it cannot realistically be reduced to zero. Accordingly, we shall adopt the following definition of system capacity:

> The capacity C_r of a system is that level of saturation, represented by the number of entering aircraft per hour, at which r% of the entering traffic must be recleared to an alternate route involving significant economic penalty.

The capacity C_r is defined in terms of an unspecified number, r, which is called the rejection rate. In examples given in Section VIII, various systems are compared on the basis of capacities computed at a 5% rejection rate. However, the final choice of r must be determined by the responsible agencies.

Mathematical techniques for evaluating the capacity C_r of a system are derived in Appendix F and discussed qualitatively in the next Section. Before proceeding with this discussion, it should be emphasized that the capacity of a system is independent of the density of traffic entering the system. Capacity is an intrinsic feature of the system and exists even in the absence of traffic. If traffic enters at a rate exceeding the capacity C_r, then requested flight plans will be rejected at a rate greater than r. If the traffic density is less than C_r, then rejections will occur at a rate lower than r.

2. Discussion of Mathematical Techniques

A mathematical model presented in Appendix F makes it possible to evaluate the traffic handling capacity of the North Atlantic System, not only in its present form, but also under various modifications of the environment, procedures, and separation standards. In this model, an air traffic system is characterized by the parameters k, T, and c, where k is the number of channels or flight levels into which entering aircraft are fed, T is the longitudinal separation standard measured in minutes, and c is the probability that a lateral conflict in the flight plans requested by two aircraft, entering the system with a longitudinal separation less than T, prevents clearance of both flight plans at the same altitude.

The longitudinal separation standard, T, is assumed in the model formulation to be a constant for all pairs of aircraft. The model is therefore appropriate for systems in which all air speeds are identical. It may also be applied to systems in which small variations in air speed sometimes cause the longitudinal separation standard to be increased, so long as the average applied separation, $T + \Delta T$, is such that ΔT is a small fraction of the basic separation standard T. This condition is satisfied in the case of subsonic jet traffic. Special consideration is given in Section VIII to a system modification, recently approved by ICAO, whereby a reduced longitudinal separation is permitted only for aircraft on the same or diverging tracks.

The analysis in Appendix F is initially based on the assumption that the controller is free to reassign aircraft to channels (flight levels) other than the requested one. The k system channels are all considered equally useful. A different model is then considered in which the controller's prerogative to reassign altitudes is limited in a more realistic manner. This second model requires computer simulation techniques. A study of the two models shows that the increase in realism does not significantly improve the final results, especially when they are used to compare the performances of alternate

systems. The simpler model is therefore used to obtain numerical results for a wide range of system parameters. This range is adequate to provide useful comparisons of the relative performances of a large variety of systems.

An additional assumption is made in Appendix F that those aircraft which are diverted laterally are separated sufficiently from the main traffic system so that they do not interfere with clearances of flight plans for aircraft entering the system later. In some cases, this assumption results in an overestimate of the capacity of systems; however, the error in the estimate is small, unless the percentage of aircraft which are diverted laterally is large. Moreover, the comparison of alternate systems, in terms of their relative capacities, is not affected significantly.

Under these assumptions, it is shown in Appendix F that, if aircraft enter the system at random times and at an average rate of λ aircraft per time interval T, then the probability, P, that an arriving aircraft is diverted laterally is given by an equation of the form

$$P = f(k, c, \lambda) \quad . \tag{VI. 1}$$

The precise form of eq. (VI. 1) is given in Appendix F and has been used to determine P as a function of the traffic density λ, for various fixed values of the system parameters k and c. The results are shown in Figures F-1 to F-10. We shall now interpret these results and indicate how they may be used.

It will be initially supposed that economic penalties are associated only with lateral diversions of aircraft from requested flight plans. Later, when the mathematical model is used to analyze the existing system or various proposed modifications, an appropriate adjustment will be made for the limited utility of certain flight levels to jet aircraft. In this connection, it is significant that pilots tend to prefer altitude diversions to lateral

revisions, up to a point. As indicated in Section VII, a diversion to a lower flight level than the one requested usually results in greater fuel consumption but more timely arrival of the aircraft.

Under the assumption that significant economic penalties are associated only with lateral diversions of aircraft from requested flight plans, the probability P defined by eq. (VI. 1) represents the rate at which flight plans are rejected with economically significant consequences. For a system characterized by fixed parameters k and c, eq. (VI. 1) defines P as a function of the traffic density λ only. Since λ designates the number of aircraft entering the system per time interval T and T is measured in minutes, $\frac{60\lambda}{T}$ represents the number of aircraft entering per hour. Suppose that a rejection rate r has been designated as the maximum acceptable level of aircraft diversions. This means that the capacity C_r of a system, characterized by the parameters k and c, is

$$C_r = \frac{60\lambda_r}{T} \quad , \tag{VI. 2}$$

where λ_r is that traffic density for which

$$P = f(k, c, \lambda_r) = \frac{r}{100} \quad . \tag{VI. 3}$$

That is, λ_r is the maximum traffic density that the system can handle, with not more than r% of the entering traffic diverted laterally.

To be specific, let us consider the North Atlantic System under the environment, procedures, and separation standards in effect during the summer months of 1961. We shall concern ourselves with the capacity of the system to handle westbound traffic when the datum line technique was

employed. This means that the flight levels 280, 310, 330, 350, 370 and 390 were all available. However, level 390 was almost never used, and levels 290 and 370 together were used only about 30% as often as any one of the levels 310, 330 or 350. Thus, we may consider that the system had effectively more than 3 but less than 4 desirable and fully useful channels. A study of requested flight plans during the summer of 1961 reveals that the average rate at which lateral conflicts occurred between pairs of requested flight plans was $c = 0.7$. We may therefore suppose that the probability P of lateral diversion of an aircraft entering the system lies between the corresponding probabilities for two systems with $k = 3$ and $k = 4$ channels, respectively, and with both systems characterized by the parameter value $c = 0.7$.

In the case of the 3-channel system, P may be determined for various values of λ from the curve in Figure F-3 labeled $c = 0.7$. Similarly, P may be determined for the 4-channel system from the corresponding curve in Figure F-4. The values of P determined from these curves for the traffic densities $\lambda = 2.5$, 3.5, and 5.5 (aircraft per time interval T) are presented in Table VI-1. For a longitudinal separation rule of T = 30 minutes,* these values of λ represent traffic densities such that aircraft enter the system at the rates of 5, 7, and 11 aircraft per hour, respectively. The last column of Table VI-1 shows the rates at which aircraft were diverted laterally on occasions when these traffic densities were actually attained during the summer of 1961. Most of the values in this column lie between those in the preceding two columns, as predicted, and indicate reasonable agreement between practical results and theoretically determined system performance.

---

*A value of T = 30 minutes underestimates the average applied longitudinal separation, because of occasional adjustments required to compensate differences in air speed.

TRAFFIC DENSITY		LATERAL DIVERSION RATE		
λ (aircraft/T)	$\frac{60\lambda}{T}$ (aircraft/hour)	3-channel system model	4-channel system model	North Atlantic System, Summer 1961
2.5	5	16%	6%	10-20%
3.5	7	25	12	21
5.5	11	39	25	28

Table VI-1

For a 5% rejection rate and a parameter value c = 0.7, the capacities of systems with 3, 4, and 5 channels are, respectively, 2.6, 4.6, and 6.8 aircraft per hour, as indicated in Figures F-3 to F-5. Therefore the capacity of the North Atlantic system would have been less than 7 aircraft per hour during the summer of 1961, if lateral diversions had been limited to the 5% rate and all flight levels (except 390) had been equally useable. Because of the limited use made of levels 290 and 370, the actual capacity at the 5% rejection level was less than 4 aircraft per hour.

In this analysis of recent system performance, we have associated economic penalties only with lateral diversions of aircraft from requested flight plans but have taken into account the limited usefulness of certain flight levels. Most ATC imposed changes in altitude were only 2,000 ft. in magnitude, with few exceeding 4,000 ft. However, if it is desired to associate economic penalties with all changes in flight level, as well as changes in latitude, it is then appropriate to represent the system as an aggregate of independent 1-channel subsystems, where each subsystem corresponds to a flight level. The capacity of the system is then limited to the sum of the

capacities of the subsystems and is smaller than the capacity of a system in which interchange of flight levels is allowed without penalty. Indeed, it is found from Figure F-1 that, when aircraft enter the system at a rate of 4 aircraft per hour, diversions in flight level or latitude occur at a rate exceeding 25%.

3. Analysis of System Modifications

In the last Section, the application of numerical results presented in Figures F-1 to F-10 was illustrated by an evaluation of the traffic capacity of the North Atlantic System during recent operation. In this Section, we shall indicate how the results of Appendix F may also be used to predict the effects of changes in the separation standards, procedures, and environment. This discussion will be brief, since a more detailed quantitative analysis of certain specific systems is given in Section VIII.

Eqs. (VI. 1) – (VI. 3) show that system capacity is determined as a function of the parameters k, T, and c. It is easily seen that these parameters reflect the effects of all three separation standards, as well as several features of the environment and procedures. The number of channels, k, depends upon the vertical separation standard and the operational limitations of aircraft. The probability, c, of lateral conflict in two requested flight plans is a function of the lateral separation standard, the effect of wind forecasts in spreading the various MTP's computed on the same day, and the geographical extent of the oceanic region over which a flight plan is checked for conflicts before clearance is granted. T is, by definition, the longitudinal separation standard itself.

Thus, the effect on capacity of proposed system modifications may be estimated by determining the concomitant changes in the parameters k, T, c and then computing the capacity associated with the modified system. For this purpose, the numerical values in Figures F-1 to F-10 may be used in the manner already described.

In order to assess the capacity of a system with an organized route structure, e.g., a fixed route system or the "jet reference system" described in Section VIII, one may first compute the capacity of each route, considered as an independent subsystem. If there are k flight levels along a particular route, then a k-channel subsystem may be associated with that route. The parameter value c = 1 applies to the subsystem, since the flight plans of all aircraft choosing to fly on the associated route necessarily conflict laterally. If there are n different routes, then the overall system may be considered as an aggregate of n different subsystems, and the total capacity is the sum of the subsystem capacities. This latter statement holds only if the controller does not divert aircraft from one route to the other. On the other hand, if economic penalties are not associated with diversions of aircraft from one route to another, then the capacity should be computed for a single system with the total number of channels equal to the sum of the channels associated with each of the various routes. These remarks will be illustrated by specific examples in Section VIII.

It is also possible to analyze the effect of a shift of the present, essentially strategic control system toward a more tactical control doctrine. The most likely shift in this direction would be a reduction in the extent of the region over which advance clearances are required. An immediate result would be a smaller value of the system parameter c. Moreover, since a system modification of this type is not likely to be countenanced before communications are greatly improved, it is possible that a reduction in the longitudinal separation standard T might also be justified. The increase in capacity that accompanies the reductions in the parameters c and T can be determined directly from eqs. (VI. 1) – (VI. 3) and the numerical results in Figures F-1 to F-10.

It is apparent, of course, that the improvement in capacity to be achieved by proposed system modifications should be related to anticipated

traffic loads. It is important to consider not only traffic loads, expressed in numbers of aircraft per day, but also the distribution of traffic in time and space. For this reason, traffic density has been defined in terms of an hourly, rather than daily rate. The percentage of requested flight plans which are rejected will obviously vary during the day with traffic density. Since the largest rejection rate occurs during traffic peaks, it may be desired to minimize this maximum rate. On the other hand, if it is desired only to restrict the total number of flight plan rejections during the course of a day, then the daily rejection rate may be computed by averaging the system performance, determined by the methods of Appendix F, over different periods of the day.

VII. ECONOMIC FACTORS

All air traffic control systems impose restrictions on the flight paths of the aircraft under their control. As a general rule, efficient use of air space can be achieved only by organizing the flow of traffic. Gains in traffic handling capacity must be balanced against the economic penalty associated with the restrictions on the operators' freedom of route selection. Therefore, it is necessary to evaluate these economic penalties before procedures can be developed which represent an acceptable compromise.

In this Section, only two types of penalties will be considered. First, restrictions in the vertical dimension which involve extra fuel costs will be examined. Then the penalties resulting from lateral diversions and restrictions will be discussed. The conclusions and numerical values presented in this Section apply only to jet aircraft operating at air speeds in the 480 knot range and at altitudes of 28,000 feet or higher. The Section concludes with an evaluation of the penalties associated with organized systems of the jet reference type. Jet reference systems, as defined in Section VIII, are organized route structures which vary from one day to the next with routes that parallel the MTP.

It is difficult to establish a reasonable comparison of vertical and lateral restriction penalties. Using a fuel flow rate of two hundred pounds per minute, one can translate the extra fuel consumed into minutes of flight. Such a comparison, however, conceals the fact that altitude diversions (usually to a lower flight level than that requested) usually mean higher air speed, and the flight time for the entire trip is often decreased. The penalty of higher fuel consumption is thus offset by the timely arrival of the aircraft at its destination. A more reasonable comparison might be made between the cost of the extra fuel for altitude restriction and the direct operating cost for the time lost in a route change. At current jet fuel prices, the fuel cost

is only about 13% of the direct operating cost. The economic value of maintaining schedule, however, must ultimately be determined by the operators.

1. Penalty for Vertical Diversion

Fuel penalties vary in a nonlinear manner with departure from optimum altitude. The penalty for small changes in altitude is slight but it increases rapidly as the altitude deviation increases. The requirement for constant flight level across the entire North Atlantic is in itself a penalty since the optimal flight profile is a gradual climb. The best choice of constant altitude flight level carries a penalty of about 800 pounds of fuel when compared with an optimum climb cruise. The optimum constant altitude flight level is often very nearly the highest altitude that the aircraft can achieve initially. Diversion, then, is usually to a lower altitude. For constant altitude flight 2000 feet below optimal constant altitude flight level, the penalty is 2300 pounds of fuel, for 4000 feet below optimum, 4200 pounds, and for 7000 feet below optimum 8200 pounds. These values were calculated for a Boeing 707-321 operating at Mach .82. They apply to a distance of 1700 air miles which is the appropriate value over the North Atlantic Oceanic air space for a westbound aircraft.

If the aircraft's gross weight at altitude is 270,000 pounds upon entering the oceanic region, the optimum constant altitude is flight level 350 (assuming standard temperature). The restrictions listed above can then be interpreted as clearances at flight levels 350, 330, 310, and 280 respectively. Table VII-1 summarizes these penalties and lists the corresponding dollar cost.

Flight Level	Excess Fuel* (pounds)	Fuel Cost (dollars)
350	800	18
330	2300	51
310	4200	92
280	8200	180

Table VII-1

Examination of records of flights through the Shannon-Prestwick OCA reveals that flight level revisions of 2000 and 4000 feet occur more frequently than route revisions, but that altitude changes of 6000 feet or more are rare.

2. Penalty for Lateral Diversion

Most of the flight plans filed for North Atlantic crossings are approximations to the minimal time path (MTP). In Appendix G, the average time penalty for diversion from the MTP is calculated. The analysis assumes that the MTP is known precisely. It can be shown that the penalty for diversion from an approximation to the MTP does not differ significantly from the penalty for diversion from the true MTP.

The results of the analysis of Appendix G are summarized by the approximating formula:

$$\bar{\tau} = \frac{P_M^2}{2A}\left[\frac{1}{D} + \frac{1}{C}\right] , \qquad \text{(VII. 1)}$$

*Excess over optimum climb cruise.

where:

$\bar{\tau}$ is the average time penalty (in minutes) for following an alternate route rather than the MTP.

A is the air speed of the aircraft (in n. mi. per min.).

P_M is the maximum lateral separation (in n. mi.) between the MTP and the alternate.

D is the length (in n. mi.) of the MTP segment corresponding to the divergent portion of the alternate.

C is the length (in n. mi.) of the analogous MTP segment for the convergent region.

Eq. (VII. 1) is suitable for computing average time penalties associated with a wide variety of alternate route structures, some of which are illustrated in Figure VII-1. It should be noticed that eq. (VII. 1) does not include a parameter for the length of the region in which the alternate route parallels the MTP. Average time penalty is only slightly affected by the length of this parallel region.

The penalty associated with a lateral diversion from the MTP depends on the geometry of the alternate route as well as the magnitude of the required lateral displacement. If the alternate diverges from the MTP laterally by 60 n. mi. in a single ten degree interval (e.g., Figure VII-1a or VII-1b) and later returns to the MTP in the same manner, the average penalty is about 1.3 minutes. If, on the other hand, a dispatcher is aware that a 60 n. mi. separation from the MTP must be maintained throughout the North Atlantic portion of a flight, he can usually plan a route (e.g., Figure VII-1c) which carries an average penalty of only 0.5 minutes. A 120 n. mi. lateral diversion in a ten degree interval carries a penalty of 5 minutes but if, as before, the 120 n. mi. diversion can be taken into account during flight planning, the penalty can be reduced to only 2 minutes. These penalties can be assigned a dollar value by assuming a direct operating cost of $2000. per hour. The results are summarized in Table VII-2.

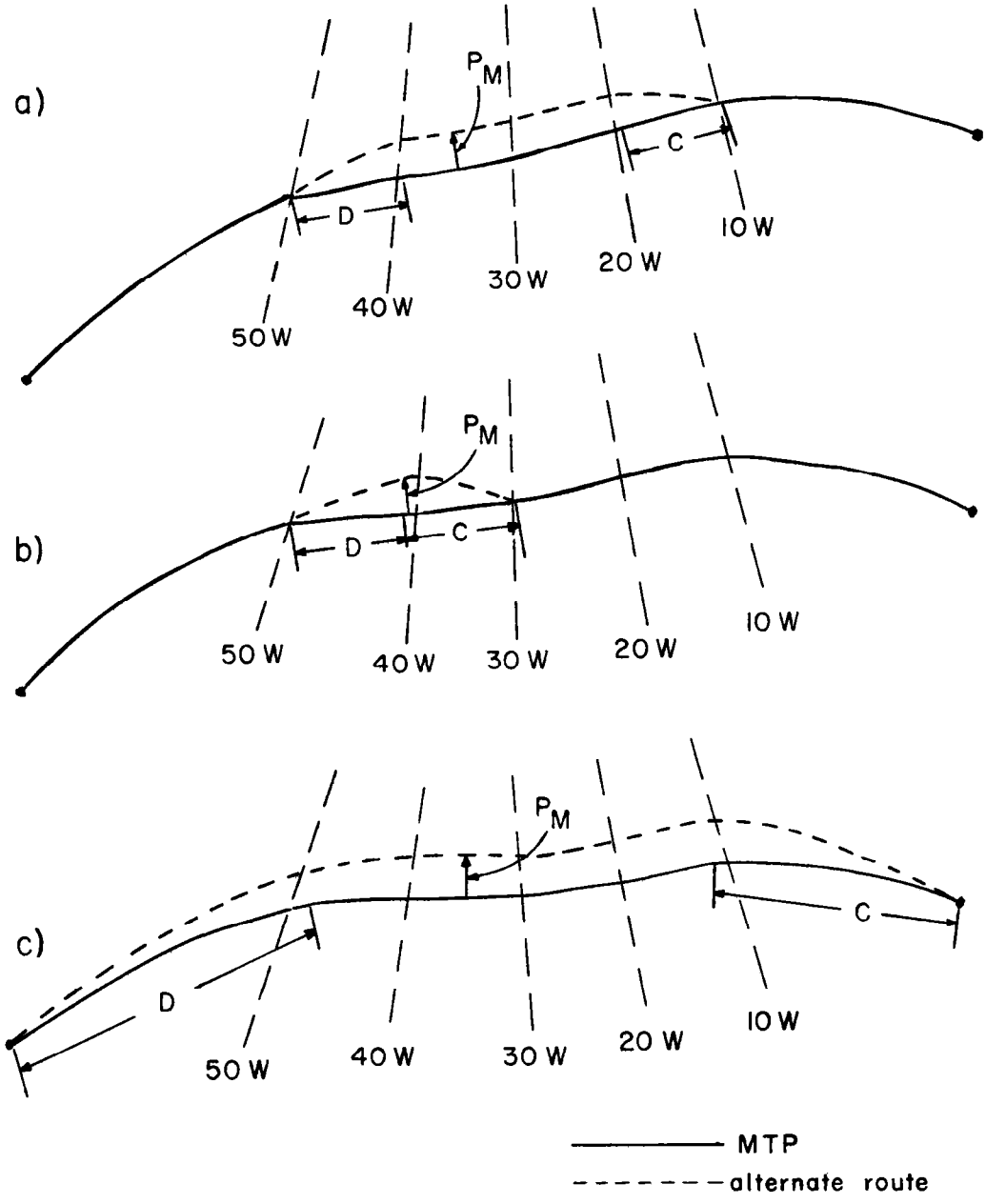

Fig. VII-1 Examples of Alternate Route Configurations

Lateral Deviation	Average Time Penalty (min)	Direct Operating Cost (dollars)
60 n. mi in 10°	1.3	42
60 n. mi. (preplanned)	0.5	17
120 n. mi. in 10°	5.0	167
120 n. mi. (preplanned)	2.0	67

Table VII-2

The penalties tabulated above refer to diversion from the requested route. Since the requested route is based on forecast winds, it is usually not the true MTP. Analysis of data presented in a report[22] on paper jet operation show that the average flight time on a forecast MTP is about 4.6 minutes longer than the average time on an exact MTP. Although this figure is based on a sample of 322 computed flight times, it is believed to be only a rough estimate because of the extreme variability of the individual flight times. Converting to a dollar value on the same basis as before, one finds that the potential saving which would result from perfect wind forecasts is about $150. per flight.

At the time eq. (VII. 1) was derived, no statistical data were available to check its validity. Since then, however, MTP studies conducted for the FAA by the Stanford Research Institute have yielded some preliminary results. An interim report[23] presents numerical values of time penalty for deviations from the MTP. These values were computed by plotting the MTP and computing the flight time on this path, laying out an alternate route and computing the time on the alternate route, and then subtracting the MTP time from the

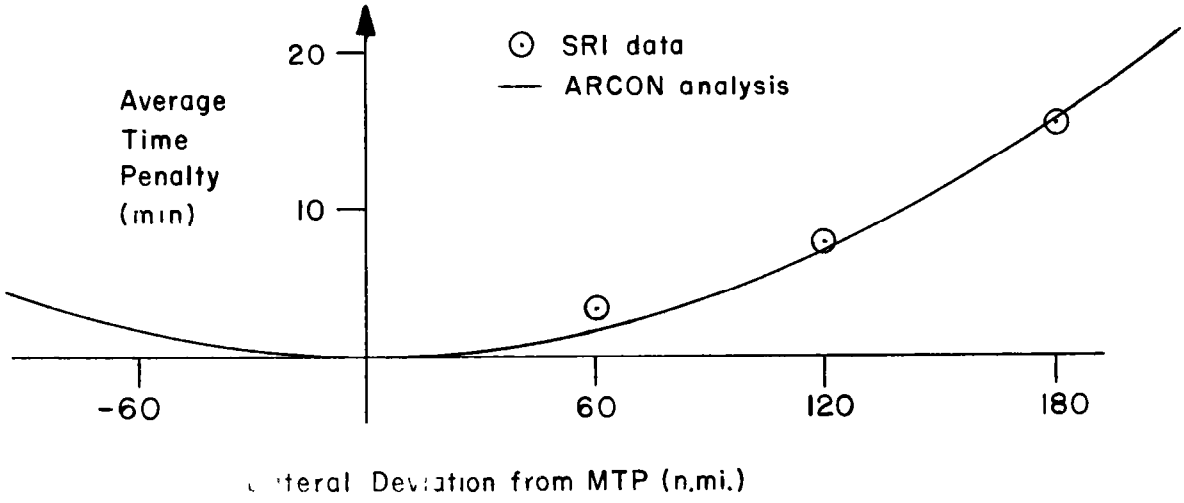

Fig VII-2 Average Time Penalty (500 kt airspeed)

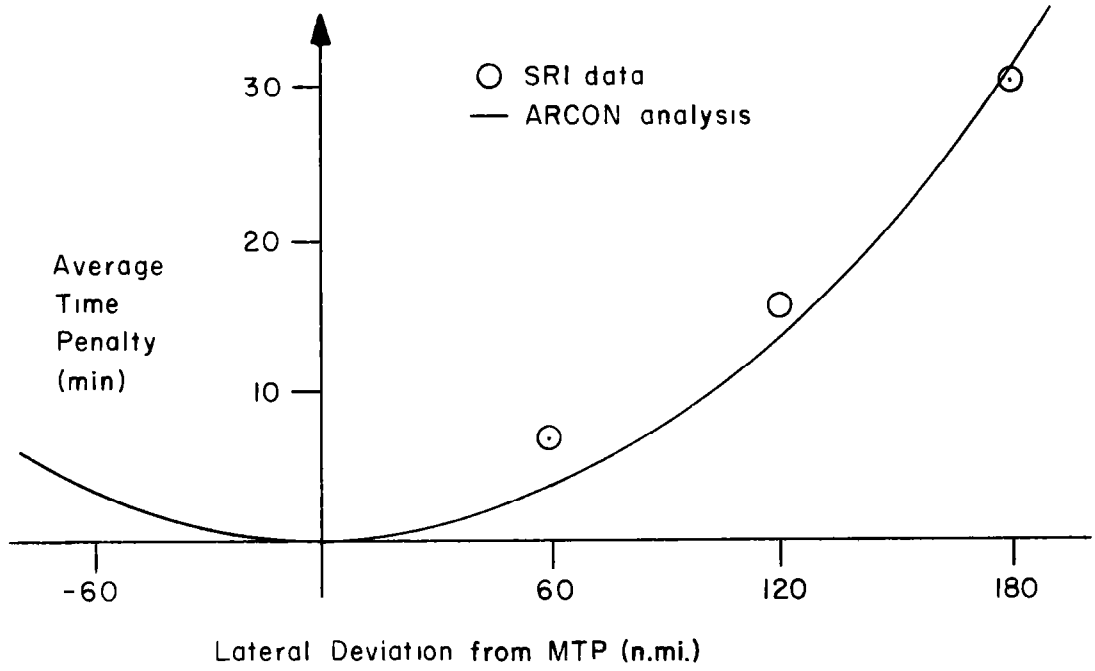

Fig. VII-3 Average Time Penalty (250 kt. airspeed)

alternate time. The cases treated include three different altitudes, two different air speeds, and three different values of maximum lateral deviation. In all cases, the geometrical layout of the alternate route (characterized by the lengths of the divergent and convergent regions) was the same. In terms of the parameters used in the ARCON analysis, the range of cases studied by the Stanford Research Institute can be summarized as follows:

A – 250 and 500 kts.

P_M – 60, 120 and 180 n. mi.

D – 250 n. mi.

C – 250 n. mi.

For each case, both eastbound and westbound MTP's on the 0000 GCT and 1200 GCT wind charts were studied.

Although these initial results do not constitute a large enough sample for a statistically sound estimate of average time penalties, it is still appropriate to compare them with values computed from the ARCON analysis. Such a comparison is presented in Figures VII-2 and VII-3. The curves in the two figures correspond to the ARCON analysis. Average time penalty ($\bar{\tau}$) is plotted against maximum lateral deviation (P_M). Figure VII-2 applies to the 500 kt. air speed while Figure VII-3 applies to the 250 kt. air speed. In both Figures the value 250 n. mi. was entered for both D and C. The circled points in the figures represent the SRI data. Each point is the average of four values (eastbound-westbound; 0000–1200 GCT) in Figure VII-2, and eight values (500 mb and 700 mb) in Figure VII-3.

Although the eastbound and westbound penalties might be assumed statistically independent, the correlation between the noon and midnight weather systems is high enough so that the penalties for same direction flights are correlated. Thus the average of four SRI values is a poorer

estimate (statistically) of the average time penalty than that which would be obtained from four independent samples. The close agreement of curves and points is fortuitous.

The Stanford Research Institute study is still in progress. A larger data sample will be useful in establishing the validity of the ARCON analysis. It is expected that the results will confirm the essentially parabolic effect (P_m^2) of the maximum lateral deviation and the inversely proportional effect ($\frac{1}{A}$) of air speed.

3. Economic Penalties in the Jet Reference System

In present practice, oceanic controllers freely reassign flight levels when the traffic load is high. If we assume that the same procedure will apply in an organized route system, the vertical restriction penalties for the two types of systems will be similar. In this Section, then, only lateral restriction penalties will be discussed.

Because of differences in forecasts and in flight planning techniques, the pattern of requested routes in the North Atlantic exhibits a random character. It is therefore difficult to make a direct estimate of the economic penalties which would result from the adoption of an organized route structure. If it is assumed that all aircraft have a common origin and destination and that the MTP is precisely defined, the calculated penalty will overestimate the actual mean loss. For a two track jet reference system (one track on either side of the MTP) the average time penalty is 0.5 minutes per flight (since the dispatcher could match the entire route to the oceanic route structure). For a three track system, one third of the aircraft (or perhaps a greater fraction during off peak loads) could fly the MTP while the remainder would be diverted two degrees north or south. The average penalty is 2/3 (2.0) or 1.3 minutes per flight.

In reality, however, the pattern of filed routes spreads considerably

in the lateral dimension. A westbound traffic sample of four peak days has been analyzed to determine the lateral spread of filed flight plans. On all four days, 80% of the flights at 20 W and 30 W were included in a lateral band four degrees wide. Although the majority of flight plan pairs were in lateral conflict at some point within the oceanic region, most of the requested routes tended to run parallel to one another rather than cross back and forth. If all paths were parallel, the adoption of the jet reference system would require one degree changes for only half of the aircraft, leading to an average penalty of only 1/2 (0.5) or 0.25 minutes. At least three tracks would be required to accommodate the spread of requests.

The method of establishing the reference MTP for an organized system should also be considered. If the reference MTP is a compromise or average of MTP's determined by a number of different operators it is reasonable to expect that this path is a better estimate (statistically) of the true MTP than any single operator's estimate. Some of the potential gain of 4.6 minutes associated with accurate MTP forecasts could be realized, and the gain may outweigh the losses.

In Section VIII it is shown that the capacity of the three track jet reference system exceeds that of the present free strategic system by a significant margin. The existing system is heavily loaded. During peak periods lateral revisions have been imposed on 10 to 20% of the traffic. The penalty for these revisions is severe because they are executed on a tactical basis. The jet reference system could easily accommodate present peak loads. In addition, traffic loads which must suffer altitude revision in the present system could be handled by the jet reference system without frequent altitude changes.

VIII. POTENTIAL SYSTEM IMPROVEMENTS

1. Introduction

The performance improvements that may be realized by different system modifications, considered either separately or in combination, will be analyzed in this Section. In Section 2, the advantages of reductions in separation standards, resulting primarily from changes in the environment, are evaluated. The performance of certain organized route systems is discussed in Section 3, and other procedural and environmental changes are considered in Section 4.

2. Reduced Separation Standards

In this Section, we shall consider the improved system performance that may be realized when modifications in the present environment permit one or more of the separation standards to be reduced. It will be assumed that no changes are made in procedures, unless the contrary is specified. Improvements in the environment which might justify reductions in the separation standards include:

Lateral Standard:	Improvements in navigation which lead to more accurate lateral track-keeping.
Vertical Standard:	Improvements in altimeters and in altitude holding.
Longitudinal Standard:	Improvements in wind and temperature forecast data, or in Machmeters, which lead to more accurate ETA's.
	Improvements in both navigation and communication which lead to more reliable enroute control of longitudinal separation.

We shall not attempt to define quantitavely the environmental changes that are required to justify a reduction in any given standard, since this

problem is considered in Section V. Instead, our present concern is with the increase in traffic capacity and economic benefits that may be derived from such reductions. For purposes of comparison, it will be useful to recall that the capacity of the present system was estimated in Section VI as 4- aircraft per hour. This estimate was computed for a 5% rejection rate and a 30 minute longitudinal separation standard.

Let us first consider a reduced longitudinal separation standard, T, which is applied uniformly to all pairs of jet aircraft. Eq. (VI.2) reveals that capacity is inversely proportional to T. That is, halving the longitudinal separation standard would double the capacity of the system. This statement is optimistic, however, since a uniform separation requirement is not employed in practice. The average applied separation, $T + \Delta T$, exceeds the basic separation standard, T, because of occasional adjustments required to compensate differences in air speed. Clearly, a reduction of T does not imply a proportionate reduction of $T + \Delta T$. Moreover, the increment, ΔT, becomes more significant as T decreases. A more accurate estimate of the increase in capacity that accompanies a decrease in the longitudinal separation standard requires a statistical determination of ΔT. Information obtained informally from controllers suggests, however, that ΔT is small for jet aircraft. Consequently, the error in the estimate of the increase in capacity, implied by eq. (VI.2), should be small for a reasonable reduction of T.

A recent ICAO ruling authorizes a reduction of the longitudinal separation from 30 minutes to 20 minutes for aircraft at the same altitude and with identical or diverging flight plan tracks. An ARCON study of flight plan data furnished by the Prestwick Control Center indicates that the conditions required for application of the 20 minute rule are satisfied by less than 10% of all pairs of filed flight plans. Therefore, only a negligible increase in system capacity is indicated.

In order to estimate the effects of changes in the other separation standards, the present system may be represented as an intermediate case between a 3-channel and a 4-channel system. The reasonableness of this representation was demonstrated in Section VI.

Let us now suppose that the lateral separation standard is cut from 2° to 1°. A study of data on requested flight plans suggests that the probability, c, of lateral conflict in two requested flight plans would be reduced from about 0.7 to 0.5. The curves in Figures F-3 and F-4, corresponding to these values of c, indicate that system capacity would increase by less than 40%. This result holds, providing all other system characteristics remain the same and capacity is defined with respect to a 5% rejection rate for both the 1° and 2° separation rules.

It is possible, however, that if the lateral separation standard were reduced, then the allowed rejection rate might be increased because the smaller lateral diversions required to resolve conflicts carry smaller economic penalties. In this case, a greater increase in system capacity would be realized. For example, if the lateral separation standard were halved and the rejection rate doubled, then system capacity would nearly double.

The effect of a reduction in the vertical separation standard is reflected by an increase in the number of system channels, k. If the standard were cut in half, then the number of channels would be doubled. Examination of the appropriate curves in Figures F-1 to F-10 reveals that, if all system characteristics are held constant, then the capacity, defined at a 5% rejection rate, is more than tripled. This result depends upon the assumption that the controller is free to assign any available altitude to an aircraft entering the system, whenever reassignment is needed to resolve conflicts in the filed flight plan.

The effect of allowing the controller freedom to reassign altitudes to

entering aircraft may be illustrated by comparing two cases. Let us consider, in one case, a system with five flight levels in which the controller may assign any available altitude to an entering aircraft in order to resolve conflicts in the requested flight plan. In the other case, we shall also consider a system with five flight levels; however, the controller is never allowed to reassign altitudes, and conflicts are resolved only by lateral diversions. The parameter values c = 0.7 and T = 30 minutes are assumed for both systems. The first case may be represented as a 5-channel system and the second case as an aggregate of 5 independent 1-channel subsystems. The capacity of the latter system is five times that of a single 1-channel system, or about 0.8 aircraft per hour, at the 5% rejection rate. On the other hand, the capacity of the 5-channel system, at the same rejection rate, is 7.0 aircraft per hour.

This striking contrast in the capacities of the two systems suggests that the new ICAO ruling which prevents VFR changes in flight level through intermediate occupied levels will have an important effect on system capacity. Although the controller will still have some freedom to reassign altitudes and the system will still have a greater capacity than could be attributed to an aggregate of separate 1-channel subsystems, it is nevertheless clear that the ICAO ruling will result in a significant increase in lateral diversions. This ruling was established, of course, because of considerations of safety rather than of capacity.

If the controller were not allowed to reassign altitudes at all, so that the system were effectively an aggregate of independent 1-channel subsystems, then halving the vertical separation standard would only double the capacity of the system. In actual practice, a reduction of the vertical separation standard from 2000 ft. to 1000 ft. would more than double, but less than triple, the capacity of the present system.

It is apparent that an important gain in system performance would be

realized from a more efficient use of available flight levels. Because VFR climbs through occupied levels are no longer permitted for aircraft entering the North Atlantic System, there is a strong argument for coordinated domestic-oceanic planning of altitude assignments for departing aircraft. The advantages of such coordination are discussed further in Section 4.

3. Organized Routes

In this Section, we shall consider the changes in system performance that would result if the present free route structure were replaced by a particular organized structure known as the "jet reference scheme." In this scheme, it would be the function of air traffic control to select on each day a track which corresponds most closely to the majority of the westbound MTP's determined by the operators and to lay out across the ocean two parallel tracks, one 1° north of the selected track and one 1° south of it. Similarly, two parallel tracks would be determined for eastbound traffic. All aircraft would be permitted to fly only on one of the two available parallel tracks or on other tracks separated from them by at least 2°. Alternatively, a 3-track system might also be considered which includes the selected track and a track separated from it by 2° on each side.

We shall evaluate the performance of these systems, first under the present environment and separation standards and then with separation standards reduced. A similar evaluation could also be made for fixed route systems. It should be pointed out, however, that greater economic penalties are associated with a fixed route structure than with one that varies from day to day with the weather. It will become apparent, moreover, that it is the organization of the routes rather than their absolute positions that contributes to the traffic handling capacity of the system.

In the following analysis, we shall consider westbound jet traffic specifically, although similar remarks will also apply to eastbound traffic.

It was shown in Section VI that, when the datum line technique is in effect, the present North Atlantic System, with its free route structure, has a capacity exceeding that of a 3-channel system but less than that of a 4-channel system. This characterization of the present system is a consequence of the number of available flight levels and certain limitations on the usefulness of some of these levels. The capacity of the system at the 5% rejection level was found to be less than 4 aircraft per hour. This result was obtained for the parameter value c = 0.7, representing the probability of lateral conflict in a pair of filed flight plans.

If we first consider a simplified jet reference scheme in which only one track is laid out across the ocean, then the probability of lateral conflict among pairs of aircraft entering the single track system is c = 1.0. In the present North Atlantic environment, this system may be considered as an intermediate case between a 3-channel system and a 4-channel system, as before, but with a value c = 1.0 instead of c = 0.7. From Figures F-3 and F-4, it is seen that the capacity of the 1-track system is between 1.8 and 3 aircraft per hour, at the 5% rejection level, if a 30 minute longitudinal separation standard is assumed. Under a new ICAO ruling, however, a 20 minute rule would apply to virtually all pairs of aircraft entering a jet reference system, since step climbs are seldom made by aircraft after entry into the oceanic region and, therefore, nearly every pair of aircraft would follow flight plans which either are identical in the vertical and lateral dimensions or provide separation in at least one of these dimensions across the entire region. Therefore a capacity of between 2.7 and 4.5 aircraft per hour, can be attributed to the single track system. A reasonable estimate would be 3.5 aircraft per hour.

We shall now consider a 2-track jet reference system. If we assume that the same number of flight levels that were available in the single track case are now available on each of the two routes, we then have two sub-

systems, each with capacities of about 3.5 aircraft per hour. The total capacity of the system is not the sum of the capacities of the subsystems, unless aircraft diverted from one route never interfere with aircraft requesting flight plans on the other route. At the 5% rejection rate, however, diversions from one route to the other would introduce little interference, and the total system capacity is about 7.0 aircraft per hour.

It may happen on some occasions that the maximum number of flight levels which are afforded by the datum line technique in the present system may not be available on both routes in the 2-track jet reference system. Accordingly, we shall consider the case in which only the flight levels 280, 310, 350, and 390 are available on the track nearest the eastbound routes and the additional levels 330 and 370 are available on the other track. Since levels 280 and 390 receive very little use, the subsystem associated with the former route may be considered as little better than a 2-channel system. In this case, the capacity is only slightly more than one aircraft per hour, at the 5% rejection rate. The capacity of the subsystem associated with the second route has already been determined as about 3.5 aircraft per hour. Thus, the total system capacity is a little over 4.5 aircraft per hour.

It can be shown in a similar manner that the capacity of the 3-track jet reference system is about 10.5 aircraft per hour, when flight levels 330 and 370 are available on all three tracks. If they are available on all but the track nearest the eastbound routes, the capacity is 8+ aircraft per hour.

In considering the effects of changes in the present separation rules on either jet reference system, we may apply the same remarks that were made in the last section to reductions in either the longitudinal or vertical rules. The lateral separation standard has a new significance, however, since it determines the number of tracks that can be fitted into a given lateral band by a jet reference scheme. Cutting the separation requirement to 1° would in some cases double the number of tracks, depending upon the

lateral spread of the westbound and eastbound reference MTP's, and also double the capacity. In the cases where the number of tracks is less than doubled, it can be shown that an increased number of flight levels can be made available on some of the routes and that the capacity would be at least doubled. As previously suggested in Section 2, the allowed rejection rate might also be increased because of the smaller lateral diversions required to resolve conflicts. If, for example, the lateral separation were cut in half and the allowed rejection rate doubled, system capacity would increase approximately 170%.

The conclusions in this and the preceding Section are summarized numerically in Table VIII-1. Each row corresponds to a set of separation standards, with a reduction in at most one of the present standards. The columns correspond to systems with different route structures. The Columns labelled "A" correspond to the case in which the flight levels 330 and 370 are available on all tracks of the jet reference systems. The columns labelled "B" correspond to the case in which these flight levels are not available on the track nearest the routes assigned to traffic in the opposite direction. In the row labelled "1° lateral rule," it is understood that the number of tracks is increased in each jet reference system and that the terms "2-track" and "3-track" in the column headings no longer apply.

The values in Table VIII-1 represent the capacities of various systems when lateral diversions are limited to a 5% rate. A diversion refers only to an ATC imposed change from the filed flight plan track. In each system, however, the flight plan track must be chosen from those that are permitted by the basic route structure of the system. Thus the values in Table VIII-1 do not reflect economic penalties associated with the loss of freedom to choose the route that would be preferred if there were no restrictions on filed flight plan tracks. It is, therefore, important to consider the advantages to an air line of the preferred route chosen under the present system compared

	Present Free Route Structure	2-track Jet Reference System		3-track Jet Reference System	
		A	B	A	B
Present separation standards	4 -	7	4.5	10.5	8
15 Min. Long. rule on same or diverging tracks; 25 min., otherwise	4 +	9 +	6	14	10.5
1° lateral rule*	5 +	14	10.5	21	17.5
1000 ft. vertical rule**	8-12	14-21	9-13.5	20-30	16-24

TABLE VIII-1

Capacity of the North Atlantic with Various System Modifications.***

with the route that would be preferred among the available choices in a jet reference system.

Data collected on flight plan requests suggests that the majority of the lateral revisions, imposed by a jet reference scheme on the routes preferred in the present system, would be 1° in magnitude, with few changes exceeding 2°. In many cases no changes would be required. The parallel routes available in either the 2-track or 3-track jet reference scheme are centered

*A greater increase in capacity may be afforded, if a greater lateral diversion rate is allowed.

**The correct values within the indicated ranges depend upon the extent to which entering aircraft may be reassigned flight levels.

***All capacities are defined at a 5% rejection rate.

about a track determined from the MTP's computed by several air lines. Since forecast MTP's are not actual MTP's, this central track may, on the average, represent a better approximation to the true MTP than one computed by an individual air line.

The lateral revisions imposed by a jet reference scheme would, of course, be known in advance by the air lines. As indicated in Section VII, the time penalty associated with a planned 1° revision in a true MTP carries an average penalty of about 0.5 minutes. The average penalty for a planned 2° revision is about 2 minutes. In considering the advantages of air line computed MTP's (which are based upon forecast rather than actual winds), it should be recognized that, under the present system, future traffic densities may result in even more frequent lateral diversions from filed flight plans than are now imposed upon aircraft entering the oceanic region. Since these diversions cannot be anticipated readily by the air line dispatchers, they carry more significant average penalties than a lateral revision which is planned in advance.

4. Other System Modifications

A general class of system modifications, not considered so far in this Section, take the form of a shift from the present strategic doctrine of control toward a more tactical approach. In a domestic system, a tactical approach is reasonable, not only because of the relatively close monitoring of aircraft positions that is possible, but also because of the distribution of traffic over a number of airways intersecting one another from many directions. In such systems, separation assurances are required only from one intersection to the next, and conflicts may be resolved by temporary, ad hoc flight plan modifications. In the North Atlantic environment, however, most of the traffic tends to move in the same general direction across the entire oceanic region, and a conflict will usually persist over a long period of time unless

resolved by an extended change in the flight plan of one or both of the conflicting aircraft.

Thus, the prevailing traffic patterns in the North Atlantic do not lend themselves readily to tactical procedures. Moreover, a significant shift toward a tactical control doctrine is not feasible without major changes in the present environment. Among the requirements are improvements in communications, navigation, and meteorological forecasting. The introduction of automation in air traffic control procedures might also be required, depending upon the extent of the shift, in order to provide more rapid conflict detection and resolution.

Extensive improvements in communications and navigation would be required to provide the controller with accurate up-to-date information on the progress of all aircraft in his area and to allow him to communicate any instructions needed to resolve conflicts. Improvements in meteorological forecasts would also be needed to enable the controller to predict the relative ground velocities of pairs of aircraft and to detect potential conflicts more accurately.

The extensive improvements required in all three areas cannot reasonably be anticipated for several years. Consequently, it is unrealistic at this time to consider a significant shift toward a tactical doctrine of air traffic control in the North Atlantic. In contemplating the eventual adoption of a tactical system, it should be noted that such an approach is not likely to be consistent with the requirements of supersonic flight. Indeed, economical operation of supersonic craft will require carefully preplanned flights, especially in the vertical dimension, and will not allow the evasive maneuvers essential to a tactical doctrine.

A limited shift toward a tactical approach which might be considered, if communications and navigation were sufficiently reliable, would be a reduction in the extent of the oceanic region over which advance separation

assurances are required. For example, westbound aircraft might be cleared to enter the Shannon-Prestwick OCA if their flight plans were free of conflicts out to 30° W instead of 40° W, as at present. Similarly, separation assurances only to 30° W, rather than 20° W, would be required at Gander. The effect on system capacity would be reflected by a reduction of the probability, c, that a lateral conflict prevents a pair of aircraft from being cleared to enter the OCA at the same flight level and without longitudinal separation. A study of flight plan requests suggest that c would be reduced by less than .04. The corresponding increase in capacity is less than 8%. Moreover, there is no guarantee that a flight plan conflict beyond the 30° W line will not still require a disadvantageous diversion of one or both of the enroute aircraft.

A different area, in which there is considerable room for improvement, is that of inter-system procedures. System performance should benefit significantly from a coordinated effort by the different ATC centers which control the regions through which transatlantic flights pass. There is a special need for more integrated control of departing flights during the period prior to entry into either the Gander or Shannon-Prestwick OCA's. In the present operation, preplanning of mid-atlantic crossings is limited and, consequently, the available air space is not always used efficiently.

As an example of the possibilities for increased efficiency, suppose that the Shannon-Prestwick controllers were able to preassign flight levels to westbound aircraft at the time of take-off, rather than upon entry into the OCA, and that a similar arrangement were made at Gander for eastbound traffic. With the present restriction on VFR climbs through occupied flight levels, it is clear that such preplanning would help to avoid the loss of opportunities for aircraft to use otherwise unoccupied flight levels.

The system would benefit even more from a level of coordination which permits the oceanic controller not only to assign clearances at the times of

take-off but also to control the take-offs themselves. A number of practical difficulties probably make this possibility unfeasible in the present system, but it may be feasible for supersonic aircraft. In this case, procedures could be employed to regulate the arrival times of such aircraft at the OCA boundaries. At present, departing aircraft approach these boundaries at randomly spaced time intervals. The resulting reduction of system capacity has been demonstrated in Section VI. If it were possible to regulate traffic so that arrivals at the OCA boundaries were evenly spaced in time,* then the capacity of the system could be more than doubled. It is, of course, impossible to regulate the departures of transatlantic flights from the various domestic airports so that arrivals at OCA boundaries are spaced at precisely equal time intervals. This would be possible only if the ETA's at the OCA boundaries were free of error; however, ETA errors for supersonic aircraft should be relatively small [cf. Section IX].

Finally, it is worthwhile to suggest a less sweeping modification of present procedures which should lead to some improvement in system performance. This modification would be directed toward more accurate prediction of longitudinal separations and would require that all ETA computations be based on the same weather forecast. The errors made by the carriers in estimating average head winds along the same flight plan track are inconsistent because of differences in wind forecasts. Differences in temperature forecasts also contribute inconsistencies in filed air speeds, since the air speed for a given Mach number is a function of temperature. Different air speeds are sometimes filed for jet aircraft planning to fly at identical Mach numbers and on the same route at about the same time. If flight plan Mach numbers were filed for jets in addition to predicted air speeds, the controller could then use the same temperature forecast to

---

*Such regulation does not imply a redistribution of air line schedules.

compute air speeds for all aircraft entering the oceanic region during the same general time period. He could also apply his own wind forecast, together with his air speed computations, to determine ETA's. The inconsistencies arising from the use of different weather forecasts in the operator computed ETA's would then be eliminated. There is no reason to believe that the controller's ETA errors would be smaller than those of the operators; however, the relative ETA errors would be reduced. It is the relative errors that determine the accuracy of predicted longitudinal separation. Consequently, the use of controller computed ETA's to check requested flight plans for conflicts might justify a reduction in the longitudinal separation standard.

IX. APPLICATIONS TO OTHER ENVIRONMENTS

The emphasis in this report has been placed on subsonic jet operations over the North Atlantic. We shall discuss briefly how the analytic techniques described in the preceding Section may be applied to other environments.

1. Other Geographical Regions

The effect of wind variability on both longitudinal and lateral separation standards has been discussed in Section V and is derived analytically in Appendices B, C, and E from statistics characterizing the winds over the North Atlantic. The basic mathematical models presented in these Appendices can be applied directly to any other region, including the Pacific and the Arctic. To obtain numerical results, however, it is necessary to provide, as inputs to the models, wind data characteristic of the region under consideration. Data on the standard deviation of the wind is available in reference 2, which provides complete coverage of the northern hemisphere, and in reference 18, which provides world wide coverage. It appears, however, that data on the spatial correlations of winds, such as that prepared for the North Atlantic,[3] is not available for other regions, although it could readily be prepared by meteorologists.

In order to apply the methods described in Sections VI and VII to analyze the traffic handling capacity and the economic features of ATC restrictions associated with regions other than the North Atlantic, it is necessary to investigate certain geographical characteristics of those regions. In particular, the distance traversed by an aircraft when crossing a region has a direct bearing on the economic penalties associated with diversions from the preferred flight plan track or altitude. This distance is also related to the system parameter c, defined in Section VI, which depends upon the extent of the geographical area over which advance conflict checking is

required. Communications coverage over the region will, of course, also influence c.

A complete analysis of the traffic problems associated with any region must also take into account the distribution of traffic in both space and time, as determined by operator scheduling, the geographical spread of origins and distinations of various flights, and other factors. Given the appropriate statistical data, the basic mathematical tools provided in this report can be readily adapted to the environments associated with other geographical regions.

2. Supersonic Aircraft

A comparison of wind effects on longitudinal separation for propeller and subsonic jet aircraft has already been made in Section V. A similar comparison may be made for subsonic and supersonic jets. It is reasonable to anticipate a comparitively small wind effect on longitudinal separation for supersonic jets, both because of the increased air speed and because of the decreased wind variability known to be characteristic of the flight levels at which supersonic aircraft will fly. Indeed, the results in Appendix C [cf. Figure C-9] show that, even when supersonic jets fly through a wind field characterized by statistics at the 300 mb. level, the effect of horizontal wind gradient on longitudinal separation is negligible.

In a recent article by C. S. Durst,[19] it is also shown that wind and temperature forecast errors result in a standard error of less than a minute in planned flight times for the entire transatlantic crossing by supersonic aircraft. This figure is in sharp contrast to the standard errors of about 7-14 minutes for subsonic jets. As Durst suggests, this improvement in punctuality will afford a real opportunity for planned air traffic control.

It is obvious that the effect of air line schedules on air traffic control problems will change because of the decrease in flight time for supersonic

jets. For example, the total transatlantic flight time is reduced from about 7 hours for subsonic jets to less than 3 hours for Mach 2 aircraft. If most eastbound flights continue to depart from North America in the early evening and most westbound flights from Europe in the afternoon (local times), then the traffic peaks in the two directions will be well separated in time. Accordingly the competition for air space by traffic in the two directions should be reduced. On the other hand, decreased flight times may encourage some spreading of flight schedules throughout the day.

Without a detailed study, the appropriate separation standards for supersonic traffic cannot be speculated upon. However, it is reasonable to expect that major improvements in navigational devices and techniques, altimeters, and communications will have developed prior to the introduction of supersonic traffic. If these improvements serve to reduce lateral, vertical, or longitudinal errors significantly, particularly large blunder errors, then significant reductions in the corresponding separation standards would be justified. Indeed, the small effect of wind variability does suggest the possibility of a reduced longitudinal separation standard. Similarly, smaller drift angles should help to improve lateral track-keeping accuracy. It is also likely that inertial navigation will be a serious contender for consideration in the supersonic era, since the navigational errors associated with an inertial system, unlike a Doppler system, grow with time rather than distance. Thus, the decrease in the time of flight between geographical locations where accurate fixes can be obtained favors the adoption of inertial systems for supersonic craft.

Finally, certain significant differences in the economic aspects of subsonic and supersonic flight should be mentioned. Because of the insensitivity of supersonic flight time to winds, the MTP will be (very nearly) the great circle route. The penalty associated with deviations from this route is thus determined by the increases in ground distance. In this case, a fixed

route system becomes feasible. The economic significance of penalties associated with lateral deviations from the great circle route and with separations from the optimal vertical flight profile cannot be determined without a study of supersonic aircraft fuel flow rates. It is likely, however, that deviations in the vertical dimension will be much more critical.

3. Automation

A computer can serve a useful purpose in reducing the controller's work load, particularly in the processing of filed flight plans and preparation of flight strips. It is also useful as a research tool in analyzing the data available in filed and cleared flight plans, pilot reports, etc. However, it does not constitute an essential feature of a strategic control system. In a tactical system, with the requirement for rapid resolution of conflicts and, perhaps, even multiple conflict situations, automation does become an essential feature of the system. However, a significant shift toward tactical procedures is considered unlikely.

One application of automation which can be recommended for any control system is the use of rapid meteorological data processing to provide more accurate, up-to-date forecasts. In particular, the processing of large numbers of reports on winds encountered by aircraft while in flight could yield useful information on current wind fields. The installation of Doppler equipment in aircraft will make reports accessible on instantaneous wind velocities encountered at a large number of points over the North Atlantic. The advantages of more accurate information on current wind fields have already been made apparent.

APPENDIX A

STATISTICAL MODEL OF WIND BEHAVIOR

1. Introduction

The purpose of this Appendix is to provide a mathematical background for the analysis of the effects of winds on the problems of air traffic control in the North Atlantic. A realistic mathematical model of the statistical behavior of the winds is formulated, providing a consistent set of relationships among the correlation functions of wind components for various required geometrical configurations in two dimensions.

The model is based mainly on the geostrophic assumption which has been thoroughly verified by many workers in the last few years.[1] The only other significant assumption made in the derivation of the model concerns the statistical nature of the two-dimensional D-value field. This field is accordingly regarded here as a stationary random variable with an autocorrelation function characterized by elliptical symmetry. This latter fact is amply justified by available data obtained in the North Atlantic in the general vicinity of the New York-Brussels great circle.[2]

There are two basic requirements for the particular form of the wind model. The first one arises from an obvious emphasis that this study must place on the evaluation of relative separations among aircraft. Thus, for example, we are far more interested in the differences between the ETA's of two adjacent aircraft than in the actual values of the individual ETA's themselves. To study such problems from a statistical point of view, we must in general know the complete joint probability density function of the winds acting on both aircraft. However, as is shown elsewhere in this report, many important questions arising in such problems can be answered when only the so-called "second order statistics" of the winds are known. This implies the knowledge of the correlation functions of suitably chosen wind components,

defined as the expected value of their product. Moreover, if we also assume that the winds are Gaussian, their joint probability density functions are completely described when only the correlation functions are known. (It should be noted here, however, that the Gaussian assumption, although an eminently reasonable one, is not necessary for the validity of the results derived in this Appendix. Also, although it is quite reasonable to assume that the winds are Gaussian, it is definitely not correct to make a similar assumption about aircraft separations.)

We conclude, therefore, that, first of all, the model must permit the calculation of wind correlation functions. The second model requirement is concerned with the type and form of available data. The best statistical data available during this study have been obtained from papers published in the U.K. by C.S. Durst[3] and are in the form of the so-called longitudinal and lateral autocorrelation functions. The model must be able to utilize these data and to express more general two-dimensional wind correlation functions in terms of them. Finally, the model should permit a simple validation of the assumptions made in its construction by demonstrating that redundant data sets are mutually consistent. As will be shown later, this last objective has been realized very well indeed, since our model can express the lateral correlation function in terms of the longitudinal one, showing excellent agreement with the two independent sets of data obtained by C.S. Durst.

2. The Geostrophic Assumption

It is well known that the wind velocity vector is to a great extent determined by the pressure pattern in its vicinity. This relationship is a direct result of the Coriolis forces caused by the rotation of the earth. In fact, in middle latitudes, using this principle alone, the wind can be computed from the pressure pattern with considerable accuracy. This method of computing the wind components is said to be based on the "geostrophic assumption".

In its most simple form, this method can be described as follows:

Determine the so-called D-value function, D(x, y), defined as the height, with respect to an arbitrary level, of a constant pressure surface in the altitude region of interest, e.g., the 300 mb surface. Associate with the function D(x, y) a vector field, F, always oriented vertically upward, and with a magnitude equal to D(x, y). Then the wind velocity vector W can be shown to be proportional to the curl of the vector F:

$$W = -a\nabla xF \quad . \tag{A1}$$

In particular, the rectangular wind components are:

$$W_x = -a\frac{\partial D}{\partial y}$$

$$W_y = a\frac{\partial D}{\partial x} \quad . \tag{A2}$$

The proportionality factor, a, varies with the latitude, but can be regarded as approximately constant throughout the region encompassing the bulk of trans-Atlantic traffic. In this region its numerical value is

$$a = 1.65 \times 10^5 \text{ knots} \quad . \tag{A3}$$

In what follows, D(x, y) will be considered a random variable. In general, the expected value of D(x, y) is itself a function of x and y. For the purposes of the following analysis, it will be convenient to write

$$D(x, y) = \delta(x, y) + D_o(x, y) \quad , \tag{A4}$$

where $D_o(x, y)$ is the expected value of $D(x, y)$. Therefore, the expected value of $\delta(x, y)$ is zero. The wind components then become:

$$W_x = -a\frac{\partial \delta}{\partial y} - a\frac{\partial D_o}{\partial y}$$

$$W_y = a\frac{\partial \delta}{\partial x} + a\frac{\partial D_o}{\partial x} \quad . \tag{A5}$$

Taking expected values of both sides, we find

$$E[W_x] = -a\frac{\partial D_o}{\partial y}$$

$$E[W_y] = a\frac{\partial D_o}{\partial x} \quad . \tag{A6}$$

This allows us to write

$$W_x = w_x - a\frac{\partial D_o}{\partial x}$$

$$W_y = w_y + a\frac{\partial D_o}{\partial x} \quad , \tag{A7}$$

with both w_x and w_y having zero expected value.

Therefore, from eqs. (A5) and (A7),

$$w_x = -a \frac{\partial \delta}{\partial y}$$

$$w_y = a \frac{\partial \delta}{\partial x} \quad . \tag{A8}$$

In the following analysis, we shall be solely concerned with the two-dimensional correlation functions of the orthogonal wind components defined by eq. (A8). In the application of the results of this analysis to the study of air traffic control problems performed elsewhere in this report, the non-zero expected value of the wind expressed by eq. (A6) will be properly taken into account. Note that the expected value of the wind is in general a function of position.

3. Wind Correlation Functions

It will be assumed here that $\delta(x, y)$, as defined by eq. (A4), is a stationary random variable and that it possesses a unique autocorrelation function:

$$\varphi_\delta(u, v) = E[\delta(x, y)\delta(x + u, y + v)] \quad . \tag{A9}$$

Differentiating eq. (A9) with respect to v, we obtain

$$\frac{\partial}{\partial v} \varphi_\delta(u, v) = E[\delta(x, y) \frac{\partial \delta}{\partial y} (x + u, y + v)]$$

$$= E[\delta(x - u, y - v) \frac{\partial \delta}{\partial y} (x, y)] \quad . \tag{A10}$$

Differentiating again,

$$\frac{\partial^2}{\partial v^2}\varphi_\delta(u,v) = -E\left[\frac{\partial\delta}{\partial y}(x-u,y-v)\,\frac{\partial\delta}{\partial y}(x,y)\right] \quad . \tag{A11}$$

The negative of the right hand side of eq. (A11) can serve as a definition of the autocorrelation function of the partial derivative of $\delta(x,y)$ with respect to y. Thus,

$$\frac{\partial^2}{\partial v^2}\varphi_\delta(u,v) = -\varphi_{\delta_y}(u,v) \quad . \tag{A12}$$

Also, differentiating eq. (A10) with respect to u, we obtain

$$\frac{\partial^2}{\partial u\partial v}\varphi_\delta(u,v) = -E\left[\frac{\partial\delta}{\partial x}(x-u,y-v)\,\frac{\partial\delta}{\partial y}(x,y)\right] \quad . \tag{A13}$$

Again, we recognize the cross-correlation function of the two partial derivatives of $\delta(x,y)$ with respect to x and y:

$$\frac{\partial^2}{\partial u\partial v}\varphi_\delta(u,v) = -\varphi_{\delta_x\delta_y}(u,v) \quad . \tag{A14}$$

In a similar manner, it can be shown that

$$\frac{\partial^2}{\partial u^2}\varphi_\delta(u,v) = -\varphi_{\delta_x}(u,v) \quad . \tag{A15}$$

Now, from eq. (A8), it follows that the autocorrelation functions of w_x and w_y can be expressed respectively as

$$\varphi_{xx}(u,v) = a^2 \varphi_{\delta_y}(u,v) \quad , \tag{A16}$$

and

$$\varphi_{yy}(u,v) = a^2 \varphi_{\delta_x}(u,v) \quad . \tag{A17}$$

Similarly, the cross-correlation function of w_y and w_x is

$$\varphi_{yx}(u,v) = -a^2 \varphi_{\delta_x \delta_y}(u,v) \quad . \tag{A18}$$

Combining eqs. (A16), (A17) and (A18), with eqs. (A12), (A14), and (A15), we finally obtain

$$\varphi_{xx}(u,v) = -a^2 \frac{\partial^2}{\partial v^2} \varphi_{\delta}(u,v) \quad , \tag{A19}$$

$$\varphi_{yy}(u,v) = -a^2 \frac{\partial^2}{\partial u^2} \varphi_{\delta}(u,v) \quad , \tag{A20}$$

$$\varphi_{yx}(u,v) = a^2 \frac{\partial^2}{\partial u \partial v} \varphi_{\delta}(u,v) \quad . \tag{A21}$$

From eq. (A21), it naturally follows that

$$\varphi_{xy}(u,v) = \varphi_{yx}(u,v) \quad . \tag{A22}$$

Eqs. (A19) through (A22) express in a compact way the correlation functions of the two orthogonal wind components in terms of the derivatives of a single autocorrelation function of $\delta(x, y)$.

4. Elliptical Symmetry Assumption

To make further use of the results of the preceeding section, it is necessary now to express $\varphi_\delta(u, v)$ as a function of a single variable. Accordingly, an additional assumption is made here ascribing a property of elliptical symmetry to the autocorrelation function of the D-value surface. In particular, the autocorrelation function $\varphi_\delta(u, v)$ is assumed to be constant along any one of a family of concentric ellipses with the major and minor axes oriented in the north-south and east-west directions respectively. In our notation, this takes the form

$$\varphi_\delta(u, v) = \varphi_\delta(s) \quad , \tag{A23}$$

with

$$s = \sqrt{u^2 + \rho^2 v^2} \quad . \tag{A24}$$

The validity of this assumption is well verified by available data.[2]

The elliptic factor ρ is related to the eccentricity e of the ellipse by

$$\rho^2 = \frac{1}{1 - e^2} \quad . \tag{A25}$$

It is found that ρ is essentially a constant in the North Atlantic region in the vicinity of the New York-Brussels great circle. Its average value there is approximately

$$\rho = 0.885 \quad . \tag{A26}$$

A physical interpretation of ρ will be provided later. [cf. eq. (A43)].

Using the assumptions expressed by eqs. (A23) and (A24), we shall now evaluate the second partial derivatives in eqs. (A19), (A20), and (A21).

Differentiating

$$s^2 = u^2 + \rho^2 v^2 \quad ,$$

we obtain

$$\frac{\partial s}{\partial u} = \frac{u}{s} \quad , \tag{A27}$$

$$\frac{\partial s}{\partial v} = \frac{\rho^2 v}{s} \quad . \tag{A28}$$

Therefore,

$$\frac{\partial}{\partial v} \varphi_\delta(s) = \frac{\rho^2 v}{s} \varphi'_\delta(s) \quad , \tag{A29}$$

with the prime denoting differentiation with respect to s.

Differentiating again,

$$\frac{\partial^2}{\partial v^2} \varphi_\delta(s) = \frac{\rho^2}{s} \varphi'_\delta(s) + \rho^2 v \frac{\partial}{\partial v}\left[\frac{1}{s} \varphi'_\delta(s)\right] \quad . \tag{A30}$$

Similarly,

$$\frac{\partial}{\partial u}\,\varphi_{\delta}(s) \;=\; \frac{u}{s}\,\varphi'_{\delta}(s) \quad , \tag{A31}$$

and

$$\frac{\partial^2}{\partial u^2}\,\varphi_{\delta}(s) \;=\; \frac{1}{s}\,\varphi'_{\delta}(s) \;+\; u\,\frac{\partial}{\partial u}\left[\frac{1}{s}\,\varphi'_{\delta}(s)\right] \quad . \tag{A32}$$

Also,

$$\frac{\partial^2}{\partial u \partial v}\,\varphi_{\delta}(s) \;=\; \rho^2 v\,\frac{\partial}{\partial u}\left[\frac{1}{s}\,\varphi'_{\delta}(s)\right] \quad . \tag{A33}$$

Now, substituting eqs. (A30), (A32), and (A33) in eqs. (A19), (A20), and (A21), respectively, we obtain

$$\varphi_{xx}(u, v) \;=\; -\,a^2\rho^2\left\{\frac{1}{s}\,\varphi'_{\delta}(s) \;+\; v\,\frac{\partial}{\partial v}\left[\frac{1}{s}\,\varphi'_{\delta}(s)\right]\right\} \quad , \tag{A34}$$

$$\varphi_{yy}(u, v) \;=\; -\,a^2\left\{\frac{1}{s}\,\varphi'_{\delta}(s) \;+\; u\,\frac{\partial}{\partial u}\left[\frac{1}{s}\,\varphi'_{\delta}(s)\right]\right\} \quad , \tag{A35}$$

$$\varphi_{xy}(u, v) \;=\; \varphi_{yx}(u, v) \;=\; a^2\rho^2 v\,\frac{\partial}{\partial u}\left[\frac{1}{s}\,\varphi'_{\delta}(s)\right] \quad . \tag{A36}$$

Setting $v = 0$ in eqs. (A34) and (A20), we have

$$\varphi_{xx}(u, 0) \;=\; -\,\frac{a^2\rho^2}{u}\,\varphi'_{\delta}(u) \quad , \tag{A37}$$

$$\varphi_{yy}(u, 0) = -a^2 \varphi''_{\delta}(u) \quad . \tag{A38}$$

Eqs. (A37) and (A38) are important because they relate to each other two independent sets of experimentally obtained data in the forms of $\varphi_{xx}(u, 0)$ and $\varphi_{yy}(u, 0)$. This point will be further treated in the next section.

The variances of the x and y wind components, w_x and w_y, are expressed by

$$\sigma_x^2 = \varphi_{xx}(0, 0) \quad , \tag{A39}$$

and

$$\sigma_y^2 = \varphi_{yy}(0, 0) \quad , \tag{A40}$$

respectively. Therefore, from eqs. (A39) and (A37),

$$\sigma_x^2 = -a^2 \rho^2 \lim_{u \to 0} \left[\frac{1}{u} \varphi'_{\delta}(u) \right] = -a^2 \rho^2 \varphi''_{\delta}(0) \quad . \tag{A41}$$

Also, from eqs. (A40) and (A38),

$$\sigma_y^2 = -a^2 \varphi''_{\delta}(0) \quad . \tag{A42}$$

Dividing eq. (A41) by (A42) yields

$$\frac{\sigma_x^2}{\sigma_y^2} = \rho^2 \quad . \tag{A43}$$

This expression provides a physical interpretation for the elliptic factor ρ defined by eq. (A24).

5. Basic Relationships Among Correlation Functions of Orthogonal Wind Components

At this point, in order to simplify the notation and to conform to current practice, it is convenient to introduce the following normalized correlation functions:

$$R_x(u, v) = \frac{1}{\sigma_x^2} \varphi_{xx}(u, v) \quad , \tag{A44}$$

$$R_y(u, v) = \frac{1}{\sigma_y^2} \varphi_{yy}(u, v) \quad , \tag{A45}$$

$$R_{xy}(u, v) = \frac{1}{\sigma_x \sigma_y} \varphi_{xy}(u, v) \quad . \tag{A46}$$

In addition to the functions listed above, we shall also define

$$R_{xu}(r) = R_x(r, 0) \quad , \tag{A47}$$

$$R_{xv}(r) = R_x(0, r) \quad , \tag{A48}$$

$$R_{yu}(r) = R_y(r, 0) \quad , \tag{A49}$$

$$R_{yv}(r) = R_y(0, r) \quad . \tag{A50}$$

Using this notation, and with the help of eq. (A43), eqs. (A37) and (A38) can now be written as

$$\sigma_y^2 u R_{xu}(u) = - a^2 \varphi'_\delta(u) \quad , \tag{A51}$$

$$\sigma_y^2 R_{yu}(u) = - a^2 \varphi''_\delta(u) \quad . \tag{A52}$$

Differentiating eq. (A51) and comparing with eq. (A52), we obtain

$$u R'_{xu}(u) + R_{xu}(u) = R_{yu}(u) \quad , \tag{A53}$$

where the prime denotes differentiation with respect to u.

Eq. (A53) is extremely useful, because it represents a simple and unique relationship between $R_{xu}(r)$ and $R_{yu}(r)$, the two known input functions in terms of which all other wind correlation functions must be expressed. This constitutes a valuable check on the validity of the assumptions made in the derivation of the wind model. As mentioned above, $R_{xu}(r)$ and $R_{yu}(r)$ represent respectively the so-called longitudinal and lateral correlation functions determined independently from experimental data by C.S. Durst in the U.K. These functions are shown plotted in Figure A-1. Also shown for comparison in the same figure is the plot of the left hand side of eq. (A53), indicating excellent agreement with the theory at least up to 600 nautical miles.

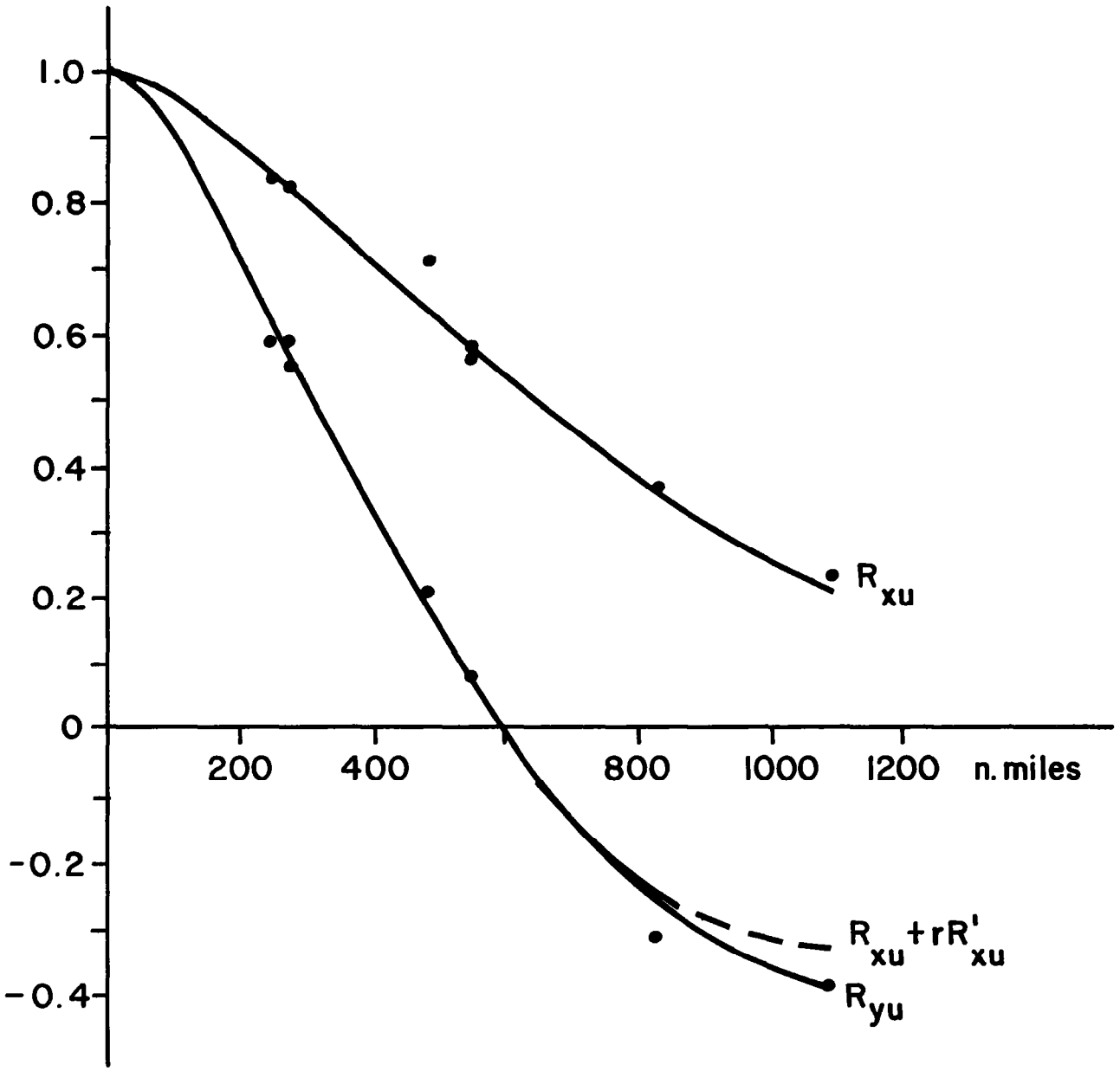

FIG. A-I: LONGITUDINAL AND LATERAL AUTOCORRELATION FUNCTIONS

(Data points from C.S. Durst[3])

The remaining part of this section will be devoted to the calculation of required wind correlation functions in terms of $R_{xu}(r)$ and $R_{yu}(r)$.

From eqs. (A34) and (A44),

$$R_x(u,v) = -\frac{a^2}{\sigma_y^2}\left\{\frac{1}{s}\varphi'_\delta(s) + v\frac{\partial}{\partial v}\left[\frac{1}{s}\varphi'_\delta(s)\right]\right\} \quad . \tag{A54}$$

But, from eq. (A51),

$$\frac{1}{u}\varphi'_\delta(u) = -\frac{\sigma_y^2}{a^2}R_{xu}(u) \quad . \tag{A55}$$

Therefore,

$$R_x(u,v) = R_{xu}(s) + v\frac{\partial}{\partial v}R_{xu}(s) \quad , \tag{A56}$$

with s defined by eq. (A24).

However, from eq. (A28),

$$\frac{\partial}{\partial v}R_{xu}(s) = \frac{\rho^2 v}{s}R'_{xu}(s) \quad , \tag{A57}$$

while, from eq. (A53),

$$R'_{xu}(s) = \frac{1}{s}\left[R_{yu}(s) - R_{xu}(s)\right] \quad . \tag{A58}$$

Substituting eq. (A57) and (A58) into eq. (A56),

$$R_x(u, v) = R_{xu}(s) + \frac{\rho^2 v^2}{s^2}\left[R_{yu}(s) - R_{xu}(s)\right] \quad , \tag{A59}$$

or

$$R_x(u, v) = \frac{1}{s^2}\left[u^2 R_{xu}(s) + \rho^2 v^2 R_{yu}(s)\right] \quad . \tag{A60}$$

Similarly, from eqs. (A35) and (A45),

$$R_y(u, v) = -\frac{a^2}{\sigma_y^2}\left\{\frac{1}{s}\varphi'_\delta(s) + u\frac{\partial}{\partial u}\left[\frac{1}{s}\varphi'_\delta(s)\right]\right\} \quad , \tag{A61}$$

and, with the use of eq. (A55),

$$R_y(u, v) = R_{xu}(s) + u\frac{\partial}{\partial u}R_{xu}(s) \quad . \tag{A62}$$

However, from eq. (A27),

$$\frac{\partial}{\partial u}R_{xu}(s) = \frac{u}{s}R'_{xu}(s) \quad , \tag{A63}$$

and, with eq. (A58),

$$R_y(u, v) = R_{xu}(s) + \frac{u^2}{s^2}\left[R_{yu}(s) - R_{xu}(s)\right] \quad , \tag{A64}$$

or

$$R_y(u, v) = \frac{1}{s^2}\left[\rho^2 v^2 R_{xu}(s) + u^2 R_{yu}(s)\right] \quad . \tag{A65}$$

To express $R_{xy}(u, v)$ in terms of $R_{xu}(s)$ and $R_{yu}(s)$, we use eqs. (A36) and (A46):

$$R_{xy}(u, v) = \frac{a^2 \rho^2 v}{\sigma_x \sigma_y} \frac{\partial}{\partial u}\left[\frac{1}{s}\varphi'_\delta(s)\right] \quad . \tag{A66}$$

With the help of eqs. (A43) and (A55),

$$R_{xy}(u, v) = -\rho v \frac{\partial}{\partial u} R_{xu}(s) \quad , \tag{A67}$$

and, using eqs. (A63) and (A58),

$$R_{xy}(u, v) = \frac{\rho u v}{s^2}\left[R_{xu}(s) - R_{yu}(s)\right] \quad . \tag{A68}$$

The results of this section are summarized in eqs. (A53), (A60), (A65), and (A68).

It is useful to note here that, from eq. (A51),

$$R_{xu}(r) = -\frac{a^2}{\sigma_y^2} \cdot \frac{1}{r}\varphi'_\delta(r) \quad , \tag{A69}$$

while, from eqs. (A50) and (A61),

$$R_{yv}(r) = -\frac{a^2}{\sigma_y^2} \cdot \frac{1}{\rho r} \varphi'_\delta(\rho r) \quad . \tag{A70}$$

Comparing (A69) and (A70), we obtain

$$R_{yv}(r) = R_{xu}(\rho r) \quad . \tag{A71}$$

6. Correlation Functions of Wind Components Along Inclined Lines

To satisfy the requirements of the analysis of wind effects performed in Appendix B, two special cases will be considered here. The first case is concerned with wind components along a straight line inclined at an angle θ with respect to the x-axis, as illustrated in Figure A-2.

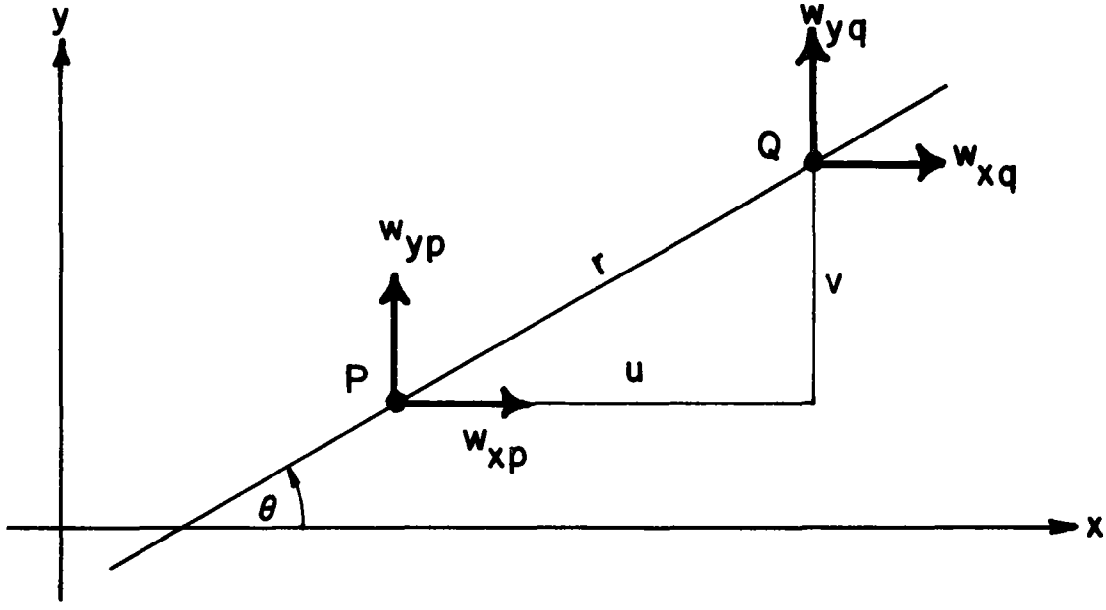

Figure A-2

The wind component along this straight line at the point P is

$$w_p = w_{xp} \cos\theta + w_{yp} \sin\theta \quad . \tag{A72}$$

At the point Q, the corresponding wind component is

$$w_q = w_{xq} \cos\theta + w_{yq} \sin\theta \quad . \tag{A73}$$

Therefore, the autocorrelation function of the wind component along the straight line is

$$\varphi_\theta(u, v) = \varphi_{xx}(u, v) \cos^2\theta + \varphi_{yy}(u, v) \sin^2\theta + 2\varphi_{xy}(u, v) \sin\theta \cos\theta \quad , \tag{A74}$$

or

$$\varphi_\theta(u, v) = \sigma_x^2 R_x(u, v) \cos^2\theta + \sigma_y^2 R_y(u, v) \sin^2\theta + 2\sigma_x \sigma_y R_{xy}(u, v) \sin\theta \cos\theta \quad . \tag{A75}$$

The variance of this wind component is

$$\sigma_\theta^2 = \varphi_\theta(0, 0) = \sigma_x^2 \cos^2\theta + \sigma_y^2 \sin^2\theta \quad . \tag{A76}$$

Thus, the normalized autocorrelation function becomes

$$R_\theta(u, v) = \frac{\rho^2 R_x \cos^2\theta + R_y \sin^2\theta + 2\rho R_{xy} \sin\theta \cos\theta}{\rho^2 \cos^2\theta + \sin^2\theta} \quad . \tag{A77}$$

With the help of eqs. (A60) and (A65), this can be written as

$$R_\theta(u,v) = \frac{\rho^2(u\cos\theta + v\sin\theta)^2 R_{xu}(s) + (\rho^2 v\cos\theta - u\sin\theta)^2 R_{yu}(s)}{(\rho^2\cos^2\theta + \sin^2\theta)\, s^2} \quad . \text{(A78)}$$

In particular, since $u = r\cos\theta$, $v = r\sin\theta$,

$$R_\theta(r) = \frac{\rho^2 R_{xu}(s) + (\rho^2 - 1)^2 R_{yu}(s)\sin^2\theta\cos^2\theta}{(\cos^2\theta + \rho^2\sin^2\theta)(\rho^2\cos^2\theta + \sin^2\theta)} \quad , \qquad \text{(A79)}$$

$$\text{with } s = r\sqrt{\cos^2\theta + \rho^2\sin^2\theta} \quad .$$

The second case to be considered here concerns the cross-correlation function of wind components along two lines inclined with respect to the x-axis at angles of θ and $-\theta$ respectively.

As in the previous case, we can write directly for the cross-correlation function of these two wind components:

$$\varphi_{\theta,\,-\theta}(u,v) = \varphi_{xx}(u,v)\cos^2\theta - \varphi_{yy}(u,v)\sin^2\theta + \\ + \varphi_{yx}(u,v)\sin\theta\cos\theta - \varphi_{xy}(u,v)\sin\theta\cos\theta \quad . \qquad \text{(A80)}$$

Thanks to eqs. (A22), (A44) and (A45), this becomes

$$\varphi_{\theta,\,-\theta}(u,v) = \sigma_x^2 R_x(u,v)\cos^2\theta - \sigma_y^2 R_y(u,v)\sin^2\theta \quad . \qquad \text{(A81)}$$

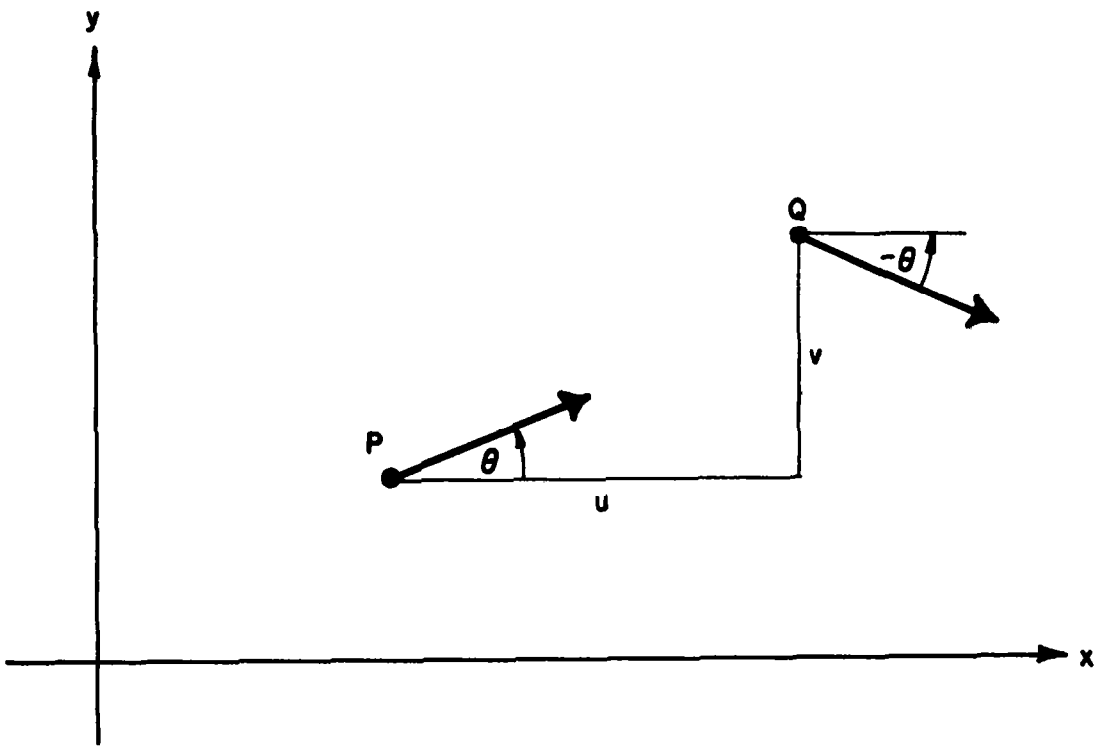

Figure A-3

In analogy with eq. (A46), let us define

$$R_{\theta,\ -\theta}(u, v) = \frac{1}{\sigma_\theta \sigma_{-\theta}} \varphi_{\theta,\ -\theta}(u, v) \quad . \tag{A82}$$

But, from eq. (A76),

$$\sigma_\theta^2 = \sigma_{-\theta}^2 = \sigma_x^2 \cos^2\theta + \sigma_y^2 \sin^2\theta \quad . \tag{A83}$$

Therefore,

$$R_{\theta,-\theta}(u,v) = \frac{\rho^2 R_x(u,v)\cos^2\theta - R_y(u,v)\sin^2\theta}{\rho^2\cos^2\theta + \sin^2\theta} \quad . \tag{A84}$$

With eqs. (A60) and (A65), this becomes,

$$R_{\theta,-\theta}(u,v) = \frac{\rho^2(u^2\cos^2\theta - v^2\sin^2\theta)R_{xu}(s) + (\rho^4 v^2\cos^2\theta - u^2\sin^2\theta)R_{yu}(s)}{(\rho^2\cos^2\theta + \sin^2\theta)(u^2 + \rho^2 v^2)} \quad . \tag{A85}$$

7. Summary of Results

For reference, we list here the main results of this Appendix.

The normalized correlation functions of the orthogonal wind components are expressed in terms of known functions by

$$\begin{cases} R_x(u,v) = \dfrac{1}{s^2}\left[u^2 R_{xu}(s) + \rho^2 v^2 R_{yu}(s)\right] \quad , & \text{(A60)} \\ R_y(u,v) = \dfrac{1}{s^2}\left[\rho^2 v^2 R_{xu}(s) + u^2 R_{yu}(s)\right] \quad , & \text{(A65)} \\ R_{xy}(u,v) = \dfrac{\rho uv}{s^2}\left[R_{xu}(s) - R_{yu}(s)\right] \quad , & \text{(A68)} \end{cases}$$

$$\text{with } s = \sqrt{u^2 + \rho^2 v^2}$$

$$\text{and } \rho = \frac{\sigma_x}{\sigma_y} \quad .$$

For correlation functions of wind components along inclined lines, we have:

$$R_\theta(r) = \frac{\rho^2 R_{xu}(s) + (\rho^2 - 1)^2 R_{yu}(s) \sin^2\theta \cos^2\theta}{(\cos^2\theta + \rho^2 \sin^2\theta)(\rho^2 \cos^2\theta + \sin^2\theta)} \quad , \tag{A79}$$

$$\text{with } s = r\sqrt{\cos^2\theta + \rho^2 \sin^2\theta}$$

$$R_{\theta,-\theta}(u,v) = \frac{\rho^2(u^2\cos^2\theta - v^2\sin^2\theta)R_{xu}(s) + (\rho^4 v^2 \cos^2\theta - u^2 \sin^2\theta)R_{yu}(s)}{(\rho^2\cos^2\theta + \sin^2\theta)(u^2 + \rho^2 v^2)} \quad . \tag{A85}$$

The two-dimensional correlation functions in these formulas are defined as follows [cf. eqs. (A44) through (A50)]:

$R_x(u,v)$ is the normalized autocorrelation of the zero-mean x-component of the wind.

$R_y(u,v)$ is the normalized autocorrelation of the zero-mean y-component of the wind.

$R_{xy}(u,v)$ is the normalized cross-correlation of zero-mean x and y-components of the wind.

$R_\theta(r)$ is the normalized autocorrelation of the zero-mean wind component along a line inclined at an angle θ with respect to the x-axis.

$R_{\theta,-\theta}(u,v)$ is the normalized cross-correlation of zero-mean wind components along lines inclined at θ and $-\theta$ with respect to the x-axis.

u and v are defined as displacements in the x and the y directions respectively, with $r = \sqrt{u^2 + v^2}$.

The two autocorrelation functions available from experimental data, and used as arguments in the formulas listed above, are:

$R_{xu}(u)$, the so-called longitudinal function, defined as the normalized autocorrelation of the zero-mean x-component of the wind in the x-direction, as illustrated in Figure A-4.

$R_{yu}(u)$, the so-called lateral function, defined as the normalized autocorrelation of the zero-mean y-component of the wind in the x-direction, as illustrated in Figure A-5.

These two functions are found to satisfy the relation

$$uR'_{xu}(u) + R_{xu}(u) = R_{yu}(u) \quad . \tag{A53}$$

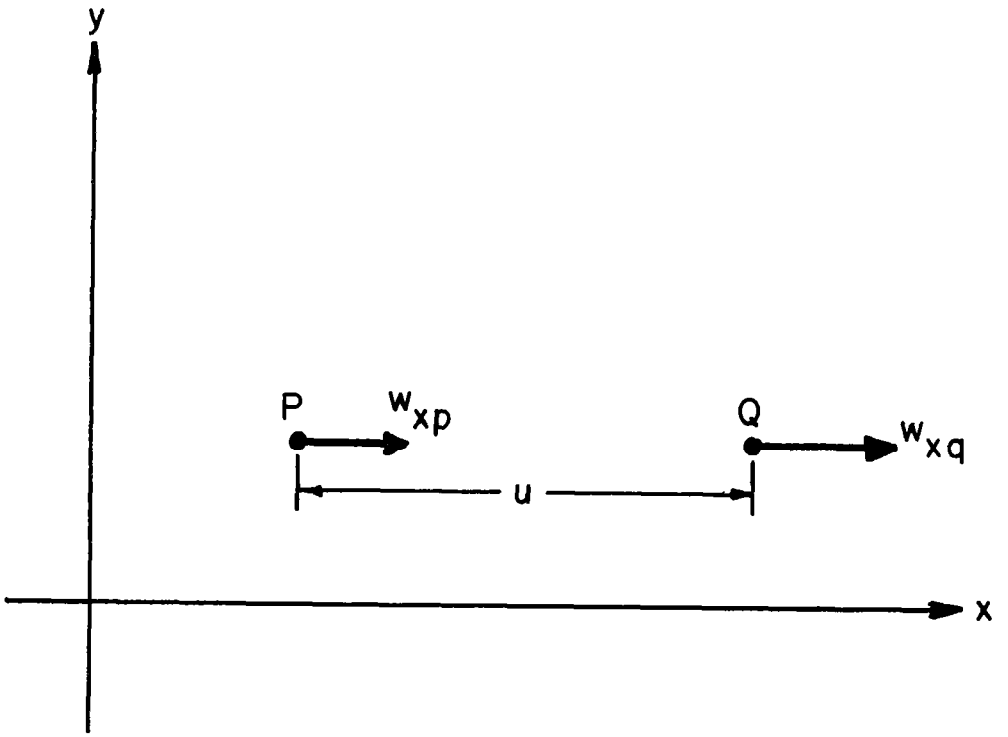

Figure A - 4

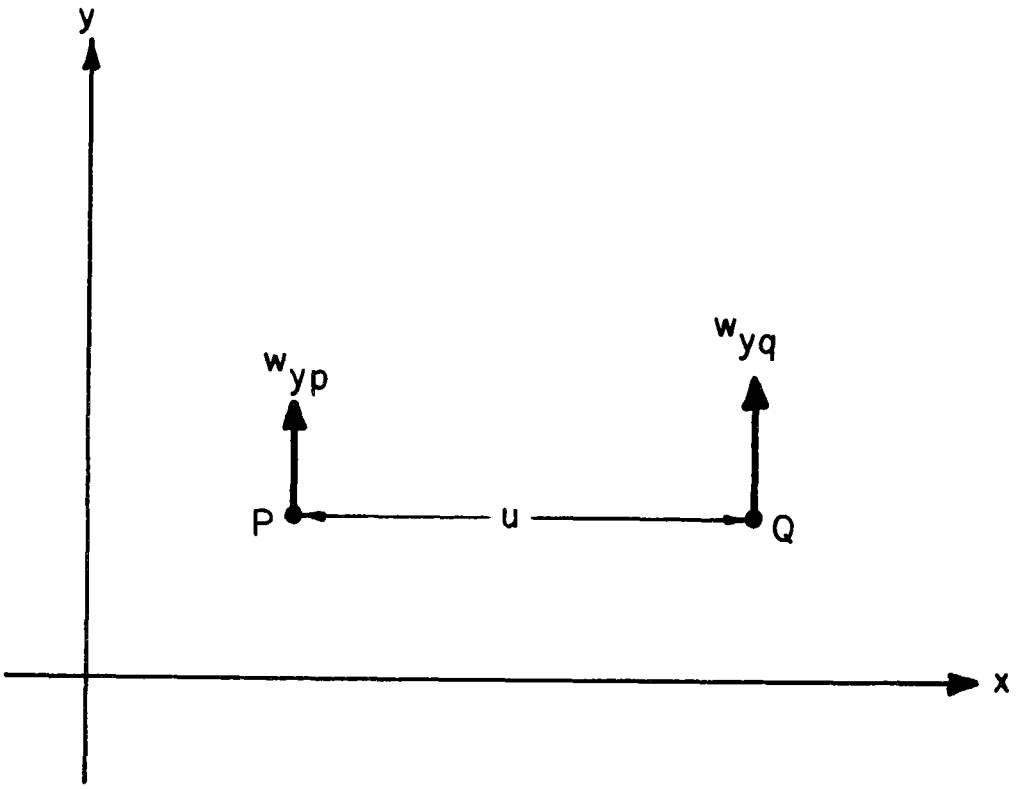

Figure A - 5

APPENDIX B

THE EFFECT OF WINDS ON LONGITUDINAL SEPARATION

1. Introduction

Consider two aircraft flying at the same altitude and at identical airspeeds along legs or segments of their actual flight paths. The segments are distinct but of the same length L. It will be assumed that the flight paths lie in a two-dimensional plane so that aircraft positions can be described by rectangular coordinates x and y, with the x- and y-axes corresponding to the east-west and north-south directions, respectively.

Two cases will be considered for the pair of flight path segments and are illustrated in Figures B-1 and B-2, respectively. In the first case, the segments are parallel to the x-axis and separated by a distance d. In the second case, the segments meet at their terminal points and form an angle 2θ which is bisected by a line parallel to the x-axis. In both cases, the abscissae of the initial and terminal points of the segments coincide.

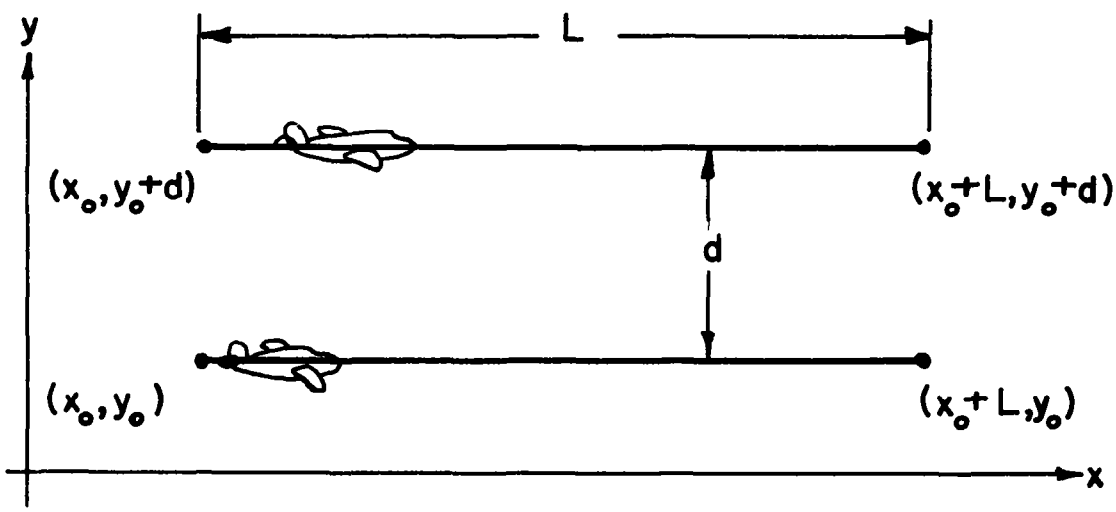

Figure B-1

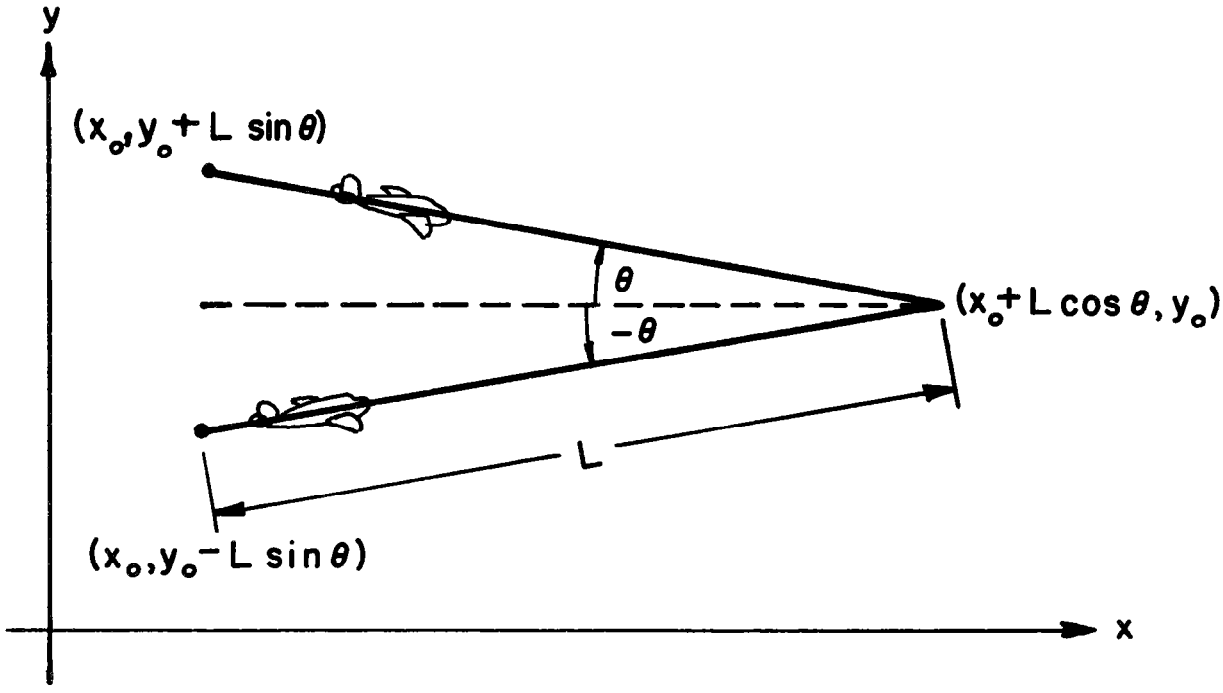

Figure B-2

The purpose of the analysis developed in this Appendix is to determine the statistics of wind effects on the longitudinal separation of a pair of aircraft which fly on the separate paths indicated in either Figure B-1 or B-2. It is assumed that in both figures the aircraft fly in the direction of the positive x-axis; i.e., toward the east. The results of subsequent analysis will also apply to westbound flights, however, since the statistical analysis of wind effects on longitudinal separation will be the same for both tail and head winds. It will become apparent that it is necessary only to determine the means and standard deviations of the appropriate tail wind components, in the geographical regions of interest, in order to apply the analysis to either eastbound or westbound flights.

The analysis is developed specifically for flight paths with the orientations indicated in Figures B-1 and B-2; i.e., for two paths parallel to the east-west axis and for two paths crossing at an angle which is bisected by a line parallel to the east-west axis. It will become apparent, however, that the same analysis can be applied to other orientations of parallel or crossing flight paths, if minor adjustments are made in certain parameters. Our primary purpose is to provide a comparison between the effects of wind on the longitudinal separation of aircraft following parallel flight paths as opposed to aircraft following crossing or converging flight paths. This comparison will not differ significantly for various flight path directions; moreover, present day air traffic flies predominately in the east-west direction in accordance with the two cases represented in Figures B-1 and B-2.

If two aircraft fly at the same airspeed along the pair of paths indicated in either Figure B-1 or B-2, and if the predicted flying times for the two paths are the same, then any difference in the actual flying times represents the relative ETA error at the terminal points of the paths. If accurate pilot reports of the ATA's at these terminal points were available, then the difference in flying times would be interpreted by the controller as a difference between the actual and scheduled longitudinal separation of the two aircraft.

In this Appendix we shall consider only the difference ΔT in flight times that arises because of the horizontal wind gradient existing at the flight level of the two aircraft. Other contributions to ΔT have been discussed elsewhere in this report.

The comparison of the statistics of flight time differences for parallel and crossing tracks is given at the end of this Appendix. In order to make this comparison, numerical evaluations are required of the mean $\mu_{\Delta T}$ and

variance $\sigma^2_{\Delta T}$ of the flight time difference for parallel tracks and also of the variance (but not the mean) of the flight time difference for crossing tracks.

In Section B.2, an approximation used in the evaluation of both the mean $\mu_{\Delta T}$ and the variance $\sigma^2_{\Delta T}$ is introduced, with specific reference to the parallel track case. The same method of approximation is used later in the evaluation of $\sigma^2_{\Delta T}$ for crossing tracks. This approximation depends upon the assumption that wind speeds are small compared to airspeed. An analysis of the error in $\mu_{\Delta T}$ caused by the approximation is given and leads to a bound on the actual error. An analysis of the error in $\sigma^2_{\Delta T}$ is intractable and is not undertaken. Instead, a comparison is made of the analytic results for the parallel track case with those obtained by a realistic computer simulation. This comparison validates the analytical approach and supports the contention that the error caused by the approximation is small.

The details of the evaluation (with approximation) of $\sigma^2_{\Delta T}$ for the parallel track case are given in Section B.3. The variance $\sigma^2_{\Delta T}$ for the crossing track case is evaluated by analogous methods in Section B.4. No computer simulation has been undertaken to determine values of $\sigma^2_{\Delta T}$ for the crossing track case. The required additional programming effort is obviated by the previously mentioned validation of the analytical approach for the parallel track case, since equivalent approximations are used in both the parallel and crossing track cases.

A comparison of the parallel and crossing track cases therefore depends upon the analytically determined approximations to $\sigma^2_{\Delta T}$. The comparison is

made in Section B.5, where numerical results of the approximations derived in Sections B.3 and B.4 are presented.

2. Approximations

In Figure B-3 an aircraft is shown flying at constant airspeed A in the direction of the positive x-axis along a flight path segment of length L. The instantaneous tail wind speed $W_x(x, y_o) = W_x(x)$ at each point on the flight path is the component of the wind velocity $\vec{W}(x)$ in the positive x-direction and varies as a function of the position of the aircraft. The instantaneous ground speed, $A \cos \lambda(x) + W_x(x)$, is also a function of aircraft position, where $\lambda(x)$ is the drift angle of the aircraft with respect to the flight path.

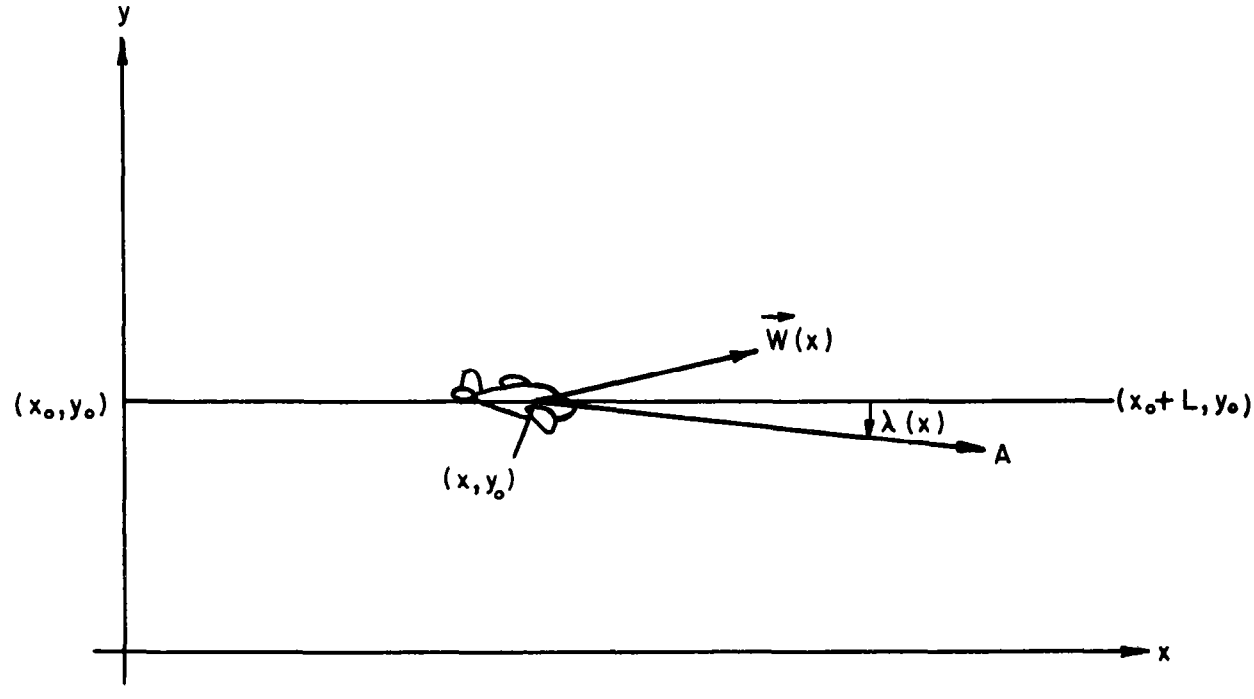

Figure B-3

The drift angle $\lambda(x)$ is determined at each point by the equation

$$A \sin \lambda(x) = - W_y(x) \quad , \tag{B1}$$

where $W_y(x)$ is the cross-track component of the wind velocity $\vec{W}(x)$. Therefore, the component of the airspeed along the flight path is

$$A \cos \lambda(x) = A \left[1 - \frac{W_y^2(x)}{A^2} \right]^{\frac{1}{2}} \quad . \tag{B2}$$

For jet aircraft speeds, it can be assumed that

$$\frac{W_y^2(x)}{A^2} < 1 \quad . \tag{B3}$$

Therefore $A \cos \lambda(x)$ can be represented by the series

$$A \cos \lambda(x) = A \left[1 - \frac{1}{2} \frac{W_y^2(x)}{A^2} - \frac{1}{8} \frac{W_y^4(x)}{A^4} - \ldots \right] \quad . \tag{B4}$$

Consider the approximation obtained by truncating the series in eq. (B4) after the first term:

$$A \cos \lambda(x) \approx A \quad . \tag{B5}$$

It is easily shown that if the airspeed A is 480 knots and the cross-track wind component W_y is 100 knots, then the error in $A \cos \lambda(x)$ caused by

approximation eq. (B5) is less than 2%. If A is 480 knots and W_y is 200 knots, then the error is less than 10%. In order to simplify subsequent mathematical calculations, we shall assume that the along-track component of the airspeed is a constant, A. Accordingly, the flight time for the route shown in Figure B-3 is taken to be

$$T = \int_0^L \frac{dx}{A+W_x(x)} \quad . \tag{B6}$$

Note that the wind at each point on the flight path has been considered as a function of position only and not of time. The reason for this is that our purpose is to evaluate the statistics of flight time differences for aircraft which traverse neighboring flight paths at about the same time; i.e., with longitudinal separations corresponding to present day separation standards. Although fluctuations in the wind at a particular point do occur within short intervals of time, the integrated effect of such fluctuations over a flight path can be shown to be small.[8] Consequently, the variation of wind with time will have a negligible effect on flight time differences compared to the effect of variations of wind with distance. For purposes of illustration, let the flight times for the three aircraft A_1, A_2, A_3 in Figure B-4 be T_1, T_2, T_3, respectively. Suppose that the lead times of aircraft A_1 over aircraft A_2 and A_3 are both small, say thirty minutes or less. Then the flight time difference $T_1 - T_3$, caused solely by the variation of wind with time, is negligible compared to the flight time difference $T_1 - T_2$, to which the variation of wind with distance contributes. We shall neglect the effect of variation of wind with time and assume that $T_1 = T_3$ and, therefore, that the flight time differences $T_1 - T_2$ and $T_3 - T_2$ are identical. Note that this assumption becomes increasingly realistic in the cases of greatest

significance, i.e., when the longitudinal separation between aircraft A_1 and A_2 becomes small.

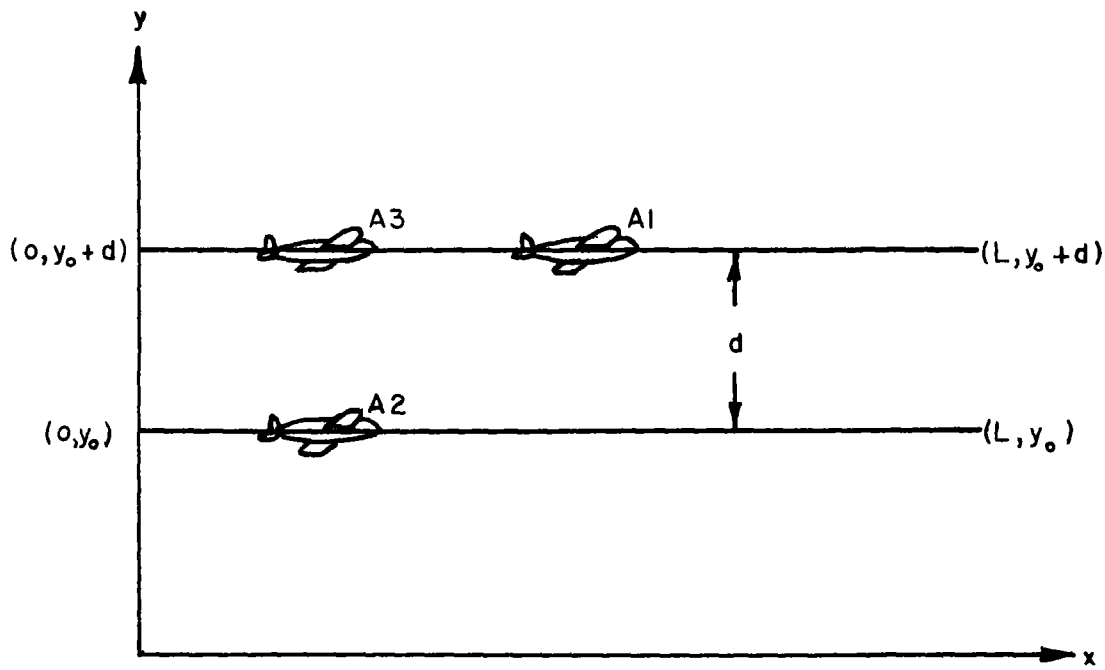

Figure B-4

Since for jet aircraft speeds, the inequality

$$\left| \frac{W_x(x)}{A} \right| < 1 \quad , \tag{B7}$$

is satisfied, eq. (B6) can be written

$$T = \frac{1}{A} \int_0^L \left[1 - \frac{W_x(x)}{A} + \frac{W_x^2(x)}{A^2} - \ldots \right] dx \quad . \tag{B8}$$

Therefore the difference ΔT in flight times for the two paths indicated in Figure B-4 is

$$\Delta T = T_1 - T_2 = \frac{1}{A} \int_0^L \left\{ \frac{W_{x2}(x) - W_{x1}(x)}{A} - \frac{W_{x2}^2(x) - W_{x1}^2(x)}{A^2} + \ldots \right\} dx \quad , \tag{B9}$$

where $W_{x1}(x)$ and $W_{x2}(x)$ represent the tail wind components on the first and second paths, respectively. In order to make the subsequent mathematical analysis tractable we shall use the approximation

$$\Delta T \approx \frac{1}{A^2} \int_0^L \left[W_{x2}(x) - W_{x1}(x) \right] dx$$

$$= \frac{1}{A^2} \int_0^L \Delta W_x(x)\, dx \quad , \tag{B10}$$

where $\Delta W_x(x) = W_{x2}(x) - W_{x1}(x)$.

Accordingly, the mean $\mu_{\Delta T}$ of the flight time difference will be represented by the approximation:

$$\mu_{\Delta T} = E(\Delta T)$$

$$\approx \frac{1}{A^2} E \left\{ \int_0^L \left[W_{x2}(x) - W_{x1}(x) \right] dx \right\}$$

$$= \frac{1}{A^2} \int_0^L \left[\mu_{x2}(x) - \mu_{x1}(x) \right] dx$$

$$= \frac{L}{A^2} \left[\mu_{x2}(\bar{x}) - \mu_{x1}(\bar{x}) \right]$$

$$= \frac{L}{A^2} \Delta\mu_x(\bar{x}) \quad , \tag{B11}$$

where, in accordance with the mean value theorem of integral calculus, $\bar{x}$ is an intermediate point in the interval $0 \leq \bar{x} \leq L$. The symbols $\mu_{x1}(x)$, $\mu_{x2}(x)$, and $\Delta\mu_x(x)$ are defined by

$$\mu_{x1}(x) = E\left[W_{x1}(x) \right]$$

$$\mu_{x2}(x) = E\left[W_{x2}(x) \right]$$

$$\Delta\mu_x(x) = \mu_{x2}(x) - \mu_{x1}(x) = E\left[\Delta W_x(x) \right] \quad . \tag{B12}$$

A study of charts in reference 2 reveals that mean winds change gradually with distance and, consequently, it is not difficult to choose a suitable "intermediate" value $\Delta\mu_x(\bar{x})$ from these charts for any specified length and geographical location of the flight paths in Figure B-4. Thus numerical values for $\mu_{\Delta T}$ can be estimated from the approximation (B11) with the aid of the charts in reference 2. Numerical values for specific parallel flight paths are given in Section B.5.

The error in $\mu_{\Delta T}$ caused by the approximation (B11) depends upon the relative magnitude of tail winds as compared to airspeed and can be estimated from an examination of the following exact expression for $\mu_{\Delta T}$:

$$\mu_{\Delta T} = \frac{1}{A^2} \int_0^L E\left\{\left[W_{x2}(x) - W_{x1}(x)\right] - \frac{W_{x2}^2(x) - W_{x1}^2(x)}{A}\right.$$

$$\left. + \frac{W_{x2}^3(x) - W_{x1}^3(x)}{A^2} \ldots .\right\} dx$$

$$= \frac{1}{A^2} \int_0^L \left\{\Delta\mu_x(x) - \frac{E\left[W_{x2}^2(x) - W_{x1}^2(x)\right]}{A}\right.$$

$$\left. + \frac{E\left[W_{x2}^3(x) - W_{x1}^3(x)\right]}{A^2} - \ldots\right\} dx \quad . \tag{B13}$$

The error in the integrand caused by neglecting all but the first term of the series expansion is dominated by the second term:

$$\frac{E\left[W_{x2}^2(x) - W_{x1}^2(x)\right]}{A} = \frac{\sigma_{x2}^2(x) - \sigma_{x1}^2(x) + \mu_{x2}^2(x) - \mu_{x1}^2(x)}{A} \quad , \tag{B14}$$

where σ_{x1}^2, σ_{x2}^2 designate, respectively, the variances of the tail winds at corresponding points on the first and second flight paths of Figure B-4. A study of charts in reference 2 reveals that differences in the variances $\sigma_{x2}^2(x)$, $\sigma_{x1}^2(x)$ are negligible for the path separations d that are of interest. Consequently, the right hand side of eq. (B14) is (very nearly)

$$\frac{\mu_{x2}^2(x) - \mu_{x1}^2(x)}{A} = \Delta\mu_x(x) \frac{\mu_{x2}(x) + \mu_{x1}(x)}{A} \quad . \tag{B15}$$

Thus a bound on the fractional error in the integrand of eq. (B13), caused by neglecting all but the first term of the series, is given by the expression

$$\frac{\mu_{x2}(x) + \mu_{x1}(x)}{A} \quad . \tag{B16}$$

The airspeed A may be taken to be about 480 knots. Charts in reference 2 suggest that a typical value for both $\mu_{x1}(x)$ and $\mu_{x2}(x)$ is about 30 knots. Thus, a bound on the percentage error in the integrand of eq. (B13), caused by truncating the series expansion after the first term, is typically about 12.5%. The same value might also be taken as a bound on the percentage error in $\mu_{\Delta T}$ caused by the approximation (B11); however, the actual percentage error in $\mu_{\Delta T}$ should be considerably less than 12.5%, because of a tendency for errors in the integrand to cancel out during the integration process.

In accordance with the approximation (B10) for ΔT, the variance $\sigma_{\Delta T}^2$ will also be represented by an approximation:

$$\sigma^2_{\Delta T} = E\left[(\Delta T)^2\right] - \mu^2_{\Delta T}$$

$$\approx \frac{1}{A^4}\int_0^L\int_0^L E\Big\{[W_{x2}(p) - W_{x1}(p)][W_{x2}(q) - W_{x1}(q)]\Big\}\,dp\,dq$$

$$- \frac{1}{A^4}\int_0^L\int_0^L \Big\{E[W_{x2}(p) - W_{x1}(p)]\Big\}\Big\{E[W_{x2}(q) - W_{x1}(q)]\Big\}\,dp\,dq$$

$$= \frac{1}{A^4}\int_0^L\int_0^L E\Big\{[w_{x2}(p) - w_{x1}(p)][w_{x2}(q) - w_{x1}(q)]\Big\}\,dp\,dq \quad , \qquad (B17)$$

where

$$w_{x1}(p) = W_{x1}(p) - \mu_{W_{x1}}(p)$$

$$w_{x2}(p) = W_{x2}(p) - \mu_{W_{x2}}(p) \quad . \qquad (B18)$$

A complete evaluation of the approximation (B17) to $\sigma^2_{\Delta T}$ is more difficult to obtain than the corresponding evaluation of $\mu_{\Delta T}$ and is deferred to Section B.3.

An analysis of the error in $\sigma_{\Delta T}$ caused by approximation (B17) is mathematically intractable and will not be given. However, an independent evaluation of $\sigma_{\Delta T}$ for the parallel track case which does not depend upon this approximation has been carried out by a computer simulation described in Appendix C. Figure B-5 shows two curves representing $\sigma_{\Delta T}$ as a function of path length for two parallel tracks separated by a distance of 28 nautical miles. One curve has been obtained by the methods of this Appendix and the other by the computer simulation. These curves show the typically close agreement between the numerical results obtained by the two approaches. Thus the computer simulation validates the analytic work in Section B.3 and

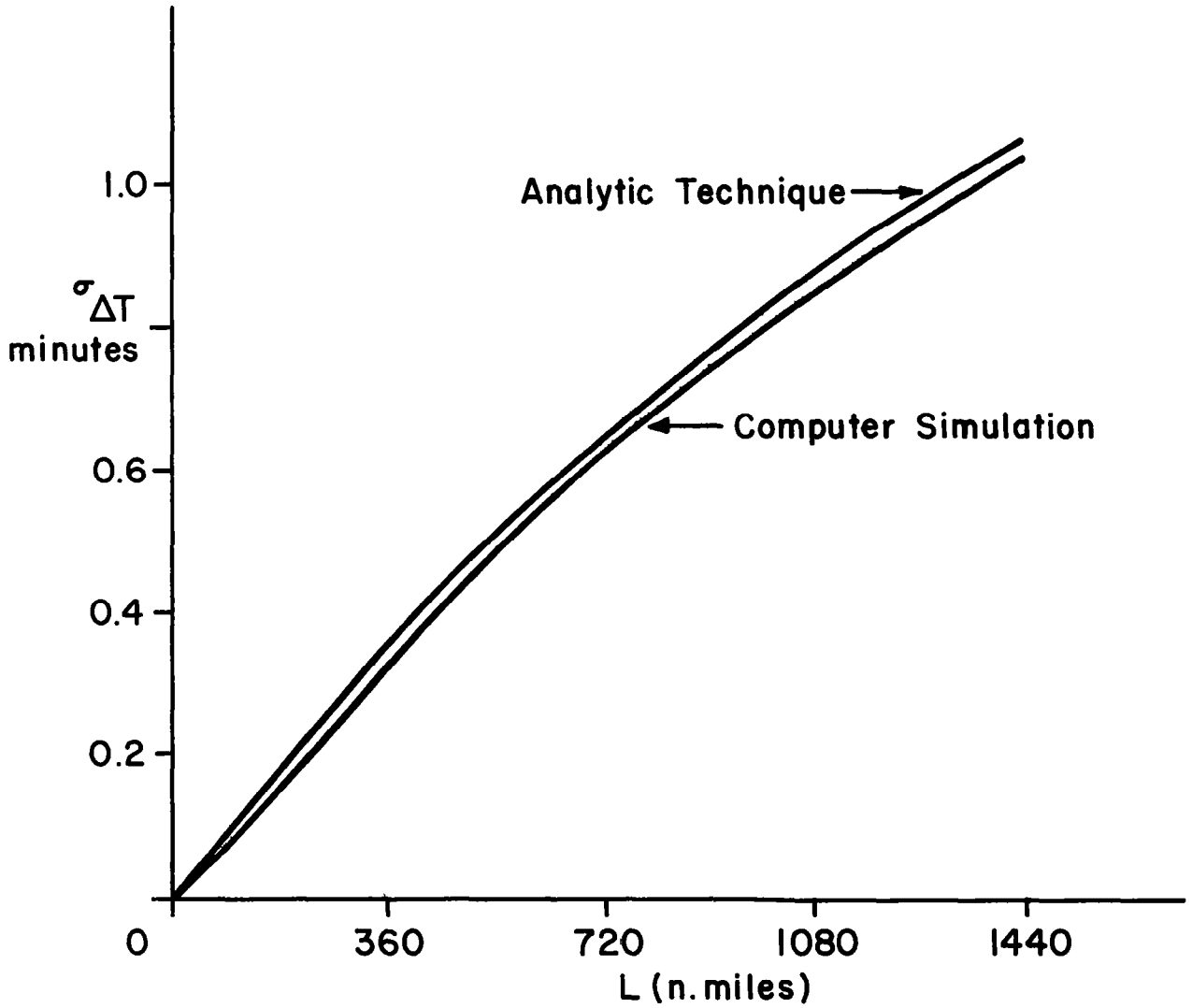

FIG. B-5: STANDARD DEVIATION OF FLIGHT TIME DIFFERENCE VS PATH LENGTH - COMPARISON OF ANALYTIC EVALUATION AND COMPUTER SIMULATION

supports the contention that the actual percentage error in $\sigma_{\Delta T}$ that results from approximation (B17) is small.

The mean and variance $\mu_{\Delta T}$ and $\sigma^2_{\Delta T}$ of the flight time difference ΔT for the crossing track case (cf. Figure B-2) can also be approximated in a manner analogous to that for the parallel track case. The approximations again depend upon the assumption that tail winds are small compared to airspeed. An evaluation of the mean flight time difference $\mu_{\Delta T}$ for the crossing track case will not be needed, for reasons given in Section B.5, and consequently is omitted. An approximation to $\sigma^2_{\Delta T}$ for the crossing track case, which is similar to the approximation eq. (B17) for the parallel track case, is evaluated in Section B.4.

The comparison of the results of Section B.3 with the results of a computer simulation have shown that the errors resulting from the approximation used in eq.(B17) to determine $\sigma^2_{\Delta T}$ analytically for the parallel track case are small. Since the approximations used in the analytic determination of $\sigma^2_{\Delta T}$ for both the parallel and crossing track cases are equivalent, the considerable additional programming effort required to determine $\sigma^2_{\Delta T}$ by computer simulation for the crossing track case is not necessary and has not been undertaken.

3. Parallel Tracks

In Section B.2, it was shown that the variance $\sigma^2_{\Delta T}$ of the flight time difference for the two parallel tracks in Figure B-6 can be approximated by

$$\sigma^2_{\Delta T} \approx \frac{1}{A^4}\int_{x_o}^{x_o+L}\int_{x_o}^{x_o+L} E\left\{\left[w_{x2}(p) - w_{x1}(p)\right]\left[w_{x2}(q) - w_{x1}(q)\right]\right\} dp\ dq$$

$$= \frac{1}{A^4}\int_{x_o}^{x_o+L}\int_{x_o}^{x_o+L} E\left\{\left[w_{x1}(p, y_o) - w_{x2}(p, y_o+d)\right]\right.$$

$$\left. x\left[w_{x1}(q, y_o) - w_{x2}(q, y_o+d)\right]\right\} dp\ dq \quad . \qquad (B19)$$

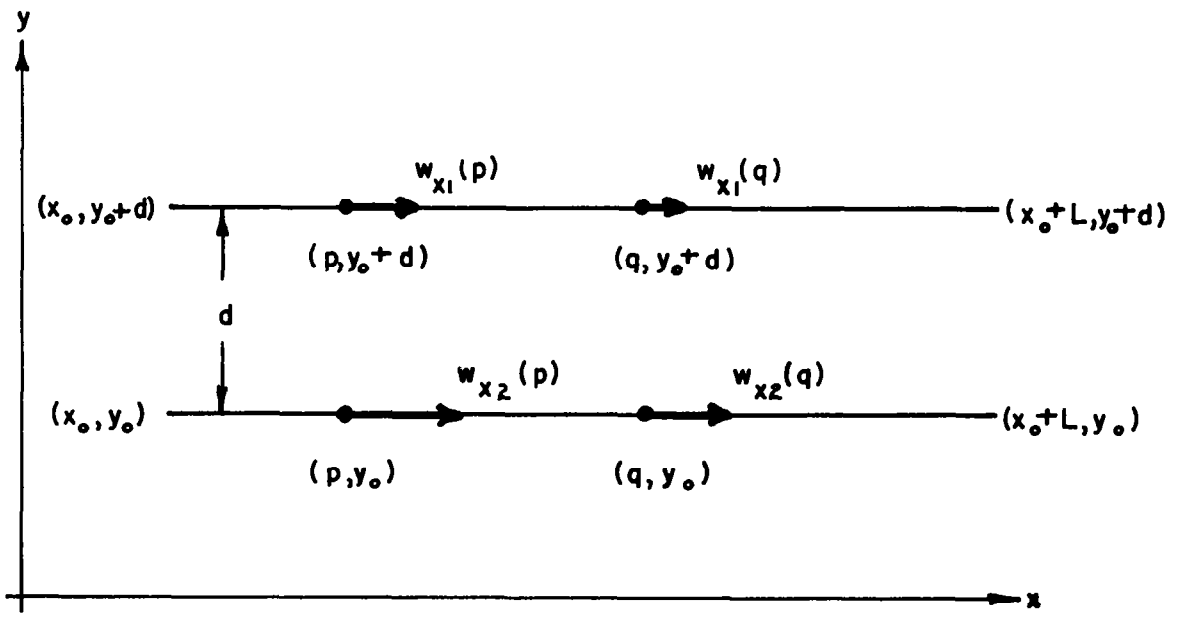

Figure B-6

In accordance with the model developed in Appendix A, the correlation of the winds at two points depends upon the relative positions of the points and not upon their absolute positions. Consequently, eq. (B19) becomes

$$\sigma_{\Delta T}^2 \approx \frac{2\sigma_x^2}{A^4} \int_0^L \int_0^L \left\{ R_x(|\, p-q\,|\,, 0) - R_x(|\, p-q\,|\,, d) \right\} dp\, dq \qquad \text{(B20)}$$

where the standard deviation σ_x of the x-direction wind component is taken to be constant in the region of interest, in accordance with the assumption of stationarity in Appendix A. Using eq. (A60) for the wind correlations appearing in eq. (B20), we have:

$$\sigma_{\Delta T}^2 \approx \frac{2\sigma_x^2}{A^4} \int_0^L \int_0^L \left[R_{xu}(|\, p-q\,|) - \frac{(p-q)^2 R_{xu}\left(\sqrt{(p-q)^2 + \rho^2 d^2}\right)}{(p-q)^2 + \rho^2 d^2} - \frac{\rho^2 d^2 R_{yu}\left(\sqrt{(p-q)^2 + \rho^2 d^2}\right)}{(p-q)^2 + \rho^2 d^2} \right] dp\, dq \,. \qquad \text{(B21)}$$

The standard deviation $\sigma_{\Delta T}$ has been determined for a variety of parallel flight paths from eq. (B21) by numerical integration. The results are presented graphically in Section (B.5). Numerical values for the functions R_{xu} and R_{yu}, appearing in eq. (B21), were taken from data in a paper by C. S. Durst.[3] The numerical value of the parameter ρ has already been given in eq. (A26), and the standard deviation σ_x is given in charts in reference 2. An examination of these charts reveals that σ_x is essentially constant along the flight paths of interest and thus supports the assumption of stationarity made in Appendix A.

4. Crossing Tracks

Consider two tracks, each of length L, crossing at an angle 2θ which is bisected by the x-axis, as in Figure B-7. The flight times for the two paths are, respectively,

$$T_1 = \int_0^L \frac{dr}{A + W_1(r\cos\theta, (L-r)\sin\theta)} = \int_0^L \frac{dr}{A + W_1(\vec{r}_1)} \quad , \quad (B22)$$

$$T_2 = \int_0^L \frac{dr}{A + W_2(r\cos\theta, (r-L)\sin\theta)} = \int_0^L \frac{dr}{A + W_2(\vec{r}_2)} \quad . \quad (B23)$$

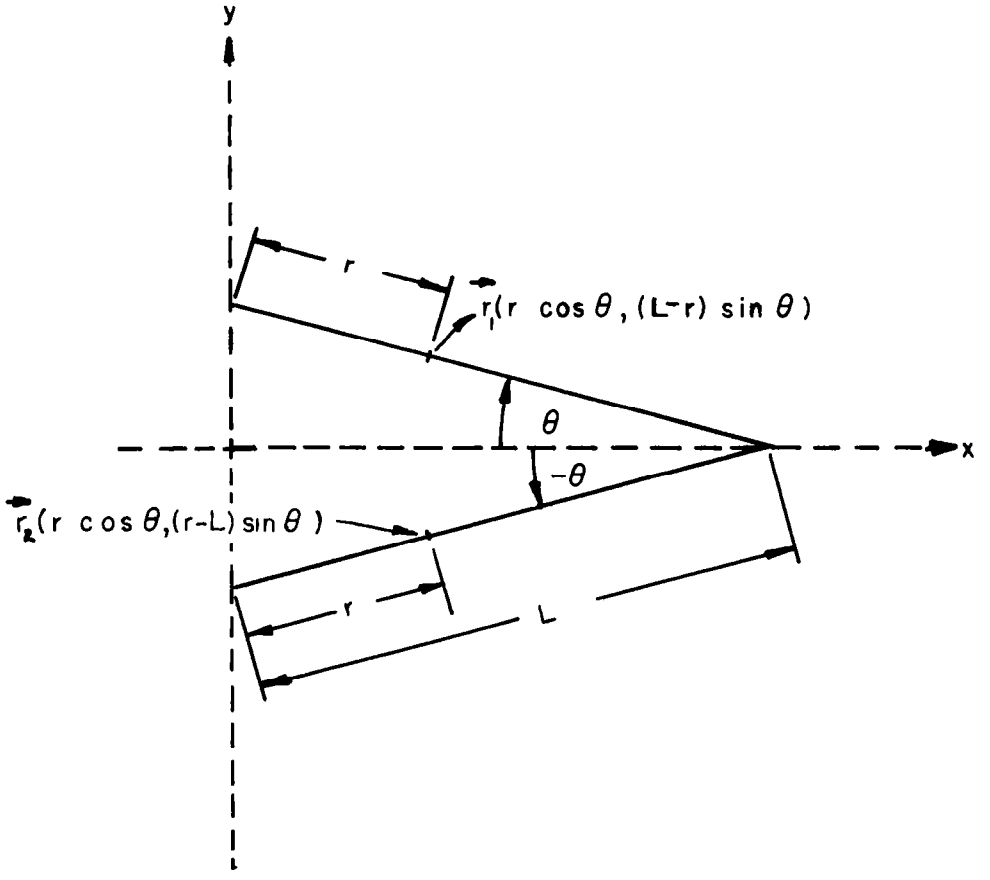

Figure B-7

where W_1 and W_2 represent tail winds along the first and second flight paths, respectively, $\vec{r}_1$ represents the vector with coordinates $(r\cos\theta, (L-r\sin\theta)$,

and $\vec{r}_2$ represents the vector with coordinates $(r\cos\theta, (r-L)\sin\theta)$.

As in the case of two parallel tracks, it can readily be shown that the variance $\sigma^2_{\Delta T}$ of the flight time difference for the two tracks is approximately

$$\sigma^2_{\Delta T} \approx \frac{1}{A^4}\int_0^L\int_0^L E\left\{\left[w_1(\vec{r}_1) - w_2(\vec{r}_2)\right]\left[w_1(\vec{s}_1) - w_2(\vec{s}_2)\right]\right\} dr\, ds \quad , \text{(B24)}$$

where w_1 and w_2 are related to the winds W_1 and W_2, respectively, by the equations:

$$w_1 = W_1 - E(W_1)$$

$$w_2 = W_2 - E(W_2) \quad . \qquad \text{(B25)}$$

Eq. (B24) may be written in the form

$$\sigma^2_{\Delta T} \approx \frac{1}{A^4}\int_0^L\int_0^L \left\{E\left[w_1(\vec{r}_1)w_1(\vec{s}_1)\right] + E\left[w_2(\vec{r}_2)w_2(\vec{s}_2)\right]\right.$$

$$\left. - E\left[w_1(\vec{r}_1)w_2(\vec{s}_2)\right] - E\left[w_1(\vec{s}_1)w_2(\vec{r}_2)\right]\right\} dr\, ds \text{(B26)}$$

The four terms in the integrand of eq. (B26) are given by

$$E\left[w_1(\vec{r}_1)w_1(\vec{s}_1)\right] = \sigma^2_{-\theta}R_{-\theta}(|\, r-s\,|)$$

$$E\left[w_2(\vec{r}_2)w_2(\vec{s}_2)\right] = \sigma^2_{\theta}R_{\theta}(|\, r-s\,|)$$

$$E\left[w_1(\vec{r}_1)w_2(\vec{s}_2)\right] = \sigma_\theta \sigma_{-\theta} R_{\theta,-\theta}(\vec{r}_1 - \vec{s}_2)$$

$$E\left[w_1(\vec{s}_1)w_2(\vec{r}_2)\right] = \sigma_\theta \sigma_{-\theta} R_{\theta,-\theta}(\vec{s}_1 - \vec{r}_2) \quad , \tag{B27}$$

where $\sigma_{-\theta}$ and σ_θ represent standard deviations of the tail winds on the first and second tracks, respectively, and the correlation functions are defined by eqs. (A78) and (A85). From eqs. (A76), (A77), (A85), it can be shown immediately that $\sigma_\theta = \sigma_{-\theta}$, $R_{-\theta}(|\, r-s\,|) = R_\theta(|\, r-s\,|)$ and $R_{\theta,-\theta}(\vec{r}_1-\vec{s}_2) = R_{\theta,-\theta}(\vec{s}_1-\vec{r}_2)$. Eq. (B26) can therefore be written

$$\sigma^2_{\Delta T} \approx \frac{2\sigma^2_\theta}{A^4} \int_0^L \int_0^L \left\{R_\theta(|\, r-s\,|) - R_{\theta,-\theta}(\vec{r}_1-\vec{s}_2)\right\} dr\, ds \quad . \tag{B28}$$

Using formulas (A78) and (A85) for the R_θ and $R_{\theta,-\theta}$ functions, eq. (B28) becomes,

$$\sigma^2_{\Delta T} \approx \frac{2\sigma^2_\theta}{A^4}\left[I_1 - I_2\right] \quad , \tag{B29}$$

where

$$I_1 = \int_0^L \int_0^L \frac{\rho^2 R_{xu}(\alpha) + (\rho^2-1)^2 \cos^2\theta \sin^2\theta R_{yu}(\alpha)}{(\cos^2\theta + \rho^2 \sin^2\theta)(\rho^2\cos^2\theta + \sin^2\theta)}\, dr\, ds \quad , \tag{B30}$$

$$I_2 = \int_0^L \int_0^L \left\{ \frac{\rho^2\left[(r-s)^2\cos^4\theta - (2L-r-s)^2\sin^4\theta\right]R_{xu}(\beta)}{(\rho^2\cos^2\theta + \sin^2\theta)\beta^2} \right.$$

$$\left. + \frac{\cos^2\theta\sin^2\theta\left[\rho^4(2L-r-s)^2 - (r-s)^2\right]R_{yu}(\beta)}{(\rho^2\cos^2\theta + \sin^2\theta)\beta^2} \right\} drds \quad . \tag{B31}$$

The arguments α, β appearing in eqs. (B30) and (B31) are

$$\alpha = \sqrt{(r-s)^2\cos^2\theta + \rho^2\sin^2\theta}$$

$$\beta = \sqrt{(r-s)^2\cos^2\theta + \rho^2(2L-r-s)^2\sin^2\theta} \quad . \tag{B32}$$

The standard deviation $\sigma_{\Delta T}$ has been determined for certain specific cases of crossing tracks from eqs. (B29) - (B32) by numerical integration. As in the case of parallel tracks, the values of the R_{xu} and R_{yu} functions required for this integration were taken from the paper by C. S. Durst.[3] Numerical results are presented in the next section.

5. Numerical Results

In Section B.2, ΔT was defined as the difference, caused by the variation of wind with distance, in flight times for two aircraft flying at identical airspeeds along two different flight paths, each of length L. In the case of a particular pair of parallel flight paths, eqs. (B11) and (B21) represent, respectively, the mean $\mu_{\Delta T}$ and variance $\sigma^2_{\Delta T}$ of the flight time difference as functions of the wind statistics, the path length L, the path separation d, and the airspeed A. These equations have been used to determine numerical values of $\mu_{\Delta T}$ and $\sigma_{\Delta T}$ for a fixed airspeed of 480 knots and for various

lengths and separations of parallel flight paths. The results are presented graphically in Figures B-10 and B-11.

Values of the mean μ_x and the standard deviation σ_x of the wind were required, respectively, for the results in Figure B-10 on the mean $\mu_{\Delta T}$ and in Figure B-11 on the standard deviation $\sigma_{\Delta T}$ of the time difference. The required wind statistics were taken from charts in reference 2 and were determined for flight paths in a region of the mid-Atlantic between 45° N and 60° N. Somewhat different results from those shown in Figures B-10 and B-11 would be obtained for other geographical regions of the North Atlantic. The results for $\mu_{\Delta T}$ might vary from those in Figure B-10 by as much as 20%; however, the results for $\sigma_{\Delta T}$ are much more significant in the applications considered in Chapter V and do not vary from those in Figure B-11 by more than 5% in the geographical regions of greatest interest. The difference in scales used in Figures B-10 and B-11 reflects the relatively small values of $\mu_{\Delta T}$.

For a pair of crossing or converging flight paths, the standard deviation $\sigma_{\Delta T}$ is represented by eq. (B29) as a function of the appropriate wind statistics, the airspeed, the path length L, and the angle of intersection 2θ. To obtain numerical results, the wind statistics were again determined for flight paths in the mid-Atlantic between 45° N and 60° N, but the results do not vary significantly for other regions. The curves in Figure B-12 represent $\sigma_{\Delta T}$ as a function of the path length L, for two fixed values of the angle θ and an airspeed of 480 knots. One curve corresponds to a value of θ such that two aircraft flying along the two crossing paths will converge 1°, or 60 n. mi., laterally as they progress 10°, or about 360 n. mi., in the longitudinal direction. In this case, the angle θ is approximately 5°, as indicated in Figure B-8. The second curve represents the case in which the aircraft converge 2° laterally as they progress 10° in the longitudinal direction. In this case, the angle θ is approximately 10°, as indicated in Figure B-9.

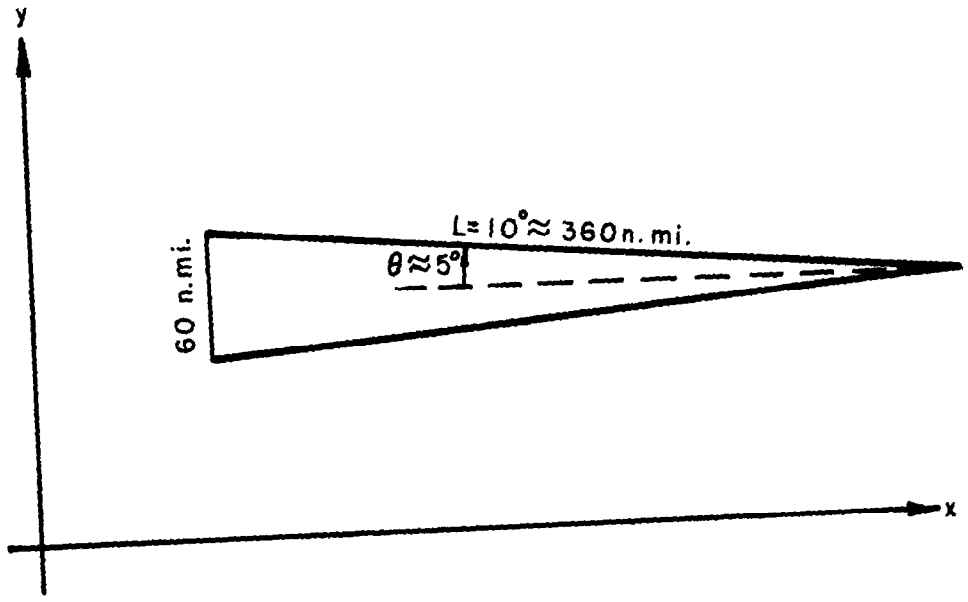

Figure B-8

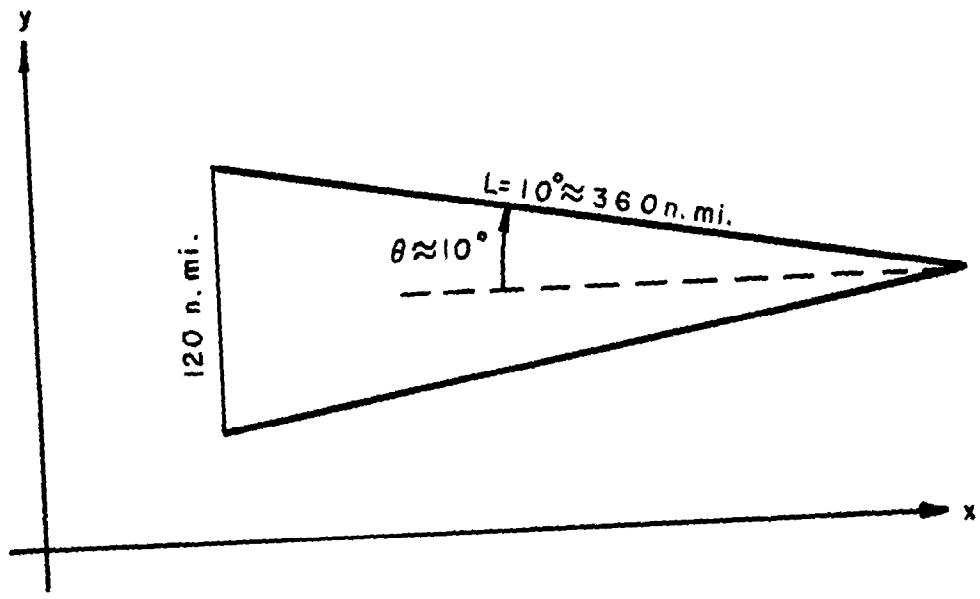

Figure B-9

A comparison of parallel and crossing tracks is provided in Figure B-13. Two curves represent $\sigma_{\Delta T}$ as a function of path length L for parallel tracks separated, respectively, by d = 60 and d = 120 nautical miles. A third curve represents $\sigma_{\Delta T}$ as a function of L for a pair of tracks crossing at an angle $2\theta = 10°$. For L = 720 n. mi., the average lateral separation of aircraft on the crossing tracks is 60 n. mi. The values of $\sigma_{\Delta T}$ at L = 720 n. mi. are 1.4, 2.0, 2.6 minutes on the three curves labeled, respectively, d = 60 n. mi., $\theta = 5°$, d = 120 n. mi. A larger value of $\sigma_{\Delta T}$ occurs for the crossing tracks than for the parallel tracks with the same average lateral separation d = 60 n. mi. This result is not surprising, since nonparallel tail wind components at two points have, in general, a smaller correlation coefficient than parallel tail wind components at the same points.

The implications of the results of this Appendix concerning separation standards are discussed in Chapter V. Two distinct types of applications are considered. In one case, we are concerned with aircraft assigned identical flight plan tracks and separated only in the longitudinal dimension, providing they follow the flight plan track exactly. If the reported air speeds are the same and the longitudinal separation is not large, say less than an hour, then identical flight times on any leg of the flight path will ordinarily be assumed by the controller. In practice, however, the two aircraft deviate laterally from the assigned flight plan. Although the two actual flight paths are not parallel and may even cross on occasions, the difference ΔT in flight times, caused by horizontal wind shear, may be associated with an equivalent pair of parallel paths having a separation d equal to the "average" lateral separation of the actual paths. The time difference ΔT then represents an error, caused by horizontal wind shear, in the planned longitudinal separation of the two aircraft.

The second type of application of the results of this Appendix is to cases in which two aircraft are assigned different flight plan tracks which

converge or cross at the same flight level. Longitudinal separation is required wherever the lateral separation standard is not satisfied. In this case, indentical flight times are not necessarily assumed by the controller for corresponding legs of the two flight paths. Instead, a difference in predicted flight times may reflect a difference in the forecast winds along the two paths. It is the actual winds, however, which determine the difference in flight times. After two aircraft have progressed a distance L along their respective paths, the longitudinal separation error, e, or the difference between the actual and predicted longitudinal separation, will depend upon the correlation of the actual and forecast winds. We shall now consider three possible techniques by which the winds along the two routes might be forecast.

In the first case, we shall suppose that the winds along the two routes are always forecast as the mean winds along those routes. For this simple forecasting technique, the mean predicted flight time difference for the two routes will be identical with the mean actual flight time difference. Consequently, the mean longitudinal separation error μ_e will be zero. Moreover, the standard deviation σ_e of the error in longitudinal separation will be identical with the standard deviation $\sigma_{\Delta T}$ of actual flight time differences, and the numerical results derived for $\sigma_{\Delta T}$ in this Appendix are directly applicable to this case.

Now suppose that the forecast winds on the two flight paths are based on the same 24-hour prognostic chart. The mean error μ_e in longitudinal separation will be assumed to be zero, since the mean forecast winds will be identical with the mean actual winds, unless the forecasting technique is biased. The standard deviation $\sigma_{\Delta T}$ of the actual flight time difference will provide a pessimistic estimate of the standard deviation σ_e of the error in longitudinal separation, since forecasting techniques based on 24-hour prognostic charts are superior (though only moderately so) to the simple forecasting technique described in the preceding paragraph.[9]

A third case occurs when the predicted flight times for the two paths are based on different wind forecasts. Since suitable statistics are not available on the correlation of forecast winds from different forecasts, the statistics of errors in longitudinal separation cannot be evaluated readily for this case. It is likely, however, that the standard deviation $\sigma_{\Delta T}$ of actual flight time differences for the two paths provides an optimistic estimate of the standard deviation σ_e of errors in longitudinal separation.

The last two possibilities considered for the wind forecasts along two different routes represent cases which occur in actual practice. The simple forecasting technique which we first considered represents an intermediate case between these two more realistic extremes. The applications of the results of the Appendix to problems related to the longitudinal separation of aircraft assigned nonidentical flight plan tracks are discussed in Chapter V. It is assumed in these discussions that the errors in predicted longitudinal separation, caused by wind differences along the two routes, are those that would occur when the simple wind forecasting technique is used; i.e., it is assumed that $\mu_e = 0$ and $\sigma_e = \sigma_{\Delta T}$. This assumption is made in all applications involving crossing or converging flight paths. It can now be made apparent why the mean flight time difference $\mu_{\Delta T}$ for such flight paths has not been evaluated. In accordance with the assumed wind forecasting technique, the mean predicted and mean actual flight time differences are identical. Therefore, the mean longitudinal separation error μ_e is zero, and an evaluation of $\mu_{\Delta T}$ is not needed.

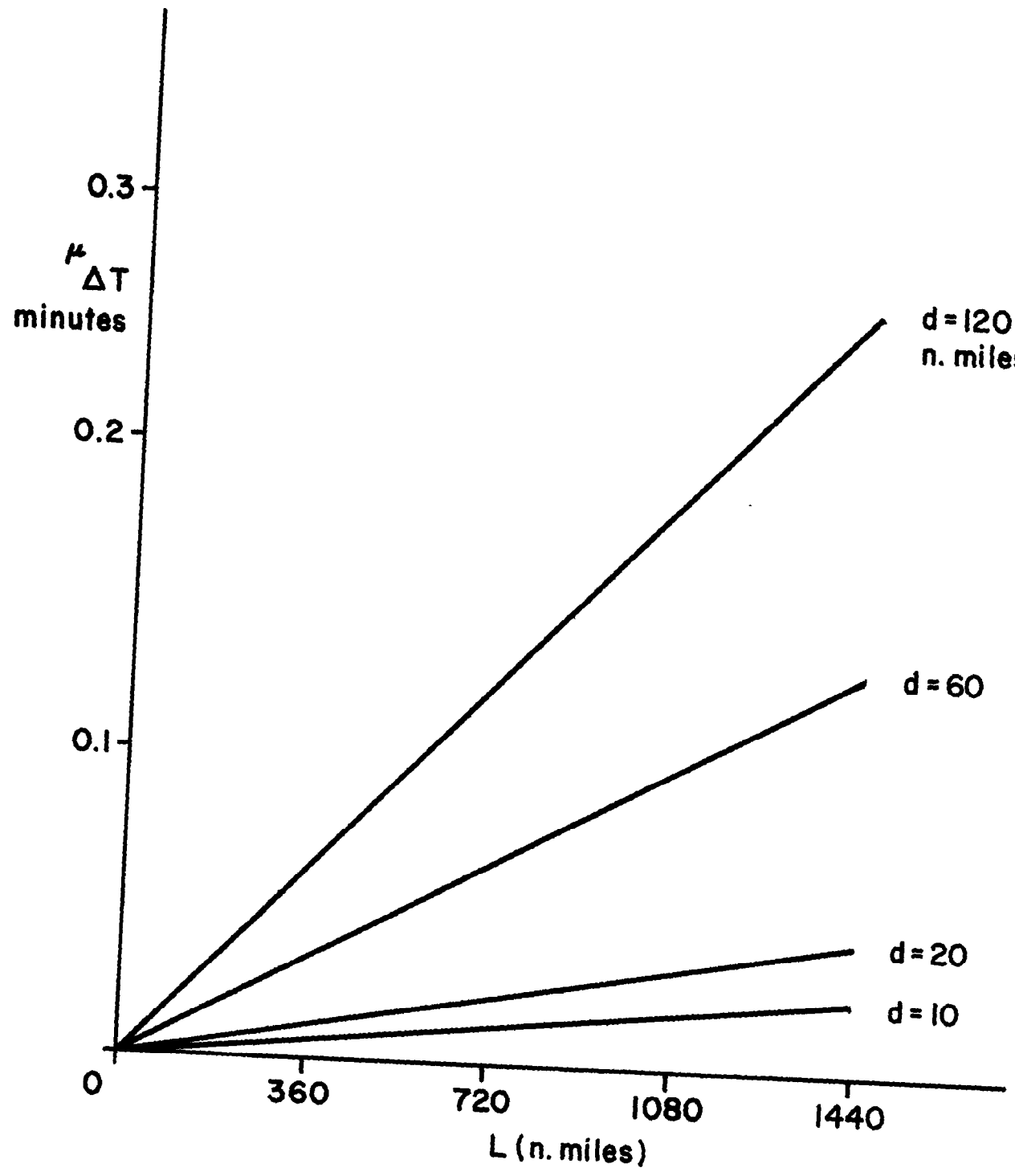

FIG. B-10: MEAN FLIGHT TIME DIFFERENCE VS PATH LENGTH - PARALLEL FLIGHT PATHS

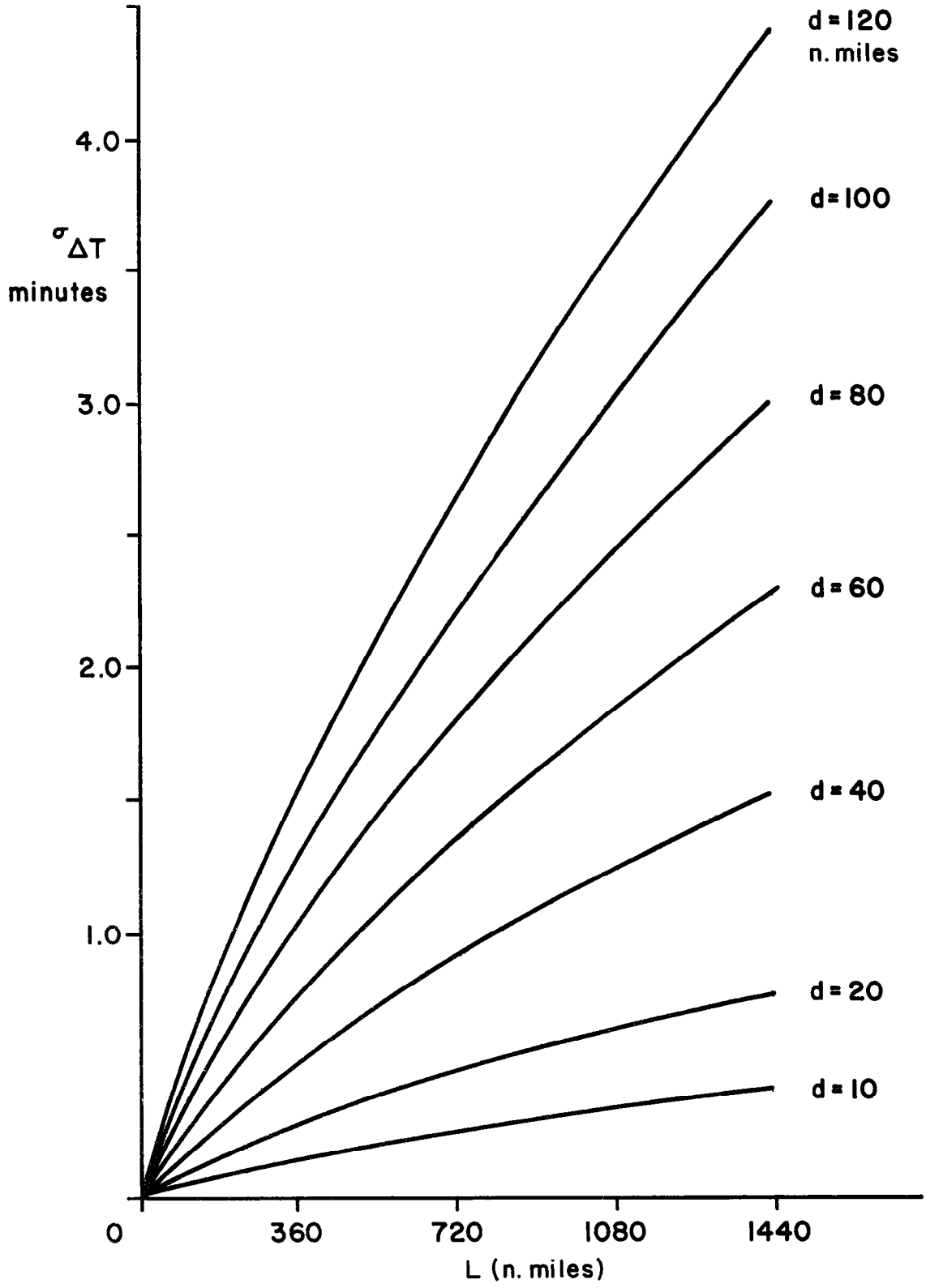

FIG. B-11: STANDARD DEVIATION OF FLIGHT TIME DIFFERENCE VS PATH LENGTH - PARALLEL FLIGHT PATHS

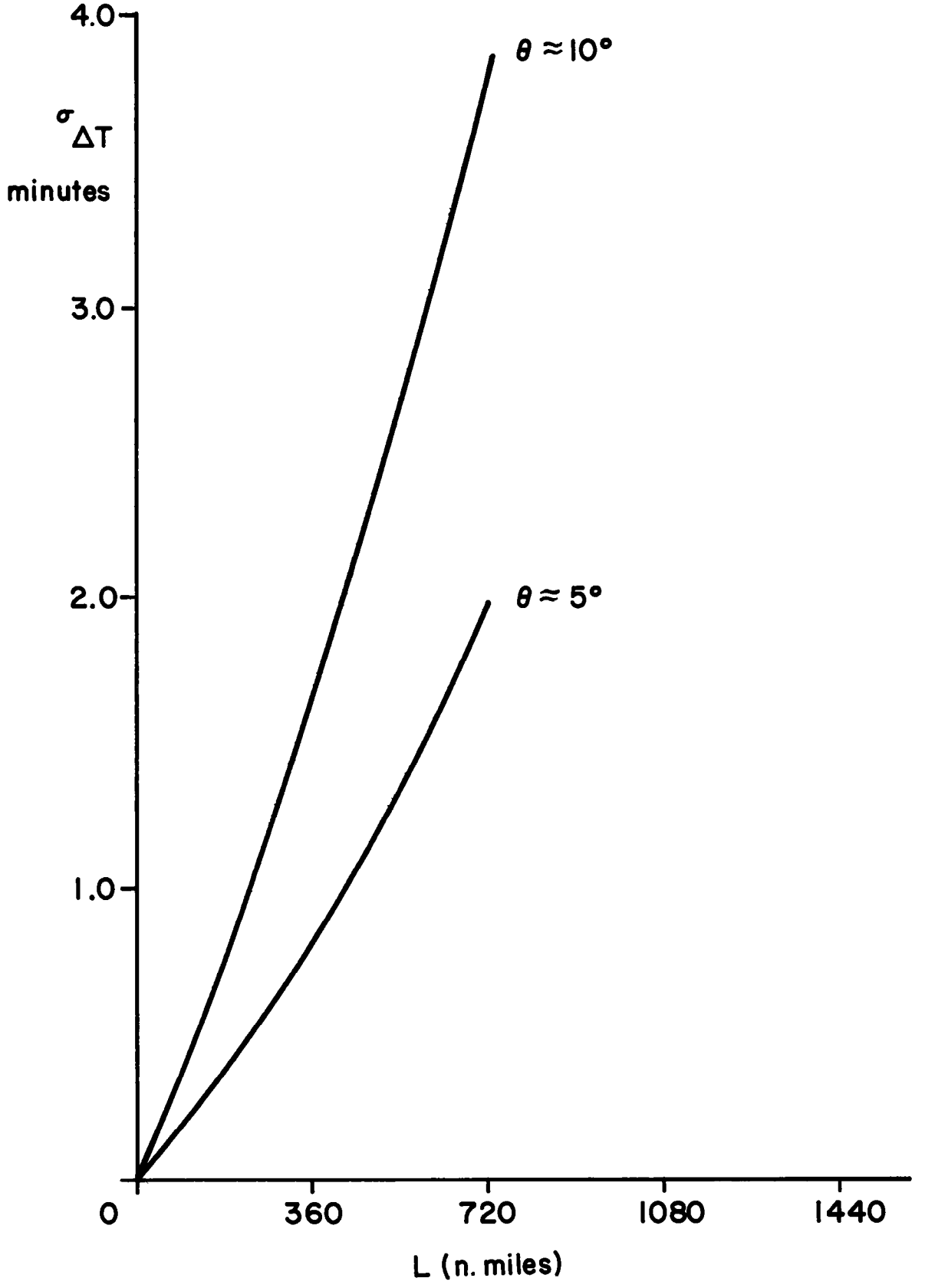

FIG. B-12: STANDARD DEVIATION OF FLIGHT TIME DIFFERENCE VS PATH LENGTH - CONVERGING FLIGHT PATHS

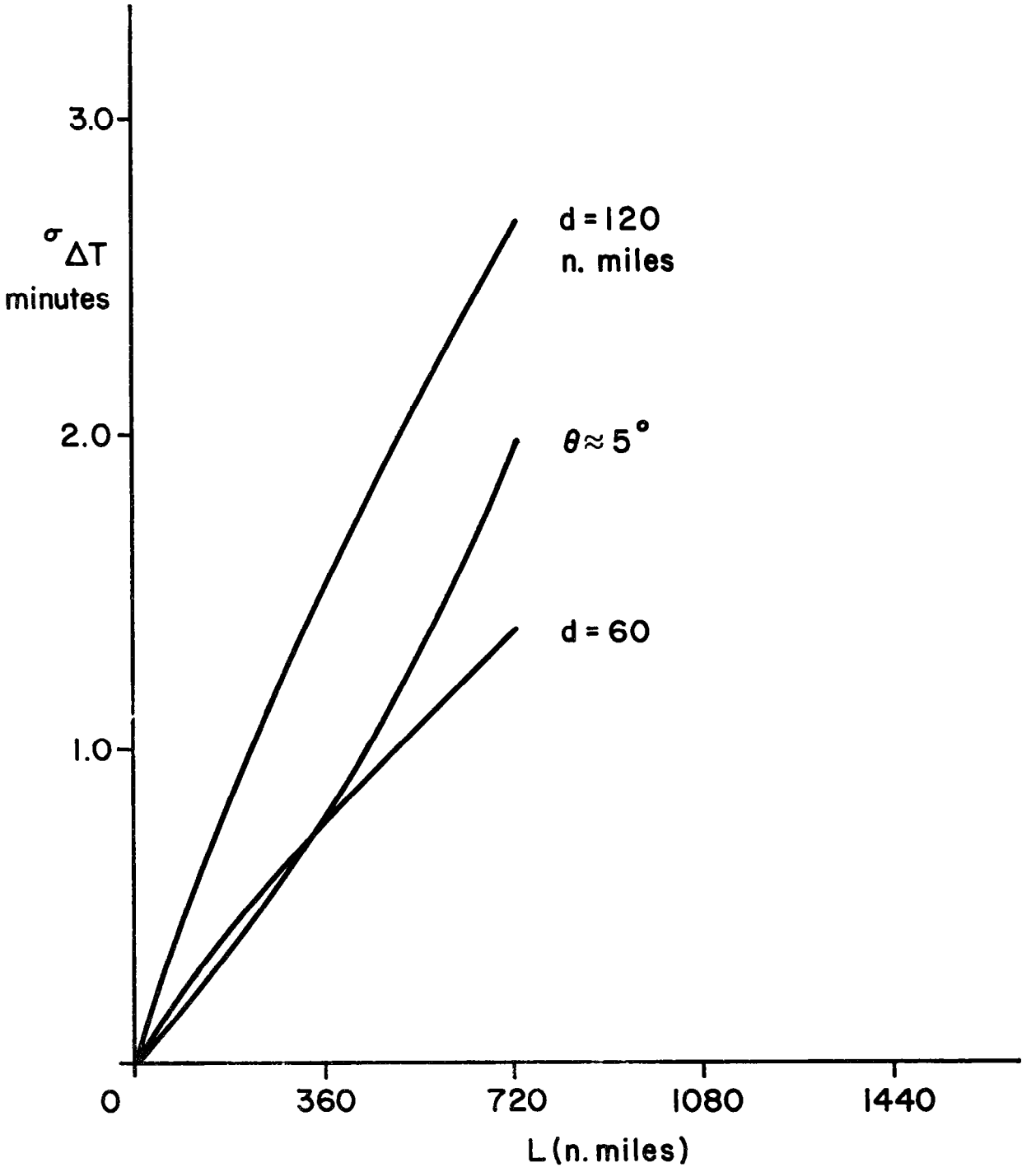

FIG. B-13: COMPARISON OF PARALLEL AND CONVERGING FLIGHT PATHS

APPENDIX C

MONTE CARLO EVALUATION OF LONGITUDINAL SEPARATIONS

1. Introduction

This Appendix describes a Monte Carlo study performed to validate certain analytical results of Appendix B concerned with the design of longitudinal separation standards. The primary objective of the validation is to obtain a statistical estimate of the errors in the predicted difference between the actual times of arrival of two aircraft following nominally the same path. Only the effects of tail winds are taken into account, and it is assumed that the air speed is known exactly. The winds are simulated by a statistical technique based on the geostrophic model derived in Appendix A. The entire simulation study, including the processing of the final results, is performed on an LGP-30 general purpose digital computer.

2. The Validation Model

The basic problem considered here is the same as that discussed in Appendix B. Aircraft entering the North Atlantic oceanic region and following nominally the same path must be given suitable longitudinal separations to ensure a sufficiently low probability of conflict throughout the entire trip. As a consequence of imperfect flight plan following, two such aircraft do not indeed fly along the same path, and are acted upon by different tail winds. This so-called "wind shear" gives rise to errors in the difference between the estimated times of arrival. In the final selection of longitudinal separation standards, such errors must be suitably compounded with errors in the air speed and errors in the initial aircraft fix from which future ETA's are predicted. It is, therefore, important to relate a measure of these errors to the length of the prediction interval which, in turn, depends on the size of the region lacking perfect communications. It should be pointed out here that, unless

the communication system in this region is highly reliable, the controller cannot shorten his prediction interval, and the longitudinal separation standards cannot be otherwise decreased unless the sources of longitudinal separation error are eliminated or minimized.

For the sake of simplicity in the validation study, it is assumed here that two aircraft flying nominally the same path actually follow two closely spaced parallel straight lines. The tail winds along these lines are produced by a pseudo-random "wind generator". Their statistical characteristics are identical with those of the geostrophic model discussed in detail in Appendix A. In addition, it is assumed here that the wind velocity has a Gaussian distribution. Finally, in accordance with Appendix B, an assumption is made that the overall effect of tail winds in a given region of space on the progress of an aircraft does not change appreciably in the time interval corresponding to aircraft separation. In other words, although winds at a point may fluctuate rapidly, their total effect, averaged over several minutes of flight, changes slowly with time.[8]

This last assumption leads to a useful simplification in the validation model. Instead of considering pairs of aircraft initially separated by an arbitrary longitudinal standard, it is sufficient to restrict attention to the cases in which both aircraft start simultaneously with zero separation. In effect, these cases are completely equivalent as far as the errors in ETA's are concerned.

The validation model, therefore, simulates the flight of a pair of aircraft starting simultaneously along two parallel paths separated by a distance related to the actual errors in lateral track-keeping. The tail winds along these paths are computed by the wind generator and added to a known air speed. In this manner, two ground speeds are obtained as functions of distance along the paths. These ground speed functions are subsequently processed to form

the difference in the time of flight of the two aircraft. These time differences are then recorded versus distance for many flights, and the results are processed statistically. In order to improve the accuracy of the estimates of the tails of the distribution of flight time differences, an elaborate statistical technique is used, devoting more computing effort to those cases which have shown an early tendency to develop large time differences.

3. Wind Simulation

Only the zero-mean tail wind component defined by eq. (A8) of Appendix A must be generated. The mean value of the wind is added later, together with the air speed.

Let us denote the zero-mean tail wind components along the two parallel paths as $w_1(x)$ and $w_2(x)$ respectively. Eq. (A60) shows that w_1 and w_2 are obviously correlated and, therefore, not easy to generate. However, advantage can be taken of the fact that their sum and difference are uncorrelated to simplify the computation. In particular, let us define two variables:

$$p = \frac{1}{2}(w_1 + w_2)$$

$$q = \frac{1}{2}(w_1 - w_2) \quad . \tag{C1}$$

The autocorrelation functions of these variables are:

$$\varphi_p(u) = \frac{1}{4}\left[\varphi_1(u) + \varphi_{12}(u) + \varphi_{21}(u) + \varphi_2(u)\right] \quad , \tag{C2}$$

$$\varphi_q(u) = \frac{1}{4}\left[\varphi_1(u) - \varphi_{12}(u) - \varphi_{21}(u) + \varphi_2(u)\right] \quad , \tag{C3}$$

where $\varphi_1(u)$ and $\varphi_2(u)$ are the autocorrelation functions of $w_1(x)$ and $w_2(x)$ respectively, while $\varphi_{12}(u)$ and $\varphi_{21}(u)$ are their cross-correlation functions. If we assume that the direction of flight is parallel to the x-axis, and if we denote the separation between the two parallel flight paths by d, then, in terms of the notation of Appendix A, these functions become:

$$\varphi_1(u) = \varphi_2(u) = \varphi_{xx}(u, 0) \quad , \tag{C4}$$

$$\varphi_{12}(u) = \varphi_{21}(u) = \varphi_{xx}(u, d) \quad , \tag{C5}$$

[cf. eqs. (A16), (A18), and (A22)].

Substituting eqs. (C4) and (C5) into eqs. (C2) and (C3), we obtain:

$$\varphi_p(u) = \frac{1}{2}\left[\varphi_{xx}(u, 0) + \varphi_{xx}(u, d)\right] \quad , \tag{C6}$$

$$\varphi_q(u) = \frac{1}{2}\left[\varphi_{xx}(u, 0) - \varphi_{xx}(u, d)\right] \quad . \tag{C7}$$

We can further express these functions in terms of the experimentally measured correlation functions R_{xu} and R_{yu} by means of eqs. (A44), (A47), and (A60):

$$\varphi_{xx}(u, 0) = \sigma_x^2 R_{xu}(u) \quad , \tag{C8}$$

$$\varphi_{xx}(u, d) = \frac{\sigma_x^2}{s^2}\left[u^2 R_{xu}(s) + \rho^2 d^2 R_{yu}(s)\right] \quad , \tag{C9}$$

$$\text{with } s^2 = u^2 + \rho^2 d^2 \quad . \tag{C10}$$

Also, noting from eq. (C1) that

$$pq = \frac{1}{4}(w_1^2 - w_2^2) \quad , \tag{C11}$$

and using eq. (C4), the cross-correlation function becomes:

$$\varphi_{pq}(u) = \frac{1}{4}\left[\varphi_1(u) - \varphi_2(u)\right] = 0 \quad . \tag{C12}$$

Thus, p and q are uncorrelated random variables with autocorrelation functions expressed by eqs. (C6) and (C7). Using eq. (C1), the winds can be simply expressed as

$$\begin{aligned} w_1 &= p + q \\ w_2 &= p - q \quad . \end{aligned} \tag{C13}$$

As is shown above, p and q can be generated independently of each other, considerably simplifying the program. In the design of the validation model it was decided to perform all computations necessary to compare the flight time of the aircraft at intervals of 120 nautical miles. Because of the smoothing process involved in the computation of flight time, it was also found sufficient to compute the wind values at the same intervals. The task of wind simulation was thus reduced to that of generating two discrete number sequences with the simple statistical properties described above.

A convenient technique of generating an infinite sequence with a prescribed autocorrelation function employs linear, time-invariant filtering of

a random sequence of mutually uncorrelated numbers. This latter sequence is usually called a "white noise" sequence. Its autocorrelation function is zero everywhere except at the origin, and its power density spectrum is a constant. In the simulation program, the white noise sequence is produced by a pseudo-random Gaussian noise generator subroutine. This ensures a Gaussian distribution of the resultant wind values, in conformance with assumptions made in the preceding Section.

The output of a realizeable discrete linear filter is a linear combination of its past and present inputs. Denoting the n-th input by f_n, the n-th output is expressed by the convolution summation:

$$p_n = \sum_{i=0}^{\infty} g_i f_{n-i} \quad . \tag{C14}$$

The g_k are the constant coefficients describing the filter. Their number is finite, and, therefore, the summation in eq. (C14) is finite. In view of eq. (C14), the k-th sample of the autocorrelation function of the p_n sequence can be written as

$$E[p_n p_{n+k}] = E\left[\sum_{i=0}^{\infty} g_i f_{n-i} \sum_{j=0}^{\infty} g_j f_{n+k-j}\right] = \sum_{i=0}^{\infty} \sum_{j=0}^{\infty} g_i g_j E\left[f_{n-i} f_{n+k-j}\right] . \tag{C15}$$

Since, however, the zero-mean input sequence, f_n, is white,

$$E\left[f_{n-i} f_{n+k-j}\right] = \begin{cases} \sigma_o^2, & j=i+k \\ 0, & \text{otherwise} \end{cases} , \tag{C16}$$

where σ_o^2 is the variance of the input sequence. Therefore,

$$E\left[p_n p_{n+k}\right] = \sigma_o^2 \sum_{i=0}^{\infty} g_i g_{i+k} \quad . \tag{C17}$$

This suggests that the p_n sequence could be generated by processing a white, Gaussian, zero-mean sequence with a linear filter whose coefficients satisfy condition (C17). The left-hand side of eq. (C17) represents the k-th sample of $\varphi_p(u)$, taken at intervals of 120 nautical miles. These samples are simply related to R_{xu} and R_{yu} through eqs. (C6), (C8), (C9), and (C10), and are, therefore, known. The required values of R_{xu} and R_{yu} are found from curves shown in Figure A-1. The problem now is to find a finite sequence g_i that will satisfy eq. (C17). Unfortunately, this problem is not simple and, in general, it does not have a unique solution. In our case, this problem was solved using an indirect iterative technique on a digital computer. The solution contains 16 coefficients and, therefore, the output of the filter in eq. (C14) is a linear combination of 16 consecutive inputs. As implied by eqs. (C6) and (C7), this solution must be obtained individually for each choice of track separation d. Of course, an analogous problem must be solved for the generation of the q_n sequence, i.e.,

$$q_n = \sum_{i=0}^{\infty} h_i f_{n-i} \quad , \tag{C18}$$

with

$$E\left[q_n q_{n+k}\right] = \sigma_o^2 \sum_{i=0}^{\infty} h_i h_{i+k} \quad . \tag{C19}$$

Denoting the filters for the generation of the p_n and q_n sequences by G and H respectively, the complete process of computing the tail winds along both paths can be summarized in the diagram in Figure C-1.

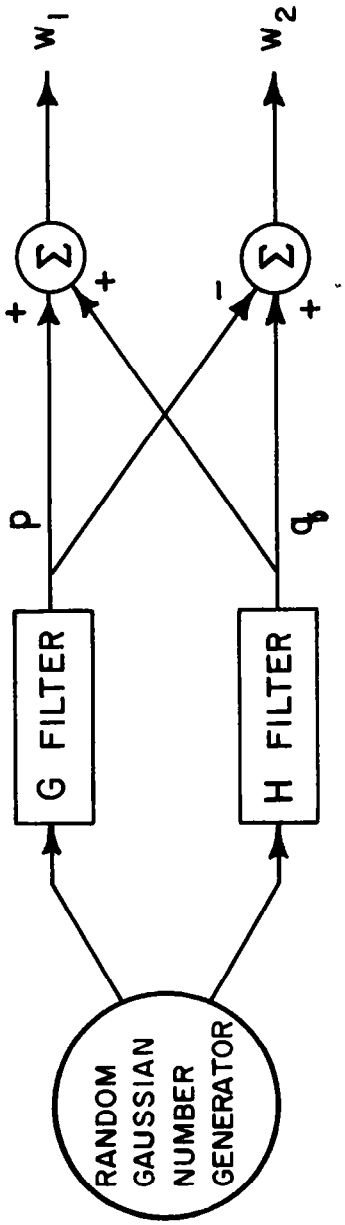

FIG. C-1 : WIND GENERATOR DIAGRAM

The successive outputs of the pseudo-random Gaussian number generator are alternately fed into the two filters, G and H, and are suitably convolved with the two corresponding sets of 16 coefficients. The outputs then are added and subtracted to produce the tail winds along both parallel paths in accordance with eq. (C13). The statistical characteristics of winds obtained in this manner are the same as those derived in Appendix A from a realistic model of wind behavior in the North Atlantic.

4. Flight Time Computation

The zero-mean tail winds produced by the process described in the preceding Section are added to the appropriate wind mean values and to the air speeds of the two aircraft to form their respective ground speeds as functions of distance at 120 mile intervals. The time of flight of each aircraft is then computed by integrating the reciprocal of its ground speed in accordance with

$$t = \int_0^X \frac{dx}{v} \quad . \tag{C20}$$

The value of this integral is obtained using trapezoidal approximation. Finally, the difference in the flight times of the two aircraft is computed at intervals of 120 miles and stored in the computer memory for statistical processing.

5. Data Processing

The object of the validation program is to determine the statistics of the difference of flight time of the two aircraft. Ideally, one would wish to obtain an accurate estimate of the probability density of the time difference,

particularly the probability of large differences, in order to evaluate the probability of longitudinal conflicts. Unfortunately, it is impractical to use simulation techniques to get reliable estimates of the probabilities of large differences, mainly because of their extremely low values. An attempt is made here to increase the accuracy of such estimates through the so-called "split" technique in order to permit a meaningful use of the results for validation purposes in other parts of this report [cf. Appendix B]. However, no attempt should be made to deduce the probability of collision from the results described in this Appendix.

The basic purpose of the split technique is to shift emphasis from low, and, therefore, more frequent values of flight time difference to its high values, occurring much less frequently. In other words, this method permits an increase in accuracy of the estimate of the probability of a rare event, at the expense of accuracy in the measurement of probabilities of more frequent events.[11] It is applied to our problem in a relatively elementary way. Whenever the time difference exceeds a preassigned threshold at a given range (say, 0.7 minutes at 600 miles), the main program is interrupted. Instead, an auxiliary program is started, performing ten independent secondary runs, all starting at the same range, with the same time difference, and with the same initial wind conditions and past history as those of the primary run at the instant of its interruption. When recording the results, however, these secondary runs are assigned only one tenth of the weight of the primary runs. Thus, the runs showing an early tendency to develop large time differences are actually split into ten secondary runs providing more fine grain data in the tails of the distribution where it is needed.

The data processing program controls the course of the simulation. Each primary run is started independently by clearing the memory of the G and H filters. The absolute value of the computed time differences is quantized by dividing it into one minute intervals. This value is then counted

at each 120 mile range interval by adding ten points to the appropriate quantum counter. When the condition for a split is satisfied, a split of ten secondary runs is performed. During the operation of the split phase, the counting is done by assigning a score of only one point to each outcome. Each complete run is terminated when the maximum range is reached. In each case, however, just before the quantization, the magnitude of the flight time difference is squared and summed in order to compute the mean square of the time difference at that range. Since it is known from theoretical considerations [cf. Appendix A] that the distribution of the time difference has a zero-mean value, this calculation serves as an estimate of the variance of the time difference.

Figure C-2 is a reproduction of a typical computer printout. In this case, the two parallel straight line paths were separated by 28 nautical miles. The legend on top is interpreted as follows:

Number of primary runs	999
Number of runs split	127
Total number of runs	2142
Air speed	480 knots
Split threshold	0.7 minutes
Split range	5x120=600 n.m.

The first column, under 0, contains the recorded score falling between 0 and 1 minutes. The column under 1 contains the score falling between 1 and 2 minutes, and so forth. The rows correspond to range increments of 120 miles. The last column represents the variance.

track separation : 28 n.m.

999	127	2142	480/480	.7	5					
R	0	1	2	3	4	5	6	7	8	9	var
120	9990	0	0	0	0	0	0	0	0	0	0
240	9990	0	0	0	0	0	0	0	0	0	0
360	9920	70	0	0	0	0	0	0	0	0	.1
480	9690	300	0	0	0	0	0	0	0	0	.2
600	9260	730	0	0	0	0	0	0	0	0	.3
720	8733	1243	14	0	0	0	0	0	0	0	.4
840	8268	1672	50	0	0	0	0	0	0	0	.5
960	7848	2031	108	3	0	0	0	0	0	0	.6
1080	7563	2238	178	11	0	0	0	0	0	0	.7
1200	7137	2524	312	17	0	0	0	0	0	0	.8
1320	6911	2624	421	33	1	0	0	0	0	0	.9
1440	6617	2785	542	44	2	0	0	0	0	0	1.1
1560	6381	2900	643	59	7	0	0	0	0	0	1.2

Figure C-2

Typical Printout

6. Simulation Results

Let us examine the last row in Figure C-2, corresponding to a range of 1560 nautical miles. The sum of the entries in this row is 9990. Therefore, an estimate of the probability that the time difference exceeds 4 minutes is 7/9990. Similarly, an estimate of the probability of exceeding 3 minutes is 66/9990, and so forth. These results are smoothed and plotted in Figure C-3 for several ranges. Each curve in this figure serves as an approximation to the probability that the time difference exceeds a value read on the abscissa. Figures C-4 and C-5 show plots of analogous results obtained for air speeds of 425 and 400 knots respectively.

The last column in Figure C-2 is a very accurate estimate of the variance of the flight time difference of the two aircraft. Figure C-6 shows plots of this estimate versus range for several air speeds. As expected, the variance increases with range, but decreases with air speed. To show the dependence on air speed more clearly, the same data is used to plot in Figure C-8 the variance of time difference as a function of air speed for several values of range. An even better insight is gained by considering the standard deviation instead of the variance. For this purpose, the square root was taken of the sample variance computed in the simulation. These results are summarized in Table C-I.

Air Speed In Knots	Range in naut. miles												Sample Size
	240	360	480	600	720	840	960	1080	1200	1320	1440	1560	
400	.3	.4	.6	.8	.9	1.0	1.1	1.3	1.4	1.5	1.5	1.6	1335
425	.3	.4	.5	.7	.8	.9	1.0	1.1	1.2	1.3	1.4	1.4	2100
450	0	.3	.4	.6	.6	.8	.8	1.0	1.0	1.1	1.2	1.3	1070
480	0	.3	.4	.5	.6	.7	.8	0.8	0.9	1.0	1.1	1.1	2142
500	0	.3	.3	.4	.5	.6	.7	0.8	0.8	0.9	1.0	1.0	500
535	0	0	.3	.3	.4	.5	.6	0.6	0.7	0.8	0.8	0.9	1184

Table C-I

Standard Deviation of Flight
Time Difference

Figure C-7 shows the functional dependence of the standard deviation on range for several air speed values. As can be seen from this Figure, the standard deviation increases linearly with range. This simple relationship permits us to estimate readily the effect of varying the size of the area lacking adequate communications on the choice of longitudinal separation standards. Thus, a proposed change in the size of the communication gap will produce a corresponding change in the standard deviation of the time separation of the aircraft. The actual value of this latter change can be obtained from Figure C-7. If now the longitudinal separation standard is changed in the same proportion as the standard deviation, the probability of longitudinal conflict will remain approximately the same.

To evaluate the effects of supersonic speeds, a number of runs were performed with an air speed of 1320 knots. The results are summarized in Figure C-9.

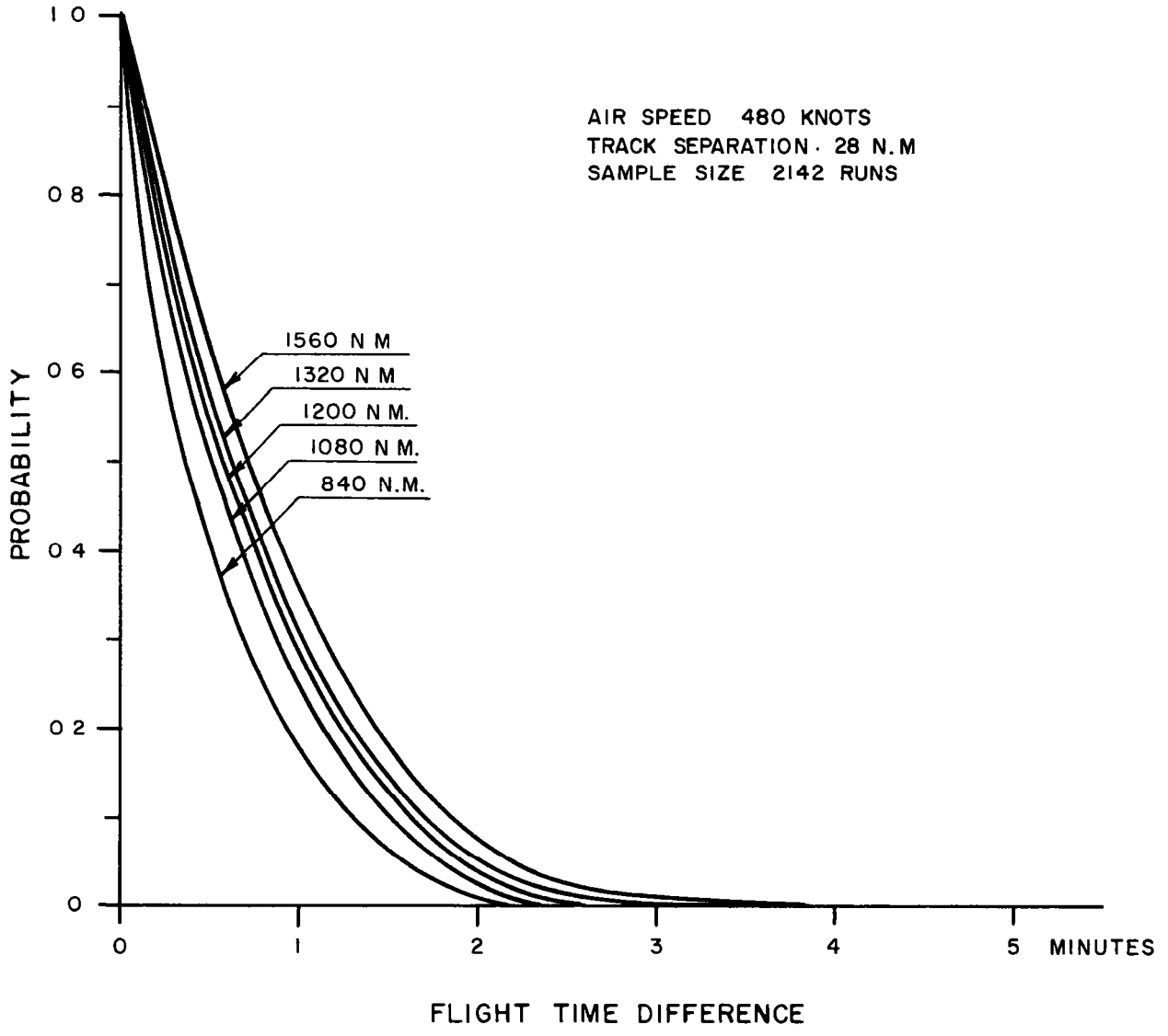

FIG. C-3: PROBABILITY THAT A GIVEN FLIGHT-TIME DIFFERENCE IS EXCEEDED

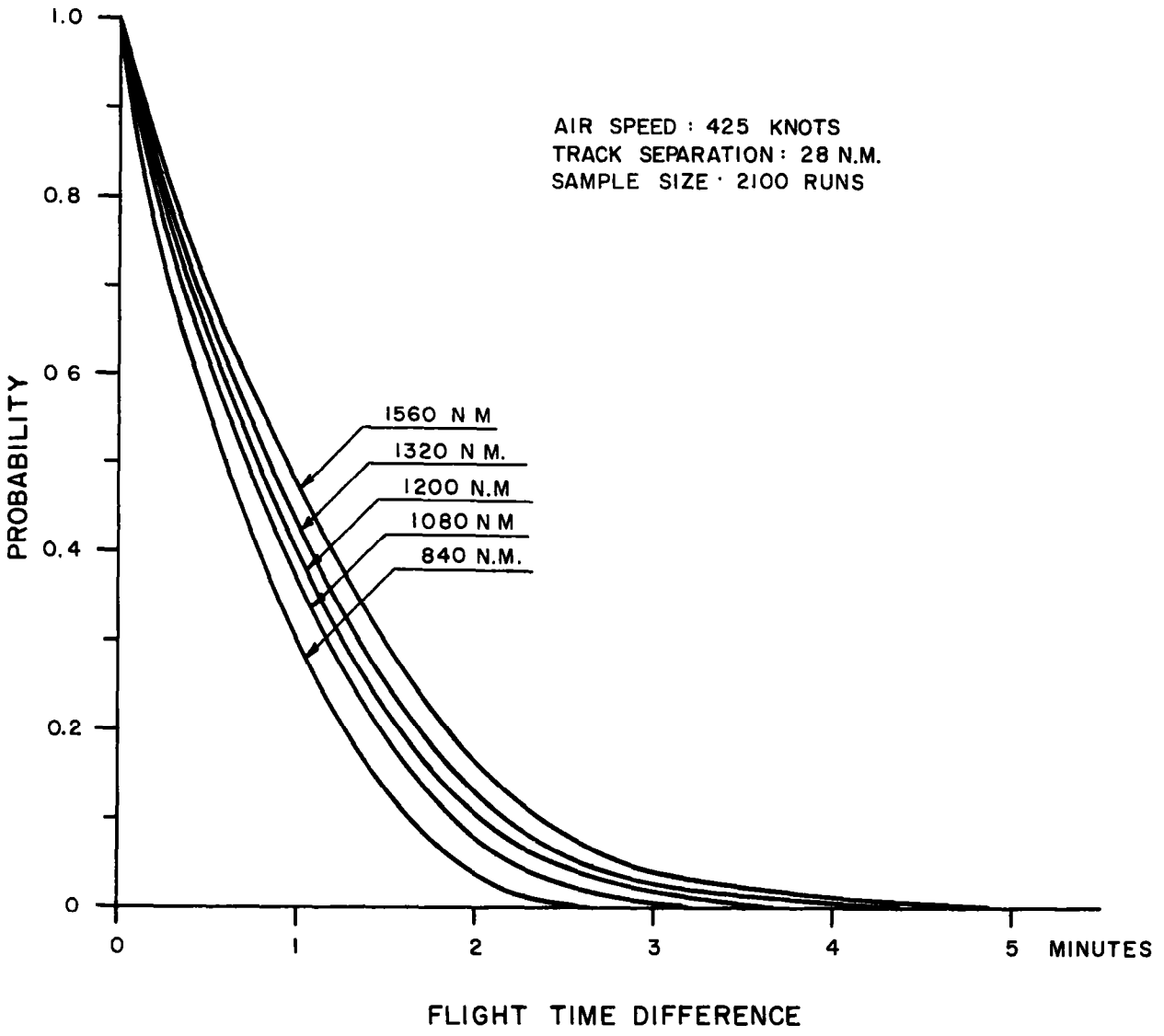

FIG.C-4: PROBABILITY THAT A GIVEN FLIGHT-TIME DIFFERENCE IS EXCEEDED

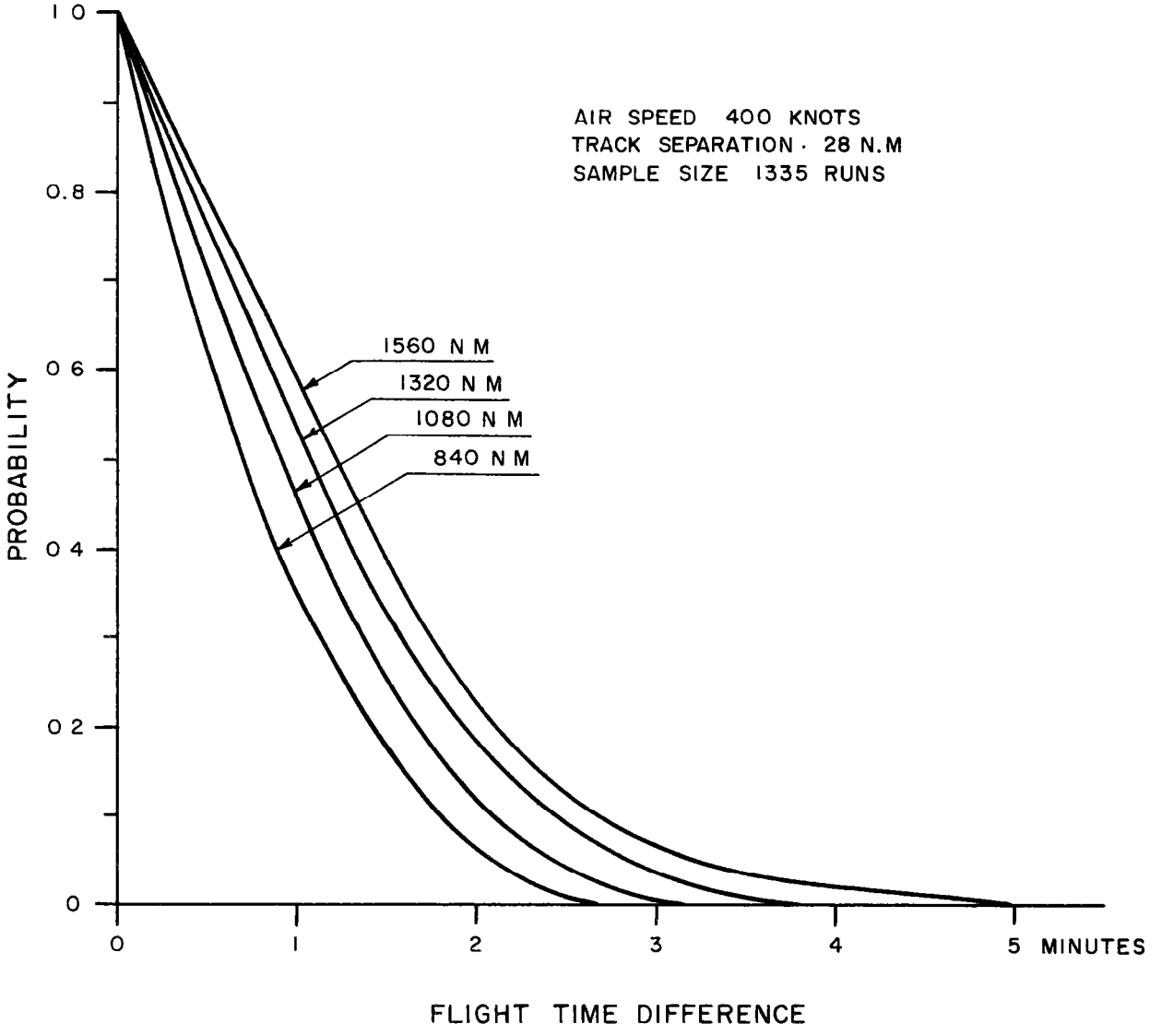

FIG.C-5: PROBABILITY THAT A GIVEN FLIGHT-TIME DIFFERENCE IS EXCEEDED

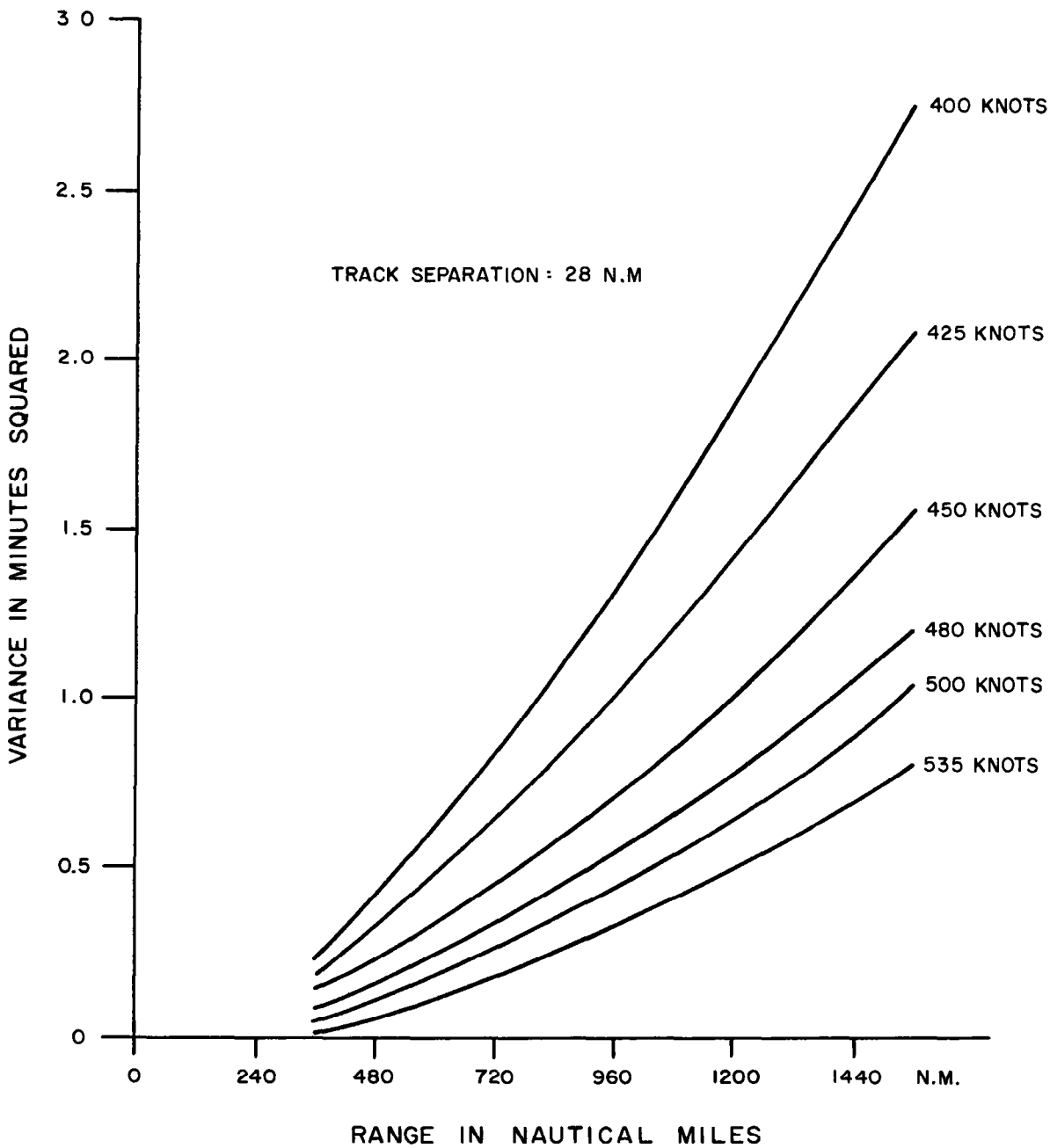

FIG. C-6 : VARIANCE OF FLIGHT - TIME DIFFERENCE VS RANGE

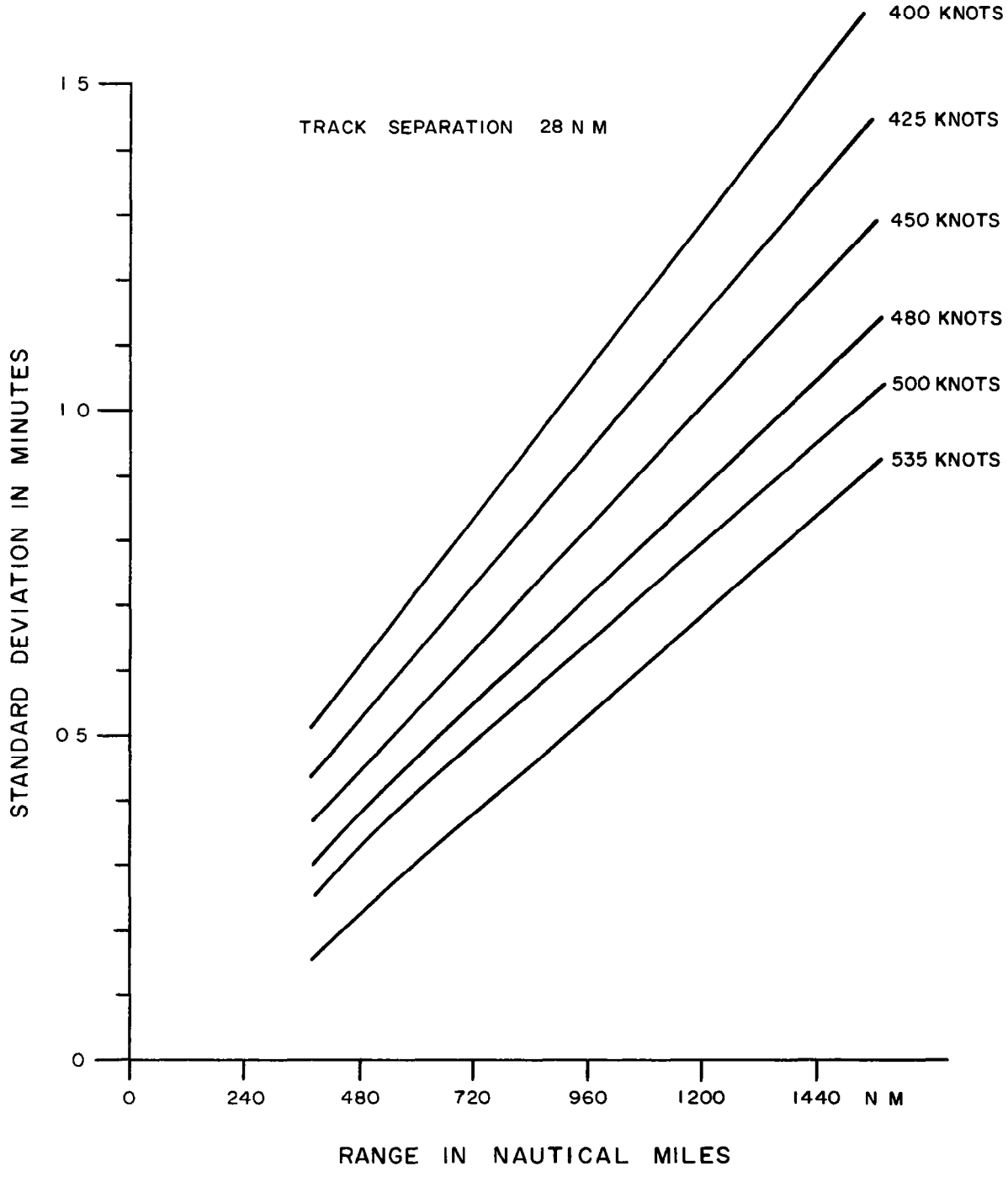

FIG. C-7: STANDARD DEVIATION OF FLIGHT TIME DIFFERENCE VS RANGE

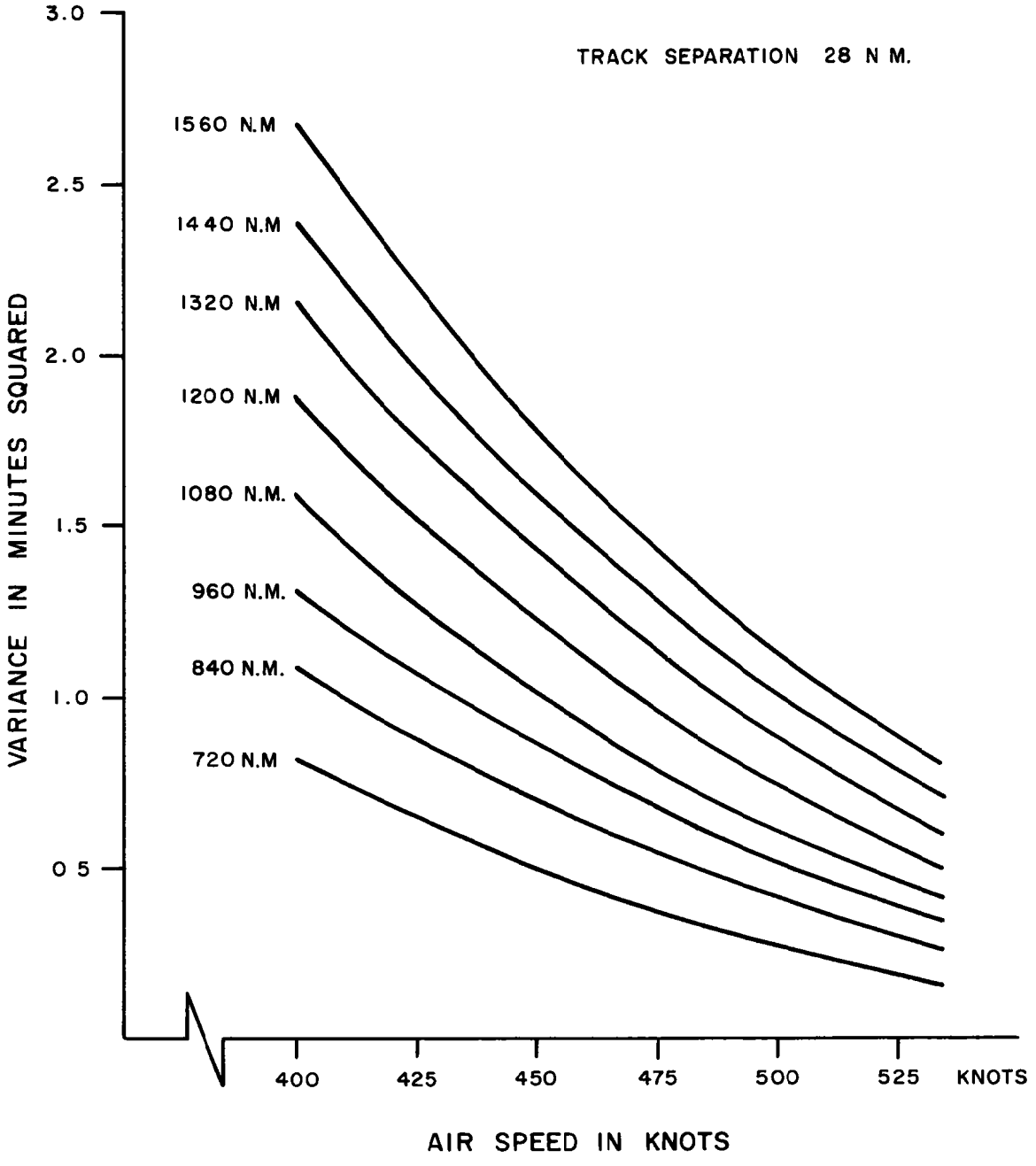

FIG. C-8 : VARIANCE OF FLIGHT-TIME DIFFERENCE VS AIR SPEED

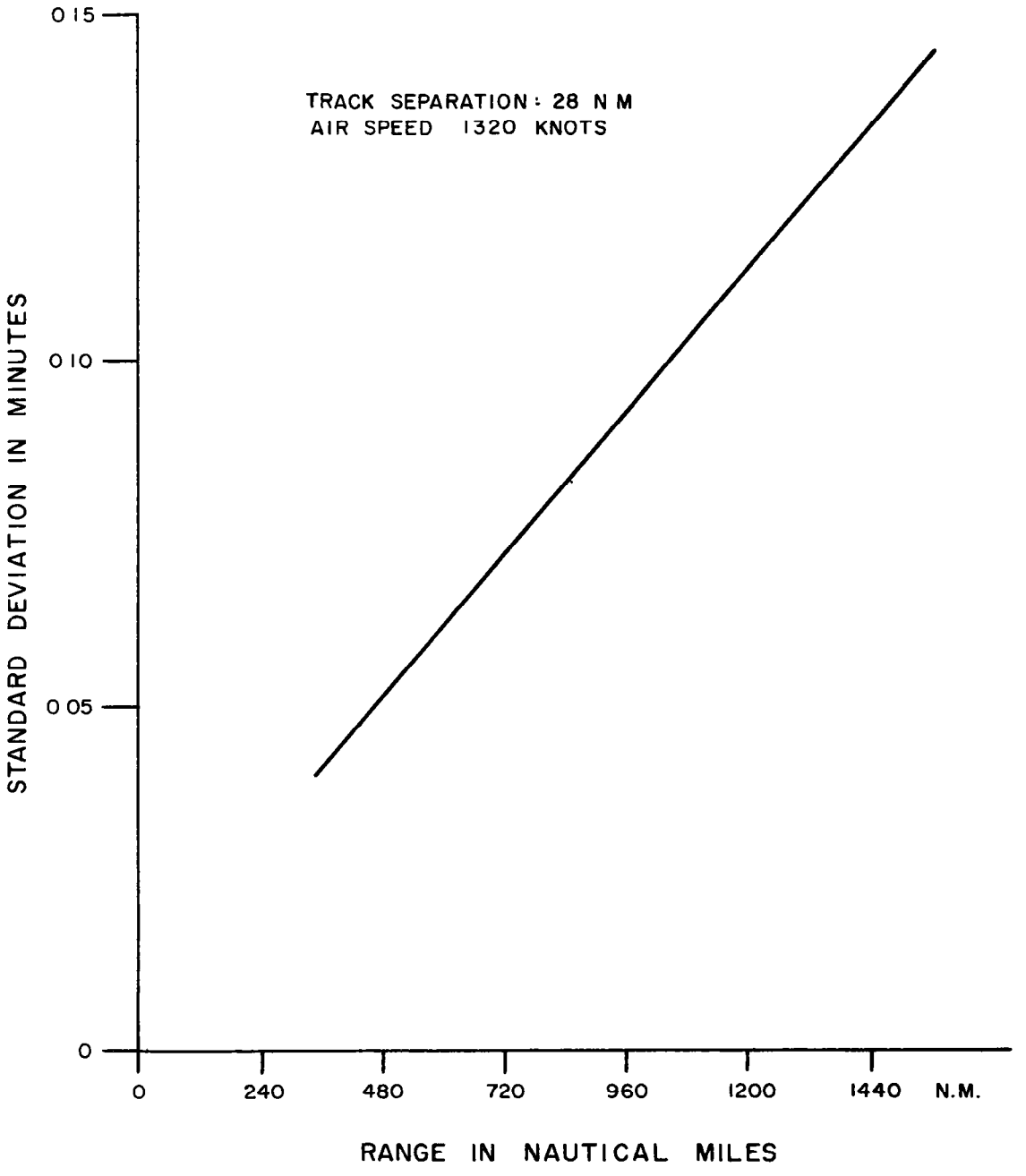

FIG. C-9: STANDARD DEVIATION OF FLIGHT TIME DIFFERENCE: SUPERSONIC CASE

APPENDIX D
ANALYSIS OF FIX ERRORS

1. Introduction

The lateral track-keeping accuracy of aircraft is limited by the accuracy of position fixes in a manner discussed in Appendix E. Because of this limitation, it is important to determine the statistics of fix errors if a meaningful relation between navigation and separation standards is to be established. A realistic statistical evaluation of fix errors is not readily attainable, however, because position-fixes obviously cannot be compared with true positions when the latter are unknown. A study based on direct comparisons between fixes and independent position measurements by radar would not provide an adequate solution, because of the errors in the radar measurements themselves and because of the unavailability of suitable radar coverage in the mid-Atlantic.

It is possible, however, to determine the statistics of fix errors from the statistics of a certain parameter which can be measured directly from fix data without knowledge of true aircraft positions. This possibility depends upon the fact that redundant data are ordinarily used to obtain fixes. It is therefore possible to define a parameter which reflects the dispersion of non-redundant subsets of the data and is statistically related to the fix error. This fact provides the basis for a measurement program which has been carried out to determine the standard deviation of fix errors for certain navigational devices and procedures.

Although some methods presented in this Appendix have appeared elsewhere,[4] they were derived independently by ARCON during the course of this project. Moreover, it is believed that many of the techniques presented here are new.

The analytical techniques derived in this Appendix were applied to data obtained from navigators' logs furnished by certain operators. Emphasis was

placed on celestial fixes because a more adequate data sample was available for this type of fix than for others.

The analysis has been confined to fixes obtained from sets of three position lines. In the absence of errors, the three lines intersect at the true aircraft position. Because of errors, however, the lines ordinarily form a triangle. Geometrical relationships between the errors and a certain parameter which can be measured directly from the triangle are established in Section D. 2. Statistical relationships are derived in Section D. 3 for those cases in which the errors in the three lines of position can be assumed to be independent. A different analysis is given in Section D. 4 for celestial navigation, since the assumptions of Section D. 3 are not valid for this case.

Numerical results of the application of the analytical techniques to data furnished by certain operators are given in Section D. 5. Results are quoted for fixes obtained entirely by celestial and entirely by Loran measurements, and also for a few mixed Loran-Consolan fixes. Less significance can be attached to the Loran and Loran-Consolan results than to those for celestial fixes, because the data sample for celestial fixes was larger and because certain assumptions essential to the analysis of Loran data make a large sample desirable. All numbers quoted in Section D. 5 are useful, however, in that they indicate the approximate magnitudes of the standard deviations of errors in various types of fixes.

It is noted in Appendix E, however, that the standard deviation of fix errors does not completely determine the distribution of track-keeping errors and does not reveal the blunder rate. A discussion of blunder errors is given in Appendix E.

2. Geometrical Relationships

We shall be concerned with fixes which are determined from sets of lines called lines of position or L. O. P. 's.* In general, an L. O. P. is

*L. O. P. 's will be assumed to be straight lines occurring on a flat earth. This assumption is justified by the relatively small dimensions of the geometrical configurations to be studied.

provided by an observation made with the aid of any of a number of navigational devices. In the absence of errors, each L.O.P. passes through the true position of the aircraft and the intersection of any two such lines occurs at this position. In practice, however, multiple-line fixes are used to provide a check on errors. Three-line fixes are most common, although four or more lines may be used. When three nonparallel L.O.P's are available, they form a triangle,* often called a "cocked hat", and the position-fix is usually taken to be somewhere near the "center" of the triangle. Our analysis will be confined to fixes of this type.

Figures D-1 and D-2 show two such triangles, with the true aircraft position T inside the triangle in Figure D-1 and outside the triangle in Figure D-2. The absolute value of the error in each L.O.P. is defined as the perpendicular distance from T. The sign of the error corresponds to the direction in which the L.O.P. is displaced from T and may be defined by any of a number of arbitrary conventions. The results of our analysis are independent of the choice of sign convention; however, it will be convenient to consider only conventions such that the signs of the L.O.P. errors associated with any given triangle satisfy the following properties:

P1: The three L.O.P. errors all have the same sign if and only if the true position T is an interior point of the triangle. (If T should lie on the perimeter, then the non-zero errors will have the same sign.)

P2: If the error associated with a given side of the triangle is positive when the true position T is on one side of the line, then the error must be negative when T is on the opposite side of the line.

Property P2 is of course satisfied by any usual definition of directed distance, and it is easy to show that sign conventions which also satisfy P1 exist. Note that under any such convention, all three errors e_1, e_2, e_3 will have the same

*In exceptional circumstances, the three L.O.P.'s may intersect in a common point. This point is rarely the true position of the aircraft, however.

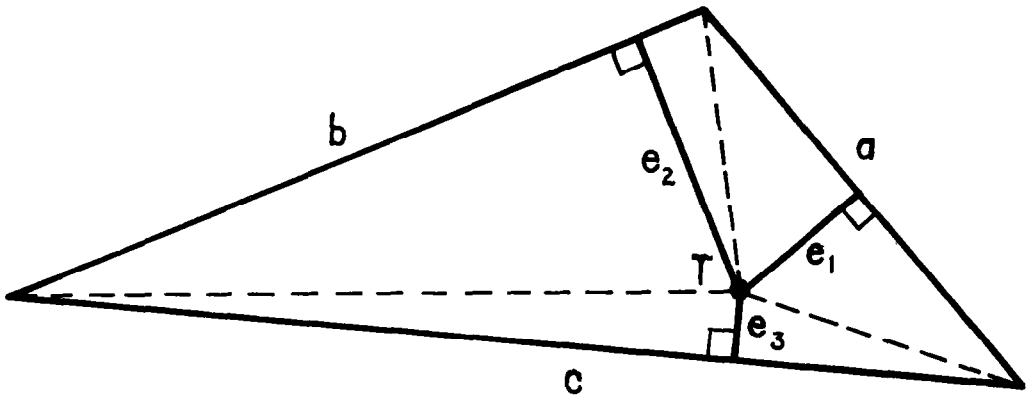

Figure D-1

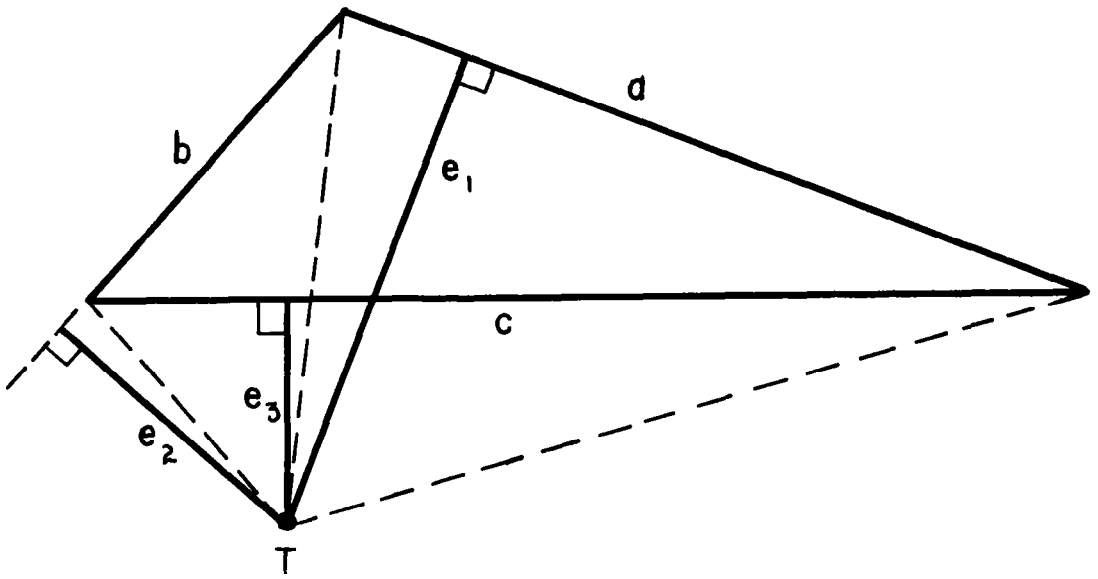

Figure D-2

sign in Figure D-1, while in Figure D-2, the signs of e_1 and e_2 are the same, but the sign of e_3 is different.

Given a triangle formed by three L.O.P.'s, it is of course impossible to determine either the magnitudes or signs of the L.O.P. errors e_1, e_2, e_3, unless the true position T is known. It will be shown, however, that given an ensemble of triangles, it is possible to express the statistics of the

ensemble of L.O.P. errors in terms of the statistics of a parameter which can be measured independently of the location of the true position T. This parameter is defined for each triangle as the following function of the three errors e_1, e_2, e_3:

$$r = f(e_1, e_2, e_3) = \frac{ae_1 + be_2 + ce_3}{a + b + c} \quad , \tag{D1}$$

where a, b, c are the lengths of the sides of the triangle associated with the errors e_1, e_2, e_3, respectively [cf. Figures D-1 and D-2] Statistical relationships between the parameter r and the errors e_1, e_2, e_3 will be developed in Sections D.3 and D.4. In this Section, we shall derive essential geometrical relationships and show how r can be determined for any given triangle without knowledge of the actual errors e_1, e_2, e_3.

A geometrical interpretation may be associated with the parameter r if one notes that the area of the triangle defined by three L.O.P.'s always satisfies the following formula:

$$A = \frac{1}{2} | ae_1 + be_2 + ce_3 | \quad . \tag{D2}$$

Eq. (D2) holds for all true positions of the aircraft and may be verified readily for each possible case by expressing A in terms of three triangles whose areas are, respectively, $\frac{1}{2} a | e_1 |$, $\frac{1}{2} b | e_2 |$, $\frac{1}{2} c | e_3 |$. (In Figures D-1 and D-2, dotted lines indicate the appropriate three triangles for these two cases.) If one recalls the properties P_1 and P_2 that must be satisfied by the signs of e_1, e_2, e_3, then eq. (D2) follows immediately in each case.

It follows from eqs. (D1) and (D2) that the absolute value of r is given by

$$|\,r\,| = \frac{A}{s} \quad , \tag{D3}$$

where s is the semi-perimeter of the triangle

$$s = \frac{1}{2}(a + b + c) \quad . \tag{D4}$$

By a standard formula of plane geometry, the area of a triangle satisfies the equation

$$A = r's \quad , \tag{D5}$$

where r' is the radius of the inscribed circle of the triangle [cf. Figure D-3]. It therefore follows from eqs. (D3) and (D5) that r is equal in magnitude to this radius, i.e.,

$$|\,r\,| = r' \quad . \tag{D6}$$

Thus | r | can be determined for any given triangle by a simple geometrical measurement.

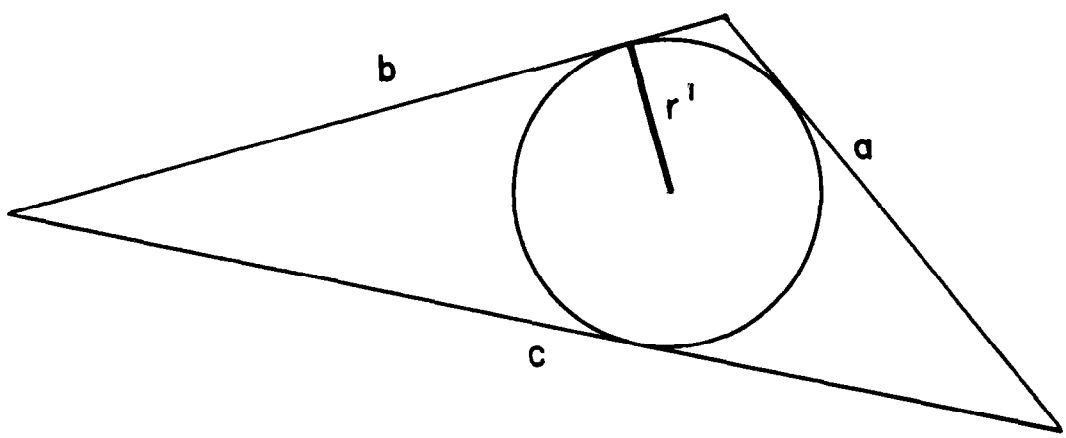

Figure D-3

The sign of r can also be determined for any given triangle without knowledge of the true aircraft position T. To see this, note that by eq. (D6), r must be either r' or $-r'$ for all possible aircraft positions; i.e., r can assume only two possible values for a given triangle. But it can be seen from eq. (D1) that r is a continuous function of the position T and therefore is a constant for all possible positions. Thus the sign of r can be determined by considering any hypothetical aircraft position T' and applying the adopted sign convention to determine the signs of the corresponding hypothetical L.O.P. errors e_1', e_2', e_3'.

Thus we have a parameter r which, by definition, is a function of the L.O.P. errors but which can be uniquely determined from information provided by the L.O.P.'s only.

It will be convenient to express formula eq. (D1) in the form

$$r = \alpha e_1 + \beta e_2 + \gamma e_3 \quad , \tag{D7}$$

where

$$\alpha = \frac{a}{a+b+c}$$

$$\beta = \frac{b}{a+b+c}$$

$$\gamma = \frac{c}{a+b+c} \quad . \tag{D8}$$

The parameters α, β, γ satisfy the identity

$$\alpha + \beta + \gamma = 1 \quad . \tag{D9}$$

In addition to the relation between the parameter r and the L. O. P. errors e_1, e_2, e_3, defined by eq. (D7), we shall need a relation between the fix error and e_1, e_2, e_3. It is first necessary, however, to establish a definition of the position-fix for each triangle. Ordinarily the fix is chosen somewhere near the "center" of the triangle, and the choice may be determined subjectively or by geometrical construction. For purposes of analysis, we shall define the fix to be the point at the center of the inscribed circle of the triangle. All statements relating to fix errors will apply to fixes determined by this convention. This choice of fix is often made under recommended navigational procedures, since in many cases it is a maximum likelihood estimate of the true position.*

In Figure D-4 a triangle is shown with fix F chosen according to our convention. The true aircraft position T is indicated as an interior point of the triangle, however, our results will not depend on the actual position T. The fix error is a vector drawn from T to F and may be analyzed in terms of orthogonal components:

$$R_x = x = \pm (r \csc C + r \cot C - e_2 \csc C - e_1 \cot C)$$

$$= \pm [(r - e_2) \csc C + (r - e_1) \cot C]$$

$$R_y = y = \pm (r - e_1) \quad , \tag{D10}$$

where the ambiguous signs depend upon the sign convention chosen for the L. O. P. errors. The magnitude R, or length of the fix-error vector, is

$$R = \sqrt{x^2 + y^2} \quad . \tag{D11}$$

*In certain cases, however, the recommended fix is placed outside the triangle.[5] Such cases are not included in our analysis.

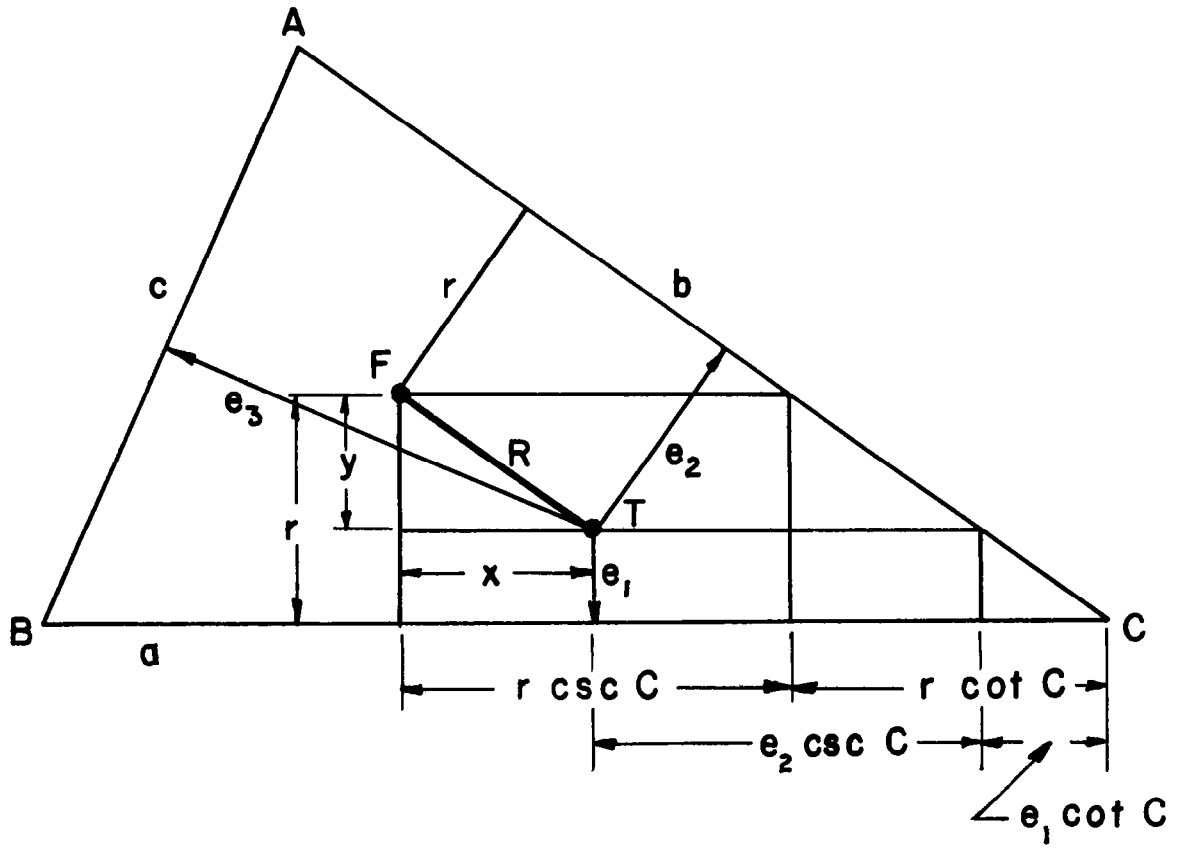

Figure D-4*

From standard formulas of trigonometry, the functions csc C and cot C satisfy

$$\csc C = \frac{ab}{2rs}$$

$$\cot C = \frac{a^2 + b^2 - c^2}{4rs} \quad , \tag{D12}$$

*A, B and C denote angles at the indicated vertices.

where s is defined by eq. (D4). Then using eqs. (D10) and (D12), together with eqs. (D8) and (D9), eq. (D11) becomes

$$R^2 = \left(\frac{s}{r}\right)^2 \left\{ [2\alpha\beta(r - e_2) + (\alpha^2 + \beta^2 - \gamma^2)(r - e_1)]^2 + \left(\frac{r}{s}\right)^2 (r - e_1)^2 \right\} . \tag{D13}$$

If the right hand side of eq. (D7) is substituted for r, eq. (D13) becomes

$$R^2 = 4\alpha\beta\gamma \left[\frac{\alpha e_1^2}{(1-2\beta)(1-2\gamma)} + \frac{\beta e_2^2}{(1-2\alpha)(1-2\gamma)} + \frac{\gamma e_3^2}{(1-2\alpha)(1-2\beta)} - \frac{e_2 e_3}{1-2\alpha} - \frac{e_1 e_3}{1-2\beta} - \frac{e_1 e_2}{1-2\gamma} \right] . \tag{D14}$$

Eqs. (D7), (D10), and (D14) have been derived from purely geometrical considerations and are basic to the statistical relationships established in the next Section between the parameter r and the L. O. P. and fix errors.

3. Statistical Relationships

In this Section, we shall consider how a sample of triangles formed by three L. O. P. 's, all generated by the same navigational technique, can be used to estimate the mean and variance of errors associated with that technique. Suppose that two such samples are available, one for each of two navigational techniques which are to be compared. Suppose that the radii of the inscribed circles of the triangles in both samples are measured and that the average radius is found to be much larger for one sample than the other. One might then suspect that both the L. O. P. errors and the fix errors are greater for the navigational technique associated with the sample with the larger average radius. We shall see that this intuitive notion is not strictly

correct, unless it is properly qualified, although it does suggest that the statistics of the parameter r should be related to the statistics of both L.O.P. and fix errors.

It can be seen from eq. (D7) that large L.O.P. errors do not necessarily imply a large radius for the inscribed circle, since the relative directions; i.e., signs, of the errors may be such that a small triangle and small value of $|r|$ results. Similarly, it can be shown that a large value of $|r|$ does not necessarily imply a large fix error. Realistic quantitative relationships between the statistics of the parameter r and the L.O.P. and fix errors will now be derived for certain important cases.

Consider an ensemble of triangles all having the same shape; i.e., all triangles are similar and α, β, γ are constant. Then it follows from eq. (D7) that the mean and mean-square values of r for this ensemble are:

$$\mu_r = E(r) = \alpha\mu_{e_1} + \beta\mu_{e_2} + \gamma\mu_{e_3} \quad . \tag{D15}$$

$$\begin{aligned} E(r^2) = {} & \alpha^2 E(e_1^2) + \beta^2 E(e_2^2) + \gamma^2 E(e_3^2) \\ & + 2\left[\alpha\beta E(e_1 e_2) + \alpha\gamma E(e_1 e_3) + \beta\gamma E(e_2 e_3)\right] \quad . \end{aligned} \tag{D16}$$

In this Section, we shall consider only the case in which the errors e_1, e_2, e_3 are independent, zero-mean random variables with identical distributions and, therefore, a common variance σ_e^2. These assumptions can be used in the analysis of cases in which all three L.O.P.'s are determined from independent measurements made by the same navigational technique and in which random measurement errors occur without a significant bias attributable to the instrument or procedure, or at least without a bias which causes the L.O.P. errors to be correlated in any significant manner. In the next Section

we shall see that these assumptions are not justified for celestial navigation and that a distinct analysis must be applied to this particular case.

Under the assumptions made in this Section, eqs. (D15) and (D16) become

$$\mu_r = \mu_e = 0 \quad . \tag{D17}$$

$$\sigma_r^2 = K\sigma_e^2 \quad , \tag{D18}$$

where

$$K = \alpha^2 + \beta^2 + \gamma^2 \quad . \tag{D19}$$

K is a constant which depends upon the shape of the triangles under consideration but does not vary widely for different triangles. In fact, K lies within the range $\frac{1}{3} \leq K \leq \frac{1}{2}$ for all possibilities. The value $K = \frac{1}{3}$ occurs for equilateral triangles, and the value $K = \frac{1}{2}$ occurs for degenerate cases; e.g., an isosceles triangle with a vertex angle of 0°.

To determine the mean fix error, recall that this error is a vector with orthogonal components defined by eq. (D10). Taking the expected value of both sides of these equations, and applying eq. (D17), we see that

$$E(R_x) = 0$$

$$E(R_y) = 0 \quad . \tag{D20}$$

Thus the mean fix error is a zero vector. To determine the variance of R, we may take the expected value of both sides of eq. (D14) and apply our

assumptions to simplify the right hand side:

$$E(R^2) = \sigma_R^2 = \frac{4\alpha\beta\gamma(1 - 2K)}{(1-2\alpha)(1-2\beta)(1-2\gamma)} \sigma_e^2 \quad , \tag{D21}$$

where K is defined by eq. (D19). Eqs. (D18) and (D21) yield the following statistical relation between r and R:

$$\sigma_R^2 = \frac{4(1-2K)\alpha\beta\gamma}{K(1-2\alpha)(1-2\beta)(1-2\gamma)} \sigma_r^2 \quad . \tag{D22}$$

Now suppose that a sample of n triangles is chosen from a population for which the assumptions of this section are justified and that a measurement program is undertaken to determine the sample mean-square value of r defined as:

$$\overline{r^2} = \frac{1}{n} \sum_{i=1}^{n} r_i^2 \quad . \tag{D23}$$

According to eq. (D17),

$$\sigma_r^2 = E(r^2) - \mu_r^2 = E(r^2) \quad . \tag{D24}$$

Therefore an estimate of the population variance σ_r^2 can be obtained from the sample value $\overline{r^2}$:

$$\sigma_r^2 \approx \overline{r^2} \quad . \tag{D25}$$

The accuracy of eq. (D25) will depend upon the validity of our assumptions, the size of the sample, and upon whether the sample is selected at random from the parent population.

From eqs. (D18) and (D22), estimates of σ_e^2 and σ_R^2 are obtained from the approximations

$$\sigma_e^2 \approx \frac{1}{K} \overline{r^2} \quad , \tag{D26}$$

$$\sigma_R^2 \approx \frac{4(1-2K)\alpha\beta\gamma}{K(1-2\alpha)(1-2\beta)(1-2\gamma)} \overline{r^2} \quad . \tag{D27}$$

The coefficients of $\overline{r^2}$ in eqs. (D26) and (D27) depend upon the shape of the triangles under consideration. For equilateral triangles, eqs. (D26) and (D27) become

$$\sigma_e^2 \approx 3 \overline{r^2} \quad , \tag{D28}$$

$$\sigma_R^2 \approx 4 \overline{r^2} \quad . \tag{D29}$$

The coefficients of $\overline{r^2}$ in eqs. (D26) and (D27) do not vary widely for various triangle shapes (for a right isosceles triangle, the coefficients become approximately 2.9 and 4.4, respectively). In practice, separate values of the coefficients can be calculated for each triangle, or suitable averages can be used for the entire sample.

In the case of triangles formed by celestial L.O.P.'s, the stars chosen for observation usually result in triangles which are nearly equilateral and the coefficients in eqs. (D26) and (D27) are close to 3 and 4, respectively.

In the next Section, however, we shall find that celestial L.O.P. errors are correlated in such a way that the assumptions and equations of this Section cannot be used. The results of this Section will be applied to certain types of fixes, but a different analysis is required for celestial navigation.

4. Celestial Navigation

Measurements of two physical quantities are required to obtain a celestial L.O.P.: the altitude of a celestial body and the time. Both measurements may be subject to random and bias errors. A bias in the time measurement results from a clock error, which displaces the L.O.P. along a latitude line. The displacement is $\frac{\tau}{4}$ cos L nautical miles, where τ is the clock error in seconds and L is the latitude of the aircraft position. The clock error has an identical effect on each of the three L.O.P.'s that determine a fix and no effect on the size of the triangle. The mean clock bias should be zero when averaged over a large number of clocks, and the variance of time measurement error is assumed to be small.

The major source of error in a celestial L.O.P. is the error in the sextant-measured altitude. This error may be represented in the form

$$e = x + d \quad . \tag{D30}$$

The component x is a random error with zero mean and variance σ_x^2 and is statistically independent from one sextant reading to the next. The component d is a bias error which has zero mean and variance σ_d^2, when averaged over a large number of sextants; however, d is ordinarily constant for a particular sextant throughout a single flight. The bias d is referred to as an "index error" by the navigator who endeavors to minimize its effect.

An error in the altitude of a celestial body causes a parallel displacement of the L.O.P. from the true aircraft position. If the sextant error is

x + d, measured in minutes of arc, then the magnitude of the L.O.P. error is $|x + d|$, measured in nautical miles. The sign of the L.O.P. error depends upon the convention used. Regardless of convention, however, a positive sextant error will always cause the L.O.P. to be displaced toward the observed celestial body, and a negative error causes a displacement away from it.

An important distinction must be made in considering the triangle formed by three celestial L.O.P.'s. Two possible cases may occur, depending upon the relative azimuths of the observed celestial bodies, and are illustrated in Figures D-5 and D-6. In both figures, triangles are shown which would result if the L.O.P. errors were caused solely by a sextant bias d. Solid lines are used to indicate the triangles which would occur if d were positive, and broken lines to indicate those resulting from a negative d. The azimuths of the three observed stars are spaced at intervals of 120° in Figure D-5, and at intervals of 60° in Figure D-6. The figures illustrate two distinct types of celestial fix, which will be termed "balanced" or "unbalanced", according to whether the three stars span an arc greater or less than 180°.

In Figure D-5 the three L.O.P.'s form an equilateral triangle centered about the true aircraft position T. The radius of the inscribed circle is equal to the absolute value of the bias d, and the fix error is zero. Both results hold for any balanced arrangement of stars, although the three L.O.P.'s form an equilateral triangle only if the star azimuths are spaced at intervals of 120°.

In the unbalanced case, an equilateral triangle is formed only if the stars are spaced at intervals of 60°, as in Figure D-6. If the triangle is equilateral, then the radius of the inscribed circle is $\frac{1}{3}|d|$, and the magnitude R of the fix error is $\frac{4}{3}|d|$. Different values of the inscribed circle radius and fix error occur for other triangle shapes. For every triangle resulting

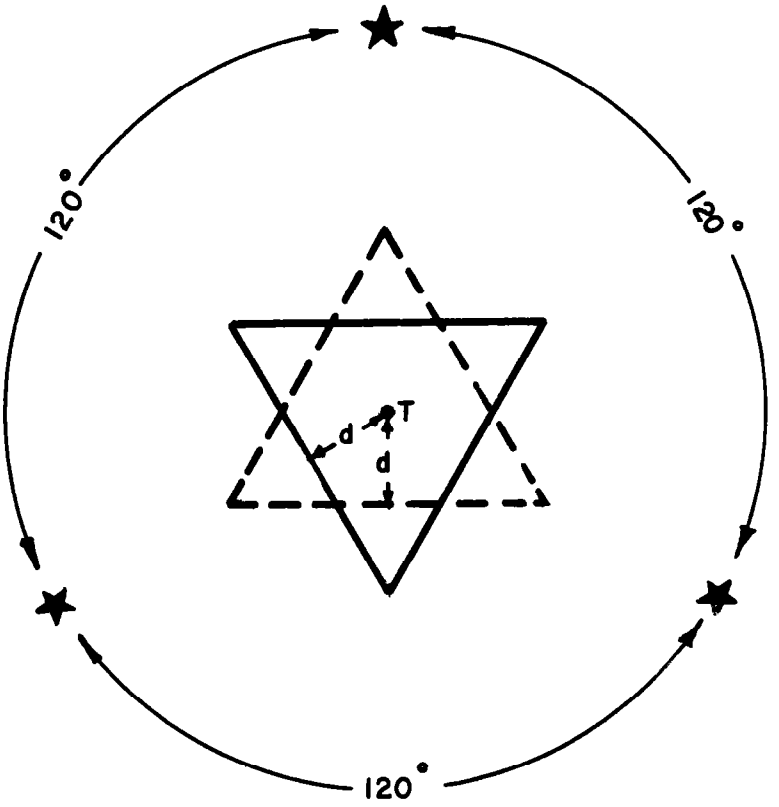

Figure D-5

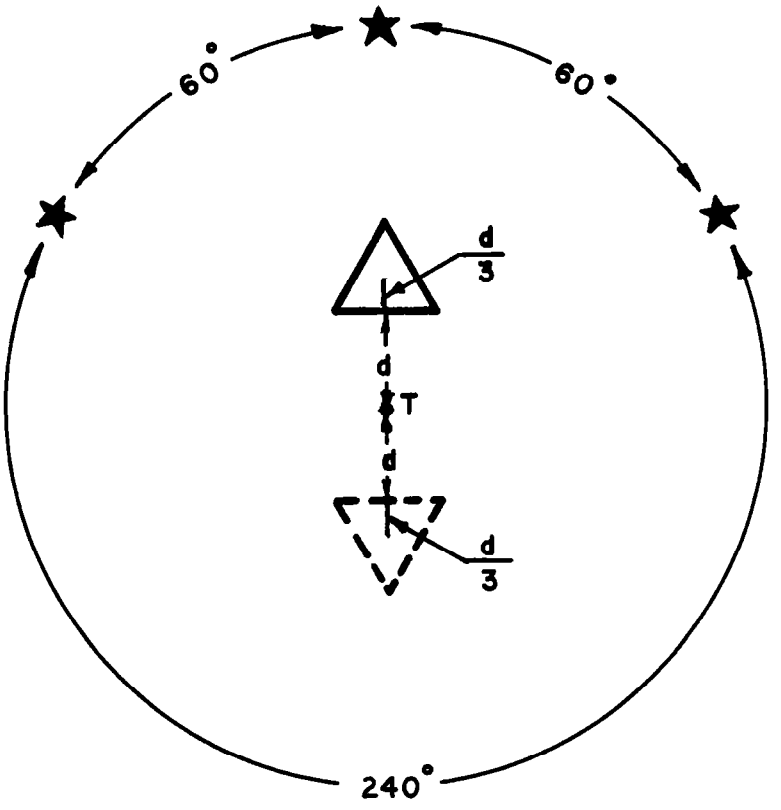

Figure D-6

from a sextant bias d and an unbalanced arrangement of observed stars, it is possible to postulate a triangle of identical shape and size resulting from a balanced star arrangement. In every case, the radius of the inscribed circle of the triangle is smaller for the unbalanced star arrangement; but the fix error is zero for the balanced case and non-zero for the unbalanced case (assuming no errors other than the sextant bias).

Of course, since L.O.P. errors include components other than the bias error d, the radius of the inscribed circle and fix error will, in general, be different from those indicated in Figures D-5 and D-6. It is easily shown, however, that the radius is larger but the fix error is smaller, in a statistical sense, for balanced star arrangements. Because of the manner in which the sextant bias is compensated when a balanced arrangement of stars is observed, it is common practice for navigators to choose such an arrangement whenever possible. Indeed, over 95% of the celestial fixes recorded in the navigators' logs studied during the project were of this type.

In order to derive realistic statistical relationships for celestial fixes obtained from balanced star arrangements, it is necessary to recognize the manner in which L.O.P. errors generated by a particular sextant on a single flight are correlated. For this purpose, it will be convenient to use the following convention to define the signs of L.O.P. errors: if an L.O.P. is displaced from the true aircraft position toward the observed star, then the error is positive; if the L.O.P. is displaced away from the star, the error is negative. (Errors in time measurement are neglected in the following analysis, and it is assumed that an L.O.P. error displaces the L.O.P. parallel to itself.) It is easily verified that the properties P1 and P2 defined in Section D.2 are satisfied by this convention, provided that the triangles are obtained from balanced star arrangements. Therefore the geometrical relationships eqs. (D7), (D10), and (D14) are satisfied for all such triangles when this convention is used.

The three L.O.P. errors associated with a triangle obtained from a balanced arrangement of observed stars may be written in the form:

$$e_1 = x_1 + d$$

$$e_2 = x_2 + d$$

$$e_3 = x_3 + d \quad . \tag{D31}$$

The sextant bias error d appears in each equation with the same sign, in accordance with the adopted sign convention. The x_i are assumed to be independent, random zero-mean variables with a common variance σ_x^2. As stated before, d has zero mean and variance σ_d^2, when averaged over an ensemble of sextants, but is constant for a particular sextant on a single flight. Therefore, the mean and variance of the L.O.P. errors are

$$\mu_e = 0$$

$$\sigma_e^2 = \sigma_x^2 + \sigma_d^2 \quad , \tag{D32}$$

if averages are taken over an ensemble of sextants. If averages are taken for a particular sextant used on a single flight, the mean and variance are

$$\mu_e = d$$

$$\sigma_e^2 = \sigma_x^2 \quad . \tag{D33}$$

Statistical relationships can now be derived for celestial fixes obtained from balanced star arrangements. Substituting the right members of eq.

(D31) for the e_1 in eq. (D7), taking expected values of both sides of the resulting equation, and recalling eq. (D9), we have:

$$\mu_r = \mu_e \quad , \tag{D34}$$

where μ_e is defined by either eq. (D32) or (D33), depending on whether a single sextant or ensemble of sextants is involved. Similarly, the expected value of r^2 is

$$E(r^2) = (\alpha^2 + \beta^2 + \gamma^2)\ \sigma_x^2 + E(d^2)$$

$$= K\sigma_x^2 + E(d^2) \quad , \tag{D35}$$

where $K = \alpha^2 + \beta^2 + \gamma^2$.
Since $E(r^2) = \sigma_r^2 + \mu_r^2$, it follows from eqs. (D34) and (D35) that

$$\sigma_r^2 = K\sigma_x^2 + \sigma_d^2 \quad , \tag{D36}$$

if averages are taken over an ensemble of sextants, but that

$$\sigma_r^2 = K\sigma_x^2 \quad , \tag{D37}$$

if averages are taken for a particular sextant and a single flight.

It can be seen from eqs. (D10) and (D34) that the fix error has orthogonal components with zero means:

$$E(R_x) = \pm [(\mu_r - \mu_e)\csc C + (\mu_r - \mu_e)\cot C] = 0$$

$$E(R_y) = \pm [\mu_r - \mu_e] = 0 \quad . \tag{D38}$$

It therefore follows that $\sigma_R^2 = E(R^2)$. Taking the expected value of both sides of eq. (D14) and simplifying the resulting expression, we have

$$\sigma_R^2 = \frac{4\alpha\beta\gamma\left\{(1 - 2K)\sigma_x^2 + 2[1 - (\alpha+\beta+\gamma)^2]E(d^2)\right\}}{(1-2\alpha)(1-2\beta)(1-2\gamma)}$$

$$= \frac{4\alpha\beta\gamma(1-2K)}{(1-2\alpha)(1-2\beta)(1-2\gamma)}\,\sigma_x^2 \quad . \tag{D39}$$

The coefficient of $E(d^2)$ vanishes in eq. (D39) independently of whether averages are taken for a single sextant or an ensemble of sextants. Thus the variance of the fix error depends only upon the random component of the L.O.P. errors.

If averages are taken for triangles generated only by a single sextant with a fixed bias, then the following useful relation between the variances σ_r^2 and σ_R^2 can be derived from eqs. (D37) and (D39):

$$\sigma_R^2 = \frac{4\alpha\beta\gamma(1-2K)}{K(1-2\alpha)(1-2\beta)(1-2\gamma)}\,\sigma_r^2 \quad . \tag{D40}$$

It is apparent from eqs. (D36) and (D39) that no useful relation between σ_r^2 and σ_R^2 can be derived, if averages are taken directly over an ensemble of triangles generated by various sextants on different flights.

Given a sample of triangles generated by a particular sextant on a single flight, an estimate of σ_R^2 can be obtained for that flight if the sample mean value $\bar{r}$ and mean square value $\overline{r^2}$ are computed. Then an estimate of σ_r^2 is given by

$$\sigma_r^2 \approx \overline{r^2} - (\bar{r})^2 \quad , \tag{D41}$$

and an estimate of σ_R^2 is provided by eqs. (D40) and (D41).

Given a large sample of triangles generated by a number of sextants used on different flights, the separate estimates of σ_r^2 obtained for each flight can be combined to obtain an estimate of σ_r^2 for the entire ensemble. An optimal method for combining the separate estimates will now be described.

Suppose that there are m groups of triangles, with each group generated by just one sextant on a single flight, and that the magnitude and sign of the parameter r is measured for each triangle. We then have a set of m groups of sample values of r. Let $n_j (1 \leq j \leq m)$ designate the number of sample values in the jth group and $r_{ij} (1 \leq i \leq n_j)$ designate the ith value in that group. Each group of samples is assumed to be drawn from a Gaussian population with mean μ_j and variance σ_r^2. The unknown mean μ_j is the sextant bias for the jth group.

We wish to estimate the variance σ_r^2 of the population from which all the sample groups are drawn. Consider the variable s_j defined for the jth group by

$$s_j = \frac{1}{n_j - 1} \sum_{i=1}^{n_j} (r_{ij} - \bar{r}_j)^2 \quad , \tag{D42}$$

where

$$\bar{r}_j = \frac{1}{n_j} \sum_{i=1}^{n_j} r_{ij} \quad . \tag{D43}$$

The variable s_j has a chi-square distribution with $n_j - 1$ degrees of freedom.[6] The mean and variance of s_j are

$$E(s_j) = \sigma_r^2 \quad , \tag{D44}$$

$$V(s_j) = \frac{2\sigma_r^4}{n_j - 1} \quad . \tag{D45}$$

Consider a linear combination of the s_j of the form

$$S = \sum_{j=1}^{m} a_j s_j \quad . \tag{D46}$$

From eqs. (D44) and (D45), the mean and variance of S are

$$E[S] = \sigma_r^2 \sum_{j=1}^{m} a_j \quad , \tag{D47}$$

$$V[S] = 2\sigma_r^4 \sum_{j=1}^{m} \frac{a_j^2}{n_j - 1} \quad . \tag{D48}$$

We wish to use a linear combination S of the form (D46) as an estimate of σ_r^2 and require that S be an unbiased, minimum variance estimate. It is seen from eq. (D47) that S will be unbiased if

$$\sum_{j=1}^{m} a_j = 1 \quad . \tag{D49}$$

The variance V(S) can be minimized, subject to the constraint (D49), by

the method of Lagrange. This method requires a solution to the following system of equations:

$$\frac{\partial}{\partial a_k}\left\{2\sigma_r^4 \sum_{j=1}^{m} \frac{a_j^2}{n_j - 1} - \lambda\left(\sum_{j=1}^{m} a_j - 1\right)\right\} = 0 \quad , \tag{D50}$$

$$k = 1, 2, \ldots, m$$

where λ is an arbitrary multiplier. After carrying out the differentiations indicated in eqs.(D50) and solving for a_k, we have

$$a_k = \frac{\lambda}{4\sigma_r^4}(n_k - 1), \quad k = 1, \ldots, m \quad . \tag{D51}$$

Taking the sum of all m eqs.(D51), and applying the constraint (D49), we have

$$\sum_{k=1}^{m} a_k = \frac{\lambda}{4\sigma_r^4} \sum_{k=1}^{m} (n_k - 1) = 1 \quad . \tag{D52}$$

Therefore, the multiplier λ satisfies

$$\lambda = \frac{4\sigma_r^4}{\Sigma(n_k - 1)} = \frac{4\sigma_r^4}{N - m} \quad , \tag{D53}$$

where N is the total number of sample values of r in all m groups. Hence each coefficient a_j is

$$a_j = \frac{n_j - 1}{N - m} \quad . \tag{D54}$$

Therefore, the unbiased, minimum variance estimate of σ_r^2 is

$$\hat{\sigma}_r^2 = S = \frac{1}{N-m} \sum_{j=1}^{m} (n_j - 1)s_j$$

$$= \frac{1}{N-m} \sum_{j=1}^{m} \sum_{i=1}^{n_j} (r_{ij} - \overline{r_j})^2 \quad . \tag{D55}$$

From eq. (D48), the variance of this estimate is

$$V(S) = 2\sigma_r^4 \sum_{j=1}^{m} \frac{a_j^2}{n_j - 1}$$

$$= \frac{2\sigma_r^4}{N - m} \quad . \tag{D56}$$

Therefore, the standard deviation of the estimate $\hat{\sigma}_r^2$ is

$$\sqrt{\frac{2}{N - m}}\, \sigma_r^2 \quad . \tag{D57}$$

5. Numerical Results

A collection of navigators' flight logs furnished by certain international operators made it possible to conduct an experimental program using methods described in the preceding Sections. The logs were recorded during the

period January, 1961 to March, 1961. The L.O.P.'s used to determine fixes were drawn on aircraft position charts by the navigator during each flight. It was, therefore, possible to measure the magnitude and sign of the parameter r, defined in Section D.2, for each triangle resulting from a 3-line fix.

By using appropriate statistical techniques described in Sections D.3 and D.4, estimates of the standard deviation σ_R of the fix error were obtained for three different operators and for three different types of fix. The estimates are given in Table D-1.

Operator	3 Celestial lines	3 Loran lines	2 Loran lines - 1 Consolan line
A	11	___	___
B	6	9-14	___
C	___	6-9	6-9

Table D-1. Estimates of σ_R.*

The methods of Section D.4 were used to analyze celestial fixes obtained from so-called balanced star arrangements. The methods of Section D.3 were used for other types of fix. The two estimates of σ_R for celestial fixes were based on a sample of 386 fixes for operator A and a sample of 68 fixes for operator B. The sample of celestial fixes for operator C was not adequate to provide useful results. Note that a significantly smaller value of σ_R was found for celestial fixes by operator B than by operator A. It is thought that this fact may be accounted for, in part, by a difference in equipment used by the two operators. The sextants used by operator A provide star altitude readings obtained by averaging measurements over a one minute period. In the case of operator B, the averaging

*Expressed in nautical miles.

process occurs over a two minute period.

In order to determine appropriate statistical methods for the analysis of Loran navigation, it should be recognized that the errors in the three Loran lines associated with a particular fix may be statistically dependent because of a timing bias in the Loran receiver. The nature of the correlation depends upon the positions of the three pairs of Loran stations relative to the aircraft, just as the correlations of the L.O.P. errors in a celestial fix depends upon the relative azimuths of the three observed stars. In the case of celestial fixes, the navigator usually chooses the stars so that sextant bias errors cancel one another, and consequently the correlations of the L.O.P. errors for such fixes consistently take a particular form. In the case of Loran fixes, the navigator ordinarily does not have the freedom to choose Loran stations in a manner which would cause the effects of a timing bias on the three L.O.P.'s to cancel one another. Consequently, the three L.O.P. errors are not consistently correlated in any prescribed manner. Accordingly, it can be shown that if an ensemble of Loran fixes is uniformly distributed over a suitable geographical region, then the effects of correlations of L.O.P. errors for particular fixes are not reflected in ensemble averages. A uniform geographical distribution of fixes is also required to justify the assumption that all three L.O.P. errors have the same variance. The statistical relationships derived in Section D.3 are then applicable.

Estimates of σ_R for Loran fixes by operators B and C are given in the second column of Table D-1. Loran equipment was not used by operator A. The data samples, which included 30 fixes for operator B and 27 fixes for operator C, were limited and did not fully meet the requirements for uniform geographical distribution of fixes. Because of the limitations of the data samples, a range of values of σ_R is given for each operator, rather than a unique ensemble average. The rather large upper limit of σ_R for operator B reflects the especially poor Loran coverage in certain geographical regions

in which many of the fixes by that operator were taken.

Indeed, it should be noted that the Loran fixes were taken by both operators primarily in regions of the mid-Atlantic where Loran accuracy is relatively poor. The reason for this is that 3-line Loran fixes are simply not used where Loran accuracy is greatest; i.e., in regions near the coastlines where only two Loran lines are available to the navigator. It is quite possible, therefore, that the data in Table D-1 reflect a significantly poorer fix accuracy than is characteristic of the regions where 2-line Loran fixes are taken.

A sample of 41 fixes made with two Loran lines and one Consolan line was available in the data provided by operator C. An estimate of σ_R obtained from this data sample is given in the third column of Table D-1 and might be compared with the corresponding estimate for fixes made with three Loran lines. Any conclusions drawn from this comparison, however, should be qualified by the fact that the fixes using a Consolan line were ordinarily taken near the coastlines. It is not surprising that experimental results reported elsewhere[7] indicate a much lower level of accuracy for Consolan L.O.P.'s taken in the mid-Atlantic.

APPENDIX E

LATERAL TRACK-KEEPING ERRORS

1. Introduction

It has been pointed out that the lateral separation required in the North Atlantic is determined by the extent to which the flight path of an aircraft departs from its flight plan. In this report the lateral deviation of an aircraft from its flight plan is called the track-keeping error. Track-keeping errors should not be confused with position estimation errors. Position estimation error is the difference between the navigator's measurement of position and the actual aircraft position, whereas track-keeping errors reflect the pilot's inability to hold the aircraft precisely on the flight plan path. In this Appendix, those factors which affect track-keeping errors are examined, and relationships between track-keeping error, position estimation error, and operational procedures are developed.

In Section 2, the factors which affect track-keeping error are discussed, and a simple model, suitable for calculating the standard deviation of track-keeping errors, is described. This model yields a rather simple but significant result, namely, that in any system of navigation utilizing intermittent position fixes, the track-keeping error standard deviation is at least as great as the standard deviation of the error in position estimation.

Section 3 discusses in detail the sources of heading error associated with various types of navigational equipment and navigational procedures in use today on the North Atlantic. The effect of wind forecast errors is described and the application of Doppler radar to drift angle measurement is discussed.

Numerical values are presented in Section 4. They have been calculated, using the model of Section 2, for each of the types of navigation described in Section 3. It is indicated that the minimum value of track-keeping error

standard deviation which can be attained at present in the North Atlantic is on the order of 10 nautical miles. In order to reduce this figure either position measurement errors must be reduced, or systems which do not rely on frequent position fixes (e.g., improved Doppler or inertial systems) must be introduced. Statistical data on track-keeping are presented for comparison.

2. Track-keeping Model

The accuracy of lateral track-keeping is affected by a large number of different parameters. Among these are:

1. Accuracy of the position fix.
2. Interval between position fixes.
3. Heading reference accuracy.
4. Air speed and air speed measurement accuracy.
5. Accuracy of estimated winds ahead.
6. Complexity of the flight plan track (frequency and magnitude of turns)
7. Operational procedures of track-keeping.

In order to arrive at a tractable model of lateral track-keeping, it is convenient to begin with a rather simple set of assumptions. First, it will be assumed that the angle between the aircraft's ground velocity vector and the flight plan track is at all times a small angle. This simplification makes it possible to neglect the longitudinal, or along track, components of fix errors. Second, it is assumed that heading errors and drift angles are always small angles so that the sines can be everywhere replaced by the angles themselves (measured in radians). Third, it is assumed that the navigator plots a position fix at regular intervals. Finally, it is assumed that after each position fix the navigator accepts the fix as a best estimate of position and chooses a new heading intended to return the aircraft to the flight plan at the time of the next fix. This last assumption meets the requirements

of the ICAO rule which states that an aircraft must choose a heading which will return it to flight plan within 200 miles, a figure typical of the distance between position fixes.

Let y_i be the true perpendicular distance of the aircraft from its flight plan at the time of the i^{th} position fix, p_i, the navigator's estimate of y_i, and f_i, the y component of fix error. (f_i is equal to the difference between y_i and p_i.) ϵ_i is the error in the heading computed by the navigator at the time of the i^{th} fix and s is the distance in nautical miles between position fixes.

There are two reasons why the navigator fails in his attempt to return the aircraft precisely to its flight plan. First, his choice of heading assumes that the position fix is correct, which it is not, and second, he cannot compute the proper heading precisely. If, initially, the aircraft is precisely on its flight plan, then:

$$y_o = 0$$
$$p_o = f_o \quad .$$

At the time of the first position fix,

$$y_1 = -f_o + s\epsilon_o$$
$$p_1 = -f_o + f_1 + s\epsilon_o \quad .$$

At the time of the second position fix,

$$y_2 = -f_1 + s\epsilon_1$$
$$p_2 = -f_1 + f_2 + s\epsilon_1 \quad ,$$

and at the i^{th} position fix,

$$y_i = -f_{i-1} + s\epsilon_{i-1}$$
$$p_i = -f_{i-1} + f_i + s\epsilon_{i-1} \quad . \tag{E1}$$

The geometry of this process is illustrated in Figure E-1.

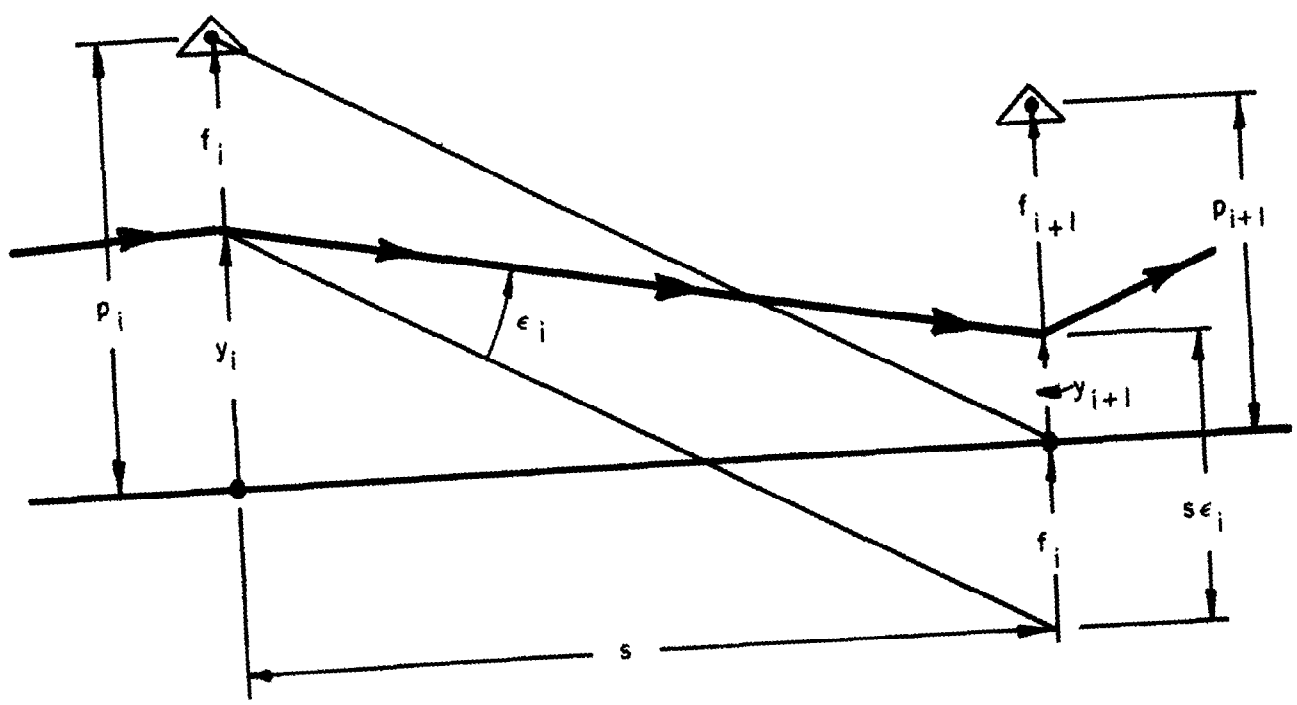

Figure E-1

These equations describe relationships among the random variables y, p, f and ϵ. In order to bring out the statistical nature of the relationship, the last two equations can be squared and expected values taken. Assuming

that each fix error is not correlated with the previous fix error and also that fix errors are independent of heading errors, the following results are obtained:

$$\sigma_y^2 = \sigma_f^2 + s^2\sigma_\epsilon^2$$
$$\sigma_p^2 = 2\sigma_f^2 + s^2\sigma_\epsilon^2 \quad . \tag{E2}$$

Also:

$$\sigma_p^2 = \sigma_y^2 + \sigma_f^2 \quad . \tag{E3}$$

In these equations σ is the standard deviation of the subscript random variable. It should be noted that no assumption is required about the statistical dependence of the heading error at one fix on the heading error at the previous fix.

Eq. (E2) implies that σ_y, the standard deviation of track-keeping error, can never be less than σ_f, the standard deviation of the fix error. A reduction in the heading errors or in the interval between position fixes will reduce the track-keeping standard deviation but can never bring it below the fix error standard deviation. The equation also implies that the standard deviation of track-keeping errors increases with the distance between fixes. This implication should be treated with caution, however, since heading errors in some cases are dependent upon the distance between fixes. This point will be discussed further in Section 3. Eq. (E3) indicates that it is possible to deduce track-keeping standard deviation from a study of navigators' logs, provided that an estimate of σ_f is at hand. This has been done in the course of the present study and the numerical results are presented in Section 4 below.

3. Heading Error

A number of sources contribute to the error in the desired heading. They include:

1. Error in the estimated drift angle.
2. Error in magnetic variation.
3. Error in compass deviation (compass calibration).
4. Error in compass following by pilot or autopilot.

Of these four sources of error, the first is frequently the most significant. Errors in magnetic variation and compass deviation are both on the order of 1 or 2 degrees. Compass following errors arise from the pilot's inability to follow precisely the chosen heading. It is difficult to estimate the magnitude of this type of error but it is believed to be small. The second and third types of error should remain constant or decrease slightly as distance between fixes is increased. The behavior of the drift angle error with increasing distance between fixes depends upon the type of navigation employed. Among the methods which might be used to estimate drift angles are the following:

a. Read the wind ahead from the meteorological forecast.
b. Assume that the wind ahead is equal to the wind calculated from past and present fixes.
c. Assume that the wind ahead is equal to the wind calculated from the measured pressure gradient.
d. Assume that the wind ahead is equal to the wind measured by Doppler radar.
e. Assume a weighted average of two or more of the above.

The drift angle is then computed from:

$$\lambda = \sin^{-1} \frac{\text{cross track wind component}}{\text{air speed}} .$$

Since the percentage error in air speed is small compared to the percentage

error in estimates of cross wind as obtained from a, b, and c above, and since wind velocity is small compared to air speed, the error in the drift angle, ϵ_λ, is given approximately by:

$$\epsilon_\lambda \approx \frac{\text{error in cross wind ahead}}{\text{air speed}} \quad . \tag{E4}$$

The standard deviation of the error in cross wind ahead depends upon the method of estimation. Each of the above mentioned methods must be discussed separately.

a. Cross wind errors from forecast winds

Statistics of forecast errors and their space correlation have been collected by C. S. Durst.[9] The standard deviation of the error in a forecast wind component is about 32 knots at 300 millibars. If the forecast applies to a route segment,the error decreases slightly as the length of the route segment increases. This behavior is illustrated in Figure E-2. These figures are based on a sample of 120 wind forecast charts prepared for the North Atlantic during the winter of 1957. Since there have been no major changes in procedures for collecting wind data and preparing wind forecasts it is believed that these figures apply in the North Atlantic today.

b. Cross wind errors from fix derived winds

There are two sources of error in cross wind ahead estimated from fix derived winds. The first arises from the fact that the fix measured wind is in error because of fix errors and heading errors at the previous fix. (Heading errors resulting from variation errors, deviation errors and compass following errors will here be lumped in one term, ϵ_c.) An analysis of the computation shows that the error in the fix derived wind ΔW_1, is given by:

Standard Deviation of Error in Forecast Wind Component

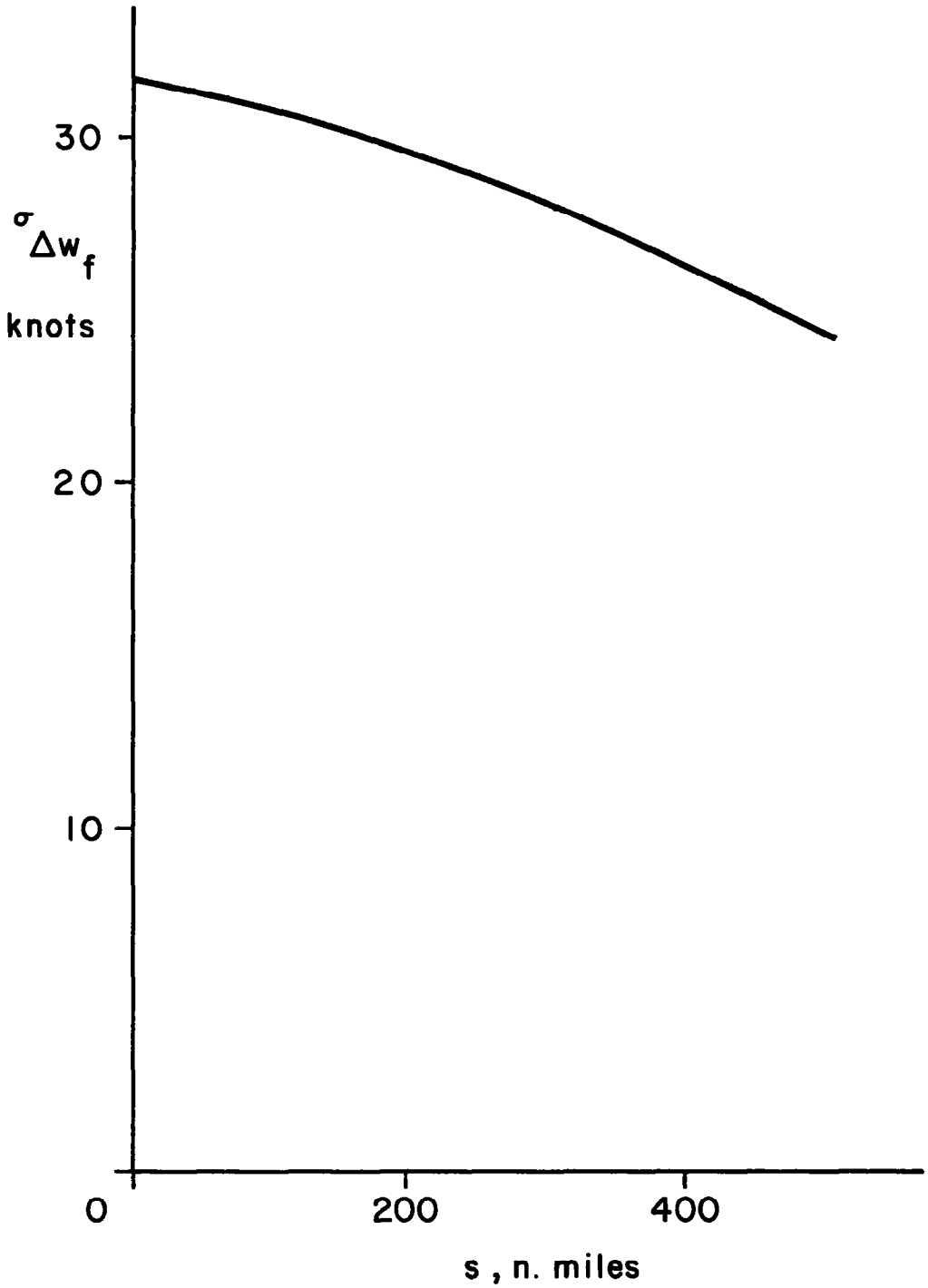

Figure E-2.

STANDARD DEVIATION OF ERROR IN FORECAST WIND COMPONENT

$$\Delta W_i = \frac{A}{s}(f_i - f_{i-1}) + A\epsilon_{c,i-1} \quad , \tag{E5}$$

where A is the air speed.

If this fix derived wind is to be used as an estimate of wind ahead then another term must be added, namely, the error made in assuming that the wind ahead is equal to the wind experienced over the previous leg. The standard deviation of this error can be computed from a knowledge of the standard deviation of the wind and its space correlation properties. It is given by:

$$\sigma_{\Delta W_e} = \sqrt{E\left[(W_{ahead} - W_{calc.})^2\right]}$$

$$\approx \frac{\sigma_W}{s}\sqrt{2\int_0^s\int_0^s\left[R_{yu}(x-z) - R_{yu}(x-z+s)\right]dx\,dz} \quad .$$

ΔW_e can be thought of as an extrapolation error. The symbols σ_W and R_{yu} refer respectively to the standard deviation of the cross track wind and to the lateral wind correlation function. R_{yu} is defined in Appendix A. A graphical integration has been performed on this expression and the results are indicated in Figure E-3.

c. Cross wind errors from pressure gradient winds

If periodic measurements are made of both pressure altitude and radio altitude of an aircraft, the navigator can compute an effective cross wind component by making use of the geostrophic assumption described in Appendix A. Assuming the errors in the measurement of the D value (pressure alt. minus

Standard Deviation of Error in Extrapolated Wind Component

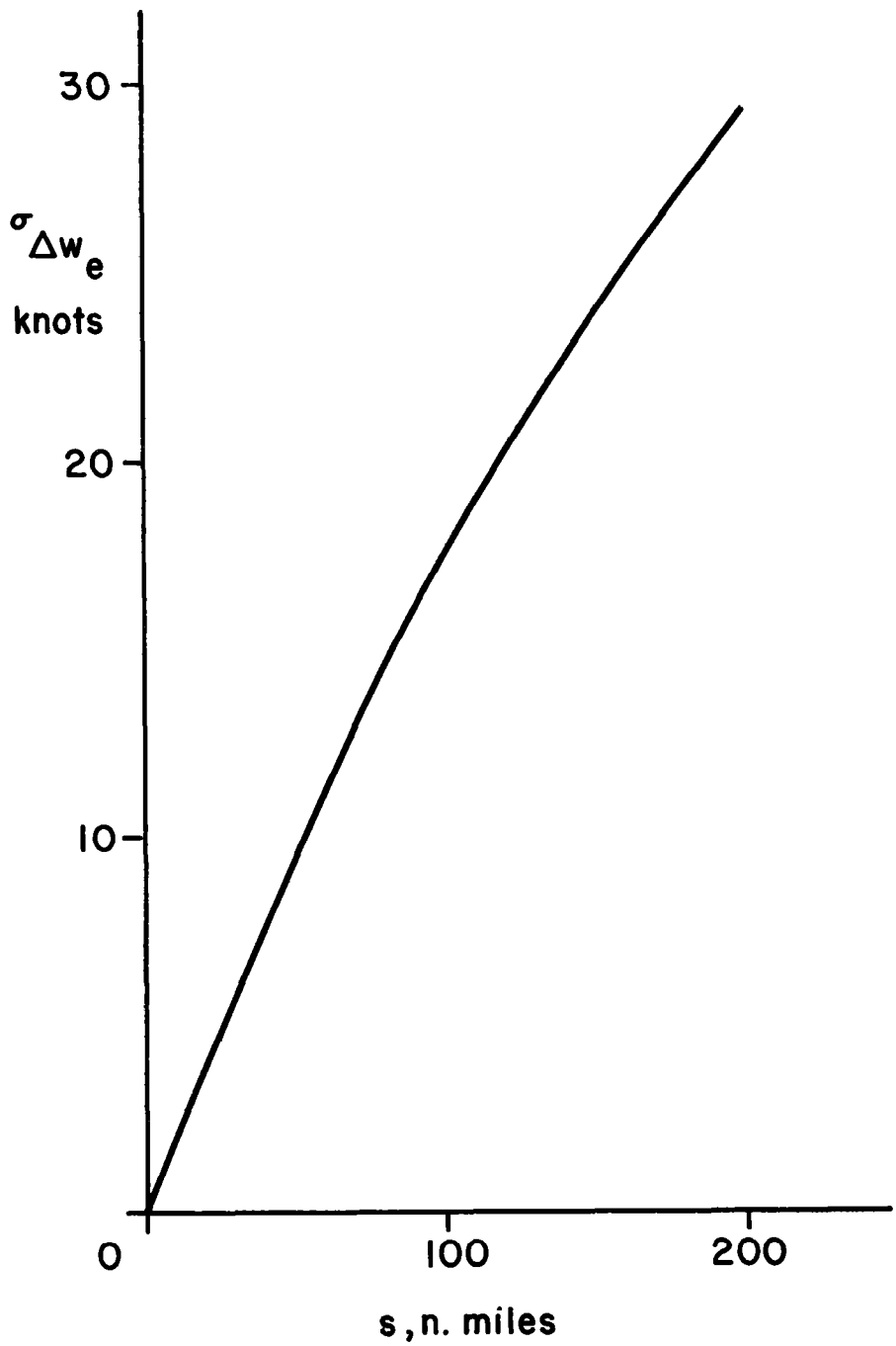

Figure E-3.

STANDARD DEVIATION OF ERROR IN EXTRAPOLATED WIND COMPONENT

radio alt.) predominate over all other error sources, it can be shown that the error in the measured cross wind is given by:

$$\Delta W_i = \frac{k}{s \sin L} (\Delta h_i - \Delta h_{i-1}) \quad . \tag{E6}$$

Δh_i is the error in the D value measurement at the i^{th} point on the flight, L is the latitude at which the aircraft is flying and k is the geostrophic constant. It may be appropriate to increase ΔW_i in this case by perhaps 10% in view of the approximate character of the geostrophic relation. If the pressure gradient cross wind is used as an estimate of cross wind ahead, then the same extrapolation error as described for the case of fixed measured winds must be added.

Quite frequently, navigators on the North Atlantic measure the pressure gradient at intervals more closely spaced than the interval between fixes. A significant decrease in track-keeping error can be achieved under these circumstances. The numerical examples of the next Section will illustrate this point.

d. Cross wind ahead errors from Doppler measured winds

The direct outputs of a Doppler radar sensor are drift angle and ground speed. There is, at present, little information available concerning the accuracy of the drift angle measurement. Data collected by Mr. Nathaniel Braverman of the FAA characterize the overall errors accumulated on long flight segments. The primary source of lateral error in these cases appears to be the heading reference system rather than the Doppler set itself. In spite of the lack of information, it is still appropriate to make the following comments on Doppler navigation.

In current practice, there are two different methods of using Doppler

radar. In the first method, periodic readings of drift angle and ground speed are taken and the drift angle measurements are used to estimate cross winds ahead. Under these circumstances the extrapolation error mentioned under fix derived winds must be taken into consideration. In the second mode, the Doppler radar outputs are connected directly to an automatic dead reckoning computer. This procedure eliminates the extrapolation errors and permits an increase in the distance between position fixes. It should be remembered, however, that the fix accuracy places a basic limit on the track-keeping accuracy, and that the only way to approach this limit is to minimize heading errors or to take frequent position fixes.

e. Cross wind errors when a weighted average is used

If two or more estimates of cross wind are available, a judiciously weighted average of these estimates can be used. The standard deviation of this average will be smaller than that of any of the individual estimates. Significant reduction of error occurs only when the errors in the separate estimates are of comparable magnitude. If, for example, two estimates from independent sources had identical standard deviations of 30 knots each, the standard deviation of the average would be about 21 knots. It is not suggested that navigators actually carry out such computations in practice; they do not have the statistical information needed to compute the weighting factors. Interviews with PAA and TWA personnel and careful study of navigators' logs indicate that an experienced navigator can arrive at compromise estimates which are almost as good as those derived by precise statistical methods. Compromises between fix derived winds and forecast winds are occasionally employed in practice.

4. Numerical Results

The heading errors discussed in the preceding Section and the track-

keeping model of Section 2 can be combined. For each type of navigation, the track-keeping error at the time of the fix is expressed in terms of the errors associated with navigation equipment, wind uncertainty, air speed, and the distance between fixes. Assumptions about statistical independence among some of the errors permit derivation of formulae for the standard deviation of track-keeping error.

All of the different instrumental errors can legitimately be regarded as independent of one another. As before, fix errors are assumed to be uncorrelated from one to the next. Although heading errors will be correlated on a particular flight, the range of choice of a numerical value for the correlation coefficient (assumed positive) has little effect on the computed track-keeping standard deviation. Only the random components of the altimeter errors will be considered, and these are defined as uncorrelated. Wind correlation has been discussed in detail in Appendices A and B.

Numerical values of track-keeping standard deviation have been computed for each case. They are summarized in Table E-I at the end of this Section. Navigational errors and other data used in the computation are:

1.	Distance between fixes	200 n. mi.	(s)
2.	Air Speed	480 knots	(A)
3.	Lateral component of fix error	7.0 n. mi.	(σ_f)
4.	Altimetry error (D value)	40 ft.	($\sigma_{\Delta h}$)
5.	Heading error (all sources except drift)	.025 radians	(σ_{ϵ_c})
6.	Geostrophic assumption error (10% of standard deviation of cross wind)	4 knots	(σ_G)
7.	Geostrophic constant	1.31×10^5 knots	(k)
8.	Latitude of flight (approximate)	55° N	(L)

Wind statistics are taken from Figures E-2 and E-3.

Some of the values listed above are estimates. They are all believed to be approximately correct. A few are taken from data collected during this

study; others are estimates based on interviews with air lines and studies of navigators' logs. The validity of the computed results is tested by comparing them with statistical data on actual track-keeping errors.

a. Navigation using forecast winds

Combination of eqs. (E1) and (E4) yields:

$$y_i = -f_{i-1} + s\epsilon_{c,i-1} + \frac{s}{A}\Delta W_f \quad ,$$

where $\epsilon_{c,i-1}$ is the heading error (exclusive of drift angle error) at the $i-1^{st}$ fix. Then:

$$\sigma_y = \left[\sigma_f^2 + s^2\sigma_{\epsilon_c}^2 + \left(\frac{s}{A}\right)^2 \sigma_{\Delta W_f}^2\right]^{\frac{1}{2}}$$

$$= 14.8 \text{ n. mi.}$$

The term involving forecast error predominates.

b. Navigation using fix derived winds

From eqs. (E3), (E4) and (E5)

$$y_i = f_{i-2} - 2f_{i-1} + s(\epsilon_{c,i-1} - \epsilon_{c,i-2}) + \frac{s}{A}\Delta W_e \quad .$$

Here, the fix error enters in two ways. It misleads the navigator about both the wind on the previous leg and about his deviation from flight plan. Unfortunately the two effects add. ΔW_e is the error made in extrapolating the found wind to the leg ahead. In computing standard deviations, the correlation coefficient (ρ) for the heading errors enters:

$$\sigma_y = \left[5\sigma_f^2 + 2s^2(1-\rho)\,\sigma_{\epsilon_c}^2 + \left(\frac{s}{A}\right)^2 \sigma_{\Delta W_e}^2\right]^{\frac{1}{2}}$$

for the extreme values $\rho = 1$ and $\rho = 0$

$$\sigma_y = \begin{cases} 22.2 \\ 19.8 \end{cases} \text{n. mi.}$$

The correct value lies somewhere in between. Inside the brackets the fix error predominates.

The standard deviation of the fix derived (found) wind can be computed. For the 200 mile interval it is 24.3 knots. It is readily understood why meteorologists use caution when interpreting pilot reported winds.

c. Navigation using a combination of forecast and fix derived winds

Although the standard deviation of the fix derived wind (in this example) is less than that of the forecast, the unfortunate correlation between fix derived wind errors and fix errors dictates weighting factors which place greater emphasis on the forecast wind. The optimal weighting factors (in this case $\frac{3}{4}$ and $\frac{1}{4}$) yield a track-keeping standard deviation of 14.0 n. mi.

In actual practice, an experienced navigator with some knowledge of meteorology will make a better estimate of winds ahead than the simple extrapolation assumed above. It is doubtful, however, that the track-keeping standard deviation could be reduced below 13 n. mi.

d. Navigation using pressure gradient winds

The error in the pressure gradient cross wind is inversely related to the distance between D value measurements. When eqs. (E1), (E4) and

(E6) are combined, it is seen that the effect of D value errors is independent of the distance between fixes. For this reason, the navigator using altimetry can hold closely to flight plan (laterally) even when fixes can only be obtained infrequently. The track-keeping error components from compass error, geostrophic error, and wind extrapolation error do increase with distance. If the D value is measured at the time of the position fix:

$$y_i = -f_{i-1} + s\epsilon_{c,i-1} + \frac{k}{A \sin L}(\Delta h_{i-1} - \Delta h_{i-2}) + \frac{s}{A}(E_G) + \frac{s}{A}\Delta W_e \quad .$$

E_G is the error in the geostrophic relation. Then:

$$\sigma_y = \left[\sigma_f^2 + s^2\sigma_{\epsilon_c}^2 + 2\left(\frac{k}{A \sin L}\right)^2 \sigma_{\Delta h}^2 + \left(\frac{s}{A}\right)^2 (\sigma_G^2 + \sigma_{\Delta W_e}^2)\right]^{\frac{1}{2}}$$

$$= 15.3 \text{ n. mi.}$$

In this case, the extrapolation error (ΔW_e) greatly exceeds all other components of the track-keeping error. The interval over which winds are extrapolated can be reduced by measuring the D value between fixes, computing the cross wind experienced, and choosing a new heading. If D readings are taken twice as frequently as position fixes, then the extrapolation error applies only to half the segment s. In common practice, most navigators measure D at 10 or 15 minute intervals. This corresponds roughly to 100 n. mi. or half the assumed distance between fixes. Applying this procedure:

$$y_i = -f_{i-1} + \frac{s}{2}(\epsilon_{c,i-1} + \epsilon_c') + \frac{k}{A \sin L}(\Delta h' - \Delta h_{i-1}) + \frac{s}{A}(E_G) + \frac{s}{2A}\Delta W_e' \quad .$$

ϵ_c' and $\Delta h'$ are the errors in compass and D value at the midpoint between

the fixes. The symbol $\Delta W'_e$ emphasizes that the extrapolation error refers here to a 100 mile interval rather than the 200 mile interval of the preceding cases (see Figure E-3). Now the track-keeping standard deviation becomes:

$$\sigma_y = \left[\sigma_f^2 + \frac{s^2}{2}(1+\rho)\,\sigma_{\epsilon_c}^2 + 2\left(\frac{k}{A \sin L}\right)^2 \sigma_{\Delta h}^2 + \left(\frac{s}{A}\right)^2 \left(\sigma_G^2 + \frac{1}{4}\sigma_{\Delta W'_e}^2\right)\right]^{\frac{1}{2}}$$

$$= \begin{cases} 9.4 \text{ n. mi. } (\rho = 0) \\ 10.1 \text{ n. mi. } (\rho = 1) \end{cases} .$$

Some navigators plot the measured D values in an attempt to smooth errors and estimate the tendency. Smaller errors should result. It should be noted, however, that the fix error predominates in this case. If the assumed 7 n. mi. error is accepted as correct, then there is little potential gain in improving dead reckoning techniques since the fix error is the lower limit on track-keeping error.

e. Navigation using Doppler radar

Since information on Doppler drift angle error is not readily available, it is not possible to compute track-keeping errors for this case. If Doppler outputs are used directly by the navigator (the first method described in Section 3d), it is possible to obtain a lower bound by assuming that the Doppler drift angle is exact. Assuming that the Doppler drift angle is read every 100 miles,

$$y_i = -f_{i-1} + \frac{s}{2}(\epsilon_{c_{i-1}} + \epsilon'_c) + \frac{s}{2A}\Delta W'_e$$

and

$$\sigma_y = \left[\sigma_f^2 + \frac{s}{2}^2 (1 + \rho)\, \sigma_{\epsilon_c}^2 + \left(\frac{s}{2A}\right)^2 \sigma_{\Delta W'_e}^2\right]^{\frac{1}{2}}$$

$$= \begin{cases} 8.7 \text{ n. mi. } (\rho = 0) \\ 9.3 \text{ n. mi. } (\rho = 1) \end{cases} .$$

If the Doppler sensed inputs are coupled directly to a dead reckoning computer, the processes of navigation and flight plan following differ significantly from those previously considered. Dead reckoning computations, which make up much of the work load of the navigator, are performed automatically. A direct indication of lateral deviation from flight plan is presented to the pilot. Whenever the DR (dead reckoning) computer is reset from a new position fix, the pilot can take immediate action to start reducing the indicated lateral deviation to zero. Since drift angle is monitored continuously there is no need to estimate wind ahead, eliminating completely the extrapolation error discussed above.

In spite of the differences cited above, the track-keeping model developed in this Appendix can be applied to the Doppler-DR computer case. The track-keeping error immediately prior to each reset of the DR computer will be the sum of the Doppler-DR error accumulated since the previous reset and the negative of the fix error at the previous reset. Assuming the cross-course Doppler-DR error to be a fixed percentage of the distance flown, the standard deviation of the track-keeping error becomes:

$$\sigma_y = \left[\sigma_f^2 + \left(\frac{k_D}{100}\right)^2 s^2\right]^{\frac{1}{2}}$$

where k_D is the standard deviation of cross-course Doppler-DR error expressed as percent of distance flown.

Data on the operational performance of Doppler-DR have been collected by Mr. Nathaniel Braverman of the FAA. He has proposed 1.5% as a typical value for k_D. Mr. Braverman also points out that the use of an accurate dead reckoning system such as Doppler-DR obviates the requirement for accurate position fix capability throughout the entire oceanic region. Accurate fixes need be obtained only in regions where the DR computer is to be reset. Studies of the sources of error in ground based Loran A equipment indicate that fix errors of less than 2 n. mi. standard deviation should be obtainable in regions covered by Loran A ground wave. These studies however did not include an analysis of air-borne equipment and procedural errors.

If it is assumed that air-borne errors could be reduced to the point where fix errors of 2 n. mi. are operationally feasible in the neighborhoods of 20 W and 40 W (corresponding to a 600 n. mi. interval between resets) the track-keeping standard deviation becomes:

$$\sigma_y = 9.2 \text{ n. mi.}$$

For this 600 n. mi. reset interval, the Doppler-DR error far outweighs the fix error. It is believed that the main limitations on Doppler-DR cross-course accuracy are the compass errors and magnetic variation errors. Further reduction of track-keeping error requires either improvements in Doppler-DR, or extension of the region of accurate fix coverage, permitting a shorter reset interval.

The numerical results calculated above are summarized in Table E-I

Dead Reckoning Technique	Track-Keeping Standard Deviation (n. mi.)
Forecast winds	14.8
Fixed derived winds (found winds)	19.8 - 22.2
Average of forecast and found winds	14.0
Pressure gradient winds	
D measured at 200 mi. intervals	15.3
D measured at 100 mi. intervals	9.4 - 10.1
Doppler	
Navigator reads drift angle every 100 mi.	8.7 - 9.3 (lower bound)
DR computer reset at 600 n. mi. intervals (fix error = 2 n. mi. at reset)	9.2

Table E-I

The validity of the model results can be checked by comparing them with the statistics of observed track deviations. A set of data based on radar observations of transatlantic jet aircraft inbound to the Goose/Gander region exhibits a standard deviation of 11.7 n. mi. This estimate is based on 137 values of track deviation. Similar data has been collected in Northern Ireland.[15] These data also apply to jet aircraft. The standard deviation of a sample of 1609 observations is 15.8 n. mi.

Navigators' logs have also been examined during this study and statistical data on the distance between the position fix and flight plan analyzed. One sample of 187 values for an air line which uses pressure derived winds has a standard deviation of 15.1 n. mi. A second group of 247 similar measurements for an air line which sometimes uses Doppler (without a DR computer) to estimate drift angle but does not use altimetry has a standard deviation of 19.9 n. mi. In both cases the parameter measured

was not the track-keeping error. Estimates of track-keeping standard deviation can be computed from eq. (E3). The computed values are 13.4 and 18.7 n. mi. respectively.

In general, the model results are low (when it is considered that most air lines use pressure derived winds). One possible explanation involves the model assumption about the choice of heading. Some air lines have indicated that aircraft do not change heading to regain flight plan unless the indicated change is two degrees or more. Other factors also suggest that the flight plan maintenance procedures implied by the model are too rigid for operational application. Since the procedure specified for the model is an optimal one, the model results can be regarded as a lower bound which can only be approached by tightening the discipline of track-keeping procedures.

APPENDIX F

SYSTEM CAPACITY

The model constructed in this Appendix makes it possible to evaluate the traffic handling capacity of oceanic control systems under various separation rules and routing procedures. Each system is represented by the model as a collection of "channels" characterized by the following parameters:

k = the number of channels. (F1)

T = the "service time" for each channel, measured in minutes. (F2)

λ = the average number of aircraft entering the system in a period T. (F3)

c = the probability that only one of two aircraft admitted to an arbitrary channel during a time T can be accommodated without economic penalty. (F4)

An intuitive appreciation of these parameters may be realized if each channel is interpreted as a flight level available to traffic flying in a fixed direction; e.g., westbound traffic. Then k is the number of flight levels available in the system to traffic flying in that direction. The "service time" T is identical to the longitudinal separation standard, which is assumed to be constant for all aircraft pairs. Assignment of two aircraft to the same channel can be made independently (i.e., without lateral separation) if and only if they enter the system with a longitudinal separation of at least T minutes.

The parameter λ designates the average number of aircraft per service time T which must be accommodated by the system of k channels. A study of data on westbound aircraft entries into the Prestwick O.C.A. reveals that arrivals occur at random time intervals and that it is reasonable to characterize the arrival distribution as exponential with mean λ/T; i.e., the number of arrivals in an interval T has a Poisson distribution.

Upon arrival, every aircraft is admitted to one of the channels (flight levels) either with or without lateral revision of the requested flight plan. Each channel includes the desired flight plan track together with a number of "side tracks" which are considered undesirable. It is assumed that the total number of tracks available in the system is arbitrarily large and, therefore, that any number of aircraft can be accommodated without delays, although only a limited number can be assigned desirable tracks at any given time. Thus queues are not allowed to form in the system. It will be assumed initially that any available channel (flight level) can be assigned to an arriving aircraft and that no economic significance is attached to the choice of channel. Economic penalties are associated only with lateral revisions of requested flight plans. A lateral revision is never imposed if it can be avoided by assignment of the aircraft to an available channel. This assumption will be modified later to achieve greater realism.

An additional assumption will be made that when an aircraft is diverted laterally, it is diverted sufficiently far from the main traffic stream so that it does not interfere with later flight plan requests. In some cases, this assumption introduces an error in the estimate of the traffic handling capacity of systems. In a later discussion, it will be shown that the error is relatively insignificant in the applications that have been considered in this report. The assumption leading to this error could be eliminated by constructing a more complicated model. The model would be useful, however, only if adequate statistical information were available on lateral conflicts between revised flight plans and flight plans which are requested later. Such information has not been available during this study.

The parameter c represents the probability that no two requested flight plans, filed for aircraft arriving with a longitudinal separation less than T, satisfy the lateral separation standard throughout the oceanic region. At least one aircraft per service time T can always be assigned to each channel without

lateral revision of the requested flight plan. We shall assume that at most two aircraft can be so accommodated; i.e.,

$$1-c = \text{probability that exactly two aircraft can be admitted to the same channel without economic penalty.} \qquad (F5)$$

This assumption is warranted by an ARCON study of flight plan data furnished by Prestwick O.C.A. The study reveals that the probability of no lateral conflicts among a set of more than two flight plans, requested at about the same time, is negligible.

Consider a system characterized by the parameters k, T, λ, c and satisfying the preceding assumptions. Let P be the probability that an arriving aircraft cannot be assigned to any channel without lateral revision of the requested flight plan. It can be shown that in the "steady state"; i.e., when traffic arrivals have reached a stable average rate λ, P is given by

$$P = \frac{\dfrac{(\lambda c)^k}{k!} + \displaystyle\sum_{i=k+1}^{2k} \left\{ \frac{\lambda^i c^{2k-i}}{i!} \prod_{j=2k-i+1}^{k} (1-c^j) \right\}}{\displaystyle\sum_{i=0}^{k} \frac{\lambda^i}{i!} + \sum_{i=k+1}^{2k} \left\{ \frac{\lambda^i}{i!} \prod_{j=2k-i+1}^{k} (1-c^j) \right\}} \; . \qquad (F6)$$

We shall derive (F6) for the special case c = 1 and indicate the additional steps required to complete the proof for arbitrary c.

The probability P can be derived by an analysis of the possible "states" of the system, where a "state" is defined by the number of "occupied" channels and the lengths of time these channels have been "occupied." A channel (flight level) is said to be "occupied" if an aircraft has been assigned to it during the last T minutes, without lateral diversion of the requested flight plan. Let the interval T be divided into n equal parts and let $\Delta t = T/n$, where n is chosen

large enough so that the probability of an aircraft arrival in an interval of length Δt is $\frac{\lambda \Delta t}{T}$ and the probability of more than one arrival is insignificant. Consider the probabilitites of the following possible system states:

$P(0, t)$ = probability that no channels are occupied at time t,

$P(1, j_1, t)$ = probability that one channel is occupied at time t and that an aircraft has been in this channel for a time $j_1 \Delta t$, where $1 \leq j_1 \leq n$.

$P(2, j_1, j_2, t)$ = probability that two channels are occupied at time t and that the two aircraft have been in these channels for times $j_1 \Delta t$, $j_2 \Delta t$, respectively. [Note that, since we assume two aircraft cannot arrive during the same interval, $j_1 \neq j_2$. We may, therefore, order the j's arbitrarily so that $1 \leq j_1 < j_2 \leq n$,]

.
.
.
.

$P(k, j_1, j_2, \ldots, j_k, t)$ = probability that all k channels are occupied and that the aircraft have been in these channels for times $j_1 \Delta t$, $j_2 \Delta t$, ..., $j_k \Delta t$, respectively. The j's are ordered so that $1 \leq j_1 < j_2 < \ldots < j_k \leq n$. (F7)

The probability of each possible system state at time $t + \Delta t$ is related to the probabilities of the possible states at time t by the following difference equations:

$$P(0,\ t+\Delta t) = \left(1 - \frac{\lambda\Delta t}{T}\right) P(0,t) + \left(1 - \frac{\lambda\Delta t}{T}\right) P(1,n,t);$$

$$P(1,1,t+\Delta t) = \left(\frac{\lambda\Delta t}{T}\right) P(0,t) + \left(\frac{\lambda\Delta t}{T}\right) P(1,n,t);$$

$$\vdots$$

$$P(s,1,j_2,\ \ldots,\ j_s,t+\Delta t) = \left(\frac{\lambda\Delta t}{T}\right) P(s-1,j_2-1,\ \ldots,\ j_s-1,t)$$

$$+ \left(\frac{\lambda\Delta t}{T}\right) P(s,j_2-1,\ \ldots,\ j_s-1,n,t);$$

$$2 \leqq s \leqq k;$$

$$P(s,j_1,j_2,\ \ldots,j_s,t+\Delta t) = \left(1 - \frac{\lambda\Delta t}{T}\right) P(s,j_1-1,j_2-1,\ \ldots,\ j_s-1,t)$$

$$+ \left(1 - \frac{\lambda\Delta t}{T}\right) P(s+1,j_1-1,\ldots,\ j_s-1,n,t);$$

$$2 \leqq j_1,\ 1 \leqq s \leqq k-1;$$

$$P(k,j_1,j_2,\ldots,\ j_s,t+\Delta t) = P(k,j_1-1,j_2-1,\ \ldots,\ j_s-1,t), \qquad 2 \leqq j_1. \quad \text{(F8)}$$

The steady state solution of these equations is

$$P(1, j_1, t) = \left(\frac{\frac{\lambda \Delta t}{T}}{1 - \frac{\lambda \Delta t}{T}} \right) P(0, t) \qquad \text{all } j_1.$$

$$P(2, j_1, j_2, t) = \left(\frac{\frac{\lambda \Delta t}{T}}{1 - \frac{\lambda \Delta t}{T}} \right)^2 P(0, t) \qquad \text{all } j_1, j_2.$$

$$\vdots$$

$$P(k, j_1, j_2, \ldots j_k, t) = \left(\frac{\frac{\lambda \Delta t}{T}}{1 - \frac{\lambda \Delta t}{T}} \right)^k P(0, t) \qquad \text{all } j_1, j_2, \ldots, j_k. \quad \text{(F9)}$$

Let $P^{(s)}$ be the probability that exactly s channels are occupied. Then $P^{(0)} = P(0, t)$. (Since we are concerned with the steady state behaviour of the system, $P^{(s)}$ will be determined, for all s, as a system parameter that is independent of time). The probability $P^{(s)}$ satisfies the equation

$$P^{(s)} = \binom{n}{s} P(s, j_1, j_2, \ldots, j_s, t),$$

$$1 \leq j_1 < j_2 < \ldots < j_s \leq n, \quad \text{(F10)}$$

for any specific selection of the j's, since $P^{(s)}$ is the sum of the probabilities associated with all $\binom{n}{s}$ such selections. It follows from (F9) and (F10) that

$$P^{(s)} = \binom{n}{s} \left(\frac{\frac{\lambda \Delta t}{T}}{1 - \frac{\lambda \Delta t}{T}} \right)^{s} P^{(0)} \quad . \tag{F11}$$

If Δt is replaced by $\frac{T}{n}$ and the limit is taken as n approaches infinity, (F11) becomes

$$P^{(s)} = \frac{\lambda^{s}}{s!} P^{(0)} \quad . \tag{F12}$$

Since $\sum_{i=0}^{k} P^{(i)} = 1$, it follows that

$$P^{(0)} = \frac{1}{\sum_{i=0}^{k} \frac{\lambda^{i}}{i!}} \quad . \tag{F13}$$

Therefore, the probability that all k system channels are occupied is

$$P^{(k)} = \frac{\frac{\lambda^{k}}{k!}}{\sum_{i=0}^{k} \frac{\lambda^{i}}{i!}} \quad . \tag{F14}$$

If c = 1, then $P^{(k)}$ is identical to the probability P that an arriving aircraft cannot be accommodated without lateral revision of the requested flight plan. For this case, the right hand sides of (F6) and (F14) coincide. If

$c \neq 1$, eqs.(F8) must be replaced by a more complex system of difference equations, corresponding to the fact that it is possible to admit as many as 2k aircraft to the system within a time interval T and without diverting them laterally. The method of analysis is identical to that given for the case $c = 1$.

Eq. (F6) is proved by determining the steady state solutions to a system of difference equations. The solutions, therefore, are characteristic of the system performance after the traffic density has reached a sustained peak; i.e., during a period when the system is most heavily taxed. The transient solutions to the difference equations reflect the system performance when the traffic flow begins to build up after a quiescent period or when the flow begins to subside after a peak period. It is clearly the steady state performance of the system that is critical.

A computer program designed to perform the calculations indicated in eq. (F6) has been used to determine values of P as a function of λ for various fixed values of k and c. The results appear in Figures F-1 to F-10. P is plotted on a logarithmic scale for ease in reading.

Note that the probability P that an aircraft is diverted from the requested flight plan cannot be reduced to zero for any system with a finite number of channels, unless there is no traffic (i.e., $\lambda = 0$), or unless aircraft arrive at regular, nonrandom time intervals. Therefore, it would be inappropriate to define the capacity of a system simply as the average number of aircraft per unit time interval that can be accommodated by the system. An appropriate definition should specify the rate at which requested flight plans are rejected. The capacity of a system may be defined with respect to a given rejection rate r as follows.

C_r = the maximum average number of aircraft which may arrive per hour, with not more than r% of the requested flight plans rejected. (F15)

In accordance with the assumptions made for the model, a flight plan is said to be "rejected" only if a lateral diversion is imposed. Since λ was defined as the average number of aircraft arrivals per time interval T, where T represents the longitudinal separation standard measured in minutes, the capacity C_r and the parameter λ are related by the equation

$$C_r = \frac{60}{T} \lambda_r \quad , \tag{F16}$$

where λ_r is that traffic density such that $P = r$.

An acceptable rejection rate r may be determined from user requirements and associated economic factors. In the applications of the results of this Appendix (cf. Chapters VI and VIII), a 5% rejection rate is used to establish a common definition of capacity for the comparison of various systems. The capacity of a system characterized by specific values of the parameters k, c, T is then determined from eq. (F16) by that value of λ such that $P = 0.05$. The value of λ may be read from the appropriate curve in Figures F-1 to F-10. Other rejection rates may also be treated in the same manner.

The effect of each separation standard on system capacity is reflected in eqs. (F6) and (F16). It can be seen from eq. (F6) that the relation between P and the parameters k, λ, and c is independent of T. Therefore, it follows from eq. (F16) that system capacity is inversely proportional to the longitudinal separation standard T. The number of system channels depends upon the vertical separation standard, and the lateral separation standard has a direct bearing on the probability c of lateral conflict between two requested flight plans. The effect of changes in the various separation standards on system capacity is discussed in Chapters VI and VIII.

A few comments on the significance of certain assumptions made in this Appendix are now in order. Eq. (F6) represents the probability that a

requested flight plan will be rejected (i.e., that the aircraft will be diverted laterally), provided that such diverted aircraft do not conflict with the requested flight plans of aircraft which arrive later. This assumption is not always justified. Therefore, in some cases, eq. (F6) underestimates the probability P that a flight plan will be rejected. Consequently, the capacity determined for a given rejection rate r from the curves in Figures F-1 to F-10 may overestimate the actual capacity of a system. The error is small, however, for low rejection rates, although it becomes more significant for large rejection rates. Moreover, the error has a negligible effect on the comparisons of alternate systems made in Chapter VIII.

The assumption that an aircraft can be assigned any available channel (flight level) does not take proper account of the operational limitations of subsonic jet aircraft. A more realistic model may be constructed, if it is assumed instead that an aircraft can be assigned to any jet altitude which is not more than one flight level above the requested level. Thus the number of channels to which a particular aircraft can be assigned depends upon the channel specified in the flight plan request. This assumption leads to a more realistic model, since the requested flight level is usually close to the maximum altitude that can be achieved by the aircraft.

A model corresponding to this assumption has been constructed with the aid of computer simulation techniques. A block diagram of the computer program is presented in Figure F-11. The computer program has been used to determine values of the probability P that a flight plan will be rejected, for a system with $k = 5$ channels and a probability $c = .6$ of lateral conflict between two requested flight plans. The results are shown in Figure F-12, where P is plotted as a function of the traffic density λ. The value $k = 5$ represents the number of flight levels available to subsonic jet aircraft in the present system, when the datum line technique is in effect. The value $c = 0.6$ was determined from a study of data furnished by Prestwick O.C.A. on flight plan requests.

For comparison, two curves are also shown in Figure F-12 which represent values of P determined by eq. (F6); that is, values corresponding to the assumption that any available channel can be assigned to an aircraft independently of the requested channel. The two curves represent systems with k = 4 and k = 5 channels, respectively. All three curves in Figure F-12 were generated for the case c = 0.6. As indicated in the figure, the probability P determined for each value of λ by the computer simulation lies between the corresponding values of P determined by eq. (F6) for the 4 and 5-channel systems. Thus the capacity of the 5-channel system, with the restrictions on available channels, lies between the capacities determined for the 4 and 5-channel systems without these restrictions.

The similarity of the curves obtained by the two modeling techniques demonstrates that the more realistic computer simulation does not provide a significant improvement over the analytic model, especially for the purpose of comparing the relative capacities of alternate systems. For this reason, a larger scale computer effort has not been undertaken to generate curves by the simulation technique for a wider range of values of the system parameters k and c.

In both models, no economic penalties are associated with vertical changes in flight plans from requested flight levels, and a flight plan is considered as rejected (with economically significant consequences) only if a lateral deviation is imposed. It would be possible to formulate a more realistic model with weighted economic penalties associated with diversions in both flight level and latitude and with the weight attached to each penalty determined by the type and extent of the diversion. Not only would such a model be cumbersome, but any useful application would require extensive statistical information in order to determine appropriate weighted penalties. Reliable statistical information is not available. Moreover, the simpler model presented in this Appendix does provide a useful comparison between

alternate systems. A choice among proposed systems must be determined by a comparative analysis of idealized system performances, since an evaluation of the absolute performance of a system can be realized only by a detailed observation and analysis of the system in actual use.

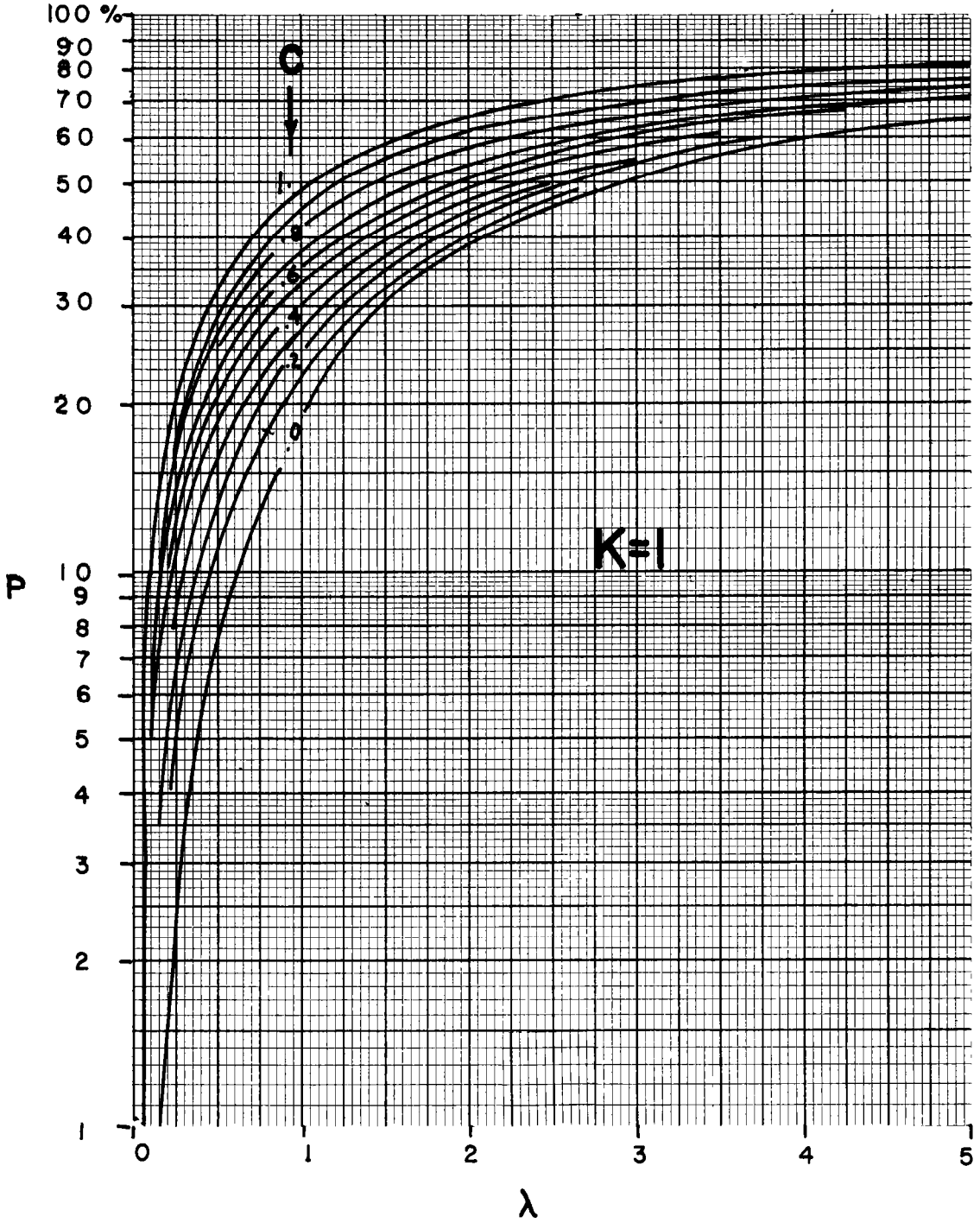

Figure F-1

CAPACITY OF 1-CHANNEL SYSTEMS.

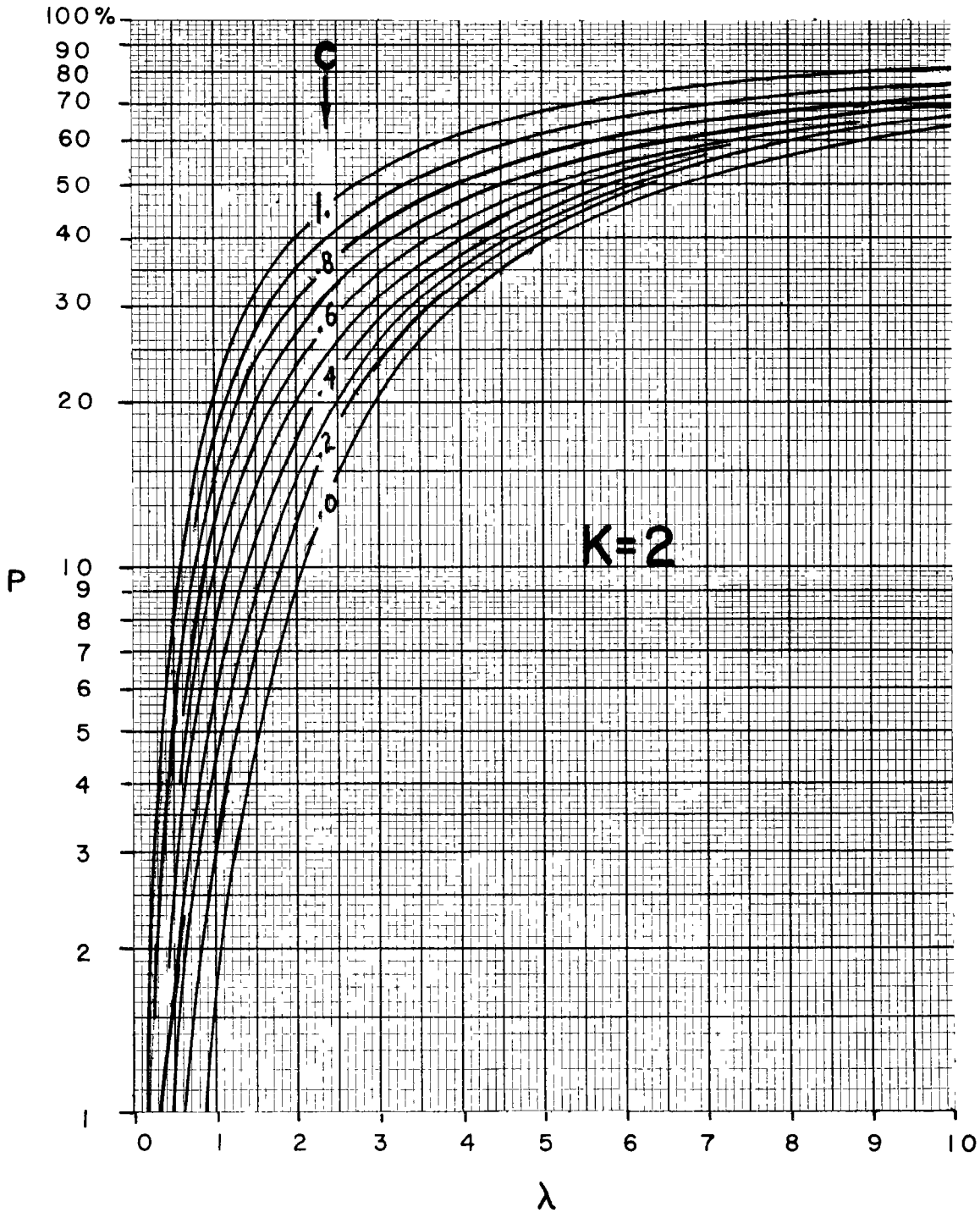

Figure F-2

CAPACITY OF 2-CHANNEL SYSTEMS.

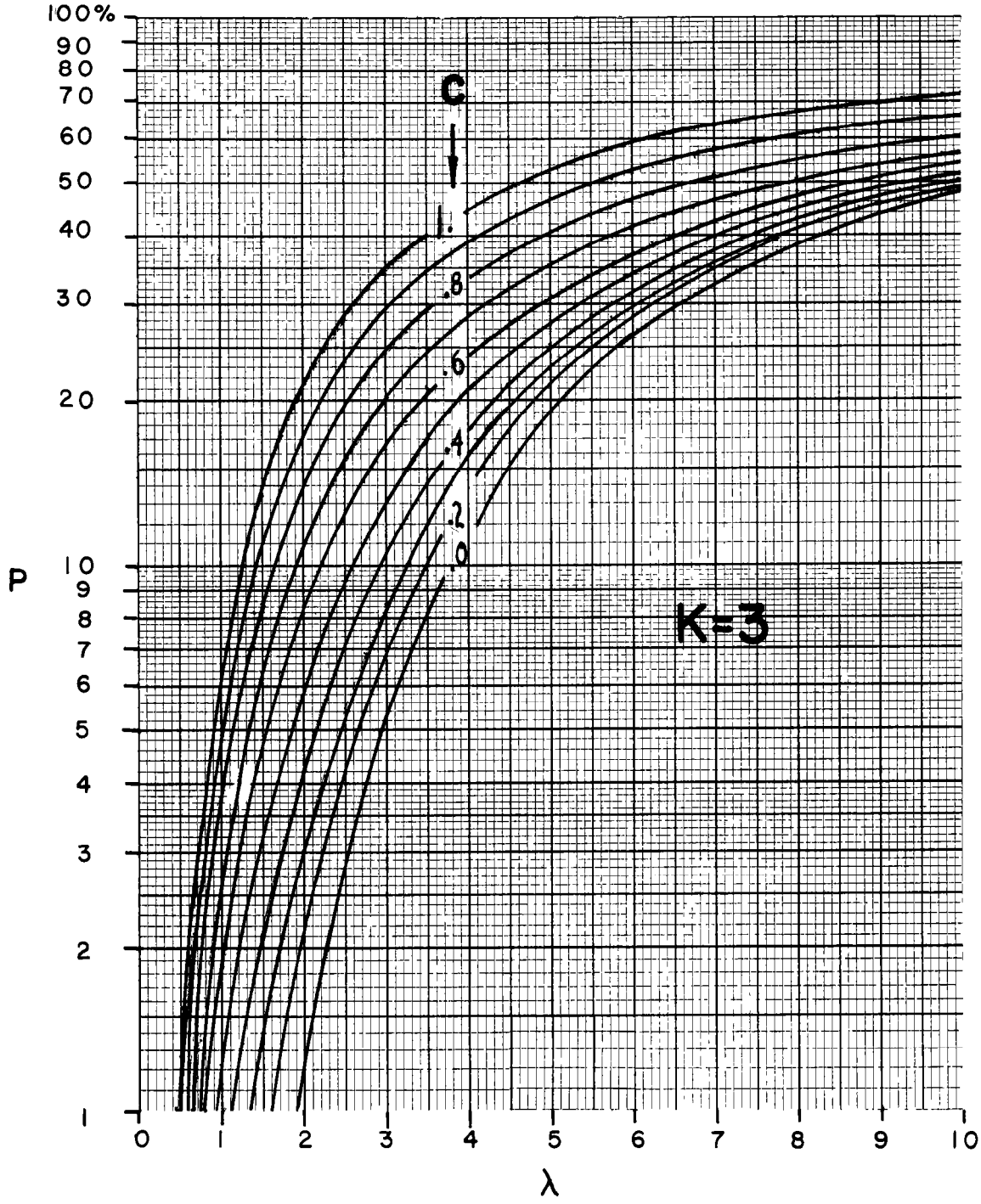

Figure F-3

CAPACITY OF 3-CHANNEL SYSTEMS.

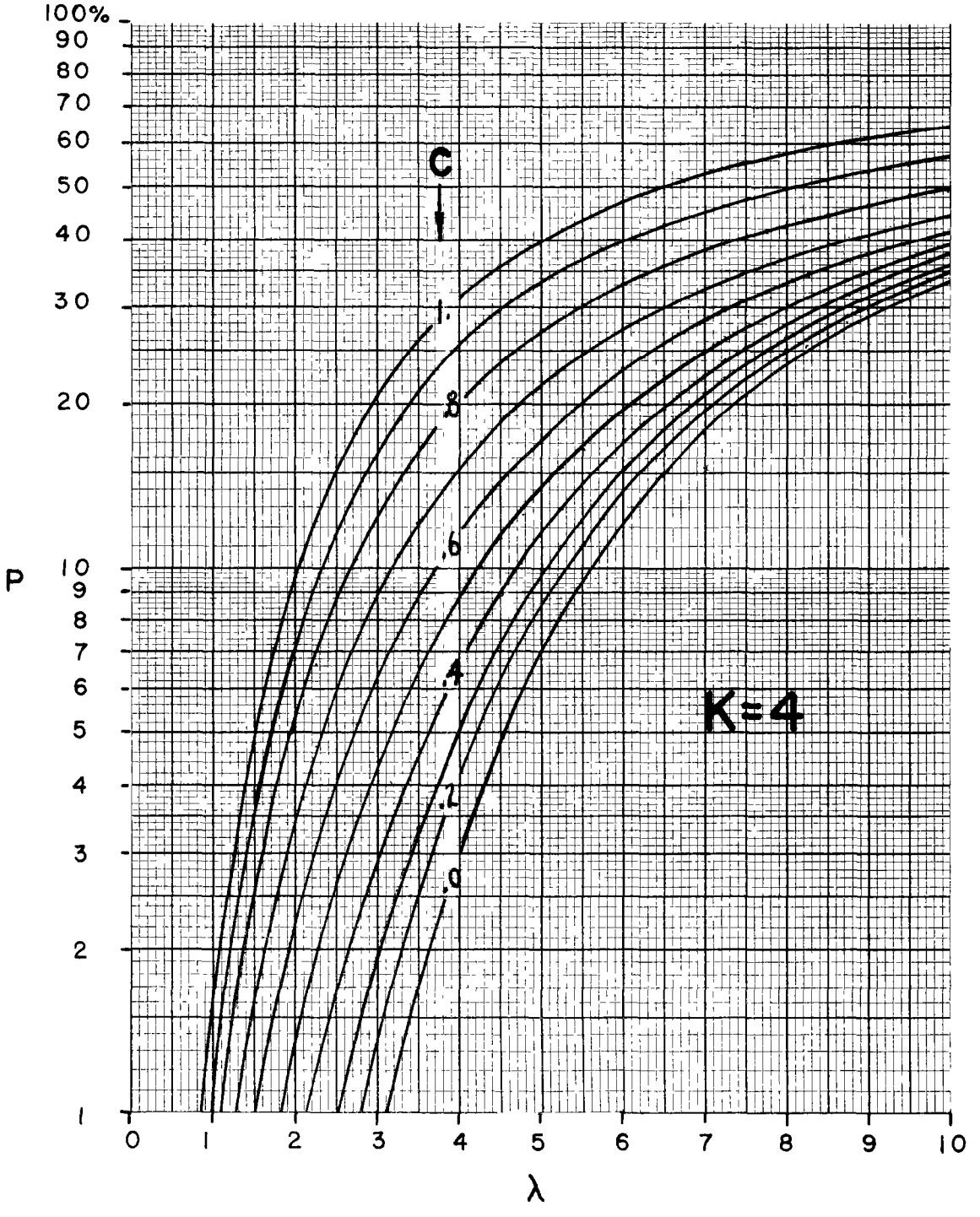

Figure F-4

CAPACITY OF 4-CHANNEL SYSTEMS.

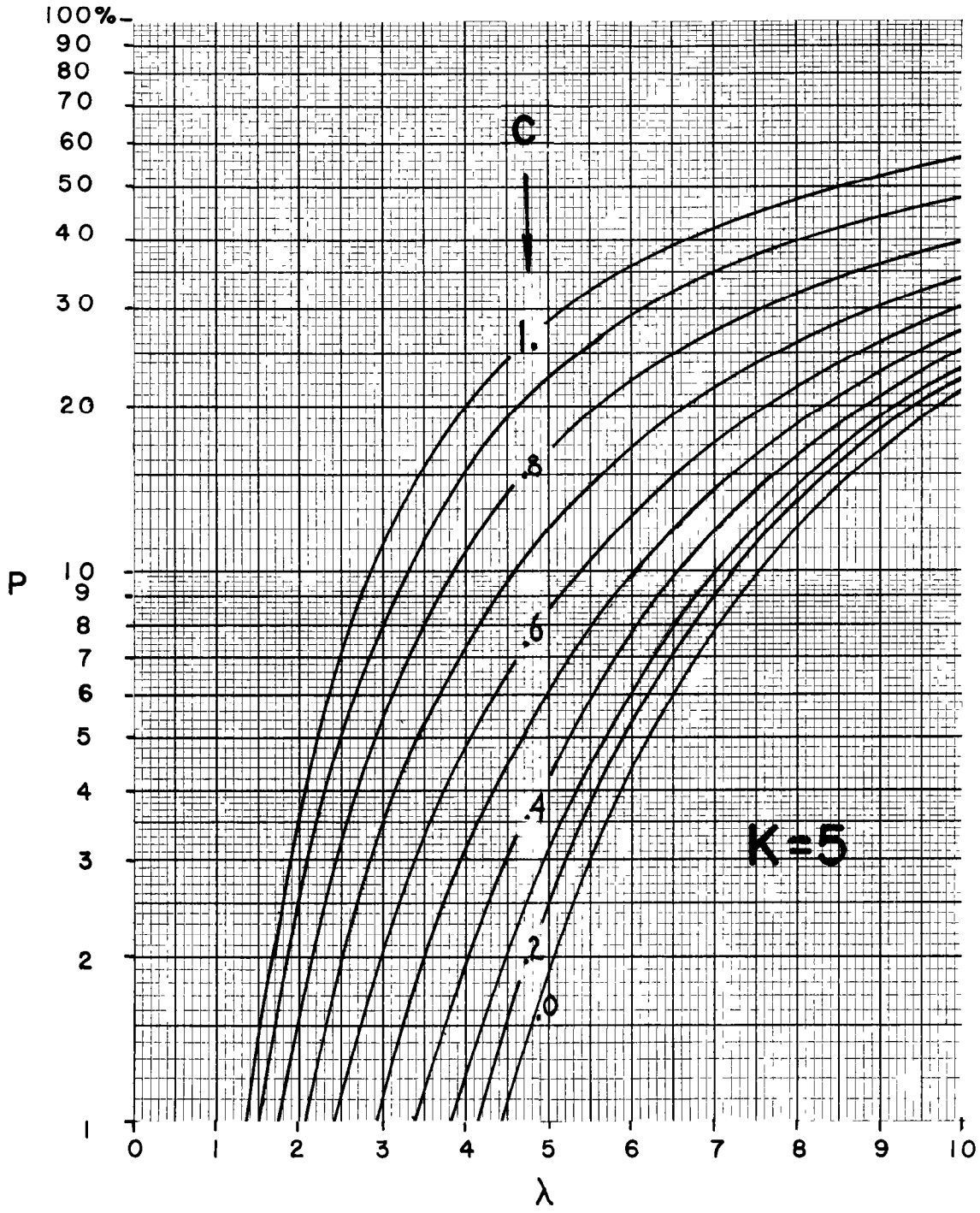

Figure F-5

CAPACITY OF 5-CHANNEL SYSTEMS.

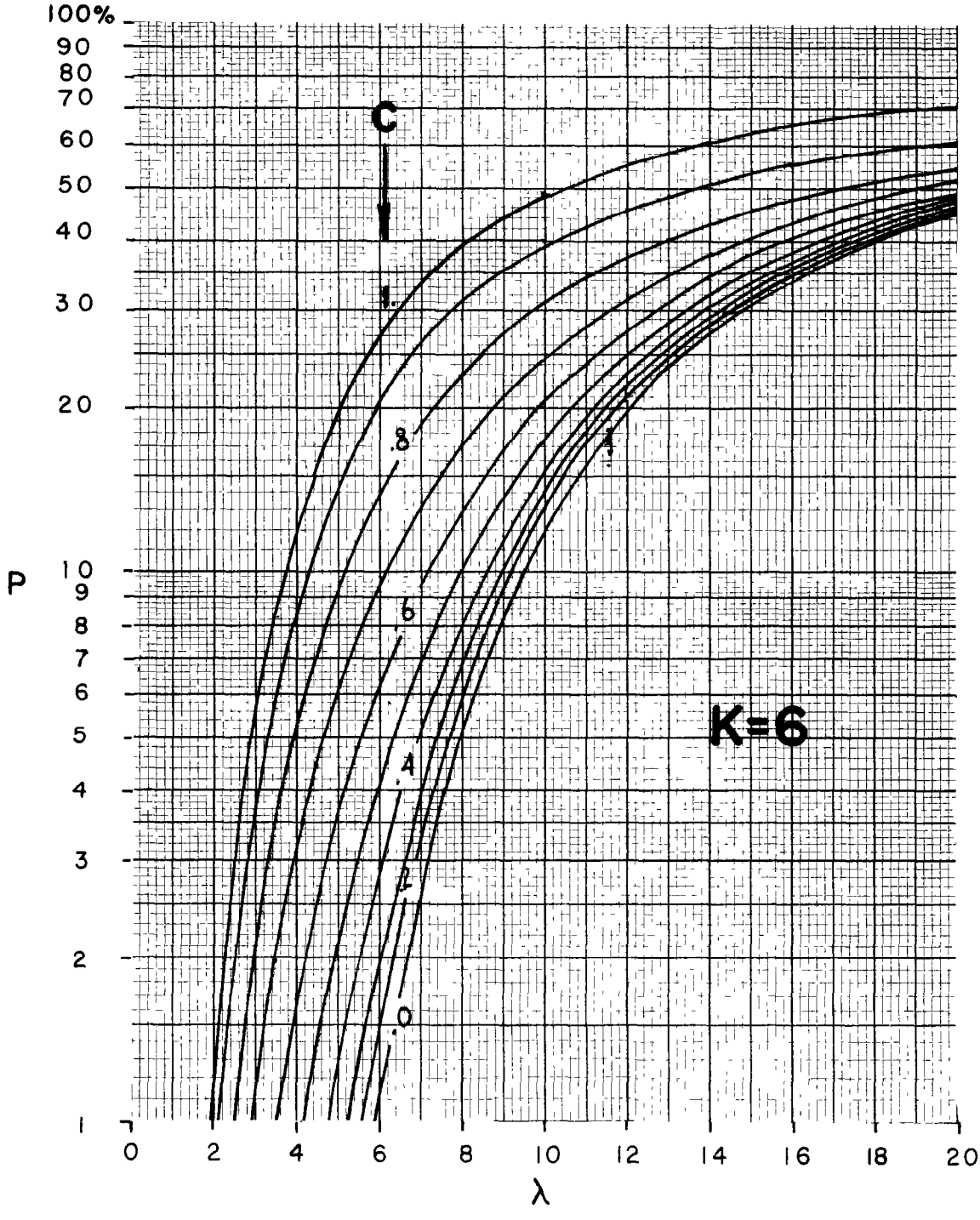

Figure F-6

CAPACITY OF 6-CHANNEL SYSTEMS.

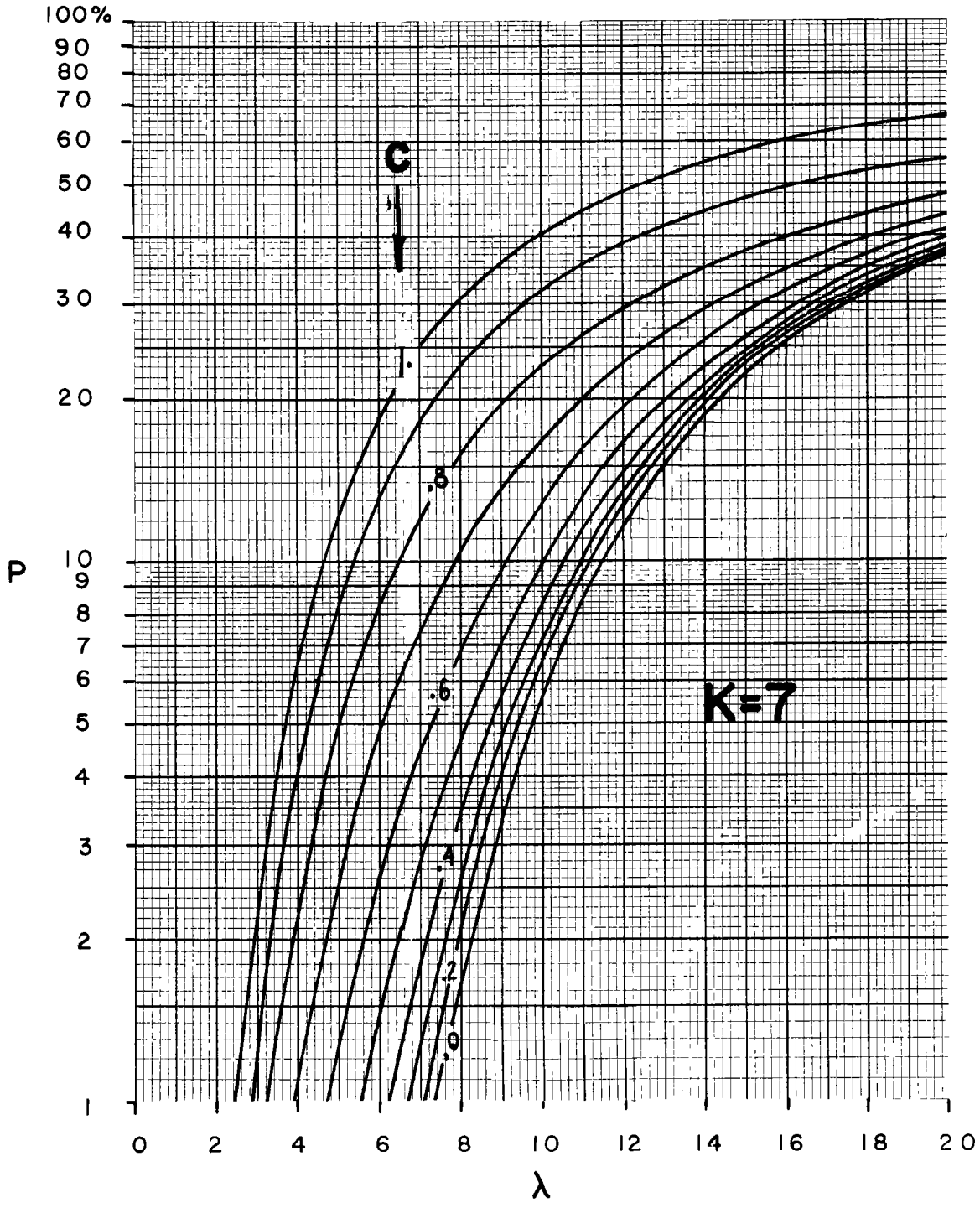

Figure F-7

CAPACITY OF 7-CHANNEL SYSTEMS.

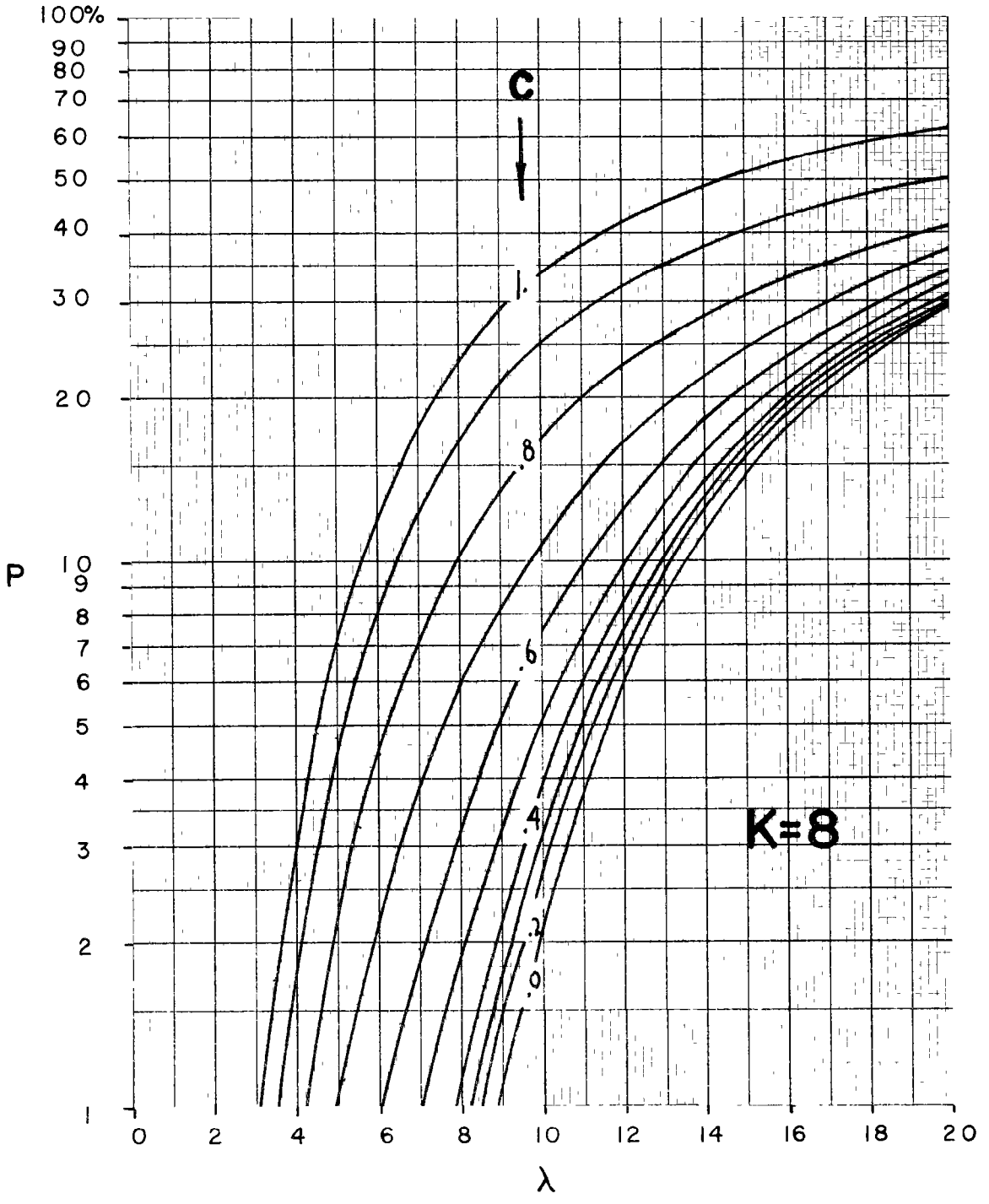

Figure F-8

CAPACITY OF 8-CHANNEL SYSTEMS.

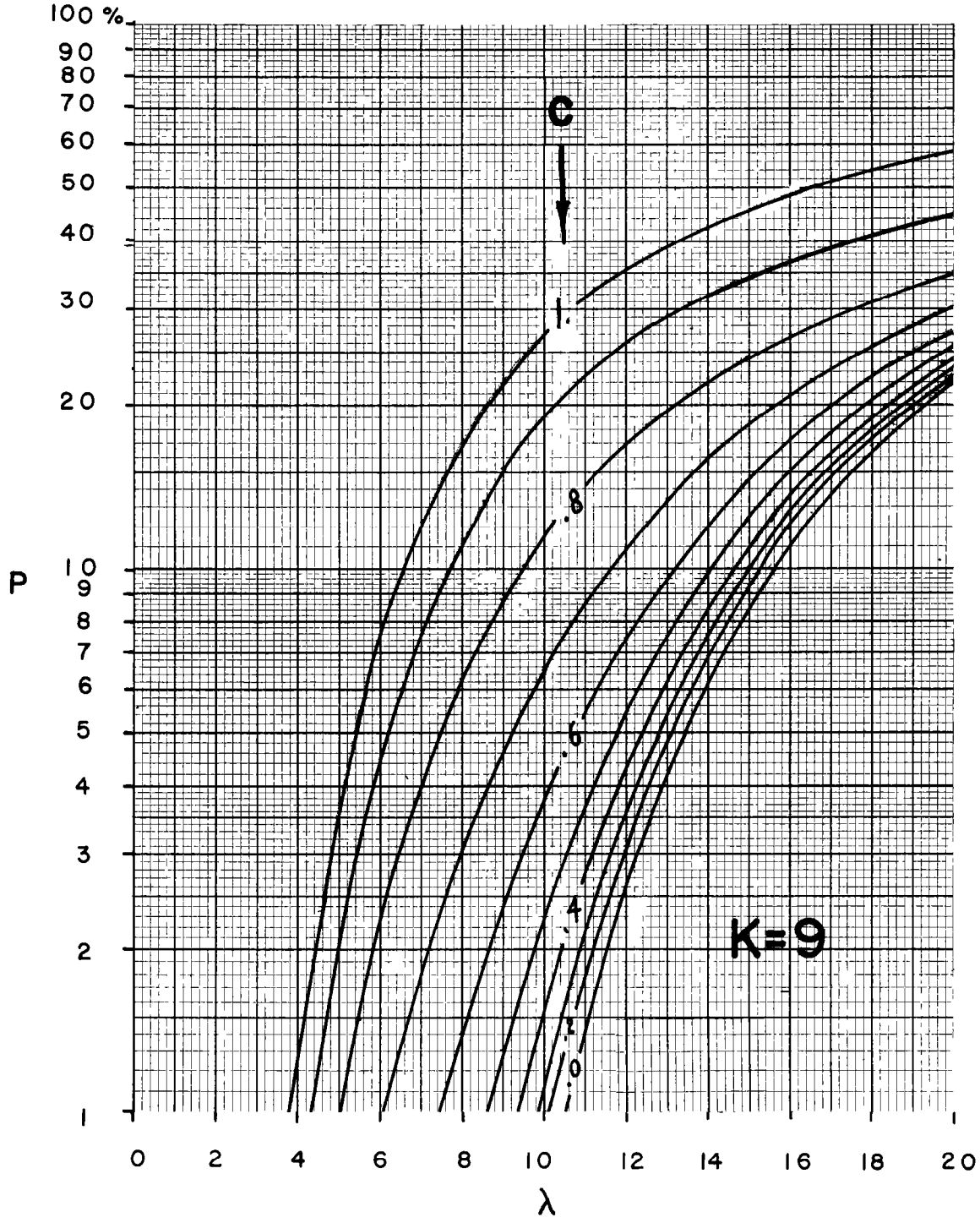

Figure F-9

CAPACITY OF 9-CHANNEL SYSTEMS.

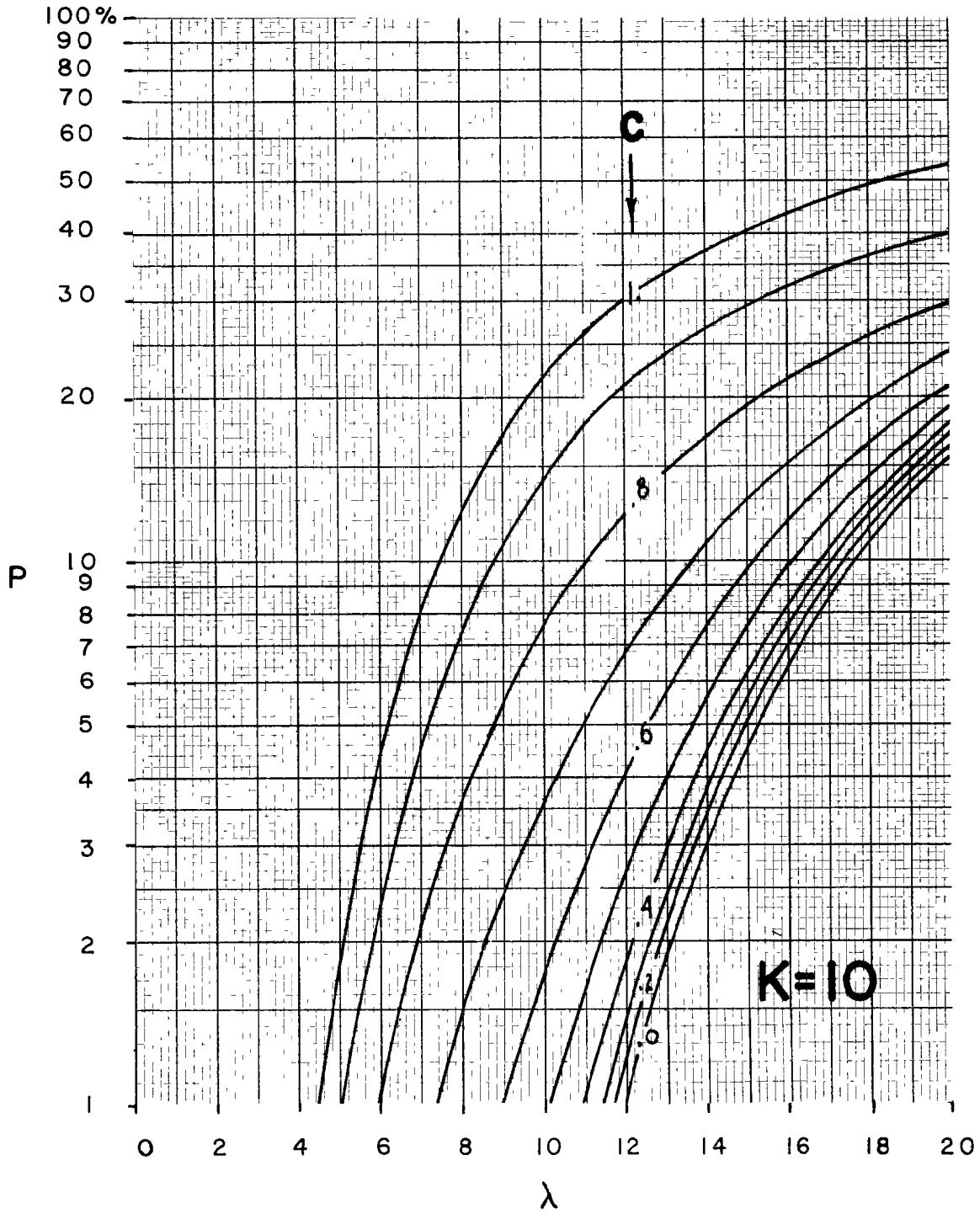

Figure F-10

CAPACITY OF 10-CHANNEL SYSTEMS.

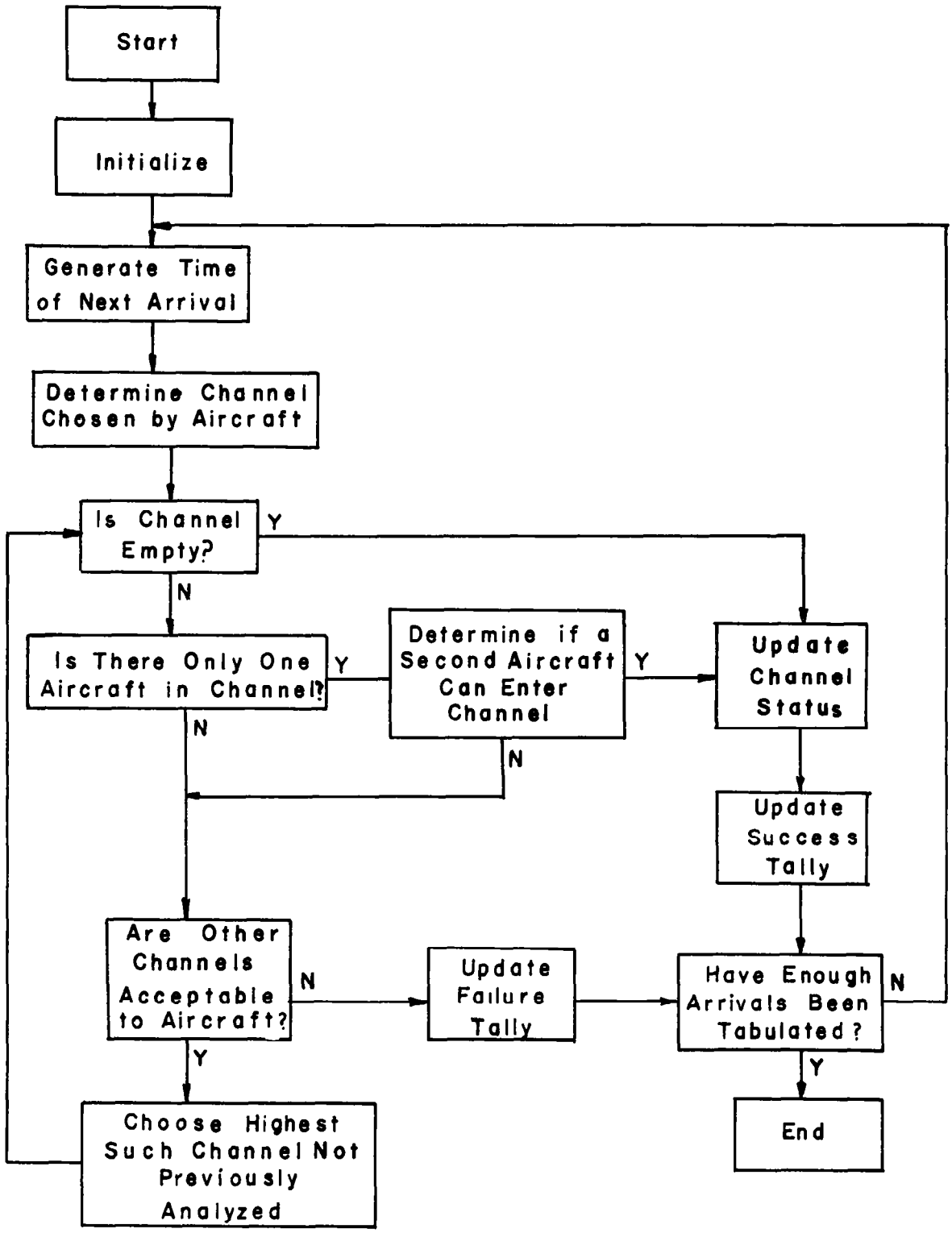

Figure F-11

BLOCK DIAGRAM OF COMPUTER SIMULATION.

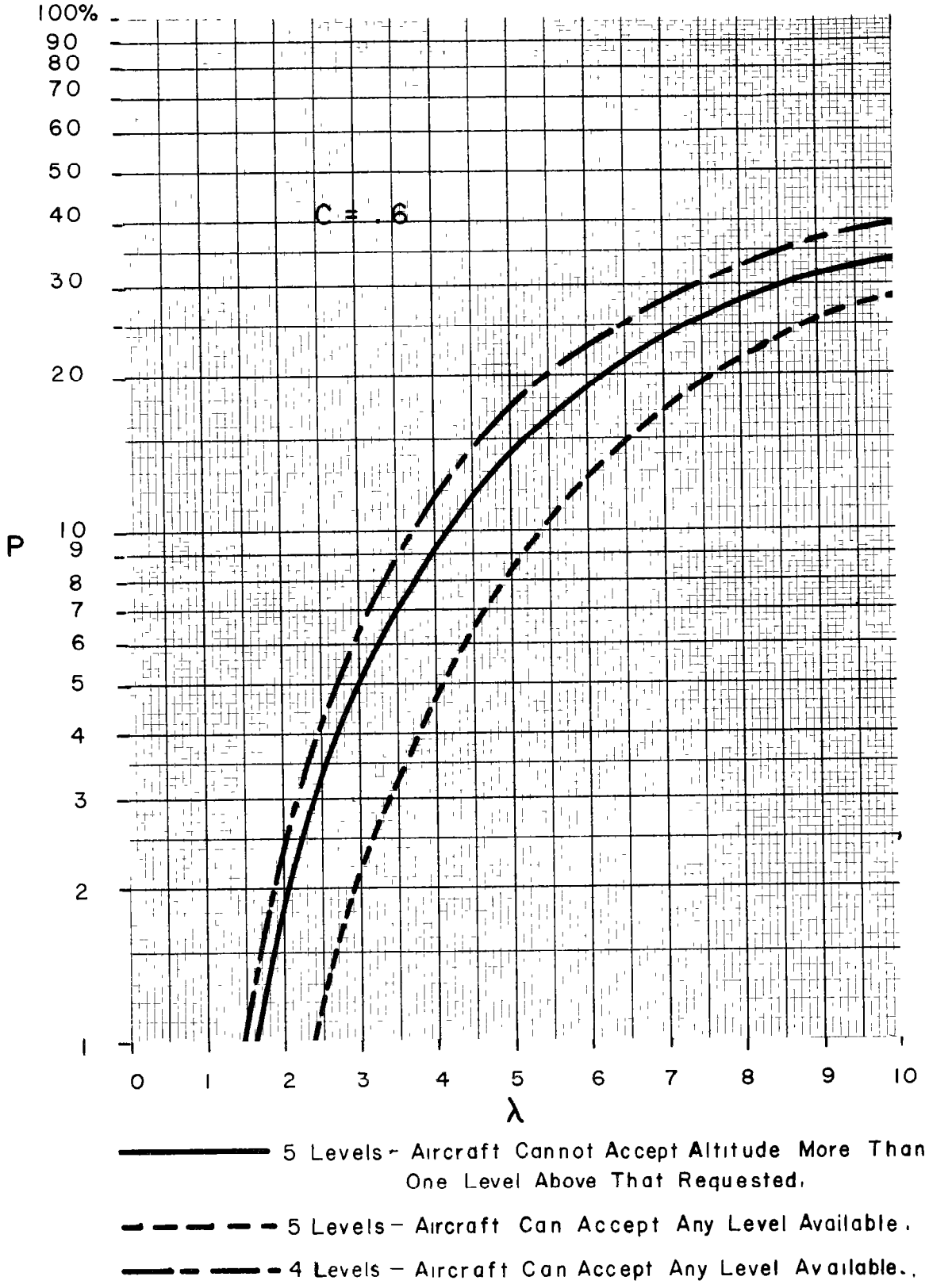

Figure F-12

COMPARISON OF ANALYTIC AND COMPUTER SIMULATION MODELS.

APPENDIX G

ANALYSIS OF THE MINIMAL TIME PATH

The minimal time path (MTP) between a specified origin-destination pair depends upon the wind field. For a particular air speed and altitude, there is, in general, only one MTP. Since it is occasionally necessary for Air Traffic Control to impose changes on flight plan routes, the economic penalty associated with rerouting should be evaluated. The analysis presented in this Appendix provides approximate values of the average time penalties associated with various types of route diversion.

In order to compute the time penalty associated with a nonoptimal route, the manner in which this alternate deviates from the minimal path (M) must be completely specified. In this study, the alternate route (A) is defined by a function P(s) whose value is the separation between M and A (measured perpendicular to M) at a point on M which is s miles from the point of origin. Clearly, P(s) = 0 for s = 0 and for s = L (the total length of the minimal route). This description is illustrated in Figure G-1. P(s) is taken positive if the alternate lies to the left of M.

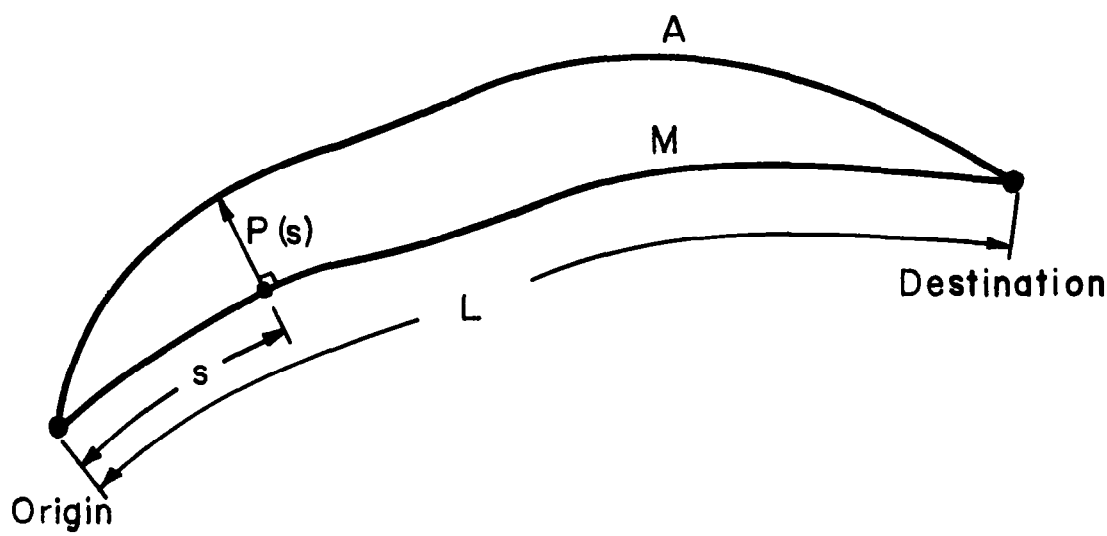

Figure G-1

The total flight time on M is.

$$T_M = \int_0^L \frac{ds}{G(s,0)} \quad ,$$

where G(s, 0) is the aircraft ground speed on M at the point s. On the alternate path, the flight time is.

$$T_A = \int_0^{L'} \frac{ds'}{G(s,P)} = \int_0^L \frac{ds'}{ds} \frac{ds}{G(s,P)} \quad .$$

ds' is the differential element of ground distance along A which corresponds (see Figure G-2) to ds on M, and G(s, P) is the ground speed at the point on A adjacent to the point s on M. The time penalty incurred on the alternate path is

$$\tau = T_A - T_M \quad .$$

Then

$$\frac{d\tau}{ds} = \frac{ds'}{ds} \cdot \frac{1}{G(s,P)} - \frac{1}{G(s,0)} \quad . \qquad \text{(G1)}$$

Since $\frac{ds'}{ds}$, and G are functions only of the wind field, air speed (assumed constant), and the alternate route specification, P(s), it is possible to compute an average value for τ since the statistics of the wind field are known.

The analysis proceeds as follows:

1. Express $\frac{ds'}{ds}$ in terms of P(s) and M.
2. Describe M in terms of the wind field.
3. Derive an expression for G(s, P) in terms of G(s, 0) and the wind field.
4. Combine the above using eq. (G1) and compute average values.

1. Computation of $\frac{ds'}{ds}$

Let the curve M (the minimal time path) be expressed parametrically by

$$x = x(s) \quad ; \quad y = y(s) \quad .$$

The alternate path is determined by the MTP and by the function P(s) which specifies the length of the segment of the line perpendicular to the MTP which lies between M and A (the alternate route).

Let the path A be specified by u(s) and v(s). We wish to find the length of the segment of arc (ds') along the path A which corresponds to an increment ds along M.

$$ds' = \sqrt{du^2 + dv^2} \quad \text{or} \quad \frac{ds'}{ds} = \sqrt{\left(\frac{du}{ds}\right)^2 + \left(\frac{dv}{ds}\right)^2} \quad .$$

The relationship between A and M is given by:

$$u(s) = x(s) - P(s) \sin \theta$$

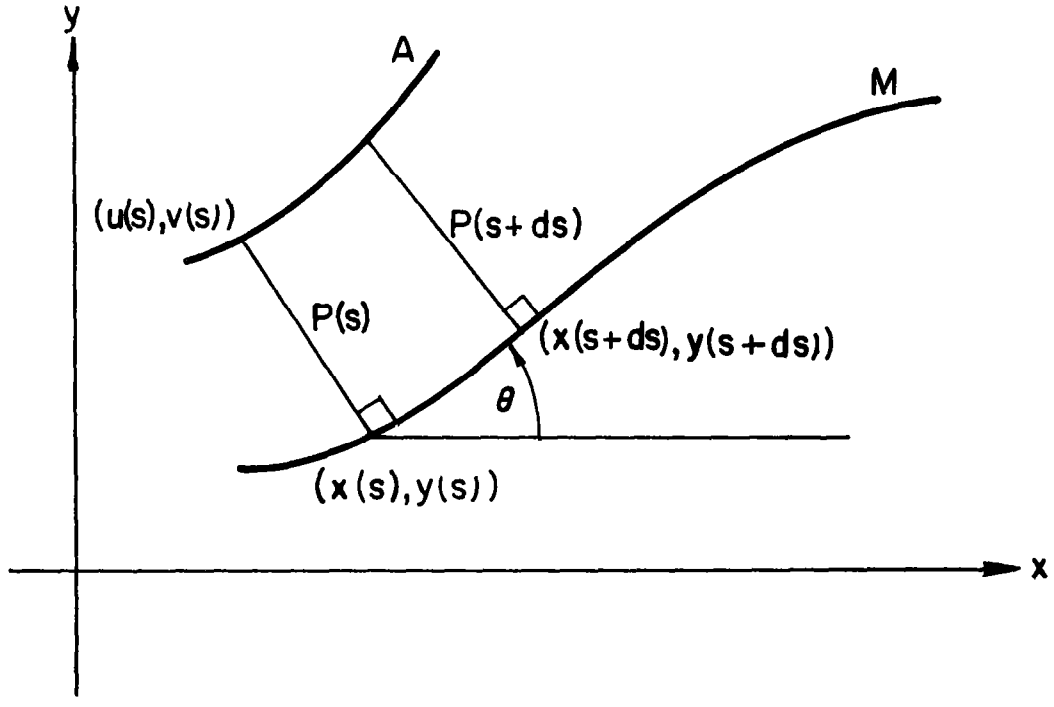

Figure G-2

and

$$v(s) = y(s) + P(s)\cos\theta$$

$$\frac{du}{ds} = \frac{dx}{ds} - P'\sin\theta - P\cos\theta\frac{d\theta}{ds}$$

$$\frac{dv}{ds} = \frac{dy}{ds} + P'\cos\theta - P\sin\theta\frac{d\theta}{ds} \quad .$$

But $$\frac{dx}{ds} = \cos\theta \; ; \; \frac{dy}{ds} = \sin\theta \quad .$$

So

$$\frac{du}{ds} = (1 - P\frac{d\theta}{ds}) \cos\theta - P' \sin\theta$$

$$\frac{dv}{ds} = (1 - P\frac{d\theta}{ds}) \sin\theta + P' \cos\theta$$

$$(\frac{du}{ds})^2 = (1 - P\frac{d\theta}{ds})^2 \cos^2\theta + P'^2 \sin^2\theta - 2P'(1 - P\frac{d\theta}{ds}) \sin\theta \cos\theta$$

$$(\frac{dv}{ds})^2 = (1 - P\frac{d\theta}{ds})^2 \sin^2\theta + P'^2 \cos^2\theta + 2P'(1 - P\frac{d\theta}{ds}) \sin\theta \cos\theta$$

$$(\frac{ds'}{ds})^2 = (\frac{du}{ds})^2 + (\frac{dv}{ds})^2 = (1 - P\frac{d\theta}{ds})^2 + P'^2$$

$$\frac{ds'}{ds} = \sqrt{(1 - P\frac{d\theta}{ds})^2 + P'^2} \quad .$$

If P(s) is of the form (Figure G-3),

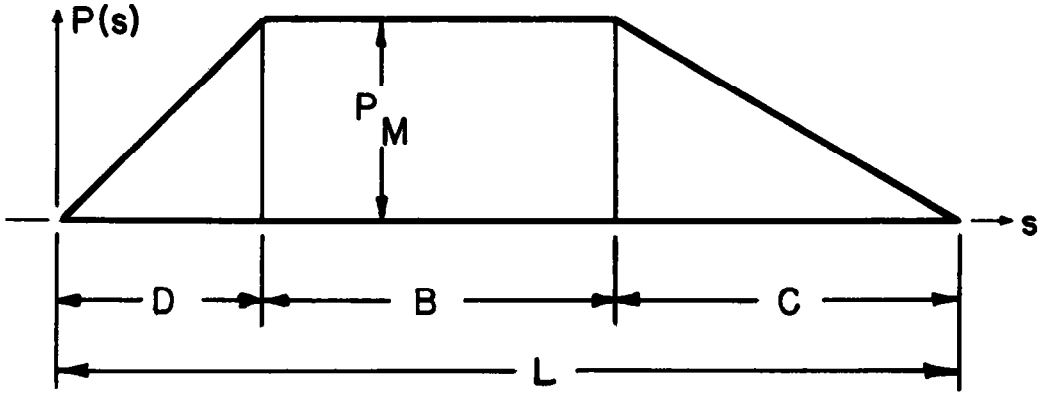

Figure G-3

$$P(s) = \begin{cases} s\frac{P_M}{D} & 0 \le s \le D \\ P_M & D \le s \le D + B \\ (L - s)\frac{P_M}{C} & D + B \le s \le L \end{cases}$$

then for the divergent region (region D)

$$\frac{ds'}{ds} = \sqrt{1 - 2s\frac{P_M}{D}\frac{d\theta}{ds} + \left(s\frac{P_M}{D}\frac{d\theta}{ds}\right)^2 + \left(\frac{P_M}{D}\right)^2}$$

$$= 1 - s\frac{P_M}{D}\frac{d\theta}{ds} + \frac{1}{2}\left(\frac{P_M}{D}\right)^2 + \text{terms in } \left(\frac{P_M}{D}\right)^3 \text{ etc.} \qquad \text{(G2a)}$$

for the middle region (region B)

$$\frac{ds'}{ds} = 1 - P_M\frac{d\theta}{ds} \qquad \text{(G2b)}$$

and for the convergent region (region C)

$$\frac{ds'}{ds} = 1 - (L - s)\frac{P_M}{C}\frac{d\theta}{ds} + \frac{1}{2}\left(\frac{P_M}{C}\right)^2 + \text{terms in } \left(\frac{P_M}{C}\right)^3 \text{ etc.} \qquad \text{(G2c)}$$

2. MTP Relationships

Since the MTP is defined by the wind field, a relationship between the two can be established. It has been shown[20] that the rate of change of aircraft heading depends only upon the "tail wind shear" (neglecting map scale factor).

$$\frac{d\varphi}{dt} = -\frac{\partial W_x}{\partial y} \quad . \tag{G3}$$

φ is the aircraft heading and the system x, y is attached to the air speed vector. If the drift angle λ (the angle between ground and air vectors) is considered positive when the wind is from the right (starboard) and if heading φ and track θ are both measured counterclockwise Figure G-4 then:

$$\varphi = \theta - \lambda \quad .$$

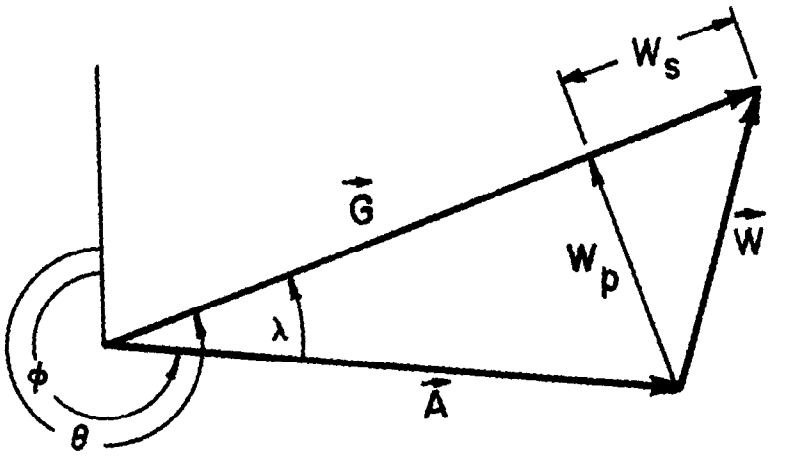

Figure G-4

Then
$$\frac{d\varphi}{dt} = \frac{d\varphi}{ds}\frac{ds}{dt} = G(s,0)\frac{d\varphi}{ds}$$

$$= G(s,0)\left[\frac{d\theta}{ds} - \frac{d\lambda}{ds}\right] \quad . \tag{G4}$$

Since the coordinate system used in this analysis is attached to the ground vector rather than the air vector, $\frac{\partial W_x}{\partial y}$ must be expressed in the s, p (ground)

system. The reader should note that the s,p coordinate system rotates as the aircraft moves along M in a manner such that the s direction is always tangent to M. Therefore, the s and p components of the wind differ at any two points both because of changes in $\vec{W}$ and because of rotations of the s,p system.

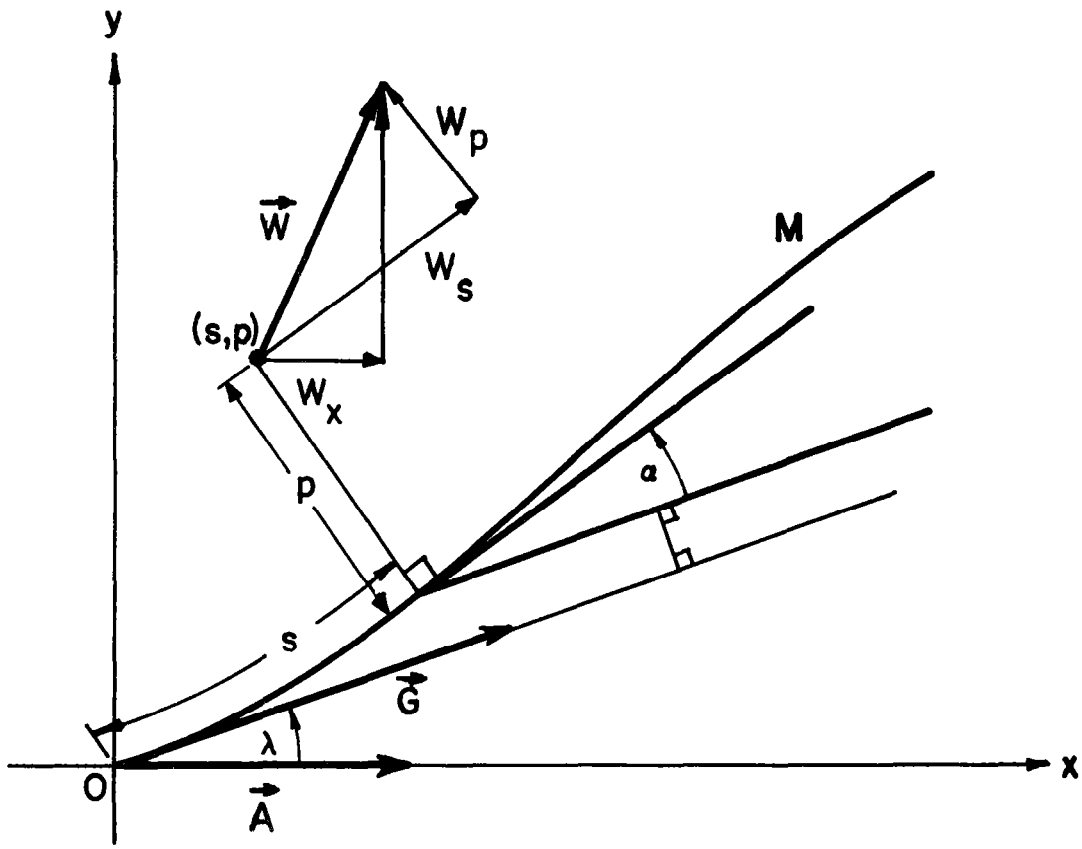

Figure G-5

In Figure G-5, the wind vector W at the point (s,p) is resolved into s and p components which are rotated $\lambda + \alpha$ from the x,y system. λ, the drift angle at the point O is fixed, but α varies along M. Thus α is a function of s but,for this purpose,λ is not.

$$W_x = W_s \cos(\lambda + \alpha) - W_p \sin(\lambda + \alpha)$$

$$\frac{\partial W_x}{\partial y} = \frac{\partial}{\partial y}\left\{W_s \cos(\lambda + \alpha) - W_p \sin(\lambda + \alpha)\right\}$$

$$\frac{\partial W_x}{\partial y} = \frac{\partial s}{\partial y}\frac{\partial}{\partial s}\left[W_s \cos(\lambda+\alpha) - W_p \sin(\lambda+\alpha)\right] + \frac{\partial p}{\partial y}\frac{\partial}{\partial p}\left[W_s \cos(\lambda+\alpha) - W_p \sin(\lambda+\alpha)\right]$$

$$\frac{\partial s}{\partial y} = \sin(\lambda + \alpha) \quad ; \quad \frac{\partial p}{\partial y} = \cos(\lambda + \alpha)$$

$$\frac{\partial W_x}{\partial y} = \sin(\lambda + \alpha)\left[\frac{\partial W_s}{\partial s}\cos(\lambda + \alpha) - \frac{\partial W_p}{\partial s}\sin(\lambda + \alpha) - \sin(\lambda + \alpha)W_s \frac{d\alpha}{ds}\right.$$

$$\left. - \cos(\lambda + \alpha)W_p \frac{d\alpha}{ds}\right] + \cos(\lambda + \alpha)\left[\frac{\partial W_s}{\partial p}\cos(\lambda + \alpha) - \frac{\partial W_p}{\partial p}\sin(\lambda + \alpha)\right] .$$

At this point we can identify $\frac{d\alpha}{ds}$ and $\frac{d\theta}{ds}$

$$\left.\frac{\partial W_x}{\partial y}\right|_{s=0} = -\sin\lambda(W_p \cos\lambda + W_s \sin\lambda)\frac{d\theta}{ds} + \cos^2\lambda \frac{\partial W_s}{\partial p}$$

$$- \cos\lambda \sin\lambda \frac{\partial W_p}{\partial p} + \sin\lambda \cos\lambda \frac{\partial W_s}{\partial s} - \sin^2\lambda \frac{\partial W_p}{\partial s} . \qquad \text{(G5)}$$

Since $W_p = A \sin\lambda$

and $G = A\cos\lambda + W_s$ (See Figure G-4),

$$\frac{\partial \lambda}{\partial s} = \frac{1}{A\cos\lambda}\frac{\partial W_p}{\partial s} \qquad \text{(G6)}$$

and $$W_p \cos\lambda + W_s \sin\lambda = G \sin\lambda \quad . \tag{G7}$$

Combining eqs. (G3) through (G7) we get (where derivatives are evaluated at $p = 0$):

$$G(s,0)\left[\frac{d\theta}{ds} - \frac{1}{A\cos\lambda}\frac{\partial W_p}{\partial s}\right] = G\sin^2\lambda\frac{d\theta}{ds} - \cos^2\lambda\frac{\partial W_s}{\partial p} + \cos\lambda\sin\lambda\frac{\partial W_p}{\partial p} - \sin\lambda\cos\lambda\frac{\partial W_s}{\partial s} + \sin^2\lambda\frac{\partial W_p}{\partial s}$$

$$G\frac{d\theta}{ds}\left[1 - \sin^2\lambda\right] = -\cos^2\lambda\frac{\partial W_s}{\partial p} + \cos\lambda\sin\lambda\left(\frac{\partial W_p}{\partial p} - \frac{\partial W_s}{\partial s}\right) + \left(\frac{G}{A\cos\lambda} + \sin^2\lambda\right)\frac{\partial W_p}{\partial s}$$

$$\frac{d\theta}{ds} = \frac{1}{G}\left[\left(\tan^2\lambda + \frac{G}{A}\sec^3\lambda\right)\frac{\partial W_p}{\partial s} + \tan\lambda\left(\frac{\partial W_p}{\partial p} - \frac{\partial W_s}{\partial s}\right) - \frac{\partial W_s}{\partial p}\right] \quad . \tag{G8}$$

3. Ground Speed

The reciprocal ground speed on the alternate path can be expressed in terms of the reciprocal ground speed on the minimal path M by using a Taylor series expansion. For any value p:

$$\frac{1}{G(s,p)} = \frac{1}{G(s,0)} + p\frac{\partial}{\partial p}\left(\frac{1}{G(s,p)}\right)\Big|_{p=0} + \frac{p^2}{2}\frac{\partial^2}{\partial p^2}\left(\frac{1}{G(s,p)}\right)\Big|_{p=0} + \cdots$$

$$= \frac{1}{G(s,0)} - \frac{p}{G^2(s,0)}\frac{\partial G}{\partial p}\Big|_{p=0} + \frac{p^2}{2}\left[\frac{2}{G^3(s,0)}\left(\frac{\partial G}{\partial p}\right)^2\Big|_{p=0}\right.$$

$$\left. - \frac{1}{G^2(s,0)}\frac{\partial^2 G}{\partial p^2}\Big|_{p=0}\right] + \cdots \qquad \text{(G9)}$$

Then $\frac{1}{G(s,P)}$ will be the reciprocal ground speed on the alternate path specified by P(s). Since the wind components are resolved along and across the vector $\vec{G}(s,0)$, the expression for G(s,p) becomes (see Figure G-6):

$$G(s,p) = \sqrt{A^2 - (W_p\cos\psi - W_s\sin\psi)^2} + W_s\cos\psi + W_p\sin\psi \quad .$$

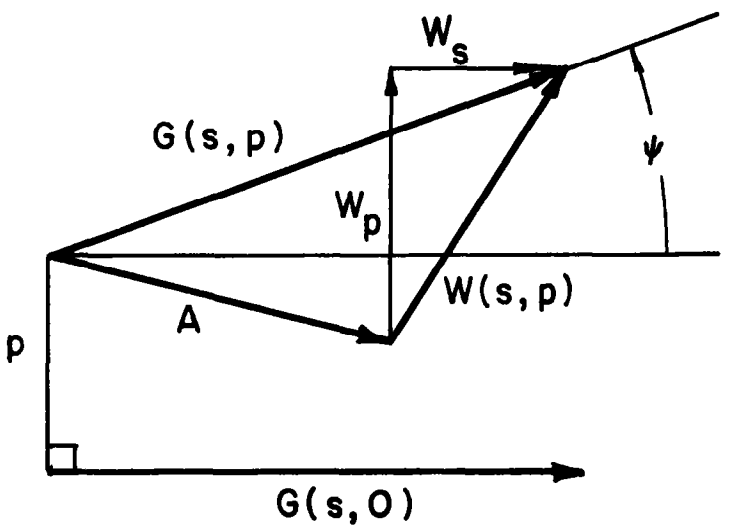

Figure G-6

Setting $\tan \psi = bp$, performing the indicated differentiations, and evaluating at $p = 0$ we find:

$$\frac{\partial G}{\partial p}\Big|_0 = \frac{-W_p \dfrac{\partial W_p}{\partial p} + bW_p W_s}{\sqrt{A^2 - W_p^2}} + bW_p + \frac{\partial W_s}{\partial p}$$

or, using $\sin \lambda = \dfrac{W_p}{A}$ and $G(s,0) = A \cos \lambda + W_s$,

$$\frac{\partial G}{\partial p}\Big|_0 = -\tan \lambda \frac{\partial W_p}{\partial p} + \frac{\partial W_s}{\partial p} + bG(s,0) \tan \lambda \quad , \tag{G10}$$

where W_s, W_p and their derivatives are evaluated at $p = 0$, and

$$\frac{\partial^2 G}{\partial p^2}\Big|_0 = -\frac{\sec^3 \lambda}{A} \left(\frac{\partial W_p}{\partial p}\right)^2 - \tan \lambda \frac{\partial^2 W_p}{\partial p^2} + \frac{\partial^2 W_s}{\partial p^2}$$

$$+ 2b \left(\tan \lambda \frac{\partial W_s}{\partial p} + \frac{\sec^3 \lambda}{A} W_s \frac{\partial W_p}{\partial p} + \frac{\partial W_p}{\partial p}\right)$$

$$+ b^2 \left(W_p \tan \lambda - W_s^2 \frac{\sec^3 \lambda}{A} - W_s\right) \quad .$$

Since we interpret

$$\tan \psi(p) = bp \quad ,$$

the expression for G(s,p) is valid for p = 0. On the alternate path, $\tan \psi(P) = bP(s)$. But $\psi(P)$ is the angle between the minimal path and the alternate and $\tan \psi(P)$ is simply $\frac{dP(s)}{ds}$ or P'. Therefore,

$$b = \frac{P'}{P(s)} \quad .$$

Using the definition of P(s) stated above,

$$b = \begin{cases} \frac{1}{s} & \text{for the divergent region} \\ 0 & \text{for the middle region} \\ \frac{1}{s-L} & \text{for the convergent region} \end{cases} \quad .$$

4. Mean Time Lost

At this point, the results of the preceding Sections can be combined (discarding terms in P_M^3 and higher). For the middle region (b = 0):

$$\frac{d\tau}{ds} = \left[1 - P_M \frac{d\theta}{ds}\right]\left[\frac{1}{G} - \frac{P_M}{G^2}\frac{\partial G}{\partial p} + \frac{P_M^2}{G^3}\left(\frac{\partial G}{\partial p}\right)^2 - \frac{P_M^2}{2G^2}\frac{\partial^2 G}{\partial p^2}\right] - \frac{1}{G} \quad .$$

Here G = G(s, 0) and all derivatives are evaluated on the MTP (p = 0).

$$\frac{d\tau}{ds} = -\frac{P_M}{G^2}\left[G\frac{d\theta}{ds} + \frac{\partial G}{\partial p}\right] + \frac{P_M^2}{G^3}\left[\frac{\partial G}{\partial p}\left(G\frac{d\theta}{ds} + \frac{\partial G}{\partial p}\right) - \frac{G}{2}\frac{\partial^2 G}{\partial p^2}\right] \quad .$$

Applying eqs. (G8) and (G10), the coefficient of P_M becomes:

$$-\frac{1}{G^2}\left[G\frac{d\theta}{ds}+\frac{\partial G}{\partial p}\right]$$

$$= -\frac{1}{G^2}\left[(\tan^2\lambda+\frac{G}{A}\sec^3\lambda)\frac{\partial W_p}{\partial s}-\tan\lambda\frac{\partial W_s}{\partial s}+\tan\lambda\frac{\partial W_p}{\partial p}\right.$$

$$\left.-\frac{\partial W_s}{\partial p}-\tan\lambda\frac{\partial W_p}{\partial p}+\frac{\partial W_s}{\partial p}\right]$$

$$= -\frac{\partial}{\partial s}\left(\frac{\tan\lambda}{G}\right).$$

For the divergent region ($b = \frac{1}{s}$):

$$\frac{d\tau}{ds} = \left[1-\frac{sP_M}{D}\frac{d\theta}{ds}+\frac{1}{2}\left(\frac{P_M}{D}\right)^2\right]\left[\frac{1}{G}-\frac{sP_M}{DG^2}\frac{\partial G}{\partial\partial}+\cdots\right]-\frac{1}{G}$$

$$= -\frac{sP_M}{DG^2}\left[G\frac{d\theta}{ds}+\frac{\partial G}{\partial p}\right]+\frac{1}{2G}\left(\frac{P_M}{D}\right)^2$$

$$+\frac{1}{G^3}\left(\frac{sP_M}{D}\right)^2\left[\frac{\partial G}{\partial p}\left(G\frac{d\theta}{ds}+\frac{\partial G}{\partial p}\right)-\frac{G}{2}\frac{\partial^2 G}{\partial p^2}\right].$$

In this region, the coefficient of P_M becomes:

$$-\frac{s}{DG^2}\left[G\frac{d\theta}{ds}+\frac{\partial G}{\partial p}\right]$$

$$= -\frac{s}{D}\left[\frac{\partial}{\partial s}\left(\frac{\tan\lambda}{G}\right)+\frac{\tan\lambda}{sG}\right]$$

$$= -\frac{1}{D}\frac{\partial}{\partial s}\left(\frac{s\tan\lambda}{G}\right).$$

The analogous coefficient for the convergent region ($b = \frac{1}{s-L}$) is:

$$+\frac{1}{C}\frac{\partial}{\partial s}\left(\frac{(s-L)\tan\lambda}{G}\right) \quad .$$

The contribution of all terms which are linear in P_M to the total time lost is:

$$-\frac{P_M}{D}\int_0^D \frac{\partial}{\partial s}\left(\frac{s\tan\lambda}{G}\right) ds - P_M\int_D^{D+B}\frac{\partial}{\partial s}\left(\frac{\tan\lambda}{G}\right) ds$$

$$+\frac{P_M}{C}\int_{D+B}^{L}\frac{\partial}{\partial s}\left(\frac{(s-L)\tan\lambda}{G}\right) ds$$

$$= -P_M\left[\frac{1}{D}\frac{s\tan\lambda}{G}\Bigg|_0^D + \frac{\tan\lambda}{G}\Bigg|_D^{D+B} - \frac{1}{C}\frac{(s-L)\tan\lambda}{G}\Bigg|_{D+B}^{L}\right]$$

$$= 0 \quad . \qquad \text{(Since } C + B + D = L\text{)} \quad .$$

Therefore, the expression for τ contains P_M only to the second and higher powers. Since τ is the time penalty for a path different from the MTP, it must be positive for all values of P_M (positive and negative). The zero value for the linear coefficient of P_M reflects this constraint.

For a particular wind field, the relationship between τ and P_M will appear something like Figure G-7. On some days, the minimum will be pronounced, while on others it will be shallow. From an economic point of view, the parameter of interest is the average value of the coefficient of P_M^2 which is a measure of the average penalty incurred for small deviations from the MTP.

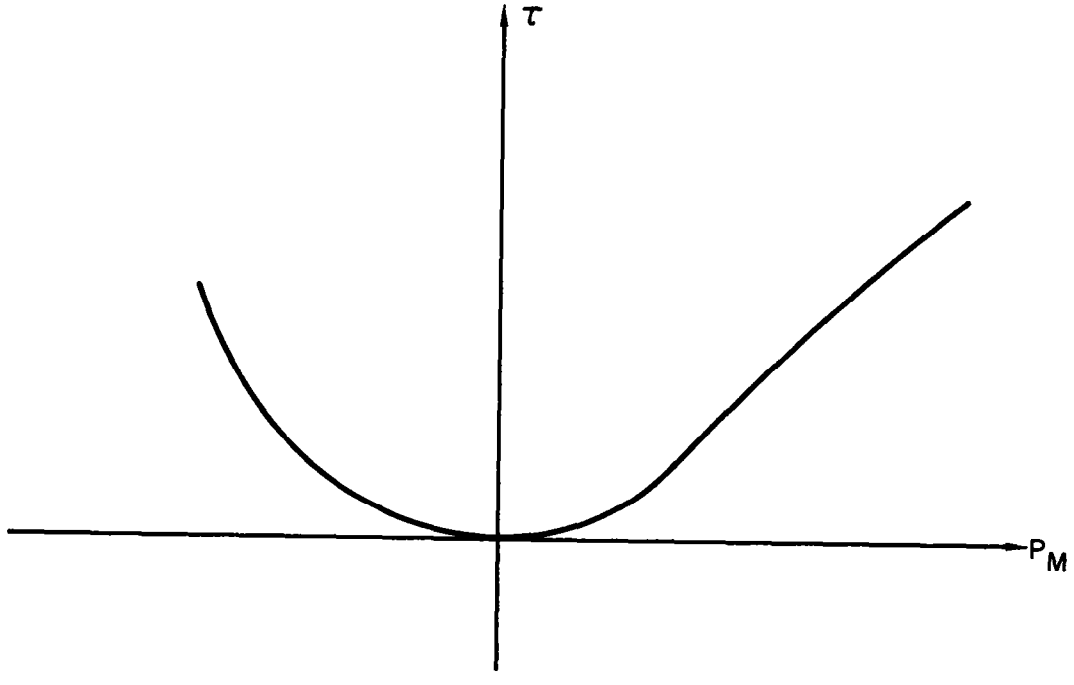

Figure G-7

To simplify the expressions for $\frac{d\tau}{ds}$, the following approximations can be introduced.

$$\tan\lambda \approx \frac{W_p}{A}$$

$$\sec^n\lambda \approx 1 + \frac{n}{2}\left(\frac{W_p}{A}\right)^2$$

$$G \approx A\left[1 + \frac{W_s}{A} - \frac{1}{2}\left(\frac{W_p}{A}\right)^2\right]$$

$$\frac{1}{G^n} \approx \frac{1}{A^n}\left[1 - n\frac{W_s}{A} + \frac{n}{2}\left(\frac{W_p}{A}\right)^2 + \frac{n(n+1)}{2}\left(\frac{W_s}{A}\right)^2\right] .$$

The validity of these approximations rests on the fact that jet air speed is much greater than typical wind velocities. In the expressions presented below, every term which as been disregarded is in the ratio W:A to some one of the terms which have been retained.

Considering only the terms in P_M^2, for the middle region:

$$\frac{d\tau}{ds} \approx \frac{P_M^2}{A^3}\left[\frac{\partial W_p}{\partial s}\frac{\partial W_s}{\partial p} - \left(\frac{A}{2} - W_s\right)\frac{\partial^2 W_s}{\partial p^2} + \frac{W_p}{2}\frac{\partial^2 W_p}{\partial p^2} + \frac{1}{2}\left(\frac{\partial W_p}{\partial p}\right)^2\right]$$

$$= \frac{P_M^2}{A^3}[Q] \quad . \tag{G11}$$

For the divergent region:

$$\frac{d\tau}{ds} \approx \frac{P_M^2}{A^3}\left\{\frac{1}{D^2}\left[\frac{A^2}{2} + \frac{3W_p^2}{4}\right] + \frac{s}{D^2}\left[W_p\frac{\partial W_p}{\partial s} - (A - W_s)\frac{\partial W_p}{\partial p}\right] + \frac{s^2}{D^2}Q\right\} \tag{G12}$$

(In the third term within the brackets, the coefficient of $(s/D)^2$ is the same as the bracketed coefficient of eq. (G11). For the convergent region:

$$\frac{d\tau}{ds} \approx \frac{P_M^2}{A^3}\left\{\frac{1}{C^2}\left[\frac{A^2}{2}+\frac{3W_p^2}{4}\right]+\frac{s-L}{C^2}\left[W_p\frac{\partial W_p}{\partial s}-(A-W_s)\frac{\partial W_p}{\partial p}\right]+\frac{(s-L)^2}{C^2}\Omega\right\}. \tag{G13}$$

The mean time penalty on the alternate path is:

$$\bar{\tau} = E\left[\int_0^L \frac{d\tau}{ds}\,ds\right] .$$

Since winds are small compared to jet air speed, percentage variation of the length (L) of the MTP will be small. Under these circumstances, the mean penalty can be approximated by:

$$\bar{\tau} \approx \int_0^{L_o} \left[\overline{\frac{d\tau}{ds}}\right] ds \quad ,$$

where L_o is the average length of the MTP.

Expected values of the terms involving winds and their spatial derivatives can be estimated by an extension of the techniques described in Appendix A. For example:

$$E\left\{\left(\frac{\partial W_p}{\partial p}\right)^2\right\} = E\left\{\left[\frac{\partial}{\partial p}(\mu_p + w_p)\right]^2\right\} = \left(\frac{\partial \mu_p}{\partial p}\right)^2 + E\left\{\left(\frac{\partial w_p}{\partial p}\right)^2\right\} \quad ,$$

where μ_p is the expected value of W_p. Interpreting eq. (All)

$$E\left\{\left(\frac{\partial w_p}{\partial p}\right)^2\right\} = -\sigma_p^2 \frac{d^2}{dr^2}\left[R_{yv}(r)\right]_{r=0} \quad .$$

Derivatives of mean winds have been estimated from mean wind charts.[2] The second derivative of the autocorrelation function is estimated from Figure A-1.

For a typical westbound flight path across the North Atlantic at flight level 290, the expected value of the quantity Q in eq. (G12) is -275 kts^2 per 100 mile unit.[2] In order to compare the average magnitudes of the three terms in eq. (G12) a value for D (the length of the divergent portion) must be assumed. Inserting 1000 n. mi. (the distance from New York to Gander), and evaluating at s = D, the expected values of these three terms are 1166, 22, and -275 kts^2 per 100 mi. unit.[2] The first term dominates the other two and the factor $A^2/2$ is primarily responsible. Since s varies in the integral from 0 to D, the second and third terms contribute even less to the total, in this divergent region, than comparison of the numerical values suggests. For smaller values of D, the dominance of the first term becomes stronger.

In the convergent region (eq. (G13)) the situation is similar. The second term is equal in magnitude (on the average) but opposite in sign to the corresponding term in eq. (G12). The contribution of these two terms to the mean time lost will be negligible.

The contribution of the term $\overline{Q}$ is negative in all three regions. If it is disregarded, the calculated penalty overestimates the correct value. Retaining only the first term in the divergent and convergent regions:

$$\bar{\tau} = \frac{P_M^2}{A^2}\left[\frac{A^2}{2} + \frac{\overline{3W_p^2}}{4}\right]\left[\frac{1}{D^2}\int_0^D ds + \frac{1}{C^2}\int_{D+B}^{L_o} ds\right]$$

$$= \frac{P_M^2}{A^3}\left[\frac{A^2}{2} + \frac{\overline{3W_p^2}}{4}\right]\left[\frac{1}{D} + \frac{1}{C}\right]$$

$$\bar{\tau} = .063\, P_M^2 \left(\frac{1}{D} + \frac{1}{C}\right) \text{ minutes} \qquad (A = 480 \text{ kt.}) \quad , \qquad (G14)$$

where P_M, D, and C are measured in n. mi.

It is apparent from this result that the wind statistics contribute negligibly to the average penalty. If the term $\overline{Q}$ is included, the penalty is reduced. Except for the factor $\frac{\overline{3W_p^2}}{4}$ (which modifies the result only by 1.4%), the penalty depends only on the geometry of the diversion. It is equivalent to the penalty associated with a path deviating from the great circle route if winds were zero everywhere.

The method used to show that wind statistical contributions are small is open to question. The values used are statistics which describe winds near a single "average" MTP whereas they should reflect wind conditions in the neighborhood of the actual MTP which moves as the weather changes. Such statistics could be collected by examining a sample of weather maps on which MTP's have been plotted. The statistics so obtained would have to be radically different from the stationary data used above before the general conclusions of this Appendix lose their validity.

Eq. (G14) shows that the penalty for a diversion depends on the length of the divergent and convergent regions. If the diversion can be planned in

advance, the penalty is less severe. If, for example, a flight must be rerouted parallel to the MTP in the oceanic portion of the flight, the dispatcher can often set up the alternate route so that D and C are both about 1000 n. mi. In this case:

$$\bar{\tau} = .45\, P_M^2 \text{ minutes} \quad .$$

Here P_M should be measured in degrees of latitude. A one degree lateral revision then carries a penalty of about one-half minute while two degrees impose a two minute penalty. If the diversion must be accomplished in a tactical manner, say in one 10° oceanic reporting interval, then (D = C = 360 n. mi.):

$$\bar{\tau} = 1.26\, P_M^2 \qquad (P_M \text{ in degrees}) \quad .$$

The penalty is about three times larger than when the diversion can be preplanned.

BIBLIOGRAPHY

1. U. S. Air Force, Air Navigation, AF Manual 51-40, Vol. I, 1959.
2. U. S. Navy, Upper Wind Statistics of the Northern Hemisphere, Navaer 50-1c-535, 1959.
3. C. S. Durst, The Statistical Variation of Wind with Distance, Quarterly Journal of the Royal Meteorological Society, October, 1960.
4. H. E. Daniels, The Theory of Position Finding, Journal of the Royal Statistical Society, Series B, Vol. XIII, No. 2, 1951.
5. U. S. Air Force, Air Navigation, AF Manual 51-40, Vol. II, 1960.
6. H. Cramer, Mathematical Methods of Statistics, Princeton University Press, 1945.
7. D. C. Willis, Dead Reckoning and Wind Finding Accuracy over the North Atlantic, Journal of the Institute of Navigation, July, 1958.
8. H. W. Ellsaesser, Lt. Col., USAF, Wind Variability, U. S. Air Force Air Weather Service Technical Report, AWS TR 105-2, 1960.
9. C. S. Durst, The Accuracy of Upper-Wind Forecasts, Journal of the Institute of Navigation, July, 1960.
10. C. E. Dunmire, Characteristics of the North Atlantic Air Traffic Control and Navigation System, Memorandum Report, Federal Aviation Agency, May, 1962.
11. H. Kahn, Use of Different Monte Carlo Sampling Techniques, Symposium on Monte Carlo Methods, John Wiley, 1954.
12. P. G. Reich, Preliminary Studies for Models of Future North Atlantic Air Traffic Control Systems, Proceedings of First Annual International Aviation Research and Development Symposium, Federal Aviation Agency, 1961.
13. W. Taylor, Cmdr., USN, A Probability Model of the Aircraft Separation Problem, Federal Aviation Agency, Bureau of Research and Development Report, April, 1960.
14. C. S. Durst, Abnormal Errors and Aircraft Separation over the North Atlantic, Journal of the Institute of Navigation, January, 1959.
15. D. E. Lloyd, Accuracy of Estimates for 10° W Made at 20° W, Ministry of Aviation, Operational Research Note No. 184, 1962.

16. K. N. Dodd, An Introduction to Air Traffic Control Procedure at Prestwick Oceanic, Royal Aircraft Establishment, Tech. Note Math. 73, June, 1961.

17. Federal Aviation Agency, North Atlantic Survey Flight Data-July 14, 1961, Traffic Analysis Branch, Systems Engineering Division, FAA, Working Paper, October, 1961.

18. Brooks, C. E. P. et al, Upper Winds over the World, Meteorological Office, Air Ministry, Geophysical Mem. No. 85, 1952.

19. C. S. Durst, Some Meteorological Aspects of Flight in the Supersonic Age, Journal of the Institute of Navigation, January, 1962.

20. I. I. Gringorten, Upper Wind Representation and Flight Planning, Air Force Surveys in Geophysics No. 89, AFCRC-TN-221, March, 1957.

21. Arcon Corporation, Air Traffic Control Theory and Design, prepared for the Mitre Corp. under Subcontract No. 49, FAA/BRD-157, July, 1961.

22. Federal Ministry of Transport (Germany), Paper-Jet, prepared by the German Meteorological Services, Federal Administration of Air Navigation Services, and Lufthansa Air Lines, 1958.

23. E. J. Weigman, Analysis of Wind and Weather Factors on the New York-London Air Route for the Peak Traffic Day of 25 August 1961, Stanford Research Institute, Peak Traffic Day Report I, July 1962.